

## University of Southampton Research Repository ePrints Soton

Copyright © and Moral Rights for this thesis are retained by the author and/or other copyright owners. A copy can be downloaded for personal non-commercial research or study, without prior permission or charge. This thesis cannot be reproduced or quoted extensively from without first obtaining permission in writing from the copyright holder/s. The content must not be changed in any way or sold commercially in any format or medium without the formal permission of the copyright holders.

When referring to this work, full bibliographic details including the author, title, awarding institution and date of the thesis must be given e.g.

AUTHOR (year of submission) "Full thesis title", University of Southampton, name of the University School or Department, PhD Thesis, pagination

DYNAMIC ANALYSIS OF ARCH DAMS  
SUBJECTED TO SEISMIC DISTURBANCES

by

H.E. ERMUTLU

Thesis submitted for the  
Degree of Doctor of Philosophy  
December, 1968

Institute of Sound and Vibration Research  
The University of Southampton

## ACKNOWLEDGMENTS

The author wishes to express his gratitude to Professor B.L. Clarkson, The Director of the Institute of Sound and Vibration Research of Southampton University, and The Directorate General of State Hydraulic Works of Turkey, who have organized the research work to be carried out; and to the Turkish N.A.T.O. Science Committee, who has supported the work financially.

The author especially wishes to thank Dr. M. Petyt, who supervised the research and gave all possible assistance.

Thanks are also due to Dr. J.R. Rydzewski for his interest and valuable suggestions on arch dam design; and to the staff members and postgraduate students in the I.S.V.R. for their assistance and helpful suggestions.

Finally, the author wishes to thank the clerical and technical staff who helped in the preparation of the thesis.

ABSTRACT

FACULTY OF ENGINEERING AND APPLIED SCIENCE  
INSTITUTE OF SOUND AND VIBRATION RESEARCH

Doctor of Philosophy

DYNAMIC ANALYSIS OF ARCH DAMS  
SUBJECTED TO SEISMIC DISTURBANCES

by HAYDAR ERHAN ERMUTLU

Three-dimensional finite element methods are developed for static and dynamic analysis of arch dams. The simple tetrahedral element, with four nodal points and three-degrees-of-freedom per node, is used in the idealization. A computer programme, which uses an iterative procedure, is prepared to give the static solution of arch dams under hydrostatic and gravity loadings.

The static analysis is extended to dynamic analysis and a computer programme is prepared to calculate the natural frequencies and corresponding mode shapes of arch dams. The hydrodynamic effect of the reservoir water and the flexibility of foundation are taken into consideration.

Since earthquake ground motions are random in nature, to satisfy the requirements of probabilistic design, a method which uses random vibration theory is developed to estimate the responses of arch dams subjected to seismic disturbances. Providing that the natural frequencies and corresponding mode shapes of an arch dam are known, by using the acceleration power spectral density of a representative earthquake ground motion

as input, then the probable responses of the structure are calculated.

The effects on the arch dam response of various parameters, such as the intensity, duration and direction of the earthquake ground motion, the velocity of earthquake waves, damping of the structure, reservoir water level and foundation flexibility, are investigated.

The probable maximum dynamic stresses developed in the arch dam during an earthquake are determined. These stresses are combined with the stresses due to static loadings and the most critical loading conditions and the total maximum stresses are discussed.

## CONTENTS

	<u>Page</u>
TABLES	
FIGURES	
SYMBOLS	
1. INTRODUCTION	1
1.1 The object of the study	1
1.2 General factors on arch dam design	3
1.3 Review of previous studies on design of arch dams to resist earthquakes	5
1.4 Concepts of the probabilistic design of arch dams to resist earthquake excitation.	11
1.5 Preview of the content of the study	14
2. STATIC ANALYSIS OF ARCH DAMS	17
2.1 Introduction	17
2.2 Finite element methods	17
2.3 Idealization of an arch dam into a finite number of three-dimensional elements	19
2.4 The theoretical basis of finite element methods, derivation of element stiffness properties	24
2.5 Assumed displacement functions for the simple tetrahedral element	27
2.6 Equilibrium of complete structure	28
2.7 Solution of equilibrium equations	31
2.8 Boundary conditions	34
2.9 Calculation of element stresses and nodal point stresses	36

	<u>Page</u>
2.10 Comparison of the types of idealizations	38
2.11 Computer programming	41
2.12 Application of the theory to the static analysis of an arch dam	42
3. DYNAMIC ANALYSIS OF ARCH DAMS	47
3.1 Introduction	47
3.2 General equations of motion for multi-degree-of- freedom systems	47
3.3 Derivation of the consistent mass matrix of an element	51
3.4 Equilibrium of complete structure	53
3.5 The evaluation of eigenvalue problem	56
3.6 General considerations on the hydrodynamic effect of the reservoir water	57
3.7 Theoretical basis of the hydrodynamic effect and the electrolytic analogy	60
3.8 Application of electrolytic analogy to approximate the hydrodynamic effect	63
3.9 Incorporation of the hydrodynamic forces in the general vibration problem	65
3.10 Effect of flexibility of the foundation	66
3.11 Computer programming	67
3.12 Application of the theory to the dynamic analysis of an arch dam	68
4. THEORY OF FORCED VIBRATION OF ARCH DAMS UNDER EARTHQUAKE EXCITATION	78
4.1 Introduction	78
4.2 Normal mode analysis	79
4.3 Response of linear single degree-of-freedom system to earthquake excitation	83
4.4 Calculation of responses from step-by-step integration of ground acceleration	86

	<u>Page</u>
4.5 General theory of stationary random vibrations	89
4.6 Application of random vibration theory to earthquake type excitation	109
4.7 Response spectra methods	115
4.8 Computer programming	120
4.9 Contributions of modes on response of an arch dam	122
5. RESPONSE OF ARCH DAMS TO EARTHQUAKES, THE EFFECTS OF VARIOUS FACTORS	125
5.1 Introduction	125
5.2 Power spectral density of earthquake acceleration	126
5.3 Response of an arch dam, reservoir in empty condition	126
5.4 Comparison of the random analysis results with those obtained by response spectra method	129
5.5 Response of an arch dam, reservoir in full condition, effect of reservoir water	130
5.6 Effect of damping ratio on the response of an arch dam	133
5.7 Effects of earthquake characteristics on the response of an arch dam	134
5.8 The direction of action of the ground acceleration	139
5.9 Effect of foundation flexibility on the response of an arch dam	143
6. STRESSES IN ARCH DAMS DUE TO EARTHQUAKES	144
6.1 Introduction	144
6.2 Calculation of dynamic stresses due to earthquakes	145
6.3 Maximum dynamic stresses	148
6.4 Maximum stresses in an arch dam during earthquake	149
6.5 Discussion of results	152

	<u>Page</u>
7. CONSIDERATIONS ON SEISMICITY OF THE DAM SITE AND THE SUMMARY OF PRINCIPAL RESULTS	155
7.1 Introduction	155
7.2 Estimation of seismic characteristics of a particular region	155
7.3 Summary of the methods of analysis	163
7.4 Summary of the principal results	166
APPENDIX A.1 Derivation of the stiffness matrix for the tetrahedral element	175
A.2 Application of iteration method to three- dimensional finite element technique	181
A.3 Inserting the boundary conditions	185
A.4 Derivation of the consistent mass matrix for the tetrahedral element	187
A.5 Summary of principal results related with random vibration theory	192
A.6 Response to random loading	195
REFERENCES	200
TABLES	207
FIGURES	

## LIST OF TABLES

- 2.1 Calculation of nodal point stresses.
- 2.2 Mechanical properties of concrete and foundation rock for Arch Dam Type-5.
- 3.1 Effect of the reservoir water on the natural frequencies of Arch Dam Type-5.
- 3.2 Effect of the flexibility of foundation on the natural frequency of fundamental mode of Arch Dam Type-5.
- 3.3 Comparison of geometrical characteristics of Kamishiiba Dam with Arch Dam Type-5.
- 3.4 Comparison of experimental results obtained for Kamishiiba Dam with the theoretical results obtained for Arch Dam Type-5.
- 3.5 Comparison of the frequency ratios obtained for the effect of the reservoir water on the natural frequencies of arch dams.

## LIST OF FIGURES

- 2.1 Idealization of an arch dam by means of tetrahedral elements.
- 2.2 A-type idealization of a brick-like block by five tetrahedral elements.
- 2.3 Division of a brick-like block into five tetrahedral elements (A-type idealization).
- 2.4 B-type idealization of a brick-like block by six tetrahedral elements.
- 2.5 Division of a brick-like block into six tetrahedral elements (B-type idealization).
- 2.6 C-type idealization of a brick-like block by six tetrahedral elements.
- 2.7 Division of a brick-like block into six tetrahedral elements (C-type idealization).
- 2.8 Possible combinations of three tetrahedral elements to construct a triangular prism.
- 2.9 Tetrahedral element, global Cartesian coordinate system.
- 2.10 A boundary nodal point and acting forces.
- 2.11 Nodal point forces acting on a portion of a three-dimensional structure.
- 2.12 Two possible idealizations of a structure by using A-type brick-like blocks.
- 2.13 Two possible idealizations of a structure by using C-type brick-like blocks.
- 2.14 Flow diagram for static analysis.
- 2.15 Arch Dam Type-5, general layout.
- 2.16 Idealization of the half of a double curvature arch dam by means of A-type brick-like blocks using five tetrahedral elements (16 x 1 x 16 mesh type).
- 2.17 Stresses and deflections of Arch Dam Type-5 under hydrostatic loading.
- 2.18 Stresses and deflections of Arch Dam Type-5 under gravity loading.
- 3.1 Flow diagram for calculating frequency and mode shape.
- 3.2 Idealization of the half of a double curvature arch dam by means of A-type brick-like blocks using five tetrahedral elements (8 x 1 x 8 mesh type).

- 3.3 First mode of vibration of Arch Dam Type-5.
- 3.4 Second mode of vibration of Arch Dam Type-5.
- 3.5 Third mode of vibration of Arch Dam Type-5.
- 3.6 Fourth mode of vibration of Arch Dam Type-5.
- 3.7 Fifth mode of vibration of Arch Dam Type-5.
- 3.8 Sixth mode of vibration of Arch Dam Type-5.
- 3.9 Seventh mode of vibration of Arch Dam Type-5.
- 3.10 Eighth mode of vibration of Arch Dam Type-5.
- 3.11 Ninth mode of vibration of Arch Dam Type-5.
- 3.12 Tenth mode of vibration of Arch Dam Type-5.
- 3.13 Modal lines of horizontal deflections for each mode of vibration of Arch Dam Type-5.
- 3.14 Coefficients of radial hydrodynamic pressures for uniform upstream acceleration.
- 3.15 Effect of the reservoir water on the mode shapes.
- 3.16 Arch Dam with its foundation included.
- 3.17 Effect of the boundary flexibility on the natural frequency of the fundamental mode.
- 3.18 Effect of the boundary flexibility on the shape of the fundamental mode.
  
- 4.1 Single degree-of-freedom system subjected to base excitation.
- 4.2 Spectrum analysis of random vibration, as determined from a magnetic tape loop.
- 4.3 The experimental determination of the power spectral density of a random function.
- 4.4 Illustration of the relationship between the force and displacement power spectral densities.
- 4.5 Three-dimensional solid structure, acting forces and displacements.
- 4.6 Flow diagram for calculating response by power spectral density method.

- 4.7 Unit modal receptances, given by equation (4.95).
- 4.8 Modal response power spectral densities, force direction X.
- 4.9 Modal response power spectral densities, force direction Y.
- 4.10 Modal response power spectral densities, force direction Z.
- 4.11 Unit modal receptances in linear scale.
- 4.12 The effect of velocity of earthquake waves on modal response power spectral densities, force direction X.
- 4.13 The effect of velocity of earthquake waves on modal response power spectral densities, force direction Y.
  
- 5.1 Smoothed power spectrum of earthquake acceleration.
- 5.2 Response power spectrum, reservoir in empty condition.
- 5.3 Response power spectrum, reservoir in empty condition.
- 5.4 Response power spectrum, reservoir in empty condition.
- 5.5 Response power spectrum, reservoir in empty condition.
- 5.6 Response power spectrum, reservoir in empty condition.
- 5.7 Response power spectrum, reservoir in empty condition.
- 5.8 Average response velocity-spectrum curves.
- 5.9 Comparison of the responses obtained by power spectrum method and response spectrum method.
- 5.10 Response power spectrum, reservoir in full condition.
- 5.11 Response power spectrum, reservoir in full condition.
- 5.12 Response power spectrum, reservoir in full condition.
- 5.13 Response power spectrum, reservoir in full condition.
- 5.14 Response power spectrum, reservoir in full condition.
- 5.15 Response power spectrum, reservoir in full condition.
- 5.16 The effect of the reservoir water on the maximum responses of crown cantilever.

- 5.17 Maximum response of crown cantilever in comparison with hydrostatic deflections.
  - 5.18 Effect of damping ratio on the response of the crown cantilever.
  - 5.19 Effect of damping ratio on the response of the dam.
  - 5.20 Earthquake and response power spectra in comparison with white noise excitation.
  - 5.21 Variation of magnification factor according to earthquake duration.
  - 5.22 Effect of earthquake wave velocity on maximum response.
  - 5.23 Effect of earthquake direction on the response of an arch dam.
  - 5.24 Earthquake direction which produces maximum horizontal responses at the points on the top arch.
  - 5.25 Comparison of response components of top arch according to the direction of earthquake with the same spectral intensity.
- 
- 6.1 Modal stresses in crown cantilever, reservoir in empty condition.
  - 6.2 Modal stresses in crown cantilever, reservoir in full condition.
  - 6.3 Maximum dynamic stresses in crown cantilever due to El-Centro 1940 earthquake.
  - 6.4 Maximum total compressive hoop stresses in crown cantilever.
  - 6.5 Maximum total tensile hoop stresses in crown cantilever.
  - 6.6 Maximum total compressive vertical stresses in crown cantilever.
  - 6.7 Maximum total tensile vertical stresses in crown cantilever.
- 
- A.1 Tetrahedral finite element, coordinate system and dimensions.
  - A.2 Assumed system of axis for inertia calculations.

## LIST OF SYMBOLS

### Matrix and other general notation

$[ \quad ]$	Rectangular matrix
$\{ \quad \}$	Column matrix
$[ \quad ]^T$	Transposed matrix
$[ \quad ]^{-1}$	Inverse matrix
$\begin{bmatrix} & \\ & \\ & \end{bmatrix}$	Diagonal matrix
$  \quad  ^2$	Modulus square
*	Complex conjugate
$\langle \quad \rangle$	Mean
Pr $[ \quad ]$	Probability
exp ( )	Exponential
erf ( )	Gaussian error function
det ( )	Determinant

### Notation used in finite element analysis

$x, y, z$	Cartesian global coordinates
$u, v, w$	Displacement components
V	Volume of tetrahedral element
$\{U\}, \{U_i\}, \{\bar{U}_i\}$	Displacements, element nodal displacements, virtual displacements
$\{A\}$	Generalized displacements
$[N(x, y, z)], [B(x, y, z)]$	Matrix of assumed displacement functions and its differential matrix
$[c]$	Nodal point coordinates
$\{\epsilon\}, \{\epsilon_0\}, \{\bar{\epsilon}\}$	Strains, initial strains, virtual strains

$\{\sigma\}$	Stresses
$[D]$	Matrix of material constants
$\{S_i\}$	Element nodal forces
$[k], [m]$	Element stiffness and mass matrices
$[m_p]$	Matrix of inertial constants
$\{f\}$	Inertia forces per unit volume

Notation used for overall structure

$[K], [M], [C]$	Stiffness, mass and damping matrices
$\{q\}, \{\dot{q}\}, \{\ddot{q}\}$	Generalized displacements, velocities and accelerations
$\{Q\}$	External forces
$[H]$	Hydrodynamic matrix
$[\Phi]$	Modal matrix
$\{\psi_r\}$	$r^{\text{th}}$ normal mode
$[M], [K], [C]$	Generalized mass, stiffness and damping matrices
$\{E\}$	Generalized forces
$\{\xi\}$	Normal coordinates

Notation used in random vibration analysis

$\omega$	Circular frequency
$f$	Frequency (Hz)
$\zeta$	Damping ratio
$\alpha(x_\alpha, y_\alpha, z_\alpha), \beta(x_\beta, y_\beta, z_\beta)$	Nodal points
$w_x(1, t), w_y(1, t), w_z(1, t)$	Response components at nodal point "1"
$P_x(\alpha, t), P_y(\alpha, t), P_z(\alpha, t)$	Discrete load components

$1/Z_{1\alpha}^x(f), 1/Z_{1\alpha}^y(f)$	Receptance
$S_w(\alpha, f), S_p(\alpha, f)$	Power spectral densities of response and loading
$S_w(\alpha, \beta; f), S_p(\alpha, \beta; f)$	Cross power spectral densities of response and loading
$R_w(\alpha, \tau), R_p(\alpha, \tau)$	Autocorrelation functions of response and loading
$R_w(\alpha, \beta; \tau), R_p(\alpha, \beta; \tau)$	Cross correlation functions of response and loading
$P_o(\alpha), P_o(\beta)$	As given in equation (4.50)
$\phi(t)$	Randomly varying quantity
$S_\phi(f), R_\phi(\tau)$	Power spectral density and autocorrelation function of $\phi(t)$
$v_x, v_y, v_z$	Convection velocity components of $\phi(t)$
$\tau_o$	Time lag
$\sigma_x$	RMS value of $x(t)$
$E_1$	Expected number of peaks in unit time
$n$	Magnification factor
$T$	Duration of earthquake
$\bar{x}_{max}(T)$	Mean maxima for duration $T$
$u_g(t)$	Ground displacement
$\ddot{u}_{g_x}(t), \ddot{u}_{g_y}(t), \ddot{u}_{g_z}(t)$	Ground acceleration components
$S_{u_g}(f)$	Power spectral density of ground acceleration
$m_x(\alpha), m_y(\alpha), m_z(\alpha)$	Inertia components of nodal point $\alpha$

## CHAPTER 1

### INTRODUCTION

#### 1.1 THE OBJECT OF THE STUDY

Earthquakes have always been one of the most disastrous natural enemies of civilization. Throughout history, several times, desperate ground shocks have shaken the crust of the earth and destroyed many cities and killed thousands of human lives.

Luckily, the occurrence of these strong ground motions is very rare, though with the increase in population of great cities and in the dimensions of the structures, the earthquakes are getting more and more disastrous. Because of the unpredictable nature of the earthquakes, the safety of civil engineering structures, particularly multi-storey buildings, chimneys, long span bridges and large dams, which are to be built in seismic zones, becomes of primary importance. Such types of structures must be designed in order to withstand an earthquake which might have a certain magnitude estimated in accordance with probabilistic considerations for the regions where the structure will be erected.

The destructive effects of earthquakes were very well recognised by civil engineers and many attempts have already been made to establish some design methods and safety criteria for the aseismic design of some certain types of structures. Among these structures, careful attention must be paid to arch dams, as these types of dams have very important specialities in many respects.

The primary function of a dam is the retention of a volume of water behind it. This function may be performed in various ways, namely by means of various types of dams.

The most commonly used dams are the gravity dams. Resistance to hydrostatic loading depends solely on its massive weight. The dam acts like a cantilever fixed at the foundation, independently of any valley walls. They are safe but not always economical.

Suitable physical and geological conditions of foundation sites may permit the hydrostatic load to be transmitted to the valley walls. In such cases, an arch dam can provide a water retaining structure requiring much less material than the equivalent gravity dam. This economy of material has made the arch dams very attractive and popular, so that the use of the arch dam form for dam design has increased considerably in recent times: five hundred of this type have been constructed in the last twenty five years.

The arch dams are designed in such a way that stresses developed in the structure are to be predominantly compressive under hydrostatic and gravity loads. This makes it possible to use unreinforced mass concrete in a very economical way. On the other hand, recent developments in design and construction techniques lead to arch dams which have very thin sections so that this tendency towards more economical dams has necessitated the assurance of the safety of that type of dam to a much higher degree; that is, some effects which could be neglected in earlier, more conservative designs, must be reconsidered in detail.

For this reason, in the design of the thin arch dams, in addition to those due to hydrostatic and gravity loads, it may be necessary to consider stresses due to temperature variation, ice formation, foundation deformation and earthquake loads. In particular, the shape of the modern arch dam is such that, if it is constructed in a highly seismic region, vibration amplitudes due to earthquake excitation may be sufficient to cause serious overstress or even collapse.

Nowadays, it is very often that engineers cannot avoid the necessity of constructing large arch dams in highly seismic regions, as the most prosperous water resources might fall in these regions. This fact leads the engineers towards detailed investigations on the response of arch dams to earthquakes in order to find out some suitable methods of analysis which are the main objects of this study.

## 1.2 GENERAL FACTORS ON ARCH DAM DESIGN

Although the theoretical basis for the dynamic analysis of structures under earthquake loading has been available for a long time, the behaviour of arch dams to earthquake excitation shows considerable difficulties because of the large number of parameters to be taken into account and because of the lack of knowledge about some of those parameters. Before discussing the details of these specific parameters, it would be useful to pay a little attention to the general factors acting on the design of arch dams.

For static analysis of arch dams the parameters encountered may be summarised as follows:

### (I) ARCH DAM:

#### (a) Geometrical properties of the dam:

Shape, curvature and thickness;

Auxiliary structures, openings, etc.

#### (b) Mechanical characteristics of the construction materials:

Modulus of elasticity, Poisson's ratio, ultimate strength,

coefficient of thermal expansion, creep properties,

permeability, shrinkage, reinforcement (if there is any).

(II) FOUNDATION ROCK:

(a) The shape of the valley

Angle of applied forces

(b) Geological and mechanical characteristics of the  
foundation rock:

Homogeneity or heterogeneity; isotropy or anisotropy;

the presence of joints, faults or other geological features;

initial stresses; long term geological movements;

deformability (in situ modulus of elasticity).

(III) APPLIED LOADS:

(a) Hydrostatic load:

Maximum level of the reservoir water.

(b) Gravity load:

Construction sequence, the shape of the dam itself.

(c) Thermal loads:

Temperature variation, solar radiation.

(d) Silt and ice loads.

(e) Uplift.

While most of these parameters can be defined accurately, some of them can only be roughly approximated. In addition to the approximations made for some parameters, the difficulties met in the analysis of such a complex problem lead the engineers to make some further assumptions in order to simplify the problem.

The detailed discussions of these parameters and assumptions have been introduced by ROCHA (ref.1) and will not be considered here.

In the case of dynamic analysis of arch dams some more parameters must be taken into consideration. These are the damping of the arch dam, the characteristics of the earthquake ground motion and the hydrodynamic effect of the

reservoir water. Each of these parameters plays an important role on the response of arch dams and shall be the main scope of this study.

### 1.3 REVIEW OF PREVIOUS STUDIES ON DESIGN OF ARCH DAMS TO RESIST EARTHQUAKES

The arch as a structural element has its origins in antiquity and dams curved in plan (the use of arch as a dam), have existed in various parts of the world for many centuries. However, as with structural theory in general, very little progress appeared for the analysis of structures of this type until the latter half of the nineteenth century. Since then, being parallel to the progress in the structural theory, construction techniques and design tools, many contributions and advances have been made in the analysis of arch dams. The detailed historical review of these advances has been given by RYDZEWSKI (ref.2) and a large bibliography has been introduced in reference 3. Herein only the major steps of these advances will be summarized and attention will be concentrated on the studies about the design of arch dams to resist earthquakes.

The early methods introduced for the analysis of arch dams consists of a vertical stack of independent horizontal arch units loaded by hydrostatic pressure and sliding freely upon one another. Such units were considered to be parts of complete cylindrical rings and the stresses were evaluated by means of the simple thin-cylinder formula. As usual the arch dams were tapered to the crest; for thicker arches near the base of the dam, thick-cylinder theory was sometimes applied. The design of such a structure demanded the choice of suitable dimensions for the height, radius and thickness of the dam. The first two of these dimensions were fixed within fairly close limits by the configuration of the site. The thickness at any level was governed by the permissible hoop stresses in the material.

Knowledge that the independent horizontal arches cannot describe correctly the behaviour of an arch dam which has vertical continuity led the

investigators to make some more attempts to introduce vertical action into the analysis of arch dams. The most successful attempt, which over many years has reached a state of considerable refinement, has been the introduction of 'Trial-Load Method' in 1921 (ref.4). This method considers the arch dam to be made up of an intersecting system of horizontal fixed-ended arches and vertical cantilever elements encastre at their bases. The applied load is then distributed between the two systems in such a way that the deflections in arch and cantilever at points of intersection become equal. In the early applications of this method, the division of the load between the arches and the cantilevers was carried out either by successive approximations or by direct solution of a set of simultaneous equations. After the United States Bureau of Reclamation began to take an active interest in this type of analysis, the accuracy of the method was improved by going beyond the simple congruence of radial displacement at the arch-cantilever nodes and by introducing the tangential displacements and torsion effects. The inclusion of these components of movement at each node made the resulting number of unknowns in the system become too large for direct solution. WESTERGAARD (ref.5) introduced a systematic process of successive trials to overcome this difficulty. Further researches have been made to refine and improve the method and so the trial-load method was found to be very satisfactory and has in fact survived, in various forms, to the present day.

Until 1956 few further advances were made in the analysis of arch dams, although existing methods, based almost without exception on trial-load type idealizations, were refined and improved. However, that year, the design of the Dokan Dam for Iraq led a group of British investigators to approach the arch problem from first principles. ALLEN, CHITTY, PIPPARD & SEVERN (ref.6) considered the dam to be a three-dimensional elastic body governed by the three-dimensional equations of elasticity, expressed in finite-difference

form, in terms of the components of displacement in cylindrical polar coordinates. The solution was carried out by a relaxation process. This paper simulated interest in arch dam analysis and subsequently several new methods, mainly based on shell theories, have been suggested by several authors. Most of these methods were edited and published by RYDZEWSKI (ref.7).

The progress of high-speed, large-capacity electronic computers has led the investigators to make new attempts to solve many problems which could not previously be solved because of the length of the necessary calculations and large number of unknowns involved. A recent proposal, so called "Finite Element Method" originated in the field of aircraft stress analysis (ref.8), is one of the methods which is suitable for computational analysis. This method, which was first applied by CLOUGH (ref.9) to plane stress analysis, is based on an idealization of the actual structure as an assemblage of a finite number of individual elements inter-connected at a finite number of nodal points. The stiffness matrices for the individual elements are derived and superposed to obtain the overall stiffness of the structure. This method is appropriate for continuum problems, like arch dams, and eliminates the necessity for arbitrary allocation of the stiffness to arches and cantilevers. The Finite Element method first introduced to the arch dam problem by CLOUGH & TOCHER (ref.10) together with ZIENKIEWICZ & CHEUNG (ref.11). Since then, many research workers have been interested in the application of finite element techniques to the arch dam analysis; however, the method has not been fully exploited yet, but the results recently introduced by several workers (ref.12,13,14) show its potential.

Parallel to the advances in the theoretical analysis, many valuable investigations have been made for the experimental analysis of arch dams and great progress has been achieved. Major contributions to model studies for

arch dams have come from ISMES of Italy (ref.15) and LNEC of Portugal (ref.16).

General model techniques of arch dams have been introduced in detail by the author of this thesis (ref.17) and shall not be reconsidered herein.

The advances in experimental and theoretical techniques which gave the designer a much fuller picture of the true behaviour of the arch dam under load has made it possible to minimize the volume of material used for the dam by structurally more efficient doubly curved shape which permits thinner sections. With increasingly sophisticated profiles of arch dams, more attention has been focused upon the loads which the structure might have to withstand. Among those loads, earthquake forces on the dam itself appear to have been considered for the first time in 1931 by MORRIS & PEARCE (ref.18). In 1933, WESTERGAARD (ref.19) published his classic paper on the water pressure produced on dams due to earthquake. Although this solution was limited to very wide, straight dams with vertical upstream face subjected to upstream acceleration, the effects of earthquakes on arch dams have for many years been analysed by this method with some modifications made by ZANGAR (ref.20) who has extended the work by means of an electric analog method to include the effects of various slopes on the upstream face of the dam. This method assumes that earthquake produces stresses by the acceleration of the mass of the dam and by changes in water pressure of the faces of the structure. The inertia forces are expressed as mass times acceleration; the hydrodynamic pressures are found to be the same as if a body of water confined between a certain parabola and the face of the dam were forced to move with the dam, while the rest of the reservoir remained inactive. The inertia forces, calculated in that manner, are then applied to structure as statical loads.

This method is valid if resonance does not occur in the structure. In an elastic structure, such as a thin arch dam, it is reasonable to assume that the ground motion is capable of producing resonance in the dam. This fact leads to the conclusion that the earthquake loadings are dynamic loadings and must be treated as such. On this premise a method has been developed in U.S. Bureau of Reclamation to determine the dynamic loadings based on the earthquake response spectra concept (ref.21). These loadings may then be used with the trial-load analysis to find the stresses in the structure caused by vibration. A similar method has been presented by SERAFIM & PEDRO (ref.22) which is based on the flexibility matrix obtained by an arch-cantilever radial adjustment.

The finite element technique has been used for the first time in earthquake studies of arch dams by TAYLOR (ref.23) who has made a comprehensive contribution on the response of arch dams to earthquakes.

The problem of hydrodynamic effect has also been investigated by many research workers. Recently theoretical expressions have been derived (ref.24) for the hydrodynamic pressure generated by earthquakes on arch dams in various shapes of valley. This work has been extended and an experimental method has been developed which uses an electric potential analogue (ref.25); however, the assumptions necessary to establish this analogy limit its applications to some extent.

Model testing is a standard technique in the static analysis of arch dams, although difficulty is sometimes encountered in loading a large scale model. These difficulties are amplified in testing models under seismic loading. The first experimental seismic model studies carried out at LNEC of Lisbon, on the design of the Tang-e-Soleyman Dam, showed the possibilities and also the difficulties of seismic model testing (ref.26). Recently such

studies have been carried out successfully at the Royal Aircraft Establishment, Farnborough (ref.27).

Some interesting results of experimental tests performed on a prototype arch dam have been introduced by OKAMOTO & TAKAHASHI (ref.28), who achieved resonant vibrations in a full scale arch dam and determined the natural frequencies and mode shapes as well as the damping ratios of the structure. These results show that the natural frequency of the system is considerably lower at high water levels than when the reservoir is empty. This is the first full scale experimental evidence of the "added mass effect" predicted by WESTERGAARD (ref.19).

Since the early recognition of the fact that the earthquake loadings are dynamic loadings and must be treated as such, the attention of the investigators has been drawn to the behaviour of the ground motion and so many attempts have been made to determine the characteristics of strong-motion earthquakes. Among those investigators, HOUSNER (ref.29) has presented a large amount of valuable results, on which most of the response calculations are based.

The first logical step for the design is to assume the earthquake excitation as a deterministic transient phenomena and to calculate the responses by means of the, so called, step-by-step integration method (ref.30). In this method a recorded accelerometerogram of a particular past earthquake should be used as input forcing function; however, the calculations involved are tedious and show considerable difficulty. To avoid the tedious part of the calculations, another approximate method, namely "Response Spectrum Method" has been introduced (ref.31) which has, up to date, been applied to most of the earthquake resistant design of structures.

Recently, the advances in the theory of random vibrations has made it possible to assume the random character of the earthquake ground motion (ref.32), and research studies in the direction of the concepts of the probabilistic design have been under progress.

#### 1.4 CONCEPTS OF THE PROBABILISTIC DESIGN OF ARCH DAMS TO RESIST EARTHQUAKE EXCITATION.

The response calculation of an arch dam at a particular seismic region, due to a future earthquake ground motion is indeterminate because the earthquake ground motions are completely unpredictable and random in nature.

The intensity of an earthquake shock on a structure depends upon:

- the amount of energy released during the tremor,
- the focal depth,
- distance from the epicenter,
- duration of the ground motion,
- geological features of the site of the structure,
- direction of earthquake shock waves.

Even for a small seismic region, as the above parameters differ for each occurrence of an earthquake, the ground motion has different characteristics which never again repeat exactly.

But, by means of statistical and probabilistic considerations, it is possible to obtain an estimated value for the most probable characteristics of the earthquake activity in a particular region. Although the scarcity of quantitative earthquake data at present permits only tentative estimations for most regions of the world, earthquake studies have taken place in those regions worst affected and recording of ground acceleration of strong earthquakes has been in progress in these regions.

Most of the research workers, concerning the dynamic analysis of civil engineering structures subjected to earthquake ground excitation, have used an acceleration time history of a recorded past earthquake for response calculations, assuming that the earthquake excitation is a deterministic transient phenomenon. As is mentioned above, the earthquake ground motions are completely unpredictable and random in nature. For this reason, the calculated responses to a past earthquake cannot be used for design purposes of structures to withstand future earthquakes, and it is necessary that the phenomena having random nature must be described in terms of probability statements and statistical averages.

To satisfy the requirements of probabilistic design, it is necessary to develop a method which uses random vibration theory for the response calculations of arch dams subjected to earthquake excitation. Such a method needs mainly the dynamical characteristics of the arch dam and the acceleration power spectral density of the representative earthquake ground motion.

The necessary dynamical characteristics of the arch dams are the natural frequencies, corresponding mode shapes and the damping ratio. The first two characteristics can be obtained theoretically by means of matrix eigenvalue analysis. As the arch dams have generally very complicated shapes and are constructed on irregular foundation valleys, these analyses possess considerable difficulties; however, the use of three-dimensional finite element techniques and the existence of large capacity fast computers recently made the solution of these analyses possible. On the other hand, hydrodynamic effect of the water in the reservoir behind the dam influences the dynamical characteristics of the dam considerably. Exact solution of this effect still does not exist, and the most practical solution seems to be the electrical potential analogy. Although the results of this analogue

need to be incorporated with the general matrix eigenvalue problem in the analysis for the reservoir in full condition..

The response of an arch dam to earthquake excitation is very dependent on the damping present; unfortunately, there is still a lack of reliable information about the magnitude of the damping present in completed dams. More experimental research must be made on prototype structures to predict the damping ratio of the arch dams.

The acceleration power spectral density of the representative earthquake ground motion can be predicted by means of statistical averages and probabilistic considerations applied to the acceleration records of previous earthquakes which have occurred in the region where the structure is to be built. As the arch dams are to be built for a long service life, the extreme value theorem might be applied to estimate the most probable maximum mean square value of the ground acceleration for the life period of the structure.

The statistical analysis of earthquake acceleration records show that the ground motions have nonstationary behaviour. However, at this stage of knowledge about nonstationary random processes, the assumption that the earthquake ground motion is to be a stationary random motion is justifiable for the response calculation of arch dams.

The only class of structures considered comprehensively in previous earthquake studies has been the multi-storey building frame. This type of structure is usually capable of resisting local tensile overstress and has a high reserve capacity for energy absorption by means of inelastic deformation. An arch dam may have only a very small amount of reinforcing steel and does not possess this capacity to resist tensile overstress. Furthermore, the resulting cracks could be disastrous in a water retaining

structure. For these reasons, in the design of an arch dam to resist earthquakes, it must be ensured that the structure remains in the elastic region of stress under the earthquake loading.

#### 1.5 PREVIEW OF THE CONTENT OF THE STUDY

The complete evaluation of the effect of an earthquake on a structure generally consists of the following three main parts :

- (a) The determination of the stiffness and inertia properties of the structure.
- (b) The calculation of the natural frequencies and the corresponding mode shapes of the structure.
- (c) The evaluation of the response of the structure to a given earthquake ground acceleration, that is, the calculation of the maximum probable displacements and stresses in the duration of the earthquake.

The determination of the stiffness properties of an arch dam is the primary problem to be solved for both static and dynamic analysis of the structure. This problem is to be discussed in Chapter 2 of this thesis in detail. The most promising and satisfactory way of obtaining the stiffness characteristics of an arch dam seems to be the use of three-dimensional finite element method. This approach, using simple tetrahedral elements has been used in all of the analysis presented in this thesis.

The determination of the inertia properties of an arch dam consistent with the stiffness properties is presented in Chapter 3. The calculation of the natural frequencies and the corresponding mode shapes of an arch dam, namely the solution of the matrix eigenvalue problem, is also to be included in this

Chapter in detail. The effects of the hydrodynamic forces of the water in the reservoir and the flexibility of the foundation are also to be discussed.

Chapter 4 contains the general theory of forced vibration of arch dams to earthquake excitation. The applicability of some available methods is to be discussed and the theory of random vibrations is to be presented. Providing that the natural frequencies and mode shapes of the structure are already known and the acceleration power spectral density of a representative earthquake is given, some methods to calculate the responses of arch dams are to be introduced.

The influence of various parameters on the response of arch dams to earthquakes is to be investigated widely in Chapter 5. Among these parameters special attention is to be paid to the damping ratio of the structure, direction and velocity of earthquake waves, spectral intensity and duration of the ground motion and the flexibility of the foundation. The condition of the reservoir water level is also to be considered. In this Chapter the response is defined in terms of displacement amplitudes.

The calculation of stresses developed in the arch dam during an earthquake is the primary object of this study. The achievement of this object, by means of the combination of the results obtained in previous Chapters, is to be explained in Chapter 6. More attention is to be paid to the calculation of most probable maximum stresses and the results obtained for reservoir in both empty and full conditions are to be presented and compared with the results of hydrostatic analysis.

In Chapter 7, attention is to be drawn to the importance of the choice of the representative earthquake whose acceleration power spectral density should be used as input in random response calculations. Suggestions are to be made for seismic regionalisation and the use of extreme value

theory for the estimation of most probable characteristics of the expected earthquake during the service life of the arch dam in the region where it is to be built. Chapter 7 will end with a summary of the methods presented which includes a review of the important results obtained.

All the numerical results introduced throughout the thesis are to be calculated for a representative arch dam. The arch dam chosen for this investigation is 120 m. high, double curvature arch dam, which is one of the selected types of arch dams by C.E.R.A. (ref.33) and designated as "Type 5". Specifications of this dam shall be given in Chapter 2.

The specifications of computer programs which have been prepared and used throughout the study are to be presented in a separately bound Appendix B. However, general programming concepts are to be included in the text wherever necessary.

## CHAPTER 2

### STATIC ANALYSIS OF ARCH DAMS

#### 2.1 INTRODUCTION

The determination of the stiffness properties of the structure is the primary problem to be solved for both static and dynamic analysis of any kind of structure. Once these properties of the structure are known, the behaviour of the structure under any kind of defined static loads can be calculated by means of well established computational methods.

In this Chapter, the determination of the stiffness properties of arch dams by means of the so-called "Finite Element Technique" and also the static analysis of an arch dam under hydrostatic and gravity loadings are to be presented. Simple tetrahedral elements are chosen for all the analysis contained in this study. The advantages and disadvantages of the application of this type of elements and also the difficulties met in the analysis and calculations shall be discussed. The results obtained shall be compared with those existing in the literature.

#### 2.2 FINITE ELEMENT METHODS

While it is relatively simple to write down the static or dynamic differential equations governing the behaviour of continuum systems, the exact solution of real problems is seldom possible. Particularly, this fact is recognised for the case of shell structures where the classical methods of structural analysis can only be applied to a small class of practical shell structures which possess constant thickness and have idealized boundary conditions. Unfortunately, all arch dams fall outside this narrow category and it is necessary to establish some satisfactory numerical solutions in

order to reduce the infinite freedoms of such a continuum to a finite number by means of replacing the distributed forces and continuous internal restraints by equivalent discrete actions.

In the physical approach of this discretisation, the structure can be considered as an assembly of a finite number of discrete elements interconnected at a finite number of nodal points and the attention then focussed on the unknown values of displacement (or force) at these nodal points where such elements are joined. The structural analysis of the individual elements and the assembled structure can be formulated in the notation of matrix algebra, in order to utilize the facilities of an electronic digital computer.

Matrix methods of structural analysis have been developed during the last fifteen years in connection with the stress analysis of highly complex aircraft structures (ref.8). As in the case of conventional structural analysis, matrix methods may also be divided into two groups, namely those formulated in terms of unknown forces and those formulated in terms of unknown displacements. ARGYRIS has developed the general theory with both forces and displacements as unknowns (ref.34). However significant differences exist in the detailed application of the methods, both of these methods are proved to be analogues and have been used in the analysis of aircraft structures.

In the field of civil engineering, considerable attention has been given to the analysis of static plate and shell problems by the displacement method and a large amount of development has been achieved. In the early studies, the method has been applied to the analysis of gravity dam sections regarded as a plane stress problem (ref.9) and thin arch dams (ref.10,11) with either single or double curvature. Since then, many engineers have been interested in the application of finite element techniques to the arch dam analysis and many valuable results have already been obtained by several research workers (ref.12,13,14).

The general procedure for analysing a structure by the finite element techniques, which has been explained comprehensively by ZIENKIEWICZ & CHEUNG (ref.35), may be summarised as follows :

- (1) The idealization of the structure into a finite number of individual elements, interconnected at a finite number of nodal points.
- (2) The evaluation of the element stiffness properties.
- (3) The structural analysis of the assemblage.

In the following paragraphs, this procedure shall be applied to the analysis of an arch dam by using three-dimensional finite elements.

### 2.3 IDEALIZATION OF AN ARCH DAM INTO A FINITE NUMBER OF THREE-DIMENSIONAL ELEMENTS

2.3.1 The choice of an adequate type of element for a certain type of structure is the first important step in the finite element methods. The array of elements must be chosen in such a way that the assembled structure is to be equivalent to the actual structure in all relevant respects.

A structural idealization comprising elements of arbitrary shape and thickness is perfectly acceptable theoretically and seems more plausible for the three-dimensional stress systems within arch dams. For thin arch dams, where the ratio of thickness to radius is less than one tenth for most of the dam, the structure may be represented as an array of plate-like elements of different thickness. Conditions of compatibility and equilibrium may be written fairly easily for rectangular plate elements, but this shape is not compatible with the geometric configuration of double curvature dams. Triangular shaped elements seem attractive from the point of view that they can describe any curved surface, provided a sufficiently large number are taken. However, the problems of displacement compatibility along the edges

of general triangular shaped elements give rise to some difficulties. Unless continuity of slope, as well as lateral displacement, is maintained across all sides there is no assurance that the analysis will converge to the correct solution with increase of the number of elements (ref.10).

Nevertheless, the first application of the finite element method to arch dam analysis has been performed by using rectangular plate elements (ref.11) and the results obtained have encouraged the investigators to extend their research on the other types of elements which might give better representation and better results.

These researches may be divided into two main groups, namely "developing plate-like elements" and "introducing three-dimensional elements".

The developments on the plate-like elements, beginning with constant thickness rectangular (ref.11) and constant thickness triangular (ref.10) elements, has been followed by general triangular elements in which the thickness is permitted to vary linearly between nodes. This type of element has recently been presented by DUNGAR & SEVERN and been applied both to static and dynamic analysis of arch dams successfully (ref.14,36).

The simplest three-dimensional element satisfying the basic requirements is the tetrahedron with four nodes and twelve degrees of freedom, first introduced by GALLAGHER (ref.37) and used by MELOSH (ref.38) and later by ARGYRIS (ref.39). As a next stage of the development, ARGYRIS recently proposed a tetrahedral element with ten nodes and thirty degrees of freedom (ref.40, 13).

An alternative family of elements has been developed by ERGATOUDIS et al (ref.41) from an eight cornered brick. Once again various degrees of freedom have been assigned. In the simplest member of this family the brick like element has eight nodes and twenty four degrees of freedom, the next one has

twenty nodes and sixty degrees of freedom, and recently a brick element with thirty two nodes and ninety six degrees of freedom has been used (ref.12). The latest development on the brick-like element has been, so called, the "isoparametric" curved brick element which has been introduced by the same group of investigators (ref.12). By means of using curvi-linear coordinates, curved brick elements with eight, twenty and thirty two nodes have been used for the analysis of arch dams.

2.3.2 In this present study the simple tetrahedral element, with four nodes (four corners) and twelve degrees of freedom, has been chosen for all the analysis of arch dams.

In spite of some necessary simplifying assumptions made for the numerical integrations involved in calculation of the element stiffness matrix, many authors have claimed that more complex elements give more accurate results for the same number of unknowns. Although the recent results obtained by the same authors have provided enough evidence to prove this claim, it is still anticipated that the use of simpler elements can also give satisfactory results for most of the analysis.

In the early beginning of this research study (August 1966), the only three-dimensional element which existed in the literature and used for the static analysis of arch dams was the simple tetrahedral element. The tetrahedron with ten nodes and the brick-like elements were all under development. As the main object of this study is the application of the finite element technique to the vibration problems of arch dams, but not to investigate some new types of elements, the most advanced element at that time, which is the simple tetrahedral element, was chosen for this study.

2.3.3 In order to idealize an arch dam as an assemblage of tetrahedral elements, the first stage is to divide the dam into brick-like building blocks. To fit the irregular shape of the structure, which is mainly near the sloped valley sides, triangular prisms are used. Such a division is shown in Figure 2.1 for one half of a symmetrical doubly curved arch dam.

The second stage is to divide the brick-like blocks and triangular prisms into tetrahedral elements. As there are several possibilities for constructing a brick-like block and a triangular prism by using tetrahedral elements, special care must be taken in this stage.

Generally, there are two possibilities to construct a brick-like block:

- (a) as an assemblage of five tetrahedrons,
- (b) as an assemblage of six tetrahedrons.

There are two possible combinations of using five tetrahedrons as shown in Figure 2.2; these combinations shall be denoted by "A-type idealizations". The assemblage of one of these combinations is shown in Figure 2.3.

The possible combinations of using six tetrahedrons can be divided into two groups. The first group is consisted of four possibilities as shown in Figure 2.4, and shall be denoted by "B-type idealizations". These four idealizations can be considered as a complete set which shall be used in calculations. The assemblage of one of these combinations is shown in Figure 2.5.

The second group of combinations with six tetrahedrons has twelve possibilities as shown in Figure 2.6 and shall be denoted by "C-type idealizations". As it can be seen, the three combinations shown in each row of Figure 2.6 have the same external pattern, but the internal diagonal is changed. While the four rows have all possible external patterns, this

figure is so arranged that, in each column there are all four possible internal diagonals. In that way, the four combinations shown in each column can be considered as a complete set, which shall be used in calculations. The assemblage of one of these combinations is shown in Figure 2.7.

A triangular prism can always be constructed by means of three tetrahedral elements; however, there are six possible combinations as shown in Figure 2.8.

In the assemblage of the whole structure by means of the types of idealizations mentioned above, to ensure the continuity of the structure, at all interfaces the diagonals should be so arranged that all the sides of adjacent elements coincide. This condition can easily be satisfied by choosing only one of the possible combinations of type-B or C idealizations, for all the structure, as the diagonals at the opposite sides run in the same direction.

For the A-type idealizations, as the diagonals at the opposite sides run in the opposite directions, the condition of continuity can only be satisfied if both of the A-type idealizations are used for adjacent blocks simultaneously.

As it is always possible to find a triangular prism which fits the adjacent idealized blocks, there is no difficulty in choosing one of the six possible combinations for triangular prisms shown in Figure 2.8, so that the condition of continuity is satisfied.

Another important point to be mentioned in the idealization of a solid structure by means of tetrahedral elements is that care must be taken to ensure that the elements do not take thin or needle-like shapes.

Before comparing the applicability and advantages of types of idealizations introduced in this section, the general theory of finite element techniques and the application of this theory to simple tetrahedral elements shall be introduced in the preceding sections, then in the light of the results of these sections the various types of idealizations shall be discussed.

#### 2.4 THEORETICAL BASIS OF FINITE ELEMENT METHODS, DERIVATION OF ELEMENT STIFFNESS PROPERTIES

The elastic properties of an element are represented by a matrix  $[k]$  which is referred to as the "element stiffness matrix". The external generalized forces  $\{S_i\}$ , which are applied to the nodal points of the element and the generalized displacements  $\{U_i\}$  of the nodal points, are related by means of the element stiffness matrix as

$$\{S_i\} = [k] \cdot \{U_i\} \quad \dots (2.1)$$

Providing the element stiffness matrix is known, it is easily possible to determine either the external forces or the nodal displacements whichever are unknown and the others are given.

For the derivation of the element stiffness matrix, the first step is to assume certain deformation patterns for the generalized displacements  $\{U\}$  of any element. Any assumed displacement function should satisfy certain requirements in order to ensure convergence to the true solution as the size of the element is reduced (ref.42), so the deformation patterns should be chosen in such a manner that the assumed displacements must be continuous over the elements; must maintain continuity with displacements of adjacent elements. The displacements along any side of the element must be selected so that

they depend only on the displacements at the nodes bounding the side. The displacement function must be a linear function of the generalized displacements; that is, in the displacement expression the coefficients of the nodal displacements must be non-dimensional and the coefficients of nodal rotations must involve a length unit to satisfy dimensional requirements. Finally, the displacement pattern should allow rigid body displacements. It is generally advantageous to assume as many deformation patterns as there are nodal degrees of freedom. The generalized displacements are thus written in the form

$$\{U\} = [N(x,y,z)] \{A\} \quad \dots (2.2)$$

where  $[N(x,y,z)]$  is a matrix of functions defining the displacements  $\{U\}$ ; and  $\{A\}$  is a column matrix of constants. These constants may be determined by introducing the nodal co-ordinates into equation (2.2), then the generalized nodal displacements  $\{U_i\}$  are given by

$$\{U_i\} = [C] \{A\} \quad \dots (2.3)$$

where  $[C]$  is a square matrix consisting of the nodal point coordinates.

The constants  $\{A\}$  can be obtained from equation (2.3) by inverting  $[C]$  matrix as follows

$$\{A\} = [C^{-1}] \{U_i\} \quad \dots (2.4)$$

Now, the internal element strains  $\{\epsilon\}$  may also be expressed in a similar form as the generalized displacements

$$\{\epsilon\} = [B(x,y,z)] \{A\} \quad \dots (2.5)$$

where the matrix  $[B(x,y,z)]$  is a differential of the matrix  $[N(x,y,z)]$ .

Substituting equation (2.4) into equation (2.5)

$$\{\epsilon\} = [B(x,y,z)] [C^{-1}] \{U_i\} \quad \dots (2.6)$$

is obtained.

The internal element stresses  $\{\sigma\}$  are given by the material stress-strain relationships, as

$$\{\sigma\} = [D] (\{\epsilon\} - \{\epsilon_0\}) \quad \dots (2.7)$$

where  $[D]$  is a matrix of material constants and  $\{\epsilon_0\}$  is included for representing the initial strains (thermal effects, etc.). By substituting equation (2.6) into equation (2.7)

$$\{\sigma\} = [D] [B(x,y,z)] [C^{-1}] \{U_i\} - [D] \{\epsilon_0\} \quad \dots (2.8)$$

is obtained.

The internal virtual work  $W_I$ , associated with the virtual strains  $\{\bar{\epsilon}\}$  is given by

$$W_I = \int_V [\bar{\epsilon}]^T \{\sigma\} dV \quad \dots (2.9)$$

where  $V$  is the volume of the element. Introducing equation (2.6) and (2.8) into equation (2.9), it becomes:

$$\begin{aligned} W_I &= \int_V [\bar{U}_i]^T [C^{-1}]^T [B(x,y,z)]^T [D] [B(x,y,z)] [C^{-1}] \{U_i\} dV \\ &= [\bar{U}_i]^T [C^{-1}]^T \int_V [B(x,y,z)]^T [D] [B(x,y,z)] dV \cdot [C^{-1}] \{U_i\} \quad \dots (2.10) \end{aligned}$$

where  $\{\bar{U}_i\}$  are the virtual nodal displacements associated with the virtual strains  $\{\bar{\epsilon}\}$ .

The external work  $W_E$  done during the virtual displacements  $\{\bar{U}_i\}$  is

$$W_E = [\bar{U}_i]^T \{S_i\} \quad \dots (2.11)$$

where  $\{S_i\}$  are the generalized external nodal forces corresponding to the nodal displacements  $\{U_i\}$  as given in equation (2.1).

Applying the theorem of virtual work gives

$$W_E = W_I \quad \dots (2.12)$$

that is

$$[\bar{U}_i]^T \{S_i\} = [\bar{U}_i]^T [C^{-1}]^T \int_V [B(x,y,z)]^T [D] [B(x,y,z)] dV. [C^{-1}] \{U_i\} \quad \dots (2.13)$$

Now, by applying a unit virtual displacement at each of the nodal degrees of freedom in sequence

$$\{S_i\} = [C^{-1}]^T \int_V [B(x,y,z)]^T [D] [B(x,y,z)] dV. [C^{-1}] \{U_i\} \quad \dots (2.14)$$

is obtained. The comparison of equations (2.1) and (2.14) gives the expression for the element stiffness matrix as

$$[k] = [C^{-1}]^T \int_V [B(x,y,z)]^T [D] [B(x,y,z)] dV. [C^{-1}] \quad \dots (2.15)$$

## 2.5 ASSUMED DISPLACEMENT FUNCTIONS FOR THE SIMPLE TETRAHEDRAL ELEMENT

For the derivation of the stiffness matrix for the simple tetrahedral element shown in Figure (2.9) which has four nodal points (in this case four corners) each of them allowed three degrees of freedom, the generalized displacement functions assumed are that :

$$\left. \begin{aligned} u &= A_1 + A_2x + A_3y + A_4z \\ v &= A_5 + A_6x + A_7y + A_8z \\ w &= A_9 + A_{10}x + A_{11}y + A_{12}z \end{aligned} \right\} \quad \dots (2.16)$$

These equations satisfy all of the necessary requirements except the continuity of slopes between adjacent elements on the free surfaces of the structure. However, by using large number of elements, that is decreasing the dimensions of elements, the effect of discontinuity of slope between

adjacent elements can be minimized.

By using the assumed displacement functions given in equation (2.16), the element stiffness matrix for the tetrahedral element can be derived by suitable interpretation of the basic matrices involved. This derivation is given in Appendix (A.1) explicitly.

## 2.6 EQUILIBRIUM OF COMPLETE STRUCTURE

Having idealized the structure as an assemblage of finite elements and determined the element stiffness properties, the extension of the process to the complete structure can be achieved by considering the equilibrium of the complete structure, that is the equilibrium of the internal and external applied forces at each nodal point.

The internal forces due to the element  $i$  are given by equation (2.1) as

$$\{S_i\} = [k_i] \{U_i\} \quad \dots (2.17)$$

To consider the equilibrium of the complete structure, it is necessary to form the overall stiffness matrix for the whole structure. As it has been shown in Appendix (A.1) that, in the finite element method adopted for tetrahedral elements, all of the elements can be defined with respect to a global coordinate system and there is no need to use any other local coordinate system for each element. So that the transformation process, which is necessary for many other types of elements is avoided. This property leads to a very simple procedure to form the overall matrices; which consists of only transferring the coefficients of the stiffness matrix of each element to the appropriate locations of the overall matrix and then adding each other algebraically. This addition can best be illustrated if equation (2.17) is rewritten in terms of a typical element  $q$  :

$$\begin{Bmatrix} S_i^{(q)} \\ S_j^{(q)} \\ S_k^{(q)} \\ S_\ell^{(q)} \end{Bmatrix} = \begin{bmatrix} k_{ii}^{(q)} & k_{ij}^{(q)} & k_{ik}^{(q)} & k_{i\ell}^{(q)} \\ k_{ji}^{(q)} & k_{jj}^{(q)} & k_{jk}^{(q)} & k_{j\ell}^{(q)} \\ k_{ki}^{(q)} & k_{kj}^{(q)} & k_{kk}^{(q)} & k_{k\ell}^{(q)} \\ k_{\ell i}^{(q)} & k_{\ell j}^{(q)} & k_{\ell k}^{(q)} & k_{\ell\ell}^{(q)} \end{bmatrix} \begin{Bmatrix} U_i^{(q)} \\ U_j^{(q)} \\ U_k^{(q)} \\ U_\ell^{(q)} \end{Bmatrix} \quad \dots (2.18)$$

where in terms of arbitrary nodal points  $m$  and  $n$ ,  $S_m^{(q)}$  and  $U_n^{(q)}$  are vectors of the form

$$S_m^{(q)} = \begin{Bmatrix} S_x \\ S_y \\ S_z \end{Bmatrix}_m^{(q)} \quad \text{and} \quad U_n^{(q)} = \begin{Bmatrix} u \\ v \\ w \end{Bmatrix}_n^{(q)} \quad \dots (2.19)$$

and the stiffness coefficient  $k_{mn}^{(q)}$  is a 3 x 3 submatrix

$$k_{mn}^{(q)} = \begin{bmatrix} k_{xx} & k_{xy} & k_{xz} \\ k_{yx} & k_{yy} & k_{yz} \\ k_{zx} & k_{zy} & k_{zz} \end{bmatrix}_{mn}^{(q)} \quad \dots (2.20)$$

The term  $k_{mn}^{(q)}$  represents the forces developed on element  $q$  at nodal point  $m$  due to unit displacements at nodal point  $n$ . Therefore, the overall stiffness term,  $K_{mn}$ , for the complete structure, which is the sum of the forces acting on all elements at nodal point  $m$  due to unit displacements at nodal point  $n$ , is given by

$$K_{mn} = \sum_q k_{mn}^{(q)} \quad \dots (2.21)$$

Obviously,  $K_{mn}$  exists only if  $m$  equals  $n$ , or if  $m$  and  $n$  are adjacent nodal points in the physical system.

Now, considering equilibrium of forces at each nodal point, the overall equilibrium equations are obtained as follows :

$$\{ S \} = [K] \{ U \} \quad \dots (2.22)$$

where  $[K]$  is the overall stiffness matrix for the complete structure.

For the application of the boundary conditions, equation (2.22) can be partitioned as :

$$\begin{Bmatrix} S_a \\ S_c \end{Bmatrix} = \begin{bmatrix} K_{aa} & K_{ac} \\ K_{ca} & K_{cc} \end{bmatrix} \begin{Bmatrix} U_a \\ U_c \end{Bmatrix} \quad \dots (2.23)$$

where the suffix  $c$  denotes the nodal points on the boundaries which have prescribed displacements, and the suffix  $a$  denotes all the other points which the external forces  $S_a$  are applied.  $U_a$  and  $S_c$  are the unknown displacement and reactions, respectively.

If the boundary nodal points are assumed to be fixed, then the prescribed boundary displacements become :

$$\{ U_c \} = 0 \quad \dots (2.24)$$

Introducing these boundary conditions, equation (2.23) can be divided into two equations :

$$\{ S_a \} = [K_{aa}] \{ U_a \} \quad \dots (2.25)$$

$$\{ S_c \} = [K_{ca}] \{ U_a \} \quad \dots (2.26)$$

Under some given external loading  $\{S_a\}$ , the unknown nodal point displacements  $\{U_a\}$  can be determined from equation (2.25); then equation (2.26) may be used to calculate the reactions on the part of the boundary along which the displacements have been prescribed.

## 2.7 SOLUTION OF EQUILIBRIUM EQUATIONS

The solution of the simultaneous equations given in equation (2.25) can be evaluated by a simple matrix manipulation :

$$\{U_a\} = [K_{aa}^{-1}] \{S_a\} \quad \dots (2.27)$$

This manipulation involves the inversion of the overall stiffness matrix. As the matrix  $[K_{aa}]$  is positive definite, its inverse can always be obtained by means of standard matrix operations.

For problems having a small number of degrees-of-freedom, this direct solution gives very satisfactory and quick results. However, in finite element analysis, for most practical problems, equation (2.25) represents a system of several hundred equations. In these cases, three major difficulties arise in the direct solution of such a large set of equations :

- (a) If  $N$  is the number of equations, then the storage required by the overall stiffness matrix is equal to  $N^2$ ;
- (b) The computing time required for solution is proportional to  $N^3$ ;
- (c) The inversion of high order matrices involves uncontrolled rounding-off errors, so the accuracy of the solution may be a serious problem.

Even on a large computer, these problems still exist; however, these difficulties may only be minimized by the use of iterative methods.

The specific iterative method used in this study, for the static analysis, is a modification of the well-known Gauss-Seidel iteration procedure (ref.43) which has been developed by WILSON (ref.44) and applied to two dimensional structural analysis. This method is adopted for three dimensional finite element technique and applied to static analysis of arch dams.

This iteration procedure, when applied to equation (2.27), involves the repeated calculation of new displacements from the equation

$$U_n^{(r+1)} = K_{nn}^{-1} \left[ S_n - \sum_{i=1, n-1} K_{ni} U_i^{(r+1)} - \sum_{i=n+1, N} K_{ni} U_i^{(r)} \right] \quad \dots (2.28)$$

where  $n$  is the number of the unknown displacement and  $r$  is the cycle of iteration. This procedure can be applied simultaneously to three components of displacement at each nodal point, therefore  $U_n$  and  $S_n$  become vectors with  $x$ ,  $y$  and  $z$  components, equation (2.19), and the stiffness coefficients are expressed in the  $3 \times 3$  submatrix form of equation (2.20).

The rate of convergence of the Gauss-Seidel procedure can be greatly increased by the use of an over-relaxation factor (ref.45). In order to apply this factor firstly the change in the displacement of nodal point  $n$  between two successive cycles of iteration is calculated from :

$$\Delta U_n^{(r)} = K_{nn}^{-1} \left[ S_n - \sum_{i=1, n-1} K_{ni} U_i^{(r+1)} - \sum_{i=n+1, N} K_{ni} U_i^{(r)} \right] - U_n^{(r)} \quad \dots (2.29)$$

then, the new displacement of nodal point  $n$  is determined from the following equation

$$U_n^{(r+1)} = U_n^{(r)} + \beta \cdot \Delta U_n^{(r)} \quad \dots (2.30)$$

where  $\beta$  is the over-relaxation factor.

The selection of an over-relaxation factor, which gives the best convergence, depends on the characteristics of the particular problem. However, experience has indicated that for most three-dimensional structures, the optimum over-relaxation factor is between 1.85 and 1.95.

The detailed formulation and the physical interpretation of this method are given in Appendix (A.2).

The objections, suggested against the direct matrix inversion method involving large amount of equations, can be minimized by using the above mentioned iterative method so that :

- (a) In this case, the stiffness matrix of equation (2.27) is no longer necessary to be fully populated. Since the complete stiffness matrix contains many zero elements, only the non-zero elements are evaluated and retained; therefore it is possible to treat large systems without exceeding the storage capacity of the computer.
- (b) By means of a good choice of the over-relaxation factor, the computing time can be reduced to minimum, in order to obtain the solution in any desired accuracy.
- (c) As each cycle of iteration is an independent procedure, the rounding off errors involved in one cycle will not accumulate during the next cycle; on the contrary, these errors might be assumed as unbalanced forces, which are to be eliminated in the preceding cycles.

For problems involving ill-conditioned matrices, this method is particularly recommended.

## 2.8 BOUNDARY CONDITIONS

Solving the simultaneous equations of equation (2.22) by means of direct matrix inversion method, for the application of the boundary conditions, the overall matrix can be partitioned as shown in section 2.6 with equation (2.23); then the rows and columns corresponding to the prescribed boundary displacements are simply deleted and the constrained matrix  $K_{aa}$  is obtained.

In case of the iteration method described in section 2.7, the application of boundary conditions requires more attention.

In fact, equation (2.30) which gives the successive equilibrium position of the nodal point after each cycle of iteration, is valid for all nodal points which are free to move in all of the x, y and z directions; however, in order for it to be applied to boundary nodal points, the flexibility coefficients of  $K_{nn}^{-1}$  submatrix must be modified to account for the specific types of restraints which may exist. Since these flexibility coefficients are independent of the cycle of iteration, this modification is performed before the start of iteration.

The forces and displacements associated with the application of equation (2.30) are illustrated in Figure 2.10 for a general boundary point that is constrained in every direction. The unbalanced forces, X, Y and Z are determined from equation (A.2.7) of Appendix (A.2).

The unknown reaction components are represented by  $R_x, R_y$  and  $R_z$ . Applying equation (2.29) to this nodal point, the displacements  $\Delta U_n$  can be expressed

in the form

$$\begin{Bmatrix} \Delta u \\ \Delta v \\ \Delta w \end{Bmatrix}_n = \begin{bmatrix} K_{nn}^{-1} \end{bmatrix} \begin{Bmatrix} X - R_x \\ Y - R_y \\ Z - R_z \end{Bmatrix}_n \quad \dots (2.31)$$

where  $K_{nn}^{-1}$  is the 3 x 3 flexibility submatrix of the nodal point  $n$ .

Obviously for points fixed in all directions, where  $\Delta u = \Delta v = \Delta w = 0$ , all of the nine coefficients of the modified flexibility matrix will be equal to zero.

If the boundary nodal point is allowed to move one or two of the three displacement directions and is not allowed to move in the other directions, in that case, the displacement terms of equation (2.31) relating to the fixed directions are taken as zero and only the corresponding reaction terms are retained. For example, if the nodal point is allowed to move in the plane of  $yz$ , i.e. is fixed in  $x$  direction, then  $\Delta u = 0$  and only the  $R_x$  reaction exists, equation (2.31) becomes

$$\begin{Bmatrix} 0 \\ \Delta v \\ \Delta w \end{Bmatrix}_n = \begin{bmatrix} K_{nn}^{-1} \end{bmatrix} \begin{Bmatrix} X - R_x \\ Y \\ Z \end{Bmatrix}_n \quad \dots (2.32)$$

The coefficients of the flexibility matrix  $K_{nn}^{-1}$  can be modified in order to obtain the effective flexibility coefficients by eliminating the unknown reaction  $R_x$  in equation (2.32) and rearranging the coefficients of the flexibility matrix. Obviously, in this effective flexibility matrix, the coefficients in the rows and columns corresponding to the fixed displacements will be equal to zero.

As an example, the detailed evaluation of the effective flexibility matrix in case of  $\Delta u = 0$  is given in Appendix (A.3).

## 2.9 CALCULATION OF ELEMENT STRESSES AND NODAL POINT STRESSES

The six components of stress  $\sigma_x$ ,  $\sigma_y$ ,  $\sigma_z$ ,  $\tau_{xy}$ ,  $\tau_{yz}$ , and  $\tau_{zx}$  within a typical element in terms of the twelve corner displacement of the element are expressed by equation (2.8). Therefore, once equation (2.22) is solved for the nodal point displacements of the finite element system, the stresses within each element may be determined by the direct application of equation (2.8) to all elements of the system.

The matrices involved in equation (2.8) are given in Appendix (A.1). As the assumed displacement functions  $N(x,y,z)$  given in equation (2.16) are linear, then the differential matrix  $B(x,y,z)$  contains only constants, so that only one set of stress components can be calculated for each element; that is, in other words, no variation in strains and stresses inside the element can be applicable for simple tetrahedral elements.

This property of the simple tetrahedral element causes considerable difficulty in stress calculations, unless the size of element is sufficiently small, which necessitates the use of large number of elements in the analysis. Furthermore, since maximum stresses generally are developed on the surfaces and on the boundaries of the structure, it is often desirable to obtain the stresses at the nodal points.

It has been shown that nodal point stresses, obtained by averaging the element stresses of all elements connected to the nodal point, produce good results for interior nodal points; however, this approach breaks down when applied to boundary nodal points (ref.46). For better approximation of nodal point stresses, WILSON (ref.44) suggested a weighted averaging method.

In case of slowly varying stress distribution, this method gives much better results, in any way, unless the stress distribution is constant through the thickness, this method may also fail to give exact stresses for boundary points. Another possible solution of this problem might be to extrapolate the interior nodal point stresses to obtain the stresses at the boundaries.

All of the above mentioned methods use the element stresses evaluated by using equation (2.8) and may give satisfactory results for nodal point stresses, whenever the stresses are varying slowly or, if there are enough number of element layers through the thickness.

Generally the number of elements and nodal points of the idealized structure is limited by the storage requirements of the existing computers and also by the computing time. It is often necessary to idealize some certain types of structures such as shells or arch dams, where the thickness is small in comparison with the other dimensions. In such cases, instead of using coarser mesh sizes with many element layers through the thickness, it can be shown that, the use of finer mesh sizes with a less number of element layers through the thickness converges more rapidly to the exact solution for the displacements. However, as the stresses in relatively thin structures generally vary rapidly through the thickness, if there is not enough number of element layers, the above mentioned methods for nodal point stresses do not give satisfactory results.

A suitable solution for the evaluation of the nodal point stresses is developed which uses the nodal point forces  $\{S_i\}$ . Firstly, in this method three components of each nodal point force are calculated for each element and expressed in terms of the twelve corner displacements by means

of equation (2.1). Then the structure is divided into some portions by cutting through the nodal points where the stresses are needed. Later the nodal point forces acting on that particular portion of structure are calculated by means of algebraic addition of the element corner forces joining at the same nodal point (Figure 2.11 a, b, and c). Finally, these nodal point reactions are transformed into normal and tangential force components with respect to the surface of the cross-section.

In case of slowly varying stress conditions, the nodal point stresses can be obtained simply by dividing the normal and tangential force components by the corresponding surface area around the nodal point. If the stresses are varying rapidly through the thickness, taking the moment effects into consideration and assuming that the stress distribution is linear, then it is possible to calculate the nodal point stresses on the surfaces by means of simple formulas given in Table(2.1) for 1 to 4 element layers through the thickness in comparison with the simple force/area formulas. Experience has shown that, in cases having more than 4 element layers, the simple force/area formula gives satisfactory results.

For the structures having large thicknesses, the assumption that the stress distribution is to be linear may not be true; then in such cases, there is no choice other than using 4 or more element layers.

## 2.10 COMPARISON OF THE TYPES OF IDEALIZATIONS

The idealization of three dimensional solid structures by means of tetrahedral elements needs special attention. As it has already been described in section 2.3.3, there are two possibilities in forming a brick with tetrahedral elements: the first is to use 5 tetrahedrals and the other 6 tetrahedrals. Further, there are two possibilities forming a brick with

5 tetrahedrals and sixteen possibilities with 6 tetrahedrals.

Now, let a solid structure be idealized by means of these possibilities. Two of these possibilities which use 5 tetrahedral elements are shown in Figure 2.12 a and b, and which use 6 tetrahedral elements are shown in Figure 2.13 a and b.

By a close inspection of Figure 2.12 a and b, it can be seen that, while only one element connected at point A1, four elements are connected at point A2. And also, while only four elements are connected at points C1 and D1, sixteen elements are connected at points C2 and D2. For the points B1, E1, B2 and E2, the condition is contrary. Naturally in these two different types of idealizations, corresponding nodal points have different stiffnesses and considering only one of these idealizations, the stiffnesses of the neighbouring nodal points are distributed in a non-homogenous way. Experience has shown that this non-homogenous distribution of stiffness does not affect the overall behaviour of the structure even for considerable coarse mesh idealizations. But it does affect the nodal point stress calculations. When using averaging methods, the stresses obtained for the corresponding points may differ largely from each other. Using the nodal point forces for stress calculations, considerable difficulties arise as these forces are distributed non-homogenously and also the forces obtained for the corresponding points differ largely from each other.

If 6 tetrahedral elements are used for the idealization, it can be seen from Figure 2.13 a and b that, in all possible cases, the stiffnesses are distributed homogeneously and may not differ largely for each of the possible cases, except for the points on the edges and at the corners like points A3 and A4. Again, the type of idealization does not affect

the overall behaviour of the structure, but the average stresses at the corresponding nodal points may differ, not as much as for 5 tetrahedral elements, except for the nodal points on the edges and at the corners at which the difference may be larger. On the other hand, for each case, a different set of nodal point forces develops so that the nodal point stresses calculated for each of these sets of forces may differ considerably.

To overcome these difficulties and to obtain a unique and homogeneous solution, it is suggested that all possible idealizations (for 5 tetrahedral elements both of two; and for 6 tetrahedral elements a set of four combinations) are used simultaneously, then take the average stiffnesses and the developed nodal point forces for stress calculations. This can easily be done without increasing the necessary computer storage by using a magnetic tape as a backing storage. The only difficulty encountered is the increase in the computing time for derivation of nodal point stiffnesses and calculation of stresses. As in the case of 5 tetrahedral elements, there are two possible combinations, and so computing time is doubled; while for 6 tetrahedral elements there are four possible combinations so that computing time is four times longer.

The influence of the type of the idealizations has been investigated on simpler systems having different types of idealizations with the same mesh size. This investigation has shown that the use of six tetrahedral elements has no advantage over five tetrahedral elements; on the contrary, more storage and computing time are involved as the number of elements and the possible combinations are more than those for the case of 5 tetrahedral elements.

So, it is decided to use the double combinations of five tetrahedral elements simultaneously, in all of the computations involved in this study.

## 2.11 COMPUTER PROGRAMMING

For the practical application of the theory developed in the previous sections, a computer programme has been written in FORTRAN language. The basic flow diagram of this programme is given in Figure 2.14 and it can be divided into five main parts :

- (1) Reading input data, arranging nodal point arrays, calculating nodal point coordinates (steps 1-4 inclusive). As the analysis may consist of hundreds of nodal points and thousands of elements, for structures which have geometrical regularities, the input data must be minimized in order to reduce the data preparation task and also to minimize the data reading time. For an arch dam which has circular arches, this economy can easily be achieved by writing considerably simple sub-routines. By doing this, the input data consists of only one card per each elevation considered in the idealization.
- (2) Arranging element arrays, calculating the element stiffness matrix (steps 5-11 inclusive). To satisfy a homogeneous stiffness distribution, two possible sets of arrays with 5 tetrahedral elements (A-type idealizations) have been used. The stiffnesses are calculated for each set and the average is taken as the nodal point stiffness. To save storage, the element arrays and stiffness matrices are stored in two separate magnetic tapes.

Although the number of elements is doubled the derivation of the stiffness matrix of tetrahedral element is very simple and very little computation is required for this derivation (Appendix A.1); therefore the computing time spent in this part is not excessive.

(3) Inversion of nodal point stiffness and application of constraints (steps 12-15 inclusive). This part consists of the formulation described in Appendix (A.2) and (A.3).

(4) Iteration to the solution of the equations (steps 16-20 incl.). Iteration continues until the maximum cycle limit is exceeded or the sum of error becomes equal or less than the tolerance limit which indicates the accuracy desired.

(5) Calculation of element and nodal point reactions and printing the results (steps 21-24). The nodal point reactions are calculated for each cut as shown in Figure 11. Direct stress calculation is not included in the programme, but can be done easily for certain critical sections according to the assumptions given in section 2.9.

The programme has been prepared in accordance with the specifications given for the ATLAS computer at Chilton, Berkshire, U.K. The listings of the main routine and the other sub-routines used in the programme are given in Appendix B, with some necessary information about the storage requirement, order of numbering the nodal points and input data.

## 2.12 APPLICATION OF THE THEORY TO THE STATIC ANALYSIS OF AN ARCH DAM

### 2.12.1 The Arch Dam to be Analyzed

The arch dam, chosen for the application of the theory developed, is 120 metres high, symmetrical double curvature arch dam, which is one of the selected types of arch dams by C.E.R.A. (ref.33) and is designated as "Type-5". General layout of this dam is shown in Figure 2.15 where a unit must be considered equal to 20 metres. Accordingly, the reference cylinder has a

radius of 173 metres and the crest length of the top arch is 320 metres. The thicknesses of the crown cantilever are 5.35 at the top and 23.35 metres at the bottom.

The mechanical properties assumed for concrete and foundation rock are given in Table (2.2).

#### 2.12.2 Idealization and Boundary Conditions

A-type idealizations with five tetrahedral elements in a brick-like block are used. As the dam is symmetrical, only one half of the structure is to be taken into consideration.

The dam is divided into sixteen horizontal parts, each segment having equal height. The half of the top arch is also divided into sixteen equal parts, then the intermediate arches are divided into equal parts accordingly. Only one element layer is used through thickness. This idealization is to be denoted as (16 x 1 x 16) mesh type and is shown in Figure 2.16.

The half of the dam contains 422 nodal points and 926 tetrahedral elements. 42 nodal points lay on the foundation and are assumed fixed in every direction, so that the boundary conditions at these points are :

$$u = v = w = 0$$

The origin of the global Cartesian coordinate system is assumed situated at the centre of the reference cylinder at the bottom of the valley and the positive directions of the axis are as shown in Figure 2.1. All of the coordinates of the nodal points are calculated with respect to this coordinate system.

There are 32 nodal points on the crown cantilever, which is in the plane of symmetry. These nodal points can only move in this plane,

that is the boundary conditions at these points are

$$u = 0 .$$

As each nodal point is allowed three degrees-of-freedom, the overall system considered consists of total 1266 degrees-of-freedom. After the exclusion of the above mentioned constraints, this number reduces to 1108. To solve 1108 simultaneous equations by conventional direct inverting method requires a computer storage approximately 2500 blocks (1 block is equal to 512 words) while the use of triple band matrices reduces the required storage to about 1000 blocks. In both of these methods it is necessary to use some backing storage which reduces the speed of the computations.

The iterative method discussed above needs only 150 blocks to solve the same problem. With the other necessary storage requirements, the total number of blocks reaches 202 blocks, which fits the present storage of ATLAS computer (210 blocks) without necessitating any extra storage. The comparison of the above numbers of blocks shows the efficiency of the iterative method presented.

No allowance is considered for the flexibility of the foundation. However, there is no difficulty to introduce the foundation flexibility, as it can be done by using some more elements inside the valley adjacent to the structure.

### 2.12.3 Loading Conditions and Results Obtained

Two loading conditions are considered for the static analysis of Arch Dam Type-5 :

- (1) Hydrostatic loading: hydrostatic pressures acting on the upstream face are assumed to be concentrated as lumped forces

acting at the nodal points on the upstream face. These forces are easily to be calculated by means of multiplying the hydrostatic pressures at the nodal points by the corresponding surface areas.

The resultant hoop and vertical stresses and the deflections of the crown section are shown in Figure 2.17 in comparison with the results obtained by means of other methods of analysis. As it can be seen from these figures, the simple tetrahedral element gives results with reasonable accuracy, even only one element layer is used in the idealization.

(2) Gravity loading: gravity loads are assumed to be lumped acting at all nodal points. These forces are easily to be calculated by means of multiplying the density of the concrete by the volume corresponding to each nodal point.

In these calculations the dam is assumed a complete structure as a whole, and the effect of construction joints is not considered.

The stresses and deflections obtained for crown section are shown in Figure 2.18. As no existing result has been published for the gravity stresses of Arch Dam Type-5, no comparison could be made.

Initially, the computer programme had been written to include the thermal stresses. But, as it is possible to use only one element layer through thickness because of the limitation of the computer storage, no attempt has been made to calculate the stresses due to temperature variations.

#### 2.12.4 Computations

The computations executed at the ATLAS Computer Laboratory, take about 26 minutes for each analysis. A period of about 9 minutes is spent

for the first three stages of the programme. Later, a period of about 16 minutes is spent for the iteration process. 300 cycles of iteration can be executed in this period of time, and by using an over-relaxation factor having the value of  $\beta = 1.87$ , during these 300 cycles, a ratio about  $1/10^6$  is achieved for the latest and initial values of unbalanced forces. The last minute of the computations is used for reaction calculations and output of the results.

## CHAPTER 3

### DYNAMIC ANALYSIS OF ARCH DAMS

#### 3.1 INTRODUCTION

In the previous chapter, the idealization of an arch dam by means of three-dimensional "tetrahedral" finite elements and the determination of the stiffness properties of the structure have been discussed in detail and the application of the methods to the static analysis of an arch dam has been presented.

In this Chapter, the other important properties of the structure, namely the inertia properties, are to be introduced. After the methods to determine these properties are presented, the problem of determining the dynamical characteristics of the structure, namely "the eigenvalue problem" will be solved.

An arch dam is a complex system consisting of its own body, the water in the reservoir behind the dam and the flexible foundation on which the dam stands. As the interaction between these members of this complex system largely affects the dynamical behaviour of the arch dam, the influences of these factors shall also be considered in detail.

#### 3.2 GENERAL EQUATIONS OF MOTION FOR MULTI-DEGREE-OF-FREEDOM SYSTEMS

The equations of motion of a general elastic linear multi-degree-of-freedom system can be obtained by utilizing the general Lagrange's equation :

$$\frac{d}{dt} \left( \frac{\partial T}{\partial \dot{q}_j} \right) - \frac{\partial T}{\partial q_j} + \frac{\partial F}{\partial \dot{q}_j} + \frac{\partial V}{\partial q_j} = Q_j \quad \dots (3.1)$$

where

- $T$  = total kinetic energy of system,
- $V$  = total potential energy of system,
- $F$  = the dissipation function,
- $q_j$  = generalized coordinate of displacement,
- $\dot{q}_j$  = velocity at generalized coordinate  $q_j$ ,
- $Q_j$  = generalized external force for each generalized coordinate.

The kinetic energy  $T$ , potential energy  $V$ , and the dissipation function  $F$  can be expressed in the quadratic forms, by matrix notation as :

$$\left. \begin{aligned} T &= \frac{1}{2} [\dot{q}]^T [M] \{\dot{q}\} \\ V &= \frac{1}{2} [q]^T [K] \{q\} \\ F &= \frac{1}{2} [\dot{q}]^T [C] \{\dot{q}\} \end{aligned} \right\} \dots (3.2)$$

where  $[M]$  ,  $[K]$  and  $[C]$  are the inertia, the stiffness and the damping matrices of the system, respectively. By substituting equation (3.2) in equation (3.1), the general equations of motion can be obtained as :

$$[M] \{\ddot{q}\} + [C] \{\dot{q}\} + [K] \{q\} = \{Q\} \dots (3.3)$$

In the case of free vibration of the structure, where  $\{Q\} = 0$ , the general equation becomes

$$[M] \{\ddot{q}\} + [C] \{\dot{q}\} + [K] \{q\} = 0 \dots (3.4)$$

Equation (3.4) represents the complex eigenvalue problem and the eigenvalues obtained from this equation are, in general, complex. However, if the damping of the system is small, the effects on the eigenvalues are

very little and negligible. With this assumption, equation (3.4) simplifies as :

$$[M] \{\ddot{q}\} + [K] \{q\} = 0 \quad \dots (3.5)$$

If the solution of this equation is assumed

$$\{q\} = \{\psi\} e^{i\omega t} \quad \dots (3.6)$$

and equation (3.6) is substituted in equation (3.5), it follows that

$$[K] \{\psi\} - \omega^2 [M] \{\psi\} = 0$$

and  $[K - \omega^2 M] \{\psi\} = 0 \quad \dots (3.7)$

The nontrivial solution of this equation can be obtained by making the determinant of the matrix multiplying the vector  $\{\psi\}$ , zero, that is

$$\det (K - \omega^2 M) = 0 \quad \dots (3.8)$$

When the determinant is expanded, a polynomial of order  $n$  in  $\omega^2$  is obtained. Equation (3.8) is known as the characteristic equation. The restrictions that  $M$  and  $K$  be symmetric and that  $M$  be positive definite are sufficient to ensure that there are  $n$  real roots for  $\omega^2$ . If  $K$  is singular, at least one root is zero. If  $K$  is positive definite, all roots are positive. The roots obtained are generally called normal values or eigenvalues and determine the natural frequencies  $\omega_r$  of free vibration modes of the system. When a natural frequency  $\omega_r$  is known, it is possible to solve the equation (3.7) for the corresponding vector  $\{\psi_r\}$  by means of a back-substitution process. The elements of vector  $\{\psi\}$  are generally normalized so that only the relative amplitudes of the generalized coordinates are to be obtained by means of an eigenvalue problem. There are  $n$  independent vectors  $\{\psi_r\}$

corresponding to the  $n$  natural frequencies which are known as natural or normal modes, or eigenvectors.

Providing the knowledge about the eigenvalues and the eigenvectors, and also the other dynamical properties of the system and the characteristics of the excitation are known, it is possible to determine the absolute amplitudes of the responses by means of, so-called, normal mode analysis. The forced vibration theory of multi-degree of freedom systems is to be considered in Chapter 4.

Although the above-mentioned theoretical treatment is quite simple and there exist some methods to solve the eigenvalue problem, the application of this theory to three-dimensional finite element techniques and especially to the vibration problems of arch dams needs more attention. The reasons are:

Firstly, as the problem is assumed to be three-dimensional, the normal mode vectors consist of three-dimensional components of the generalized displacements, so that, the application of the conventional lumped inertia method might cause more inconsistency with the idealization of the structure and displacement functions assumed in section 2.5.

Secondly, the dams are constructed to retain the water behind them and the reservoir is usually full of water, so that the vibration of dams involves consideration of the hydrodynamic effects of the reservoir water and the dynamical behaviour of the complete reservoir-dam system.

Finally, the arch dam, mainly, transmits the forces acting on it to the foundation on which it stands. As the dimensions of the structure and so the contact surface with the foundation are large, the interaction between the dam and the foundation has a considerable effect on the dynamical behaviour of the dam.

Before describing the method adopted for the solution of eigenvalue

problem, first the concept of consistent mass matrix is to be presented. Following the introduction of the general solution for the eigenvalue problem, the possibilities of considering the effects of the reservoir water and the flexibility of the foundation is to be discussed in detail.

### 3.3 DERIVATION OF THE CONSISTENT MASS MATRIX OF AN ELEMENT

Since the early introduction of the finite element techniques, the formulation of the stiffness matrix has always received close attention, but in the application to dynamic problems it has lately been realized that the inertia matrix is also important and it affects the frequencies and mode shapes. The conventional method of lumping the inertia at the nodes of the structure can only be adequate for simple structures where the elements of structure assumed to be weightless and concentrated masses to be present in fact at the nodes which are only permitted a single degree of freedom, then the resulting simple diagonal mass matrix which implies no inertial coupling is justified to be valid.

The dynamic representation of continuum structures which are idealized by means of elements having many nodes each with several degrees of freedom and the mass of each element is distributed over its volume, requires special care in allocating the inertias.

An appropriate method for the solution of this problem has been proposed by ARCHER (ref.47) which is a procedure consistent with the approximations involved in deriving the element stiffness matrix, and so the resulting element mass matrix is called the "consistent mass matrix".

In this method, the inertia coefficients of the element mass matrix are derived by a method analogous to that used for the derivation of the

coefficients of the element stiffness matrix as described in section 2.4. Since the same displacement pattern is used as for the stiffness matrix, the new inertia matrix is consistent with the stiffness matrix, and allows for the three dimensional coupling terms. This method is therefore very well suited to continuum type structures such as arch dams.

The finite element method described in section 2.4 can be extended to vibration problems by including the work done by the inertia forces in equation (2.12) as

$$W_E + W_M = W_I \quad \dots (3.9)$$

The inertia forces per unit volume acting on a three dimensional element are

$$\{f\} = \omega^2 [m_p] \{U\} \quad \dots (3.10)$$

where  $[m_p]$  is a matrix of inertial constants, and  $\omega$  is the frequency of vibration. The work done by these forces in the virtual displacement  $\{\bar{U}\}$  is

$$W_M = \int_V [\bar{U}]^T \{f\} dV = \omega^2 \int_V [\bar{U}]^T [m_p] \{U\} dV. \quad \dots (3.11)$$

Considering the displacement pattern introduced in equation (2.2) and equation (2.4) and substituting  $\{U\}$  into equation (3.11) :

$$W_M = \omega^2 [\bar{U}_i]^T [C^{-1}]^T \int_V [N(x,y,z)]^T [m_p] [N(x,y,z)] dV. [C^{-1}] \{U_i\} \dots (3.12)$$

is obtained.

The application of the theorem of the virtual work including inertia forces equation (3.9) gives :

$$\begin{aligned} [\bar{U}_i]^T \{S_i\} + \omega^2 [\bar{U}_i]^T [C^{-1}]^T \int_V [N(x,y,z)]^T [m_p] [N(x,y,z)] dV [C^{-1}] \{U_i\} \\ = [\bar{U}_i]^T [C^{-1}]^T \int_V [B(x,y,z)]^T [D] [B(x,y,z)] dV [C^{-1}] \{U_i\} \quad \dots (3.13) \end{aligned}$$

where  $\{S_i\}$  is the vector of nodal forces corresponding to nodal displacements  $\{U_i\}$ .

If now, a unit virtual displacement is applied at each of the nodal degrees of freedom in sequence, an equation of the form

$$\{S_i\} = [k] \{U_i\} - \omega^2 [m] \{U_i\} \quad \dots (3.14)$$

is obtained. Where  $[k]$  is the element stiffness matrix already given by equation (2.15) and  $[m]$  is the element consistent inertia matrix which is defined as

$$[m] = [C^{-1}]^T \int_V [N(x,y,z)]^T [m_p] [N(x,y,z)] dV [C^{-1}] \quad \dots (3.15)$$

and represents the equivalent point inertias required at the nodal points to produce the same loading as the distributed inertias.

The derivation of the consistent mass matrix for the tetrahedral element assuming the displacement pattern of equation (2.16) is given in Appendix (A.4).

### 3.4 EQUILIBRIUM OF COMPLETE STRUCTURE

Having idealized the structure as an assemblage of finite elements and determined the element stiffness and inertia properties, the extension of the process to the vibration of the complete structure can be achieved by considering the equilibrium of the complete structure, that is the equilibrium of the internal and external applied forces at each nodal point.

The internal forces due to the element  $i$  are given by equation (3.14)

as

$$\{S_i\} = [k_i] \{U_i\} - \omega^2 [m_i] \{U_i\} \quad \dots (3.16)$$

Now to consider the vibration of the complete structure, it is necessary to form the overall mass and stiffness matrices for the whole structure. As it has been shown in Appendix (A.1) that, in the finite element method adopted for tetrahedral elements, all of the elements can be defined with respect to a global coordinate system and there is no need to use any other local coordinate system for each element, so that to avoid the transformation process which is necessary for many other types of elements. This property leads to a very simple procedure to form the overall matrices, which consists only of transferring the coefficients of the mass and stiffness matrices of each element to the appropriate locations of the overall matrices and then adding each other algebraically.

Considering equilibrium of forces at each nodal point, the overall equilibrium equations are obtained as follows :

$$\{S\} = [K] \{U\} - \omega^2 [M] \{U\} \quad \dots (3.17)$$

where  $[K]$  and  $[M]$  are the overall stiffness and inertia matrices for the complete structure.

For the application of the boundary conditions, equation (3.17) can be partitioned as:

$$\begin{Bmatrix} S_a \\ S_c \end{Bmatrix} = \begin{bmatrix} K_{aa} & K_{ac} \\ K_{ca} & K_{cc} \end{bmatrix} \begin{Bmatrix} U_a \\ U_c \end{Bmatrix} - \omega^2 \begin{bmatrix} M_{aa} & M_{ac} \\ M_{ca} & M_{cc} \end{bmatrix} \begin{Bmatrix} U_a \\ U_c \end{Bmatrix} \quad \dots (3.18)$$

where the suffix c denotes the nodal points on the boundaries which have prescribed displacements, and the suffix a denotes all the other points at which the external forces  $S_a$  are applied.  $U_a$  and  $S_c$  are the unknown displacements and reactions respectively.

In this analysis, all the boundary nodal points are assumed to be fixed, then the prescribed boundary displacements become :

$$\{U_c\} = 0 \quad \dots (3.19)$$

If the natural modes of vibration of the structure are required then the nodal forces at the interior points are also taken to be zero:

$$\{S_a\} = 0 \quad \dots (3.20)$$

Imposing these conditions to equation (3.18)

$$[K_{aa}] \{U_a\} - \omega^2 [M_{aa}] \{U_a\} = 0 \quad \dots (3.21)$$

is obtained. In practice, the matrices  $[K_{aa}]$  and  $[M_{aa}]$  in equation (3.21) are obtained by deleting the rows and columns of the overall matrices  $[K]$  and  $[M]$ , respectively, which correspond to the zero displacements. Having obtained  $\omega$  and  $\{U_a\}$  from equation (3.21), the following equation may be used to calculate the reactions on the part of the boundary along which the displacements have been prescribed :

$$\{S_c\} = [K_{ca}] \{U_a\} - \omega^2 [M_{ca}] \{U_a\} \quad \dots (3.22)$$

### 3.5 THE EVALUATION OF THE EIGENVALUE PROBLEM

The determination of the natural frequencies and the normal modes of the system by using Equation (3.7), consists of many complicated calculations and some methods have already been developed and widely used for the solution of the matrix eigenvalue problem.

The most efficient method for matrices with the order less than 50 seems to be the Householder's method (ref.48). But, as the matrix used in this method is a fully populated matrix, and so, if its order is large the method is inefficient with regard to storage requirements.

The dynamical analysis of complex structures such as arch dams, by means of finite element techniques, generally involves larger order matrices, and some special methods must be used which satisfy the storage requirements.

The method used in this study for the solution of the eigenvalue problem was developed by PETYT (ref.49), in which only the non-zero square triple band matrices of the  $[K - \omega^2 M]$  matrix are stored, and very little working space is required. Thus, for large order matrices the method is more efficient with regard to storage requirements than the HOUSEHOLDER's method; however, the method of obtaining the roots is very slow in comparison with the Householder's technique.

The method considered here consists of evaluation of the determinant of the  $[K - \omega^2 M]$  matrix for a range of values of  $\omega^2$ , until a change in sign of the determinant is found, indicating a root for the equation (3.8). The determinant is evaluated by means of the Gauss elimination procedure with partial pivoting (ref.50). In addition, a floating fixed point arithmetic is adopted for the determinant evaluation process, so that it could be possible to evaluate the determinants in the range  $10^{-9999} \leq |\det| \leq 10^{9999}$ .

When a change in sign of the determinant occurs, the rule of false position (ref.51) is then used to iterate to the root, correct to a specified number of significant figures. Again, the Gauss elimination procedure followed by a back-substitution is used to evaluate the corresponding eigenvector. During these processes, magnetic tapes are used as intermediate storage.

In these calculations, the inertia matrix  $[M]$  should be considered as the effective mass matrix which includes the hydrodynamic matrix, for the reservoir in full condition as shall be described in section 3.9.

### 3.6 GENERAL CONSIDERATIONS ON THE HYDRODYNAMIC EFFECT OF THE RESERVOIR WATER

The hydrodynamic effect of the reservoir water has attracted close attention of scientists since the early beginning of the construction of large dams, and many theoretical and experimental studies have been made up to date.

The first study on this subject was published by WESTERGAARD (ref.19) in 1933 and his work has influenced the designer for a long time in considering hydrodynamic forces on dams during earthquakes. In this work, the complete system of the dam and the reservoir water is divided into two uncoupled systems: the first one is the dam itself vibrating alone, by ignoring the hydrodynamic effects, and the latter is the hydrodynamic pressures on the rigid dam acting as statical forces during earthquake.

The assumptions involved in Westergaard's solution are :

- (a) The dam is rigid, infinitely long and has a vertical upstream face;
- (b) The reservoir extends to infinity in the upstream;
- and (c) The effect of surface waves is neglected.

Considering the compressibility of water, the two dimensional flow problem was solved for a harmonic ground motion in the horizontal direction

perpendicular to the dam axis. The hydrodynamic pressures on the dam are shown to be opposite in phase to the ground acceleration, and this is equivalent to the inertia forces of an added mass moving with the dam. The magnitude of this mass depends on the frequency of the harmonic ground motion.

BRAHTZ & HEILBORN (ref.52) investigated the influence of the finite lengths of the reservoir in the upstream directions and showed that if the ratio of the length of reservoir to the height of the dam ( $L/H$ ) is bigger than 3, the effect of length is practically negligible. The experimental results obtained by HOSKINS & JACOBSEN (ref.53) support the above conclusion. Later, KOTSUBO (ref.54) has shown that Westergaard's solution is valid only when the period of the harmonic excitation is greater than the fundamental natural period of the reservoir, and recently BUSTAMENTE et al (ref.55) investigated the effect of length of reservoir for a wider range of periods of excitation and they showed that for shorter periods, the length plays an important role in stationary harmonic motion in the case of high dams. But in practical situations, the reservoir usually extends to large distances, so the length of reservoir may be taken as infinite without introducing any appreciable errors.

Considering the water to be incompressible, ZANGAR (ref.20) showed that the two dimensional flow problem can be solved by using an electric analogy and he determined the pressure distributions for the dams with sloping upstream faces.

The three dimensional flow problem was introduced by WERNER & SUNDQUIST (ref.56) and they solved this problem for some particular shapes of structures considering whether the water is compressible and incompressible according to

the complexity of the shape. Later, KOTSUBO (ref.24), using the three dimensional solution, investigated the dynamic water pressure distribution in horizontal direction for the case of cylindrical arch dams lying on rectangular section valley.

Most of the investigators have ignored the waves that may be generated at the free surface of water. CHZHEN-CHEN (ref.57) allowed for the existence of a surface wave in an incompressible fluid and showed that the effect of surface waves can be neglected with a little loss of accuracy.

The foregoing has concerned responses to only horizontal harmonic ground motions. KOTSUBO (ref.58) determined the hydrodynamic response of a reservoir behind an arch dam for a harmonic ground motion in the vertical direction; and recently CHOPRA (ref.59) has studied the hydrodynamic forces on dams during earthquakes, considering the horizontal component as well as the vertical component of earthquakes being random in character.

Another approach to the solution of the problem was suggested by BUSTAMENTE & FLORES (ref.60) who introduced a hydrodynamic spectra considering the validity of modal analysis to determine the hydrodynamic pressures caused by earthquakes.

The hydrodynamic boundary conditions for a particular arch dam and valley are likely to be difficult to handle theoretically and the resulting solution would have no general application. So, the electric analog method, firstly introduced by ZANGAR for two dimensional solution, was developed by ZIENKIEWICZ & NATH (ref.25) and extended to a three dimensional solution for arch dams subject to any arbitrary distribution of boundary acceleration. Also ZIENKIEWICZ et al (ref.61) demonstrated the incorporation of the hydrodynamic forces obtained by means of the electric analogy, in the general

vibration problems of the dam and the reservoir water as a complete system.

Recently, as a result of experiments made on an idealized model dam to find the generalized modal coefficients by means of the displaced-frequency technique, SKINGLE et al (ref.62) showed that the reservoir water acts not only as a mass but also as a stiffness, and the stiffness effect increases for higher modes. However, comparing with the electric potential analogue method, the effective mass of the reservoir water measured by the displaced-frequency technique has been found to be in poor agreement; the differences in frequencies obtained by both methods are not as great as the differences in generalized mass; assuming the possibility that, to some extent the error in the analogue values of mass are offset by the zero stiffness terms associated with the analogue solution.

### 3.7 THEORETICAL BASIS OF THE HYDRODYNAMIC EFFECT AND THE ELECTROLYTIC ANALOGY

If the water is considered as an ideal non-viscous fluid, the problem of the pressure in three dimensional flow is closely related with the theory of sound; and further, if the displacements in the water body are assumed small, the general Eulerian equations (ref.63) may be simplified as follows :

$$\left. \begin{aligned}
 \frac{\partial p}{\partial x} &= \frac{\gamma}{g} \cdot \frac{\partial^2 u}{\partial t^2} \\
 \frac{\partial p}{\partial y} &= \frac{\gamma}{g} \cdot \frac{\partial^2 v}{\partial t^2} \\
 \frac{\partial p}{\partial z} &= \frac{\gamma}{g} \cdot \frac{\partial^2 w}{\partial t^2}
 \end{aligned} \right\} \dots (3.23)$$

where  $x, y, z$  are Cartesian rectangular coordinates,  
 $u, v, w$  are generalized displacements in rectangular coordinate system,  
 $t$  is time,  
 $g$  is gravity acceleration,  
 $\gamma$  is unit weight of water,  
 $p$  is dynamic water pressure.

The condition of continuity for a compressible fluid in simple harmonic motion is

$$\frac{\partial u}{\partial x} + \frac{\partial v}{\partial y} + \frac{\partial w}{\partial z} = \frac{p}{K} \quad \dots (3.24)$$

where  $K$  is the compressibility of water. Now introducing the expression for the velocity of sound in water,  $s$  :

$$s = \sqrt{gK/\gamma} \quad \dots (3.25)$$

after some transformations in equations (3.23) and (3.24), the general differential equation for the pressure in three dimensional flow can be obtained as

$$\frac{\partial^2 p}{\partial x^2} + \frac{\partial^2 p}{\partial y^2} + \frac{\partial^2 p}{\partial z^2} = \frac{1}{s^2} \cdot \frac{\partial^2 p}{\partial t^2} \quad \dots (3.26)$$

By means of assuming some simplified boundary conditions, such as non-existence of surface waves, infinitely long reservoir, simple harmonic earth movements, rigid reservoir walls moving as a whole with the ground, it is possible to evaluate the solution of equation (3.26) for some simple geometrical shapes (ref.24 and 56). However, none of these results can be

generalized for the design of arch dams; a very important practical conclusion obtained is that if the depth of water in the reservoir is less than one quarter of the velocity of sound in water multiplied by the period of the ground motion, then resonance in an infinitely long reservoir cannot occur, that is the flow is stable under all conditions and so the effects of the compressibility of water may be neglected.

This conclusion leads equation (3.26) for a non-viscous and incompressible fluid to become :

$$\frac{\partial^2 p}{\partial x^2} + \frac{\partial^2 p}{\partial y^2} + \frac{\partial^2 p}{\partial z^2} = 0 \quad \dots (3.27)$$

which is known as Laplace's equations. On the other hand, the same equation governs the potential in an electrolyte.

Providing the above similarity conditions, it was firstly shown by ZANGAR (ref.20) for two dimensional flow, later by ZIENKIEWICZ & NATH (ref.25) for three dimensional flow, that an electric potential analogue may be used to determine fluid pressures developed on a structure subjected to a prescribed system of accelerations.

Assuming the  $z$  axis is in the vertical direction, from a consideration of the boundary conditions it can be shown that the hydrodynamic pressures of three dimensional flow is

$$\frac{\partial p}{\partial n} = -\gamma \cdot a_n \quad \dots (3.28)$$

where  $n$  is a coordinate normal to the boundary between the fluid and the wall containing it, and  $a_n$  is the acceleration of boundary wall in the direction of the normal. At the free surface of the fluid, for  $z = 0$ , if surface waves are ignored

$$p = 0 \quad \dots (3.29)$$

In case of the flow of electric current through a homogeneous isotropic conducting medium, for the electric potential  $\phi$ , the boundary conditions are

$$\frac{\partial \phi}{\partial n} = - \gamma \cdot a_n \quad \dots (3.30)$$

on solid boundaries, and

$$\phi = 0 \quad \dots (3.31)$$

on the free surface. Since by the definition

$$i_n = - e \frac{\partial \phi}{\partial n} \quad \dots (3.32)$$

where  $i_n$  is the current density, and  $e$  is the conductivity of the fluid, then the solid boundary condition becomes

$$i_n = e \gamma a_n \quad \dots (3.33)$$

From the similarity between the above equations, it can easily be shown that, if the input current density is identified with the accelerations of the dam, then the measured potentials will be analogous with the pressures arising therefrom.

### 3.8 APPLICATION OF ELECTROLYTIC ANALOGY TO APPROXIMATE THE HYDRODYNAMIC EFFECT

The methods developed for the application of the electrolytic potential analogue have been described in detail elsewhere (ref.23,25 and 62) and shall only be considered herein briefly.

In the practical application of the analogue to a dam and reservoir it facilitates measurement of the potentials and obviates difficulties associated

with polarisation, if oscillatory currents are used. The frequency of the oscillatory current need not be related to any of the dam resonance frequencies since by virtue of the assumption of incompressibility of the fluid, the pressure generated per unit acceleration is independent of the frequency of the motion. It is necessary, however, that the applied frequency be such that the fluid behaves as a purely resistive medium and frequencies supplied by a low frequency oscillator working at 1-1.5 kHz through a 10 watt amplifier are found to be convenient and satisfactory.

In order to obtain the so-called hydrodynamic influence coefficient matrix from the analogue, the face of the dam is divided into a number of areas corresponding to each nodal point on that face, and a brass electrode is bonded to each of the divided areas so that the centre of the electrode coincides with the nodal point. The linear dimensions of each electrode are one half of the dimensions of the area appropriate to it (ref.25). All other fluid-wall boundaries are lined with non-conducting polythene sheet. The free surface zero potential is maintained by a sheet of thin brass foil glued to the underside of a piece of plywood which floated on the free surface. A dilute solution of copper sulphate is generally used as electrolyte.

With these conditions satisfied, unit current density applied to an electrode and the change in potential at all other electrodes is measured, the process is then repeated for all of the electrodes in turn. The matrix of potentials can then be converted to a matrix of pressures per unit acceleration and this matrix can be used to calculate the pressures at the electrode points due to a given set of accelerations at those points.

### 3.9 INCORPORATION OF THE HYDRODYNAMIC FORCES IN THE GENERAL VIBRATION PROBLEM

Assuming the hydrodynamic water pressures to act on a rigid dam, it has already been shown that it is possible to obtain the hydrodynamic pressure constants for every point of an arch dam having arbitrary shape, by means of an electrolytic analogy. Now, the problem is in what way these constants can be incorporated with the elastic structure in the general vibration problem.

The effect of the hydrodynamic water pressures during the vibration of the dam can be incorporated in the general vibration problem by the introduction of the "hydrodynamic matrix" (ref.61). The coefficients of this matrix are formed by integrating the hydrodynamic pressures over the area corresponding to each nodal point on the face of the dam, and resolving these forces in coordinate directions. As the hydrodynamic forces are generated due to the acceleration of points on the dam, and are acting in the reverse direction of the motion of the point, these forces can be inserted into the equation of the undamped motion as :

$$[M] \{\ddot{q}\} + [K] \{q\} = - [H] \{\ddot{q}\} \quad \dots (3.34)$$

where  $[M]$  is the consistent mass matrix for the structure, and  $[H]$  is the hydrodynamic matrix.

Equation (3.34) can be rewritten in the following form :

$$[M + H] \{\ddot{q}\} + [K] \{q\} = 0 \quad \dots (3.35)$$

Equation (3.35) is identical to equation (3.5), the equation of the undamped free vibration of the system. The only difference is that the elements of inertia matrix are increased by the addition of the hydrodynamic coefficients. This form of the increased inertia matrix is generally called

the "effective mass matrix" and equation (3.35) can also be treated as it has been done for equation (3.5), in order to determine the eigenvalues and the corresponding eigenvectors for the reservoir in full condition of the dam.

### 3.10 EFFECT OF FLEXIBILITY OF THE FOUNDATION

In such structures like arch dams, where the interaction between the structure and the foundation is considerably large, the effects of the flexibility of the foundation on the behaviour of structure must be taken into consideration.

In the static analysis of arch dams generally, some allowance is made for foundation deformation on the basis of the in situ foundation modulus. A similar approach can be utilized in the dynamic problems. For this it is necessary to include some foundation yield terms in the stiffness matrix for those elements abutting the foundation. Further terms are also required in the mass matrix to represent the inertia of the foundation.

The finite element techniques make it possible to introduce the foundation flexibility and inertia, simply by carrying the fixed boundaries some distance into the foundation and considering some foundation elements adjacent to the base of the dam. The only difficulty involved is that the increased number of nodal points and overall degrees of freedom makes the computation much slower and necessitates larger storage capacity.

As it is possible to assign different mechanical properties to each element, variations of foundation modulus across the valley can also be handled easily.

The foundation conditions are obviously peculiar to each site and no general conclusions can be derived from assigning a particular value to the

foundation modulus. However, to demonstrate the effect of the flexibility of the foundation on the dynamical characteristics of the arch dams, several values of foundation modulus are taken into consideration in this study, as well as rigid foundation.

### 3.11 COMPUTER PROGRAMMING

The flow diagram of the FORTRAN programme, which has been written for calculating the natural frequencies and mode shapes of arch dams, is given in Figure 3.1. This programme can be divided into four main parts :

(1) Arranging nodal point arrays, calculating nodal point coordinates (as section 2.11.1) and arranging the element arrays for both sets of A-type idealizations and writing these arrays into a magnetic tape (steps 1-7 inclusive).

(2) Calculating the element stiffness matrices for each set of idealization (as appendix A.1), then transferring to the overall stiffness matrix. Taking the averages of the overall stiffness terms, applying the prescribed constraints and writing into the second magnetic tape (steps 8-17 inclusive).

(3) After clearing the storage for the overall matrix, the same procedures as the second stage are applied in order to obtain the overall mass matrix (as appendix A.4). But, before applying constraints, if the reservoir is in full condition, the hydrodynamic matrix is also calculated (as section 3.9) and then added to the overall mass matrix. The overall mass matrix is also written into the second magnetic tape (steps 18-30 inclusive).

(4) In this stage, the frequencies and mode shapes are calculated by using the method described in section 3.5. Then, the constraints are re-inserted into the eigenvector and the results are printed (steps 31-34).

As very large matrices are involved in the calculations, the same storage is used for overall stiffness and mass matrices and also the product matrix  $[K - \omega^2 M]$  in successive stages and both K and M matrices are kept in a magnetic tape during the eigenvalue evaluation stage.

The most important feature of this programme is the use of the planar type storage. The details of this storage and the requirements for the order of numbering the nodal points, some other necessary information and input data are given in Appendix B with the listings of the main routine and the other sub-routines used in the programme. This programme has also been prepared in accordance with the specifications given for the ATLAS computer at Chilton, Berkshire, U.K.

### 3.12 APPLICATION OF THE THEORY TO THE DYNAMIC ANALYSIS OF AN ARCH DAM

#### 3.12.1 The Arch Dam to be Analysed

Arch Dam Type-5, whose characteristics have been given in section 2.12.1 and has already been used for the static analysis, is to be used for the application of the theory developed in this Chapter.

#### 3.12.2 Idealization and Boundary Conditions

A-Type idealizations with five tetrahedral elements in a brick-like block are used. As the dam is symmetrical, only one half of the structure is to be taken into consideration.

The dam is divided into 8 horizontal parts, each segment having equal

height. The half of the top arch is also divided into 8 equal parts, then the intermediate arches are divided into equal parts accordingly. Only one element layer is used through thickness. This idealization is to be denoted as (8 x 1 x 8) mesh type and is shown in Figure 3.2.

The half of the dam contains 120 nodal points and 233 tetrahedral elements. 22 nodal points lay on the foundation and are assumed fixed in every direction, so that the boundary conditions at these points are

$$u = v = w = 0 \quad .$$

The origin of the Global Cartesian coordinate system is assumed situated at the centre of the reference cylinder at the bottom of the valley and the positive directions of the axis are as shown in Figure 2.1. All of the coordinates of the nodal points are calculated with respect to this coordinate system.

There are 16 nodal points on the crown cantilever, which is in the plane of symmetry. During the symmetrical vibrations of the structure, these nodal points can only move in this plane, that is the boundary conditions at these points are

$$u = 0 \quad .$$

In case of antisymmetrical vibrations, the points on the plane of symmetry can only move in the direction perpendicular to this plane, that is the boundary conditions at these points are

$$v = w = 0 \quad .$$

These boundary conditions are confirmed with the results of the analysis made on the whole structure by using a coarser mesh idealization. All of the

mode shapes obtained for these analyses resembled the mode shapes obtained by using half of the dam having the above-mentioned boundary conditions.

As each nodal point is allowed three degrees of freedom, the overall system considered consists of total 360 degrees of freedom. After the exclusion of the constraints, this number reduces to 278 for analysis of symmetrical modes and to 262 for antisymmetrical modes.

To solve an eigenvalue problem having that much degrees of freedom by conventional methods needs a computer storage approximately 250 blocks (1 block is equal to 512 words) without working space. The application of planar storage reduces the required storage for the same problem to 143 blocks. With the necessary working space for the calculations, this requirement increases up to 188 blocks, which fits the present storage of the ATLAS computer.

In this analysis, the flexibility of the foundation is also to be considered. Details of the introduction of boundary elements and the necessary revisions made in computations are explained in section 3.12.5.

### 3.12.3 Natural Frequencies and Mode Shapes of Arch Dam Type-5 on Rigid Foundation, reservoir in empty condition

The first ten natural frequencies and corresponding mode shapes computed for Arch Dam Type-5, on rigid foundation, in reservoir empty condition, are given in Figures 3.3 to 3.12. In each of these figures, the normalized deflection components of top arch, and displacements of crown cantilever and the cantilever at the mid distance between the crown and abutment are shown.

By the inspection of these figures, the vibrational modes can be divided into some groups according to the predominant component of the deflections :

(a) Radial modes: the second, third, sixth and ninth modes have the character of radial vibrations.

(b) Vertical modes: the fifth and eighth modes have shown considerable effect of vertical deflections.

(c) In the fundamental and seventh mode, the  $y$  component of deflection predominates, while these modes resemble cantilever vibrational modes.

(d) In the fourth and tenth modes, the tangential component of deflection predominates and the vibration mostly takes place in the direction perpendicular to the plane of symmetry.

The zero modal lines of horizontal deflections for each mode are shown in Figure 2.13 with the classification given above. As it can be noted that, for radial modes, the modal lines are almost in vertical direction, while for cantilever vibration the modal line is in horizontal direction. In the vertical modes, modal lines show more complex patterns. The tangential modes have modal line patterns similar to radial modes.

The three dimensional analysis introduced in this study shows that there may be some more important modes of vibrations besides the radial modes, in the frequency range interested. Among these modes, the fundamental mode contributes in the direction of  $y$  axis; the fourth mode (tangential) contributes large amount in case of excitation in direction of  $x$  axis, and the fifth mode contributes in case of vertical excitation.

#### 3.12.4 Effect of Reservoir Water

The hydrodynamic effect of the reservoir water on the dynamical characteristics of arch dams are investigated by using the results of electrolytic potential analogue described in section 3.8 and incorporating the calculated

hydrodynamic matrix in the general vibration problem as in section 3.9.

In this study no attempt has been made to apply the electrolytic analogue to obtain the hydrodynamic pressure coefficients, as these coefficients have already been determined by TAYLOR (ref.23) for Arch Dam Type-5 by using this analogy and so no advantage is to be gained by repeating the same procedures for the same structure. The radial hydrodynamic pressure coefficients which are obtained by TAYLOR are given in Figure 3.14. These coefficients are used in the following calculations and the values necessitated for the nodal points contained in (8 x 1 x 8) mesh type, the coefficients are obtained by means of interpolation.

The analysis has been carried out for the first five modes. The natural frequencies obtained are given in Table (3.1) in comparison with the frequencies obtained for the reservoir in empty condition. According to these results, the added mass effect of the reservoir water reduces the natural frequencies of Arch Dam Type-5 to 0.89~0.92 of the frequencies corresponding to the reservoir in empty condition.

The mode shapes are also modified by the hydrodynamic effect of the reservoir water. No general conclusion could be drawn from these modifications as they are solely dependent upon the corresponding mode shapes for the reservoir in empty condition. In order to give an idea about the differences between the mode shapes for the corresponding vibration modes in reservoir empty and full conditions, the normalized deflections of crown cantilever are shown in Figure 3.15 for the first three symmetrical modes.

#### 3.12.5 Effect of Boundary Flexibility

The idealization of the arch dam with its foundation included is shown in Figure 3.16. The foundation elements are so arranged that the depth

of these elements is at least 1.5 times of the thickness of the dam on the intersection surfaces.

For the half of the dam, 66 boundary points are added to the overall structure, it means that overall degrees-of-freedom reaches up to 558 and with the addition of 150 foundation elements, the overall number of elements reaches to 383. To handle a problem having 558 degrees-of-freedom is difficult even by the use of planar storage. To overcome this difficulty the programme has been modified in order not to include the stiffness and mass terms associated with the new boundary nodal points; as all of these nodal points are assumed to be fixed in every direction. This is simply done by altering the subroutine which transfers the element matrices into overall matrices, so that the terms corresponding to the new boundary points are not to be transferred. By doing this, the overall degrees-of-freedom for symmetrical modes is kept 342 and for antisymmetrical modes 324, which are fitted for the present storage capacity of ATLAS computer without any extra effort.

To demonstrate the effect of the foundation flexibility on the natural frequencies and mode shapes, four different ratios for the elasticity modulus of foundation to the elasticity modulus of concrete: 1/1, 1/2, 1/4 and 1/8 are chosen and the natural frequencies and mode shapes for only fundamental mode are calculated. The natural frequencies obtained are given in Table (3.2) and are shown in Figure 3.17. The alterations in the mode shape with respect to the flexibility of the foundation are also shown in Figure 3.18.

These results show that the flexibility of the foundation affects the natural frequencies and mode shapes considerably. The natural frequencies decrease as the flexibility of foundation increases with  $E_b/E_c = 1/8$ , the frequency reduces to 3/4 of the frequency corresponding to rigid boundary. For more flexible foundations, much more reduction in frequency is expected.

The mode shape is also altered considerably and the differences are more noticeable at the lower sections. The curvatures at these sections are getting smoother, while the tangent at the intersection point with the foundation is no longer vertical and the slope of this tangent decreases. Naturally, by the introduction of foundation elements, the point at the bottom of the structure is also allowed to move and the displacement of this point reaches to some large values as the flexibility of the foundation increases.

### 3.12.6 Computations

With the planar storage, by using the special subroutines to evaluate the determinant of  $[\dot{K} - \omega^2 M]$ , each evaluation of the determinant of a matrix of the order 278 takes slightly more than 2 minutes at the ATLAS computer. Accordingly, the computing time spent depends on the initial estimation of the root, the step size used and the number of significant figures required for the accuracy of the root. A close estimate helps to minimize the necessary steps to find out a change in the sign of the determinant and a small step size helps to minimize the necessary cycles of iterations to obtain the root with the accuracy desired.

Experience has shown that no better accuracy can be expected by using more than 8 significant figures and 6 significant figures give quite appropriate results.

With a close estimation and a small step size, the evaluation of a frequency and the modal shape takes about 10 minutes computing time, while a far estimation and a large step size may necessitate about  $\frac{1}{2}$ -hour computing time. Because of this reason the initial estimation is very important, but a good estimation needs knowledge about the variation of the determinant. This

can be done by tracing the determinant function in the frequency range desired, such a trace may provide valuable information about the approximate locations of the roots and may save a lot of computing time.

On the other hand, for making more economy in the computations, the programme given in Figure 3.1 is divided into two parts: the first part consists of the calculation of stiffness and mass matrices and writing this information into a private magnetic tape (the first 3 parts introduced in section 3.11), which takes slightly more than 4 minutes at ATLAS computer. The second part is the evaluation of frequency and mode shape (the fourth part of section 3.11), which uses directly the information stored in the private magnetic tape, so that the stage of preparing the mass and stiffness matrices is not repeated for each evaluation of a mode.

In the case of flexible boundaries, as explained in section 3.12.5, the order of the matrices is increased up to 342, which increases computing time for each evaluation of determinant up to about 3 minutes. So, the evaluation of eigenvalue problem is getting slower.

### 3.12.7 Discussion of the Results

In this Chapter the application of three dimensional finite element techniques to the dynamic analysis of arch dams by using simple tetrahedral elements has been demonstrated. The hydrodynamic effect of the reservoir water has been taken into consideration by means of the pressure coefficients obtained from electrolytic analogy and the effect of the boundary flexibility has also been investigated theoretically. However, no experimental investigations could be carried out simultaneously, the theoretical results presented in this Chapter cannot be confirmed by any experimental results. Nevertheless, there exist some experimental results carried out by other investigators which can be compared with.

OKAMOTO & TAKAHASHI (ref.28) have presented some valuable results obtained by experiments made on a prototype dam named KAMISHIIBA DAM, which has geometrical characteristics almost coinciding with Arch Dam Type-5. These characteristics are compared in Table (3.3). KAMISHIIBA DAM is slightly lower and has more thicker sections, so that it is stiffer than Arch Dam Type-5 and higher frequencies are expected.

Okamoto and Takahashi have given the first four modes obtained by means of exciting the dam radially by the application of a strong exciter positioned in proper places accordingly. These four modes exactly coincide with the first, second, third and sixth modes obtained in this study theoretically. Since KAMISHIIBA DAM was excited for all modes radially, the fourth and fifth modes obtained in this study might have been missed by Okamoto and Takahashi because of the tangential and vertical characteristics of these two modes respectively.

The existence of the modes having different characteristics other than radial modes can be traced by using three dimensional methods of analysis without any difficulty as demonstrated in this Chapter.

The natural frequencies obtained for KAMISHIIBA DAM (ref.28) and Arch Dam Type-5 (theoretically) are given in Table (3.4) comparatively. The differences between the lower modes are as large as expected due to the differences in the geometrical characteristics. Although the frequencies obtained for higher modes are closer to each other. This is due to the fact that the calculated higher frequencies may have more percentage of error, so that they are getting higher than the exact values. If the mesh size of the idealization is reduced, the errors involved in the higher frequencies are expected to become smaller.

The effect of the reservoir water on the natural frequencies has also been investigated by GAUKROGER et al (ref.27) by means of the experiments performed on the dynamical model of HENDRIK VERVOERD DAM and frequency ratios between 0.85 and 0.92 have been obtained. The prototype experiments on KAMISHIIBA DAM have provided frequency ratios 0.91 and 0.85, while the results obtained in this study for Arch Dam Type-5 are between 0.89 and 0.92 (Table 3.5). However, the hydrodynamic effect is very much dependent upon the geometrical characteristics of each particular dam, the results obtained for different structures by using different techniques are quite close to each other. This result shows that, with the exception of the dams having extremely peculiar geometrical shapes, the hydrodynamic effect of the reservoir water reduces the natural frequencies of arch dams to 0.85-0.92 of the frequencies corresponding to the reservoir in empty condition. The validities of the assumption that the hydrodynamic effect can be represented as an added mass and the use of electrolytic potential analogue technique to predict the excessive pressure coefficients, are also confirmed by these results.

No general result could be derived for the way these frequency ratios vary for lower or higher modes, as no regular decrement or increment has been noticed as the mode number increases.

Although the results given in section 3.12.5 cannot be generalized for each particular arch dam, nevertheless these results show that the flexibility of the foundation should be taken into consideration for the dynamic analysis of arch dams, especially when the in situ modulus of elasticity of the foundation is less than 1/2 of the modulus of elasticity of concrete. If this ratio is much less than 1/2, large amounts of reductions in the natural frequencies are to be expected, and if the effect of the boundary flexibility is ignored in such a case, that might cause considerable unconservative errors in response calculations, which endanger the safety of the structure.

## CHAPTER 4

### THEORY OF FORCED VIBRATION OF ARCH DAMS UNDER EARTHQUAKE EXCITATION

#### 4.1 INTRODUCTION

Providing the dynamical characteristics of the structure are known, it is possible to determine the absolute amplitudes of the responses under a prescribed excitation by means of normal mode analysis methods.

As it has already been shown in the previous chapter, the natural frequencies and mode shapes of an arch dam can be calculated by using finite element techniques which also consider the hydrodynamic effect of the reservoir water and the flexibility of the foundation rock. If the damping ratio of the system is assumed to be estimated from experiments made on prototypes, all of the necessary dynamical characteristics of the system are said to be known for response calculations.

The main difficulty met in the response calculation of a structure to earthquake ground excitation is to define the excitation itself, because of the unpredictable behaviour of the ground motion. This difficulty has led most of the investigators to use an explicit definition of the ground acceleration obtained from seismograph records of some strong earthquakes occurring in the past. In this case, assuming that the earthquake excitation is to be a deterministic transient phenomenon, the responses of the structure can be determined by means of step-by-step integration method.

In fact, the earthquake ground motions are completely random in nature, so that the calculated responses to a past earthquake cannot be used for design purposes of structures to withstand future earthquakes, and it is necessary to

describe the ground excitation in terms of probability statements and statistical averages. To satisfy these requirements, the responses of the structure must be calculated by means of a method which uses random vibration theory.

In this Chapter, firstly, the theory of normal mode analysis and the formulation of the responses of single and multi-degree of freedom systems to earthquake excitation are to be summarized. Later, random vibration theory, probabilistic and statistic relationships, and the application of these theories to the response calculations under earthquake ground excitation are to be presented.

## 4.2 NORMAL MODE ANALYSIS

### 4.2.1 Undamped Free Vibration of Multi-degrees of Freedom Systems

The equation of undamped free vibration of a multi-degree of freedom system can be written in matrix notation as :

$$[M] \{\ddot{q}\} + [K] \{q\} = 0 \quad \dots (4.1)$$

where  $[M]$  = mass matrix,

$[K]$  = stiffness matrix

$\{q\}$ ,  $\{\ddot{q}\}$  = generalized coordinates of displacements and accelerations respectively.

The use of equation (4.1) leads directly to the solution of eigenvalue problem and the  $n$  eigenvalues (natural frequencies) and eigenvectors (normal modes) can be obtained as described in Chapter 3.

The general solution of equation (4.1) contains contributions from all normal mode solutions, and a free vibration will in general take the form :

$$\left. \begin{aligned}
 q_1 &= \psi_{1I} \sin(\omega_I t + \phi_I) + \psi_{1II} \sin(\omega_{II} t + \phi_{II}) + \dots + \psi_{1N} \sin(\omega_N t + \phi_N) \\
 \cdot & \quad \cdot \quad \quad \quad \cdot \quad \quad \quad \cdot \quad \quad \quad \cdot \\
 \cdot & \quad \cdot \quad \quad \quad \cdot \quad \quad \quad \cdot \quad \quad \quad \cdot \\
 \cdot & \quad \cdot \quad \quad \quad \cdot \quad \quad \quad \cdot \quad \quad \quad \cdot \\
 \cdot & \quad \cdot \quad \quad \quad \cdot \quad \quad \quad \cdot \quad \quad \quad \cdot
 \end{aligned} \right\} \dots (4.2)$$

$$q_n = \psi_{nI} \sin(\omega_I t + \phi_I) + \psi_{nII} \sin(\omega_{II} t + \phi_{II}) + \dots + \psi_{nN} \sin(\omega_N t + \phi_N)$$

where  $\omega_I, \omega_{II}, \dots, \omega_N$  = natural frequencies,

$(\psi_1; \psi_2; \dots; \psi_n)_I, (\psi_1; \psi_2; \dots; \psi_n)_{II}, \dots$  = normal modes,

$\phi_I, \phi_{II}, \dots, \phi_N$  = phase angles.

It is clearly seen that in equation (4.1) all the generalized coordinates appear in all the equations, in general, so that there is always coupling between the coordinates and also equation (4.2) uses  $n^2$  terms. It becomes much easier to handle the problem if it is considered not as a set of  $n^2$  terms but as a summation of  $n$  simple harmonic motions. This simplification forms the basis of normal mode analysis.

#### 4.2.2 Normal Coordinates

The coupling terms in equation (4.1) arise from the product terms. But it can be shown that there can always be found another set of generalized coordinates which is denoted by  $\xi_1, \xi_2, \dots, \xi_N$  such that there are no product terms, so coupling cannot occur.

For small displacements, any set of generalized coordinates can be expressed in terms of any other by a linear transformation :

$$\{q\} = [d] \{\xi\} \dots (4.3)$$

It is possible to choose the  $n^2$  coefficients  $d_{rs}$  in any way and to satisfy the condition that the  $(n^2 - n)$  coefficients  $m_{rs}, k_{rs}$  of the product terms are

zero. If this is done, by writing the kinetic and potential energy formulas of the system and applying Lagrange's equation, Equation (4.1) becomes :

$$[\mathcal{M}] \{\ddot{\xi}\} + [\mathcal{K}] \{\xi\} = 0 \quad \dots (4.4)$$

where  $[\mathcal{M}]$  and  $[\mathcal{K}]$  are diagonal matrices of generalized mass and generalized stiffness.

Each separate equation of equation (4.4) is now identical to that obtained for a simple spring-mass system. Each equation has its own solution with its own natural frequency,  $\omega_r = \sqrt{k_r/m_r}$  and the value of each  $\xi_r$  represents the contribution of the  $r^{\text{th}}$  normal mode. Such  $\xi_r$  are known as normal (principal) coordinates.

Now, supposing a system to be vibrating in, say, its first normal mode, then  $\xi_2 = \xi_3 = \dots = \xi_n = 0$  and from equation (4.3) it can be seen that

$$\{q\} = \{d_{i1}\} \cdot \xi_1 \quad \dots (4.5)$$

and so, the ratio of the coefficient d's in any one column of equation (4.3) gives the shape of the normal mode corresponding to its  $\xi_r$ , thus

$$\{q\} = [\Phi] \{\xi\} \quad \dots (4.6)$$

where,  $[\Phi] = [\{\psi_I\}, \{\psi_{II}\}, \dots, \{\psi_N\}]$  is modal matrix.

#### 4.2.3 Forced Vibration of Multi-degree-of-freedom Systems

In case of forced vibration, a vector of external forces  $[Q]$  must be replaced on the right-hand-side of equation (4.1),

$$[M] \{\ddot{q}\} + [K] \{q\} = \{Q\} \quad \dots (4.7)$$

and so, a vector of generalized forces  $\{E\}$  must be replaced on the right hand side of equation (4.4)

$$[M] \{\ddot{\xi}\} + [K] \{\xi\} = \{E\} \quad \dots (4.8)$$

The generalized forces  $E_r$  are defined such that

$$\sum_j Q_j \cdot \delta q_j = \sum_r E_r \cdot \delta \xi_r \quad \dots (4.9)$$

and so, each equation of (4.8) would then represent forced vibration in one of the normal modes.

#### 4.2.4 The Effect of Damping

The effect of viscous damping can be allowed for in Lagrange's equations either by inserting suitable  $Q_j$  on the right hand sides or by adding terms  $\frac{\partial F}{\partial \dot{q}_j}$  on the left hand sides (where  $F$  is a quantity often called the dissipation function). As  $F$  can be shown to be similar in form to the kinetic energy  $T$  it can for small motions be expanded in the same way, and so

$$F = \frac{1}{2} [\dot{q}]^T [C] \{\dot{q}\} \quad \dots (4.10)$$

for a system having  $n$  degrees of freedom, where  $[C]$  is the damping matrix and again for small vibrations  $c_{rs}$  can be considered constant.

Now using the general form of Lagrange's equation

$$\frac{d}{dt} \left( \frac{\partial T}{\partial \dot{q}_j} \right) - \frac{\partial T}{\partial q_j} + \frac{\partial F}{\partial \dot{q}_j} + \frac{\partial V}{\partial q_j} = Q_j \quad \dots (4.11)$$

the general equation of motion is obtained as :

$$[M] \{\ddot{q}\} + [C] \{\dot{q}\} + [K] \{q\} = \{Q\} \quad \dots (4.12)$$

By the introduction of normal coordinates, equation (4.12) becomes

$$[\mathcal{M}] \{\ddot{\xi}\} + [\mathcal{C}] \{\dot{\xi}\} + [\mathcal{K}] \{\xi\} = \{E\} \quad \dots (4.13)$$

As it is described in section 4.2.2  $[\mathcal{M}]$  and  $[\mathcal{K}]$  matrices are diagonal, but it is not in general possible at the same time to express  $F$  without product terms, so that the  $[\mathcal{C}]$  matrix generally includes non-diagonal terms. However, if damping is small, it is permissible to neglect the coupling effect arising from the product terms, in which case the equation of motion becomes

$$[\mathcal{M}] \{\ddot{\xi}\} + [\mathcal{C}] \{\dot{\xi}\} + [\mathcal{K}] \{\xi\} = \{E\} \quad \dots (4.14)$$

Again, each equation of (4.14) is identical in form to that obtained for a simple spring-mass-dashpot system and all of the results obtained for that simple system can be applied to each individual modal system of the multi-degree-of-freedom system.

#### 4.3 RESPONSE OF LINEAR SINGLE DEGREE OF FREEDOM SYSTEM TO EARTHQUAKE EXCITATION

As it is mentioned in the previous section, the formulae derived for the single-degree-of-freedom system can be applied to multi-degree-of-freedom system without any difficulty, considering that the normal modes can be treated separately as individual simple structures. According to this consideration, the response of linear single-degree-of-freedom system to earthquake excitation is to be analyzed firstly.

The mathematical model of a linear single-degree-of-freedom system subjected to ground motion excitation is shown in Figure 4.1. The equation of motion can be written as :

$$-m\ddot{y} - k(y - u_g) - c(\dot{y} - \dot{u}_g) = 0 \quad \dots (4.15)$$

where  $m$  = the mass of the system  
 $k$  = the stiffness of the system  
 $c$  = the viscous damping of the system  
 $y$  = the absolute displacement  
 $u_g$  = ground displacement  
 $x$  = displacement relative to the base.

From the engineering point of view, the relative displacements are of more importance as the stresses developed in the structure are directly related with the relative displacements. As the relative, absolute and ground displacements are related with

$$x = y - u_g \quad \dots (4.16)$$

substituting equation (4.16) into equation (4.15) :

$$-m(\ddot{x} + \ddot{u}_g) - kx - c\dot{x} = 0 \quad \dots (4.17)$$

and it follows that

$$m\ddot{x} + c\dot{x} + kx = -m\ddot{u}_g \quad \dots (4.18)$$

It is seen from this equation that the relative motion  $x$  is the same as that for a structure resting on a fixed base and subjected to a horizontal force  $-m\ddot{u}_g$ .

Dividing both sides of equation (4.18) by  $m$  :

$$\ddot{x} + 2\zeta\omega_0\dot{x} + \omega_0^2x = -\ddot{u}_g \quad \dots (4.19)$$

is obtained where

$$\omega_0 = \sqrt{\frac{k}{m}} \text{ is the natural circular frequency}$$

$$\text{and } \zeta = \frac{c}{2\omega_0 m} \text{ is the fraction of critical damping.}$$

The solution of equation (4.19) can be obtained as if the earthquake acceleration time history  $\ddot{u}_g(t)$  is considered motions consisting of random arrays of concentrated acceleration pulses. The motion is assumed to begin from the rest. By using Duhamel's integral, the equation for the displacement of the mass  $m$  relative to the base, when the base is given an arbitrary horizontal acceleration is obtained as :

$$x = -\frac{1}{p} \int_0^t \ddot{u}_g(\tau) e^{-\omega_0 \zeta (t-\tau)} \sin p (t-\tau) d\tau \quad \dots (4.20)$$

where  $t$  = time at which  $x$  is evaluated,

$\tau$  = time variable of integration,

$p = \omega_0 \sqrt{1 - \zeta^2}$  damped natural frequency.

The numerical evaluation of equation (4.20) is rendered troublesome by the fact that  $\ddot{u}_g(t)$  is a complicated function requiring 500-1000 points to define it, and by the requirement that a maximum value at some unknown time must be determined by scanning the total response time for each point.

For this reason, analogue computation techniques are particularly well suited to such response calculation, and since 1941 many attempts have been made on this area. Firstly in 1941, BIOT (ref.64) introduced a mechanical analogue in the form of a torsion pendulum. Next, in 1949, HOUSNER & McCANN (ref.65) developed an electric analogue computer which is much more convenient and greatly speeded up the process and increased the accuracy. Lately, this type of electric analogue computer has been further developed by CAUGHEY et al (ref. 66) and is being used regularly in earthquake response spectrum analysis.

Besides the analogue computation techniques, in spite of the above-mentioned difficulties, the recent developments of the high speed digital

computers has made the numerical evaluation possible. Although there are still difficulties in digitizing the recorded earthquake accelerograms, many efforts are being made to overcome this difficulty (ref.67 and 68).

#### 4.4 CALCULATION OF RESPONSES FROM STEP BY STEP INTEGRATION OF GROUND ACCELERATION

The theoretical derivation of the response of a linear, elastic, multi-degree of freedom system to any given external dynamic excitation can be performed using normal mode analysis and the convolution integral by means of, so called, step-by-step integration method used by CLOUGH (ref.30) for earth dams and lately applied to arch dam vibrations by TAYLOR (ref.23) successfully.

The general equation of motion including damping, earthquake acceleration and the hydrodynamic effects can be written :

$$[\bar{M}] \{\ddot{q}\} + [\bar{C}] \{\dot{q}\} + [\bar{K}] \{q\} = - [\bar{M}] \{\ddot{u}_g(t)\} \quad \dots (4.21)$$

where  $[\bar{M}]$  is the effective inertia matrix including the hydrodynamic effects of the reservoir water as described in section 3.9.

With the introduction of the transformation of equation (4.6), equation (4.21) becomes :

$$[\bar{M}] [\bar{\Phi}] \{\ddot{\xi}\} + [\bar{C}] [\bar{\Phi}] \{\dot{\xi}\} + [\bar{K}] [\bar{\Phi}] \{\xi\} = - [\bar{M}] \{\ddot{u}_g(t)\} \quad \dots (4.22)$$

By premultiplication of both sides by the transpose of the model matrix  $[\bar{\Phi}]^T$ ,

$$\begin{aligned} [\bar{\Phi}]^T [\bar{M}] [\bar{\Phi}] \{\ddot{\xi}\} + [\bar{\Phi}]^T [\bar{C}] [\bar{\Phi}] \{\dot{\xi}\} + [\bar{\Phi}]^T [\bar{K}] [\bar{\Phi}] \{\xi\} \\ = - [\bar{\Phi}]^T [\bar{M}] \{\ddot{u}_g(t)\} \quad \dots (4.23) \end{aligned}$$

where  $[\bar{\Phi}]^T$  denotes the transposed matrix.

According to the orthogonality relationship, by this transformation the inertia and the stiffness matrices are reduced to diagonal form. Although, even after this transformation, the damping matrix generally contains non-diagonal terms, in case of lightly damped structures, the product damping matrix is also assumed to be reduced to diagonal form, so that equation (4.23) can be written in terms of generalised matrices :

$$[\mathcal{M}]\{\ddot{\xi}\} + [\mathcal{C}]\{\dot{\xi}\} + [\mathcal{K}]\{\xi\} = -[\Phi]^T [M] \{\ddot{u}_g(t)\} \quad \dots (4.24)$$

This equation is identical to equation (4.14) and the right-hand-side of this equation represents the generalised force vector in case of earthquake type excitation, which is denoted by  $\{E\}$  as follows :

$$\{E\} = -[\Phi]^T [M] \{\ddot{u}_g(t)\} \quad \dots (4.25)$$

Now it is possible to consider each normal mode of equation (4.24) as an independent vibratory system and to calculate the responses of each mode by applying the results obtained for single degree-of-freedom system in section 4.3.

Let the equation (4.24) be rewritten for the  $r^{\text{th}}$  normal mode :

$$\mathcal{M}_r \ddot{\xi}_r + \mathcal{C}_r \dot{\xi}_r + \mathcal{K}_r \xi_r = -[\psi_r]^T [M] \{\ddot{u}_g(t)\} \quad \dots (4.26)$$

where

$$\mathcal{M}_r = [\psi_r]^T [M] \{\psi_r\} \quad \dots (4.27)$$

is called the generalized mass of the  $r^{\text{th}}$  mode, and  $\{\psi_r\}$  is the eigenvector of the  $r^{\text{th}}$  mode. Dividing both sides of equation (4.26) by  $\mathcal{M}_r$  :

$$\ddot{\xi}_r + 2\zeta_r \omega_r \dot{\xi}_r + \omega_r^2 \xi_r = -\frac{1}{\mathcal{M}_r} [\psi_r]^T [M] \{\ddot{u}_g(t)\} \quad \dots (4.28)$$

where

$\omega_r$  = the undamped natural frequency of  $r^{\text{th}}$  mode,

$\zeta_r$  = fraction of critical damping in  $r^{\text{th}}$  mode.

As it is easily seen, equation (4.19) and equation (4.28) are identical in form and so, by the application of the same treatment as for the single-degree-of-freedom system, the response of the  $r^{\text{th}}$  mode can be obtained :

$$\xi_r = -\frac{1}{p_r \mathcal{M}_r} [\psi_r]^T [M] \left\{ \int_0^t \ddot{u}_g(\tau) e^{-\omega_r \zeta_r (t-\tau)} \sin p_r (t-\tau) d\tau \right\} \dots (4.29)$$

where  $p_r = \omega_r \sqrt{1 - \zeta_r^2}$  is the damped natural frequency.

By inspection of equation (4.29) it can be seen that the maximum relative response of  $r^{\text{th}}$  mode depends upon the integral and becomes maximum when

$$\int_0^t \frac{\ddot{u}_g(\tau) e^{-\omega_r \zeta_r (t-\tau)} \sin p_r (t-\tau) d\tau}{p_r} \dots (4.30)$$

reaches to its maximum. The maximum value of this term can be expressed as "the relative displacement response spectrum" for a given ground acceleration  $\ddot{u}_g(t)$  and is denoted by  $S_d$ .

$$S_d = \left[ \int_0^t \frac{\ddot{u}_g(\tau) e^{-\omega_r \zeta_r (t-\tau)} \sin p_r (t-\tau) d\tau}{p_r} \right]_{\max} \dots (4.31)$$

The time history and the maximum values of each modal response,  $\xi_r$ , can be calculated from equations (4.29) and (4.31), and the total amplitudes at time  $t$ , may be obtained by the use of the transformation

$$\{q(t)\} = [\phi] \{\xi(t)\} \dots (4.32)$$

Equation (4.29) may be evaluated by means of "step-by-step" integration method and the time histories of total displacements may be obtained by using equation (4.32). The total maximum values of displacements can be determined by scanning these time histories. The evaluation of this process has been described by several authors (ref.23,30) in detail and will not be considered here.

Although, assuming that the earthquake excitation is a deterministic transient phenomenon, so that  $\ddot{u}_g(t)$  can be described explicitly, the step-by-step integration method gives the exact solution for the responses of multi-degree-of-freedom systems to a given earthquake excitation, the calculations involved are tedious and show considerable difficulties. On the other hand, this method can only provide the responses to a recorded accelerogram of a particular past earthquake. No doubt, the earthquake ground motions are completely unpredictable and the calculated responses to a past earthquake cannot be used for design purposes of structures to withstand future earthquakes, because of the necessity that the phenomena having random nature must be described in terms of probability statements and statistical averages.

For this reason, in the next sections, the general results obtained for the responses of structures to general type of random excitations are to be presented briefly and the application possibilities of these results to earthquake type of excitation are to be discussed.

#### 4.5 GENERAL THEORY OF STATIONARY RANDOM VIBRATIONS

4.5.1 A random vibration is one whose instantaneous value is not predictable in advance, and it is essential to its nature that any relationship between the magnitude of the quantity and time, measured during a certain

interval, will never exactly recur in any other. Although the time variation of a random vibration cannot be predicted, if the physical quantities which vary in a random manner do exhibit a degree of statistical regularity, in other words, the random variable does possess the properties of stationarity, then it is possible to predict the probability of a given value being within a certain range, on a statistical basis.

The general statistical theory of random processes is a very large subject, so that, it is not to be included herein and the reader is referred to the text books written on this subject (ref.69,70). Most of the formulae developed in this section shall be based directly on the results of the previous works that are summarized in these text books.

However, the "power spectral density" of the randomly varying quantity plays the most important part in this analysis. Accordingly, the concept of the power spectral density and its properties shall be described briefly. On the other hand, definitions of the other important quantities and their relationships are to be given in Appendix (A.5).

#### 4.5.2 Power Spectral Density: Definition and Determination

In case of a harmonic vibration, the power, which is the rate of doing work, is proportional to the square of the amplitude of the vibration. If two frequencies are present in a vibration, the power is proportional to the sum of the squares of the individual amplitudes associated with two frequencies.

A random vibration can be considered to be a sum of a large number (tending to infinity) of harmonic vibrations of appropriate amplitudes and phase. The total power is again the sum of the power of the component harmonic vibrations, and it is of interest to know how this power is distributed

as a function of frequency. Therefore "power spectral density" is defined as the power per unit frequency interval. A plot of this quantity indicates the frequency distribution of power.

The analysis of random vibration always involves a record of finite length. Assuming that such a record has been produced on a magnetic tape and is to be analyzed by an electronic analyzer as a stationary process, the tape can be formed into a loop of arbitrary length and made to repeat indefinitely on the analyzer. By such a procedure, an arbitrary fundamental period corresponding to the length of the loop is established, and the contents of the record may be defined in terms of the Fourier coefficients of integral multiple harmonics of the loop frequency  $\omega_1$ .

The periodic function  $x(t)$  then can be represented by the real part of the Fourier series

$$x(t) = \sum_{r=-\infty}^{\infty} C_r e^{ir\omega_1 t} \quad \dots (4.33)$$

where the complex amplitude  $C_r$  is defined by the equation

$$C_r = \frac{1}{T} \int_{-T/2}^{T/2} x(t) e^{ir\omega_1 t} dt \quad \dots (4.34)$$

and  $T$  is the loop period.

The mean-square value of  $x(t)$ , which is a stationary property of  $x(t)$  can be determined in terms of the coefficients, as

$$\begin{aligned} \langle x^2(t) \rangle &= \frac{1}{T} \int_{-T/2}^{T/2} x^2(t) dt = \sum_{r=-\infty}^{\infty} |C_r|^2 \\ &= C_0^2 + 2 \sum_{r=1}^{\infty} |C_r|^2. \end{aligned} \quad \dots (4.35)$$

This equation indicates that the contribution to the mean-square value in any frequency interval is the summation of all the components within that frequency band.

If now the length of the loop and the loop period are doubled, the number of spectral lines will be doubled. Since the mean-square value of the entire spectrum must remain essentially constant, the values of the new coefficients  $|C'_r|^2$  must decrease to approximately one-half their former values, as shown in Figure 4.2. The sum of the lengths of the  $|C_r|^2$  lines, up to any frequency, is the same in each diagram of Figure 4.2, and the increment in  $\langle x^2(t) \rangle$  divided by the increment in frequency is essentially the same in each case,

$$\frac{\Delta \langle x^2(t) \rangle}{\Delta \omega} = \frac{2 |C_r|^2}{\omega_1} = \frac{2 |C'_r|^2}{\frac{1}{2} \omega_1} = S(\omega_r) \quad \dots (4.36)$$

The quantity  $S(\omega_r)$  is the "power spectral density" at  $\omega = \omega_r$ . The dimensions are the square of the parameter represented by  $\Delta \langle x^2(t) \rangle$  in equation (4.36) per unit of frequency.

As the length of the loop is increased, more and more spectral lines are introduced; the magnitude of  $|C_r|^2$  decreases correspondingly, but  $S(\omega_r)$  remains finite. In the limiting case, as  $T \rightarrow \infty$  or  $\Delta \omega \rightarrow 0$ , the spectrum becomes continuous, and the discrete values of  $S(\omega_r)$  approach a smooth function  $S(\omega)$  :

$$S(\omega) = \lim_{\Delta \omega \rightarrow 0} \frac{\Delta \langle x^2(t) \rangle}{\Delta \omega} = \frac{d \langle x^2(t) \rangle}{d\omega} \quad \dots (4.37)$$

The mean-square value can be expressed by the integral

$$\langle x^2(t) \rangle = \int_0^{\infty} S(\omega) d\omega \quad \dots (4.38)$$

The power spectral density of a random time function may be determined by feeding the function  $x(t)$  into a spectrum analyzer that transmits only those frequency components within the passband of the analyzer,  $\bar{\omega} \pm \frac{1}{2} \Delta\omega$ . The output in the passband, namely,  $\Delta\langle x^2(t) \rangle$  is then indicated by a "mean-square" meter (figure 4.3). The mean power spectral density  $S(\bar{\omega})$  over the pass band, at  $\bar{\omega}$ , is determined by dividing the meter reading by  $\Delta\omega$ . This division may be incorporated directly in the calibration of the meter. The complete distribution of  $S(\omega)$  then is determined by changing the frequency  $\bar{\omega}$  in increments of  $\Delta\omega$ .

#### 4.5.3 Relationship between the Power Spectral Densities of Input (Loading) and Output (Response)

The relationship between the input (loading) and output (response) of a linear system for any time function  $P(t)$ , whether random or not, may be expressed in terms of Duhamel's (convolution) integral

$$x(t) = \int_{-\infty}^t P(\tau) h(t-\tau) d\tau = \int_0^{\infty} h(\tau) P(t-\tau) d\tau \quad \dots (4.39)$$

where  $h(t)$  is the response of the system to a unit impulse  $\delta(t)$  which represents Dirac's delta function, and  $P(t)$  is the input forcing, which may have existed from  $t = -\infty$ . In the usual form of the above integral, the input is assumed to be zero for  $t < 0$ , in which case the range of integration becomes 0 to  $t$  in both integrals.

The spectral aspects of the system are defined by a response function which is directly significant only for harmonic excitation. Letting  $P(t) = e^{i\omega t}$  represent such a harmonic excitation, and noting that there is no provision for starting or stopping such a function, its substitution into equation (4.39) results in the following :

$$\begin{aligned}
x(t) &= \int_0^{\infty} e^{i\omega(t-\tau)} h(\tau) d\tau = e^{i\omega t} \int_0^{\infty} e^{-i\omega\tau} h(\tau) d\tau \\
&= \frac{1}{Z(i\omega)} e^{i\omega t} \dots (4.40)
\end{aligned}$$

where

$$\frac{1}{Z(i\omega)} = \int_0^{\infty} e^{-i\omega\tau} h(\tau) d\tau \dots (4.41)$$

is defined as the complex response function, or simply the receptance of the system. Since  $h(\tau)$  is assumed to be zero for  $\tau < 0$ , the receptance is the Fourier transform of the impulsive response function  $h(\tau)$ .

It is often desirable to work in terms of actual frequency  $f$ , rather than the circular frequency. In such cases the symbol  $1/Z(i\omega)$  for receptance may be replaced by  $1/Z(if)$ , then equation (4.41) becomes :

$$\frac{1}{Z(if)} = \int_0^{\infty} e^{-i2\pi f\tau} h(\tau) d\tau \dots (4.42)$$

If the spectral density of the forcing function  $P(t)$  is denoted by  $S_p(f)$ , and also the spectral density of the resulting displacement  $x(t)$  is denoted by  $S_x(f)$ , by means of using the above definitions and the relationships of the auto-correlation functions given in Appendix (A.5), it can be shown (ref.70) that, the power spectral densities of excitation and response are related by

$$S_x(f) = \left| \frac{1}{Z(if)} \right|^2 S_p(f) \dots (4.43)$$

where  $\left| \frac{1}{Z(if)} \right|^2$  denotes the modulus squared (See Appendix (A.6)).

This is a particularly simple relationship, so that the spectral density of the displacement at any frequency is equal to the spectral density of the excitation multiplied by the modulus squared of the receptance of the system at that frequency. The receptance of a system can always be determined in terms of frequency, either analytically or by measuring the response experimentally over the frequency range, and as it is concerned only with the modulus  $|\frac{1}{Z(if)}|$ , the experimental determination need not concern itself with phase and a straightforward response curve is sufficient.

In order to illustrate the relationship of equation (4.43), the actual quantities  $P(t)$  and  $x(t)$ , the spectrum  $S_p(f)$  of the input force  $P(t)$ , the response curve (receptance) obtained by discrete frequency excitation and the spectral density  $S_x(f)$  of the resulting displacement  $x(t)$  are shown in Figure 4.4 which are obtained using an analogue computer circuit to simulate a system having two degrees of freedom and fairly heavy damping (ref.70).

Once the spectral density of the output has been found by equation (4.43) there is no difficulty in principle in obtaining other related quantities such as the mean-square value by equation (4.38).

#### 4.5.4 The Response of a Three-Dimensional System subjected to Distributed Random Excitation.

4.5.4.1 The evaluation of the response calculations of a three-dimensional system subjected to distributed random excitation is involved, lengthy and tedious formulation (see Appendix (A.6)). To avoid the longest part of this evaluation, the primary formulation shall not be included herein and the evaluation is to be started from the results already existing in literature.

4.5.4.2 Consider a three-dimensional body of volume  $V$ , as shown in Figure 4.5 subjected to a distributed dynamic loading represented by discrete loads acting at points  $\alpha(x_\alpha, y_\alpha, z_\alpha)$ ,  $\beta(x_\beta, y_\beta, z_\beta)$ , ... in, say,  $x$  direction of intensities  $P_x(\alpha, t)$ ,  $P_x(\beta, t)$  ... These loads can be assumed either the inertia loads distributed in the volume or any external forces acting on the surface of the body. It is desired to determine the response  $w_x(l, t)$  of the point "l" which is at  $x = x_1$ ,  $y = y_1$  and  $z = z_1$ , for example in  $x$  direction. In the analysis it will be convenient to refer loadings at two representative positions  $\alpha(x_\alpha, y_\alpha, z_\alpha)$  and  $\beta(x_\beta, y_\beta, z_\beta)$ . Now it is possible, for example, to denote receptances by  $1/Z_{1\alpha}^x$  (if),  $1/Z_{1\beta}^z$  (if), that is, giving the response at point  $l(x_1, y_1, z_1)$  in  $x$  direction, to concentrated point loading  $e^{i\omega t}$  at the point  $\alpha(x_\alpha, y_\alpha, z_\alpha)$  acting in, say,  $y$  direction, and at the point  $\beta(x_\beta, y_\beta, z_\beta)$  acting in, say,  $z$  direction. For simplicity, the analysis shall be continued with the assumption that all of the loads are acting only in one specified direction and also only one of the three response components of point  $l$  is to be taken into account. That can be done without losing the generality of the problem. According to the above considerations, the receptances can be re-written as  $1/Z_{1\alpha}^x$  (if) and  $1/Z_{1\beta}^z$  (if) respectively and the response as  $w(l, t)$ .

In specifying cross-spectral densities, it becomes necessary to adopt a more explicit set of symbols which will distinguish between displacements and loads. Therefore,  $S_w(\alpha, \beta; f)$  is used to represent the cross-spectral density of the displacements,  $w(\alpha, t)$ ,  $w(\beta, t)$  and  $S_p(\alpha, \beta; f)$  to represent the cross-spectral density of the discrete loads  $P(\alpha, t)$ ,  $P(\beta, t)$ . The direct spectral densities will be denoted by  $S_w(\alpha, f)$  and  $S_p(\alpha, f)$  respectively.

The corresponding cross-correlation and auto-correlation functions will be denoted by  $R_w(\alpha, \beta; \tau)$ ,  $R_p(\alpha, \beta; \tau)$ ,  $R_w(\alpha, \tau)$  and  $R_p(\alpha, \tau)$  respectively.

The cross-correlation function and cross-spectral density of the discrete loading are, by definition :

$$R_p(\alpha, \beta; \tau) = \langle P(\alpha, t) P(\beta, t + \tau) \rangle \quad \dots (4.44)$$

and

$$S_p(\alpha, \beta; f) = 2 \int_{-\infty}^{\infty} R_p(\alpha, \beta; \tau) e^{-i2\pi f \tau} d\tau \quad \dots (4.45)$$

It can be shown, (ref.70) that the response can be expressed in terms of these quantities; that is, the spectral density of the motion  $w(l, t)$  under the discrete loading  $P(\alpha, t)$ ,  $P(\beta, t)$  ....., acting at points  $\alpha$ ,  $\beta$ , ....., is given by (Appendix (A.6)),

$$S_w(l, f) = \sum_{\alpha=1}^{\infty} \sum_{\beta=1}^{\infty} \frac{1}{Z_{1\alpha}^*(if) \cdot Z_{1\beta}(if)} S_p(\alpha, \beta; f) \quad \dots (4.46)$$

where "\*" denotes complex conjugate.

Equation 4.46 can be expanded by expressing the receptances in terms of the normal mode shapes and system constants (Appendix (A.6)) :

$$\frac{1}{Z_{1\alpha}(if)} = \sum_r \frac{\psi_r(l) \psi_r(\alpha)}{4 \pi^2 \mathcal{M}_r (f_r^2 - f^2 + i2\zeta_r f_r f)} \quad \dots (4.47)$$

where :  $r$  = normal mode number

$\psi_r$  = the normal mode shape of  $r^{\text{th}}$  mode,

$\mathcal{M}_r$  = the generalized mass in  $r^{\text{th}}$  mode (as equation 4.27)

$f_r$  =  $\frac{\omega_r}{2\pi}$  natural frequency of  $r^{\text{th}}$  mode

$\zeta_r$  = fraction of critical damping in  $r^{\text{th}}$  mode.

By substituting equation (4.47) into equation (4.46) and changing the orders of summations

$$S_w(1,f) = \sum_r \sum_s \frac{\psi_r(1) \psi_s(1)}{16\pi^4 \mathcal{M}_r \mathcal{M}_s (f_r^2 - f^2 - i2\zeta_r f_r f) (f_s^2 - f^2 + i2\zeta_s f_s f)} \times \sum_\alpha \sum_\beta \psi_r(\alpha) \psi_s(\beta) S_p(\alpha, \beta; f) \dots (4.48)$$

If the damping is small and the natural frequencies of the system are well separated, it is convenient to approximate equation (4.48) by neglecting the product terms, which contain imaginary parts and make the problem much more difficult to handle; and then only the contribution from the individual modes needs to be taken into consideration. With this simplification, equation (4.48) becomes :

$$S_w(1,f) = \sum_r \left[ \frac{\psi_r^2(1)}{16\pi^4 \mathcal{M}_r^2 [(f_r^2 - f^2)^2 + 4\zeta_r^2 f_r^2 f^2]} \times \sum_\alpha \sum_\beta \psi_r(\alpha) \psi_r(\beta) S_p(\alpha, \beta; f) \right] \dots (4.49)$$

4.5.4.3 Equation (4.49) is the general formula that gives the spectral density of the motion at any point in terms of the cross-spectral densities of the discrete loading; and of the receptances of the system. Until now, no assumption is made about the way in which the loading intensities at different points are correlated, although, only it is assumed that there is a stationary cross-correlation between the intensities at any

two points, and that this can be described by means of the cross-spectral density  $S_p(\alpha, \beta; f)$  for every pair of points  $\alpha, \beta$ .

Now if it is assumed that there is direct correlation, so that the loading intensities at all points vary proportionally to a single randomly varying quantity  $\phi(t)$ , it is possible to express the loading intensities as

$$\left. \begin{aligned} P(\alpha, t) &= P_0(\alpha) \phi(t) \\ \text{and } P(\beta, t) &= P_0(\beta) \phi(t) \end{aligned} \right\} \dots (4.50)$$

It follows that :

$$R_p(\alpha, \beta; \tau) = \langle P_0(\alpha) \phi(t) P_0(\beta) \phi(t+\tau) \rangle = P_0(\alpha) P_0(\beta) R_\phi(\tau) \dots (4.51)$$

where  $R_\phi(\tau)$  is the autocorrelation function of  $\phi(t)$ ; and so, the cross-spectral density of the loading becomes :

$$S_p(\alpha, \beta; f) = P_0(\alpha) P_0(\beta) S_\phi(f) \dots (4.52)$$

where  $S_\phi(f)$  is the spectral density of  $\phi(t)$ .

Substituting equation (4.52) into equation (4.46) :

$$\begin{aligned} S_w(l, f) &= \sum_{\alpha} \sum_{\beta} \frac{1}{Z_{1\alpha}^*(if) \cdot Z_{1\beta}(if)} P_0(\alpha) P_0(\beta) S_\phi(f) \\ &= \sum_{\alpha} \frac{1}{Z_{1\alpha}^*(if)} P_0(\alpha) \cdot \sum_{\beta} \frac{1}{Z_{1\beta}(if)} P_0(\beta) S_\phi(f) \\ &= \left| \sum_{\alpha} \frac{1}{Z_{1\alpha}(if)} P_0(\alpha) \right|^2 S_\phi(f) \dots (4.53) \end{aligned}$$

is obtained, where  $| \quad |^2$  denotes the modulus square.

Substituting the receptances into equation (4.53) and changing the order of summations :

$$\begin{aligned}
 S_w(1,f) &= \left| \sum_{\alpha} \sum_r \frac{\psi_r(1) \psi_r(\alpha)}{4\pi^2 \mathcal{M}_r (f_r^2 - f^2 + i2\zeta_r f_r f)} P_o(\alpha) \right|^2 S_{\phi}(f) \\
 &= \left| \sum_r \frac{\psi_r(1)}{4\pi^2 \mathcal{M}_r (f_r^2 - f^2 + i2\zeta_r f_r f)} \sum_{\alpha} \psi_r(\alpha) P_o(\alpha) \right|^2 S_{\phi}(f) \dots (4.54)
 \end{aligned}$$

As in equation (4.48) the above formula contains product terms of different modes which consist of imaginary parts. Again, by the assumptions that the damping is small and the peaks are well separated, these product terms can be neglected and equation (4.54) is approximated as :

$$S_w(1,f) = \left[ \sum_r \frac{\psi_r^2(1)}{16\pi^4 \mathcal{M}_r^2 [(f_r^2 - f^2)^2 + 4\zeta_r^2 f_r^2 f^2]} \left[ \sum_{\alpha} \psi_r(\alpha) P_o(\alpha) \right]^2 \right] S_{\phi}(f) \dots (4.55)$$

4.5.4.4 Further with the addition to the assumptions introduced in section 4.5.4.3, if the randomly varying quantity  $\phi(t)$  is considered to move past the structure at a constant velocity  $v_x$ , so that different points experience the same randomly varying quantity but with time-lags corresponding to their positions. In such a case :

$$\left. \begin{aligned}
 P(\alpha,t) &= P_o(\alpha) \phi(t) \\
 \text{and } P(\beta,t) &= P_o(\beta) \phi(t + \tau_o)
 \end{aligned} \right\} \dots (4.56)$$

where  $\tau_o = \frac{x_{\beta} - x_{\alpha}}{v_x}$  is the time lag between points  $\alpha$  and  $\beta$ ;  $x_{\beta}$  and  $x_{\alpha}$  are the coordinates of the points in the direction of the component the quantity velocity considered (here it is assumed that the quantity is acting in  $x$  direction).

From this definition, it follows that :

$$\begin{aligned}
 R_p(\alpha, \beta; \tau) &= \langle P_o(\alpha) \phi(t) P_o(\beta) \phi(t + \tau_o + \tau) \rangle \\
 &= P_o(\alpha) P_o(\beta) R_\phi(\tau_o + \tau) \quad \dots (4.57)
 \end{aligned}$$

then the cross-spectral density of the loading becomes :

$$\begin{aligned}
 S_p(\alpha, \beta; f) &= 2 \int_{-\infty}^{\infty} P_o(\alpha) P_o(\beta) R_\phi(\tau_o + \tau) e^{-i2\pi f \tau} d\tau \\
 &= 2 P_o(\alpha) P_o(\beta) e^{i2\pi f \tau_o} \int_{-\infty}^{\infty} R_\phi(\tau_o + \tau) e^{-i2\pi f(\tau_o + \tau)} d(\tau_o + \tau) \\
 &= P_o(\alpha) P_o(\beta) e^{i2\pi f \tau_o} S_\phi(f) \quad \dots (4.58)
 \end{aligned}$$

where  $S(f)_\phi$  is the spectral density of  $\phi(t)$ .

Substituting equation (4.58) into the general equation of the spectral density of response, equation (4.46) :

$$\begin{aligned}
 S_w(l, f) &= \sum_{\alpha} \sum_{\beta} \frac{P_o(\alpha)}{Z_{1\alpha}^*(if)} \cdot \frac{P_o(\beta)}{Z_{1\beta}(if)} e^{i2\pi f(x_\beta - x_\alpha)/v_x} \cdot S_\phi(f) \\
 &= \sum_{\alpha} \frac{P_o(\alpha)}{Z_{1\alpha}^*(if)} e^{-i2\pi f x_\alpha/v_x} \cdot \sum_{\beta} \frac{P_o(\beta)}{Z_{1\beta}(if)} e^{i2\pi f x_\beta/v_x} \cdot S_\phi(f) \\
 &= \left| \sum_{\alpha} \frac{P_o(\alpha)}{Z_{1\alpha}(if)} e^{i2\pi f x_\alpha/v_x} \right|^2 \cdot S_\phi(f) \quad \dots (4.59)
 \end{aligned}$$

Substituting the receptances into equation (4.59) and changing the order of summations :

$$\begin{aligned}
S_w(1,f) &= \left| \sum_{\alpha} \sum_r \frac{\psi_r(1) \psi_r(\alpha) P_o(\alpha)}{4\pi^2 \mathcal{M}_r (f_r^2 - f^2 + i2\zeta_r f_r f)} e^{i2\pi f x_{\alpha} / v_x} \right|^2 S_{\phi}(f) \\
&= \left| \sum_r \frac{\psi_r(1)}{4\pi^2 \mathcal{M}_r (f_r^2 - f^2 + i2\zeta_r f_r f)} \sum_{\alpha} \psi_r(\alpha) P_o(\alpha) e^{i2\pi f x_{\alpha} / v_x} \right|^2 S_{\phi}(f) \\
&\dots (4.60)
\end{aligned}$$

If damping is small and peaks are well separated, equation (4.60) can be simplified as :

$$\begin{aligned}
S_w(1,f) &= \left[ \sum_r \frac{\psi_r^2(1)}{16\pi^4 \mathcal{M}_r^2 [(f_r^2 - f^2)^2 + 4\zeta_r^2 f_r^2 f^2]} \left| \sum_{\alpha} \psi_r(\alpha) P_o(\alpha) e^{i2\pi f x_{\alpha} / v_x} \right|^2 \right] S_{\phi}(f) \\
&\dots (4.61)
\end{aligned}$$

By using the identity of complex numbers :

$$e^{i\theta} = \cos \theta + i \sin \theta \quad \dots (4.62)$$

the modulus square in equation (4.61) can be expanded :

$$\begin{aligned}
\left| \sum_{\alpha} \psi_r(\alpha) P_o(\alpha) e^{i2\pi f x_{\alpha} / v_x} \right|^2 &= \left| \sum_{\alpha} \psi_r(\alpha) P_o(\alpha) [\cos(2\pi f x_{\alpha} / v_x) + i \sin(2\pi f x_{\alpha} / v_x)] \right|^2 \\
&= \left| \sum_{\alpha} \psi_r(\alpha) P_o(\alpha) \cos(2\pi f x_{\alpha} / v_x) + i \sum_{\alpha} \psi_r(\alpha) P_o(\alpha) \sin(2\pi f x_{\alpha} / v_x) \right|^2 \\
&= \left[ \sum_{\alpha} \psi_r(\alpha) P_o(\alpha) \cos(2\pi f x_{\alpha} / v_x) \right]^2 + \left[ \sum_{\alpha} \psi_r(\alpha) P_o(\alpha) \sin(2\pi f x_{\alpha} / v_x) \right]^2 \quad \dots (4.63)
\end{aligned}$$

and the result of equation (4.63) substituted into equation (4.61),

$$S_w(l, f) = \left[ \sum_r \frac{\psi_r^2(l)}{16\pi^4 \mathcal{M}_r^2 [(f_r^2 - f^2)^2 + 4\zeta_r^2 f_r^2 f^2]} \right. \\ \left. \times \left[ \sum_\alpha \psi_r(\alpha) P_o(\alpha) \cos(2\pi f x_\alpha / v_x) \right]^2 + \left[ \sum_\alpha \psi_r(\alpha) F_o(\alpha) \sin(2\pi f x_\alpha / v_x) \right]^2 \right] \cdot S_\phi(f) \quad \dots (4.64)$$

is obtained.

It can be noted that, in case of the wave length  $\lambda_x$  of  $\phi(t)$  is much larger, compared to the dimensions of the structure

$$\lambda_x \gg x_\beta - x_\alpha \quad \dots (4.65)$$

that is, the time lag is being so small,

$$\tau_o = \frac{x_\beta - x_\alpha}{v_x} \approx 0 \quad \dots (4.66)$$

then the sine terms in equation (4.64) approach to zero and cosine terms to unity, so that the resultant equation becomes identical with equation (4.55).

After determining the power spectral density, it may be possible to obtain the other very important statistical and probabilistic characteristics of the random variable.

#### 4.5.5 The Relation between the Power Spectral Density and the Probability Density of a Random Variable

By definition (ref.69), the spectral density and the mean-square value (variance) of the randomly varying function  $x(t)$ , having zero mean value, are related with

$$\langle x^2(t) \rangle = \sigma_x^2 = \int_0^\infty S_x(f) df. \quad \dots (4.67)$$

But, in general, a knowledge of the spectral density of a quantity is not in itself sufficient to define its probabilistic characteristics, and so, there is no simple relationship connecting, for example, the probability density of the excitation with that of the response.

If the excitation is proved to have Gaussian instantaneous value distribution, it can be shown (ref.70) that the response is also Gaussian, and in this case the probability densities of excitation and response can be obtained immediately from their spectral densities by using the mean-square value (variance) from :

$$p_x(x) = \frac{1}{\sigma_x \sqrt{2\pi}} e^{-x^2 / 2\sigma_x^2} \quad \dots (4.68)$$

Although equation (4.68) gives full information about the probability of the signal having a certain value in any instant of time, in structural design point of view, the peak values of the signal are more important than the instantaneous values.

For the machine components subjected to random excitation, the number of occurrence of peaks having certain levels in unit time, is of significant importance and so, the safety or failure of the component depends directly on the peak distribution of the response. This dependence has been first suggested by MINER (ref.71) and "cumulative fatigue damage" and "fatigue life" theories are based on this phenomenon.

On the other hand, in case of civil engineering structures, like arch dams, subjected to earthquake type of excitation, generally the duration of excitation is too short to cause a fatigue failure; but, even only one peak of the response which exceeds a certain critical level, may cause a sudden

failure of the structure. For this reason, the expected maximum level of the peaks in the duration of excitation is the most significant measure to the safety of the structure, and that can only be evaluated by means of the knowledge about the peak distribution of the response.

#### 4.5.6 General Theory of the Gaussian Peak Distribution of a Random Variable.

It has been shown by RICE (ref.72) that signals which exhibit Gaussian (normal) instantaneous value distribution can be represented by an infinite number of sine waves combined in random phase, independent of spectrum shape. However, the peak values will, to a great extent, be influenced by the spectrum shape. Rice found a general formula for the peak distribution as a function of spectrum shape, as long as the above statement of Gaussian distributed instantaneous values holds true.

The probability of peaks of a random variable  $x(t)$ , occurring within the range  $dx$ , in time interval  $dt$ , can be obtained from Rice's general formula as :

$$\Pr \left[ \text{peak in } dx, dt \right] = \frac{dx \, dt \, \sqrt{-R''}}{2 \sqrt{2} \pi R} \cdot \frac{x}{\sqrt{2R}} \cdot \exp \left( - \frac{x^2}{2R} \right) \\ \times \left[ 1 + \operatorname{erf} \frac{kx}{\sqrt{2R}} + \frac{1}{\sqrt{\pi}} \frac{\sqrt{2R}}{kx} \exp \left( - \frac{k^2 x^2}{2R} \right) \right] \quad \dots (4.69)$$

where:  $\exp$  and  $\operatorname{erf}$  denote exponential and Gaussian error functions respectively and

$$k^2 = \frac{R''^2}{R R''' - R''^2} \quad \dots (4.70)$$

where, the following autocorrelation and spectrum relationships are used:

$$\left. \begin{aligned} R &= R(0) = \langle x^2(t) \rangle = \int_0^{\infty} S_x(f) df = \sigma_x^2 \\ -R'' &= -R''(0) = \langle x'^2(t) \rangle = 4\pi^2 \int_0^{\infty} f^2 S_x(f) df \\ R'''' &= R''''(0) = \langle x''^2(t) \rangle = 16\pi^4 \int_0^{\infty} f^4 S_x(f) df \end{aligned} \right\} \dots (4.71)$$

From equation (4.69) the expectation of peaks occurring in any time interval, within any range of  $x$ , can be determined by suitable integration. Thus, for example, the expectation  $E_1$  of peaks occurring in unit time which are greater than  $n$  times the root mean square value  $\sigma_x$ , is given by

$$\begin{aligned} E_1 &= \frac{1}{2\pi} \sqrt{\frac{-R''}{R}} \int_{n\sqrt{R}}^{\infty} \frac{x}{\sqrt{2R}} \exp\left(-\frac{x^2}{2R}\right) \left[ 1 + \operatorname{erf} \frac{kx}{\sqrt{2R}} \right. \\ &\quad \left. + \frac{1}{\sqrt{\pi}} \frac{\sqrt{2R}}{kx} \exp\left(-\frac{k^2 x^2}{2R}\right) \right] d\left(\frac{x}{\sqrt{2R}}\right) \dots (4.72) \end{aligned}$$

The value of the integral in equation (4.72) depends on the value of the integrand for all types of  $x$  within the range of integration; in cases of practical interest, however, the lower limit is normally large, so that only large values of  $x/\sqrt{2R}$  have to be considered. Moreover in practice the quantity  $RR''/R''^2$  is close to unity, so that  $k$  is large also. This makes possible a considerable simplification, for with  $kx/\sqrt{2R}$  large

$$\left. \begin{aligned} \exp\left(-\frac{k^2 x^2}{2R}\right) &= \exp\left(-\frac{k^2 n^2}{2}\right) \approx 0 \\ \text{and } \operatorname{erf}\left(\frac{kx}{\sqrt{2R}}\right) &= \operatorname{erf}\left(\frac{kn}{\sqrt{2}}\right) \approx 1 \end{aligned} \right\} \dots (4.73)$$

Now, the integration of equation (4.72) is much simpler. The expectation of peaks in unit time which are greater than  $n$  times the RMS value can be obtained as

$$\begin{aligned}
 E_1 &= \frac{1}{\pi} \sqrt{\frac{-R''}{R}} \int_{n\sqrt{R}}^{\infty} \frac{x}{\sqrt{2R}} \exp\left(-\frac{x^2}{2R}\right) d\left(\frac{x}{\sqrt{2R}}\right) \\
 &= \frac{1}{\pi} \sqrt{\frac{-R''}{R}} \left[ -\frac{1}{2} \exp\left(-\frac{x^2}{2R}\right) \right]_{n\sqrt{R}}^{\infty} \\
 &= \frac{1}{2\pi} \sqrt{\frac{-R''}{R}} \exp\left(-\frac{n^2}{2}\right) \dots (4.74)
 \end{aligned}$$

By the inspection of equation (4.74) it can easily be seen that the frequency of occurrence of peaks above a certain level depends on two factors: the first one can be written explicitly as :

$$\frac{1}{2\pi} \sqrt{\frac{-R''}{R}} = \left[ \frac{\int_0^{\infty} f^2 S_x(f) df}{\int_0^{\infty} S_x(f) df} \right]^{\frac{1}{2}} \dots (4.75)$$

which is equal to the half of the number of zero crossings per unit time, a very important characteristic of the random process, and will have a large value if high frequencies predominate.

The second factor is the quantity  $\exp\left(-\frac{n^2}{2}\right)$  which decreases rapidly as the level considered increases.

#### 4.5.7 The "Mean Maxima" of the Random Variable for a Prescribed Time Duration

The expected number of peaks in unit time which are greater than  $n$  times the RMS value,  $E_1$  has been given by equation (4.74). If the random variable

is assumed to have lasted  $T$  times of unit time, in other words, the duration of the random variable is denoted by  $T$  (that is, if the time unit is a second, then the duration is  $T$  seconds, etc.) it is clear that the expectation of peaks in duration  $T$  which are greater than  $n$  times the RMS value,  $E_T$ , can be obtained simply by :

$$E_T = E_1 T \quad \dots (4.76)$$

Now, according to the considerations of the probability of failure, it is possible to determine a certain level of the peaks, so that at least one peak exceeds this level during the time interval  $T$ . This level can be expressed as the "mean maxima,  $\bar{x}_{\max}(T)$ , for the duration  $T$ " and can be obtained by making  $E_T = 1$  in equation (4.76). Then it follows :

$$E_1 T = 1 \quad \text{and} \quad E_1 = \frac{1}{T} \quad \dots (4.77)$$

Substituting the new value of  $E_1$  into equation (4.74) :

$$\frac{1}{T} = \frac{1}{2\pi} \sqrt{\frac{-R''}{R}} \exp\left(-\frac{n^2}{2}\right) \quad \dots (4.78)$$

and resolving equation (4.78) for  $n$ ,

$$n = \sqrt{2} \left[ \ln \left( \frac{T}{2\pi} \sqrt{\frac{-R''}{R}} \right) \right]^{\frac{1}{2}} \quad \dots (4.79)$$

is obtained. Substituting the values of equation (4.75), equation (4.79)

becomes :

$$n = \sqrt{2} \left[ \ln \left( \frac{A^{\frac{1}{2}}}{\sigma_x} \cdot T \right) \right]^{\frac{1}{2}} \quad \dots (4.80)$$

where

$$A = \int_0^{\infty} f^2 S_X(f) df$$

$$\sigma_x = \left( \int_0^{\infty} S_X(f) df \right)^{\frac{1}{2}}$$

By the definition, the "mean maxima" for the duration  $T$  can be determined as :

$$\bar{x}_{\max}(T) = n \sigma_x \quad \dots (4.81)$$

This is the value, which must be taken into account for the design of the structure.

#### 4.6 APPLICATION OF RANDOM VIBRATION THEORY TO EARTHQUAKE TYPE EXCITATION

4.6.1 In section 4.3 it was shown that the relative motion of a single-degree-of-freedom system subjected to a ground motion excitation is the same as that for a system resting on a fixed base and subjected to a force equal to the mass of the system multiplied by the earthquake ground acceleration. For a multi-degree-of-freedom system, the forces applied to each nodal point at time  $t$  can be written as :

$$P_x(\alpha, t) = -m_x(\alpha) \ddot{u}_{g_x}(t) \quad \dots (4.82)$$

where the suffix  $x$  denotes the direction of the force applied and  $\ddot{u}_{g_x}(t)$  is the acceleration time history of the earthquake ground motion component in that direction.

If the velocity of earthquake waves is assumed to be large enough in comparison with the dimensions of the structure, each point of the structure is subjected to the same ground acceleration  $\ddot{u}_{g_x}(t)$  at the same time, and the mass of each point  $m(\alpha)$ , is a constant for each individual point. In other words, the forces acting on each point are the product of a randomly varying single quantity (the earthquake ground acceleration); and a constant (mass of each point).

According to these assumptions, in the case of the vibration of a multi-degree-of-freedom system subjected to earthquake ground excitation, it can be said that the forces acting on each point of the structure are directly correlated.

In fact, by the comparison of equation (4.82) and equation (4.50), it can easily be seen that both equations are identical in form, so that

$$\left. \begin{aligned} P_O(\alpha) &= m_x(\alpha) \\ \phi(t) &= \ddot{u}_{g_x}(t) \end{aligned} \right\} \dots (4.83)$$

can be written, and by means of these transformations, the results obtained in section 4.5.4.3 can be directly applicable, i.e. equation (4.55) becomes:

$$S_w(l, f) = \left[ \sum_r \frac{\psi_r^2(l)}{16\pi^4 \mathcal{M}_r^2 [(f_r^2 - f^2)^2 + 4\zeta_r^2 f_r^2 f^2]} \left[ \sum_\alpha \psi_r(\alpha) m_x(\alpha) \right]^2 \right] S_{\ddot{u}_{g_x}}(f) \dots (4.84)$$

where the suffix  $x$  denotes the component of the earthquake ground motion considered and  $S_{\ddot{u}_{g_x}}(f)$  is the power spectral density of the acceleration of that component. Similar equations can be written for  $y$  and  $z$  components of the ground motion.  $S_w(l, f)$  may be the response spectral density of displacement component in any of the three directions of point "1".

4.6.2 The use of equation (4.84) is acceptable providing the following assumptions hold true :

- (a) The behaviour of the random variable is stationary,
- (b) The instantaneous value distribution of the random variable is Gaussian,

- (c) The length of earthquake waves is large enough in comparison with the dimensions of structure,
- (d) The damping of the structure is small,
- (e) The natural frequencies of the system are well separated.

The first two assumptions are related with the excitation and the latter two are with the dynamical characteristics of the structure. The third assumption is related with both the excitation and the structure.

As this study is mainly concerning the behaviour of arch dams subjected to earthquake ground excitation, the validity of the above assumptions shall be discussed considering that the structure is an arch dam.

The damping of arch dams has been investigated by OKAMOTO & TAKAHASHI (ref.28) by means of experiments made on real arch dams and the damping ratio has been found 3.5-4.5% of critical. Although, in reservoir full condition, for higher modes some 6-7% of critical values have been obtained, it is still possible to accept that the damping of arch dams is small enough.

In case of strong ground motions, the recorded accelerograms have shown that most of the energy involved is in the frequency range up to 5 Hz, and the frequencies higher than 10 Hz. have practically no importance (ref.73). However, usually the medium size arch dams might have from 5 to 12 natural frequencies in that frequency range, and some of these might be quite close to each other, but generally the contributions of neighbouring modes on each other are small, so that the cross terms of equation (4.54) can be neglected.

The recorded accelerograms of strong earthquakes have been analyzed for the test of Gaussian instantaneous value distribution and it was shown (ref.32) that the Chi-square test gives satisfactory answer as the value obtained falls well in the confidence interval.

The predominant period of earthquake ground motion is approximately 0.4 second (ref.73) and the duration of strong earthquakes is about 30 seconds, so that there are large enough number of pulses which makes it possible to analyze the random variable assuming that it is stationary. In fact, the behaviour of earthquakes is shown to be non-stationary and several attempts have been made to find a reasonable solution for non-stationary behaviour of earthquake motions (ref.74,75,76); none of these attempts could produce a method which is easily applicable for design purposes and there is an open area for research in this direction. So, this study is confined to the assumption of stationary random motion, which is justifiable at this stage of knowledge about non-stationary random processes.

For civil engineering structures like multi-storey buildings, chimneys, water tank towers, etc., it can be assumed that each point of the structure is subjected to the same ground acceleration at the same time, because generally the horizontal dimensions of these types of structures are so small in comparison with the length of earthquake waves. But, for the structures like large arch dams, as the ratio of dimensions of the structure to the length of earthquake waves might have some considerable values and this causes phase differences between the motions of each point of the structure so that some alterations in modal responses might be expected.

4.6.3 To investigate the effect of the velocity of earthquake waves on the response of arch dams, it may be possible to adopt the results of random vibration theory obtained in section 4.5.4.4. In fact, if the randomly varying quantity  $\phi(t)$  is replaced by the earthquake acceleration and is considered to move past the structure at a constant velocity, so that different points

experience the same ground acceleration but with time-lags corresponding to their positions. In this case, the equation (4.56) can be written as :

$$\left. \begin{aligned} P_x(\alpha, t) &= -m_x(\alpha) \ddot{u}_{g_x}(t) \\ P_x(\beta, t) &= -m_x(\beta) \ddot{u}_{g_x}(t + \tau_0) \end{aligned} \right\} \dots (4.85)$$

where the suffix  $x$  denotes the direction of the earthquake and  $\tau_0 = \frac{x_\beta - x_\alpha}{v_x}$  is the time lag between the points  $\alpha$  and  $\beta$ ;  $x_\beta$  and  $x_\alpha$  are the coordinates of the points in the earthquake direction considered and  $v_x$  is the velocity of the earthquake waves.

By introducing the above transformations, equation (4.64) becomes :

$$S_w(1, f) = \left[ \sum_r \frac{\psi_r^2(1)}{16\pi^4 \mathcal{M}_r^2 [(f_r^2 - f^2)^2 + 4\zeta_r^2 f_r^2 f^2]} \right] \times \left[ \left[ \sum_\alpha \psi_r(\alpha) m_x(\alpha) \cos(2\pi f x_\alpha / v_x) \right]^2 \left[ \sum_\alpha \psi_r(\alpha) m_x(\alpha) \sin(2\pi f x_\alpha / v_x) \right]^2 \right] S_{u_{g_x}}''(f) \dots (4.86)$$

where  $S_{u_{g_x}}''(f)$  and  $S_w(1, f)$  are the same as in equation (4.84).

Although the transmission of earthquake waves between the valley and the structure might be more complicated than the model introduced above, it is believed that the assumptions considered can provide a close approximation to the real phenomena.

4.6.4 Having the power spectral density of the responses using either equation (4.84) or equation (4.86) for a given earthquake acceleration power spectral density as input, the other statistic and probabilistic values of

the response can be obtained by using the formulae obtained in section 4.5.5 and 4.5.7 :

The variance (mean square value) :

$$\langle w_1^2(t) \rangle = \sigma_{w_1}^2 = \int_0^{\infty} S_w(l, f) df \quad \dots (4.87)$$

The root mean square value (standard deviation):

$$\sigma_{w_1} = \sqrt{\langle w_1^2(t) \rangle} = \left( \int_0^{\infty} S_w(l, f) df \right)^{\frac{1}{2}} \quad \dots (4.88)$$

Gaussian instantaneous value probability distribution function:

$$p_{w_1}(w) = \frac{1}{\sigma_{w_1} \sqrt{2\pi}} \exp \left( -\frac{w^2}{2 \sigma_{w_1}^2} \right) \quad \dots (4.89)$$

The mean maxima for the earthquake duration T :

$$\bar{w}_{1 \max}(T) = \sqrt{2} \left[ \ln \left( \frac{\int_0^{\infty} S_w(l, f) df}{\sigma_{w_1}^2} \cdot T \right) \right]^{\frac{1}{2}} \cdot \sigma_{w_1} = n \sigma_{w_1} \quad \dots (4.90)$$

This concludes the theory of stationary random analysis of lightly damped structures to earthquake type excitation providing the acceleration power spectral density of the ground motion is known. Up to date, some of the recorded strong motion earthquake accelerograms have been analyzed by several authors (ref.32,77) and the power spectral densities were evaluated.

As the occurrence of the strong earthquakes is seldom, the processing of statistical data which is necessary for probabilistic design of structures subjected to earthquakes, is very slow. Though, in the random analysis of this study, a representative power spectral density of a strong earthquake is to be taken into account and the response of an arch dam subjected to this earthquake is to be presented in Chapter 5. In addition, some

suggestions are also to be considered in Chapter 7 about the choice of the earthquake power spectral density for probabilistic design purposes.

#### 4.7 RESPONSE SPECTRA METHODS

4.7.1 In the previous sections, two methods have been described for the response calculation to earthquake excitation, namely the step-by-step integration method and random analysis methods; the first one is a deterministic procedure, the latter is statistical and probabilistic.

Here, it must be necessary to pay attention to another method, which is now widely used in design of structures subjected to earthquake excitation. This method is called "Response Spectra Method" and based on the exact calculation of response to a particular earthquake, but, by means of some approximations, the tedious part of exact calculations is eliminated and also it becomes possible to introduce some statistical means into the calculation. Besides, the applicability of this method to earthquake analysis of earth dams by CLOUGH & CHOPRA (ref.78), and of arch dams by SERAFIM & PEDRO (ref.22) and by SEVERN & TAYLOR (ref.79) has been demonstrated. Having these characters, this method seems to be an intermediate method between the exact and random solutions, and must be considered in some detail.

##### 4.7.2 The Basis of Response Spectra Method

As it has been described in section 4.4 that, although the calculation of the response of an actual structure to an earthquake exciting force is a problem which is simple in principle, but is complicated in practice, because of the large number of parameters involved and the lengthy numerical computations required. The introduction of the concept of the "response spectrum"

by BENIOFF (ref.80) and BIOT (ref.31) was an effort to reduce the number of basic parameters for such dynamic problems.

The response spectrum provides, in effect, a way of separating that part of the response calculation which depends upon the particular earthquake exciting force from that part which involves mainly the properties of the structure.

As it has been shown in section 4.4 , the response of the  $r^{\text{th}}$  mode is given by :

$$\xi_r = \frac{1}{p_r \mathcal{M}_r} [\psi_r]^T [M] \left\{ \int_0^t \ddot{u}_g(\tau) e^{-\omega_r \zeta_r (t-\tau)} \sin p_r (t-\tau) d\tau \right\} \dots (4.91)$$

where  $p_r = \omega_r \sqrt{1 - \zeta_r^2}$  .

It may be noted in equation (4.91) that the response of the  $r^{\text{th}}$  vibration mode  $\xi_r$  depends directly upon the magnitude of the integral. The terms outside the integral are constants and depend on the modal characteristics of the structure. The integral has the dimensions of velocity; its maximum value is called the spectral relative velocity and is denoted by  $S_v$ , that is :

$$S_{v_r} = \left[ \int_0^t \ddot{u}_g(\tau) e^{-\omega_r \zeta_r (t-\tau)} \sin p_r (t-\tau) d\tau \right]_{\max} \dots (4.92)$$

From the form of the integral, it is clear that, for a given earthquake acceleration history,  $\ddot{u}_g(t)$ , the spectral velocity depends only upon the frequency of vibration,  $\omega_r$ , and the damping ratio,  $\zeta_r$ . Thus, a family of spectral velocity curves can be constructed for any given earthquake, each curve presenting the maximum velocity as a function of frequency for a given damping ratio.

Now, it is possible to define the "relative velocity response spectrum" as the maximum relative velocity in a single degree of freedom, linear, spring-mass-dashpot system acted upon by a prescribed force-time relationship, plotted for various values of natural frequency and damping.

It has been shown by HUDSON (ref.81) that the exact expression of relative velocity response spectrum obtained by differentiating the exact expression of relative displacement response spectrum given in equation (4.31) is slightly different from equation (4.92). It has been proposed by FUNG (ref.82) that the relative velocity spectrum defined by equation (4.92) should be called the "pseudo-velocity spectrum" to distinguish it from the true velocity spectrum derived from equation (4.31). However, providing that the system is lightly damped, this difference is negligible and the following relationships hold true :

$$\left. \begin{aligned} S_{a_r} &\approx \omega_r S_{v_r} \\ S_{d_r} &\approx \frac{1}{\omega_r} S_{v_r} \end{aligned} \right\} \dots (4.93)$$

where  $S_{a_r}$  and  $S_{d_r}$  are the acceleration response spectrum and the displacement response spectrum respectively, and can be defined in a similar way as for velocity spectrum.

By the introduction of the relative velocity response spectra of equation (4.92) into equation (4.91), the maximum response of the  $r^{\text{th}}$  mode can be obtained directly by

$$\xi_{r \text{ max}} = - \frac{[\psi_r]^T [M]}{p_r \mathcal{M}_r} \{S_{v_r}\} \dots (4.94)$$

providing that the damping ratio  $\zeta_r$ , the natural frequency  $\omega_r$  and the mode shape  $\psi_r$  of the structure and the relative velocity spectrum of the particular earthquake are already known. Since the velocity and acceleration spectra have been evaluated by several authors for all earthquakes from which reliable records have been obtained, the maximum modal response which would have been engendered by any of these earthquakes can be obtained without the necessity of evaluating Duhamel's integral which is the most tedious part of the exact analysis procedure.

Furthermore, it is possible to obtain a mean response spectrum for a number of earthquakes considered together (ref.83) so that some statistical aspects can also be included in the analysis.

#### 4.7.3 Superposition of Modal Responses

For a single-degree-of-freedom system, the response obtained from response spectrum analysis will be the true maximum. However, in complicated structures, the maximum response cannot be obtained directly from the modal maxima because the response spectrum curves give only the relationship between the frequency and the maximum value of the response at that frequency, but the time at which this maximum occurs is not preserved in the spectrum curves. Since the maximum values of the individual modes will in general occur at different times for the different modes, the phase relationships between the maxima are lost, and hence the exact way in which the various modes combine cannot be determined. Therefore, it is necessary to establish an appropriate method of calculating an approximate value of maximum response.

The first method, suggested by BIOT (ref.31) as a suitable method of mode combination, was to take the sum of the absolute values of the individual

modes. This absolute sum would evidently give the worst possible combination and would thus set an upper bound on the response. Since it is unlikely that the maximum response values in the individual modes would all occur at the same time with the same sign, the true maximum response would usually be somewhat less than the absolute sum. Although this method of combination has the practical advantage of that any error is always on the safe side, in most cases the overestimation resulting from this technique may be considerable and leads to non-economical design.

For structures like multi-storey buildings, considering that the first mode contributes the greater part of the total response with the higher modes essentially providing a correction of the first mode effects, CLOUGH (ref.84) suggested a simple method of approximating the total response, by adding to the first mode some appropriate portion of the higher modes. However, as it will be shown in Chapter 5, this method is not justifiable for three-dimensional structures such as arch dams.

The most appropriate method, proposed by ROSENBLUETH (ref.85) is based on ideas drawn from probability and random vibration theory, and considers that the maximum mode responses might be combined as the square root of the sum of the squares to give the most probable combination. This criterion would evidently lead to lower values of total response than the absolute sum, and hence might be a more realistic assessment of average conditions.

Further, considering the assumptions of conservative design, firstly JENNINGS (ref.86), later MERCHANT & HUDSON (ref.87) have argued that the square root of the sum of the squares method might lead to non-conservative design and have suggested other methods which involve a weighted average of the absolute sum and the square root of the sum of the squares, in order to reduce the possibility of non-conservative deviations. However, the

deviations of all above-mentioned methods from exact maxima have been calculated by MERCHANT & HUDSON (ref.87) for multi-storey buildings, and recently by SEVERN & TAYLOR (ref.79) for arch dams subjected to some particular recorded ground motions, and it was shown that the method proposed by MERCHANT & HUDSON ensures the non-conservative deviation to be limited to any desired level, but the expense of an increased number of positive deviations. In spite of these arguments about the non-conservative deviations involved in ROSENBLUETH's method for the design of structures subjected to future earthquakes, this method is assumed to be the most adequate in the point of view of probabilistic design.

#### 4.8 COMPUTER PROGRAMMING

The flow diagram of the FORTRAN programme, which has been written for calculating the responses of an arch dam by means of the random analysis methods presented in this Chapter, is given in Figure 4.6. This programme uses the natural frequencies and mode shapes obtained in Chapter 3, and the power spectral density of earthquake acceleration as the input. The programme is mainly the evaluation of either equation (4.84) or equation (4.86) according to the velocity of earthquake waves considered.

The steps from 1 to 9 include reading the input data, arranging nodal point and element arrays, calculating the overall mass matrix and reading the frequencies and mode shapes. The mass matrix includes the hydrodynamic matrix if the reservoir is in full condition. Then the generalized masses are calculated for each mode as equation (4.27).

The evaluation of equation (4.84) or equation (4.86) is executed in four stages :

(1) "Unit modal receptances", defined as

$$\frac{1}{Z_r(f)} = \left| \frac{1}{Z_r(if)} \right|^2 = \frac{1}{(f_r^2 - f^2)^2 + 4\zeta_r^2 f_r^2 f^2} \quad \dots (4.95)$$

are calculated for each mode.

(2) For each loading condition (earthquake direction, intensity and wave velocity), according to the value of the earthquake wave velocity, the control follows one of the two routes: If the value of velocity is infinite, then equation (4.84) is evaluated; if the wave velocity has a finite value, then equation (4.86) is evaluated. According to the direction of the earthquake waves, the square of total modal forces are calculated, for velocity =  $\infty$  :

$$P_r^2(x) = \left[ \sum_{\alpha} \psi_r(\alpha) m_x(\alpha) \right]^2 \quad \dots (4.96a)$$

and for velocity <  $\infty$  :

$$P_r^2(x, f) = \left[ \sum_{\alpha} \psi_r(\alpha) m_x(\alpha) \cos(2\pi f x_{\alpha} / v_x) \right]^2 + \left[ \sum_{\alpha} \psi_r(\alpha) m_x(\alpha) \sin(2\pi f x_{\alpha} / v_x) \right]^2 \quad \dots (4.96b)$$

Then the "modal response spectral densities" defined as, for velocity =  $\infty$  :

$$S_r(x, f) = \frac{P_r^2(x)}{16\pi^4 \mathcal{M}_r^2} \cdot \frac{S_{\ddot{u}_{gx}}(f)}{Z_r(f)} \quad \dots (4.97a)$$

and for velocity <  $\infty$  :

$$S_r(x, f) = \frac{1}{16\pi^4 \mathcal{M}_r^2} \cdot \frac{P_r^2(x, f) S_{\ddot{u}_{gx}}(f)}{Z_r(f)} \quad \dots (4.97b)$$

are calculated.

(3) After determining the "response spectral densities" of each mode for either case, the power spectral density of displacement at each nodal point in any of three directions can be calculated from :

$$S_w(l,f) = \sum_r \psi_r^2(l) S_r(x,f) \quad \dots (4.98)$$

(4) Last stage includes the calculation of variance as equation (4.87), the RMS value as equation (4.88), magnification factor and the mean maxima of the displacement for the earthquake duration T, as given in equation (4.90).

#### 4.9 CONTRIBUTIONS OF MODES ON RESPONSE OF AN ARCH DAM

In order to demonstrate the application of the computation stages explained in the previous section, the unit modal receptances equation (4.95), which are calculated for the first five natural frequencies of Arch Dam Type-5 for the reservoir in empty condition, are shown in Figure 4.7.

The modal response spectral densities calculated from equation (4.97a) for the velocity of earthquake waves is infinite, are also shown in figures 4.8, 4.9 and 4.10 for the same structure.

In calculation of all of these spectra where each of these figures corresponds to one of the three loading directions, the acceleration spectral density of earthquake is assumed having the same intensity in all directions (this acceleration spectral density shall be given in section 5.2).

In the case of the earthquake acting in x direction (perpendicular to the river course), the symmetrical modes have no contribution, and only the antisymmetrical modes contribute (figure 4.8). For the excitations in

y and z directions, only symmetrical modes contribute and the antisymmetrical modes have no contribution (figures 4.9 and 4.10).

As the unit modal receptances (figure 4.7) and also the power spectral density of earthquake acceleration (section 5.2) decrease for the higher frequencies and also the higher modes are having more complex shapes which causes some cancellations of dynamic forces, the contribution of higher modes are generally much smaller than lower modes. The only exception is noticed in vertical vibration, where the fifth mode has a contribution bigger than the first and third modes. This is because the fifth mode is to be considered as the first vertical mode of vibration (section 3.12.3) where all the vertical displacements have the same sign.

According to these results, in the response calculations to be presented in the next Chapter, only the first five modes will be taken into consideration and the contributions of higher modes shall be neglected without introducing any considerable error.

The last stages of the response calculations which are the evaluation of the displacements of nodal points in any direction desired, and the power spectral densities obtained as the results of these calculations, shall be given in Chapter 5 in detail.

In Figures 4.7, 4.8, 4.9 and 4.10, the vertical axis is taken in logarithmic scale, in order to demonstrate the effect of higher modes, and in these figures the effects of higher modes seem to be in the same magnitude as the lower modes. In fact, if these figures are drawn in linear scale, the differences between the modes become more distinguishable. This has been done for the unit modal receptances given by equation (4.95) and figure 4.7 is re-drawn with linear vertical axis as shown in Figure 4.11. As it is seen

from this figure, even if the natural frequencies are not very well separated, for a lightly damped structure the peaks are quite sharp and the contribution from the neighbouring modes are so small that this conclusion confirms the assumptions made in section 4.5.4.2 in order to simplify equation (4.48) by neglecting the cross terms.

The inclusion of the velocity of earthquake waves into the calculation affects the modal response spectral densities considerably. In this case the modal forces and modal response spectral densities are calculated by using equations (4.96b) and (4.97b). The modified modal spectral densities corresponding to Figure 4.8 and Figure 4.9 are shown in Figure 4.12 and Figure 4.13 respectively. As it can be noticed that the velocity of earthquake waves affects the modal responses largely for the excitation in x direction (figure 4.12), as the velocity decreases. This effect is much less for the excitation in y direction (figure 4.13). The influence of the velocity of earthquake waves on the response of the arch dam shall also be discussed in Chapter 5 in detail.

## CHAPTER 5

### RESPONSE OF ARCH DAMS TO EARTHQUAKES

#### THE EFFECTS OF VARIOUS FACTORS

##### 5.1 INTRODUCTION

In Chapter 3, the determination of the dynamical characteristics of arch dams, and in Chapter 4 the theoretical background of random vibration analysis have been described and a probabilistic method to calculate the responses of arch dams under earthquake excitation has been introduced. In this Chapter, in the light of the previous Chapters, the results obtained for the response of an arch dam subjected to a prescribed earthquake excitation shall be presented and the effects of various factors on these responses shall be discussed in detail.

These factors can be divided into two groups :

- (1) The factors related with the vibrating system, which are :
  - the damping present in completed structure;
  - the hydrodynamic effect of the reservoir water;
  - the flexibility of foundation rock.
- (2) The factors related with the earthquake ground motion, which are :
  - the shape of the power spectral density of the ground acceleration and the spectral intensity;
  - duration of the earth tremor;
  - velocity of earthquake waves;
  - direction of earthquake waves.

In the following investigations, firstly the responses of Arch Dam Type-5,

on rigid foundation, reservoir in empty condition and having nominal damping ratio, which is subjected to an earthquake which has prescribed acceleration power spectral density, shall be calculated. Then the effects of the above factors shall be taken into consideration separately.

## 5.2 POWER SPECTRAL DENSITY OF EARTHQUAKE ACCELERATION

In the random analysis of this study, a representative power spectral density of a strong earthquake is to be taken into consideration and the responses of Arch Dam Type-5 subjected to this earthquake are to be calculated. This power spectrum, which is calculated by RAVARA (ref.32) from the recorded accelerogram of the N-S component of EL-CENTRO, CALIFORNIA, earthquake, May 18, 1940, is given in Figure 5.1. This smoothed spectrum shows that, most of the energy involved is in the frequency range up to 5 Hz., and the frequencies higher than 10 Hz. have practically no importance.

The variance of this spectrum is equal to  $3820 \text{ cm}^2 \text{ sec}^{-4}$  and the RMS value is equal to  $61.8 \text{ cm sec}^{-2}$ . The duration of EL-CENTRO, 1940, earthquake is 30 seconds. The depth of the epicentre has been estimated as 24 Km. and the epicentral distance of the recording instrument was 48 Km.

## 5.3 RESPONSE OF AN ARCH DAM, RESERVOIR IN EMPTY CONDITION

Eight of the ten frequencies calculated for Arch Dam Type-5 fall inside the effective frequency range (0-10 Hz) of a strong ground motion. Since the power contents decrease very rapidly for frequencies higher than 5 Hz (Figure 5.1), it was shown in section 4.9 that, the contributions of the higher modes are very small and can be neglected. For the purpose of not increasing the computational work involved, it is decided to use the first five modes (the first two symmetric

modes, the first two antisymmetric modes and the first vertical mode) in the following calculations.

By using the first five natural frequencies and mode shapes obtained for Arch Dam Type-5, on rigid foundation and reservoir in empty condition as given in section 3.12.3, the calculated displacement power spectral densities of two critical points on the top arch of the dam; one of them is on the axis of symmetry (nodal point C), the other is on the half way between symmetry axis and the abutment (nodal point A), are shown in Figures 5.2 to 5.7.

The structure is assumed to be subjected to an earthquake ground motion which has the characteristics equal to EL-CENTRO, 1940, earthquake (section 5.2). An average damping ratio 4% is taken into consideration for all modes, according to OKAMOTO & TAKAHASHI (ref.28). The velocity of earthquake waves is assumed infinite, so that equation (4.84) is used in this response calculation.

In Figure 5.2 and Figure 5.3, the earthquake is assumed to act in a horizontal direction perpendicular to the axis of symmetry; while, in Figure 5.4 and Figure 5.5, in the horizontal direction parallel to the axis of symmetry and in Figure 5.6 and Figure 5.7, in vertical direction. For each of these cases, the earthquake component is assumed to have the same spectral intensity (as figure 5.1). The response power spectral densities of the three components of displacements for the nodal points C and A are calculated simultaneously and are shown in each figure.

As it has been explained in section 4.9, it can also be seen by examining these figures that, in case of the ground excitation in the direction parallel to the axis of symmetry or vertical, only the symmetrical modes contribute; while the ground excitation is in the direction perpendicular to the axis of symmetry, only the antisymmetrical modes contribute to the responses of the symmetrical arch dam.

In Figure 5.2, the y and z components of the displacement of nodal point C are zero, as in antisymmetrical vibrations, this point can move only in x direction. On the contrary, in Figure 5.4 and Figure 5.6, the x component is zero as in symmetrical vibrations, the point C can move only in yz plane.

The contribution of a mode to the response of a nodal point depends upon the response of the particular mode and the normalized deflection in the direction of displacement component considered, as given in equation (4.98).

The factors, on which the modal responses are dependent, have been discussed in section 4.9 and it has been shown that the contributions of higher modes are generally much smaller than lower modes with the exception noticed in the case of vertical excitation. The effect of this general conclusion is very much noticeable on the power spectral densities of displacements shown in Figures 5.2 to 5.7. It is also clear that the fifth mode predominates the responses in the case of vertical vibrations. Naturally these general conclusions are expected to be altered as the response power spectral density of a displacement component is directly related with the normalized deflection in each individual mode, so that the modal responses are modified by the mode shapes in the calculation of displacement power spectral densities. However, even these modifications do not affect the general conclusion that the contributions of higher modes are much less than lower modes for horizontal excitation and horizontal components of the displacements. But, the effect of fifth mode is getting more noticeable in vertical excitation and for the vertical components of displacements in horizontal excitation.

The mean maximum displacements for earthquake duration 30 seconds are calculated from the power spectral densities of responses according to

section 4.5.7 and equation (4.90). The results obtained for the responses of the crown cantilever shall be introduced in section 5.5, in comparison with the results obtained for the reservoir in full condition.

#### 5.4 COMPARISON OF THE RANDOM ANALYSIS RESULTS WITH THOSE OBTAINED BY THE RESPONSE SPECTRUM METHOD

It would be interesting to compare the results obtained by the random vibration analysis with those obtained by using response spectrum methods described in section 4.7. For the calculation of responses of Arch Dam Type-5, the average response velocity spectrum curves calculated by HOUSNER (ref.83) for EL-CENTRO, CALIFORNIA, May 18, 1940, earthquake, are used. These response spectrum curves are given in Figure 5.8. In the superposition of modal responses, the square root of the sum of the squares is taken into consideration as proposed by ROSENBLUETH (ref.85).

The responses at various nodal points are calculated assuming various damping ratios for the structure. The results are classified according to the predominant frequency which affects each individual response component, and the curves obtained for the ratio of responses corresponding to the power spectrum method and the response spectrum method are given in Figure 5.9 in the frequency range 3.0 to 7.5 Hz. taking the damping ratio as parameter.

With the damping ratio 4%, the maximum differences in that frequency range between the results obtained by the two methods are less than  $\pm 15\%$ . For the lower frequencies the responses obtained by the power spectrum method is greater, while for higher frequencies it is less than the responses obtained by the response spectrum method. The power spectrum method gives larger values as the damping ratio decreases; for higher damping ratios the condition is reversed.

The above conclusions are solely dependent upon the acceleration power spectral density and the velocity response spectrum curves used in the calculations; however, both curves are originated from the same recorded accelerogram of EL-CENTRO, 1940, earthquake, but derived by different investigators. Although, these curves used in two different methods have slightly different spectral characteristics, both of the methods can give reasonably close responses for an arch dam with a damping ratio about 4%.

#### 5.5 RESPONSE OF AN ARCH DAM, RESERVOIR IN FULL CONDITION, EFFECT OF RESERVOIR WATER.

By using the first five natural frequencies and mode shapes obtained for Arch Dam Type-5, on rigid foundation and reservoir in full condition as given in section 3.12.4, the calculated displacement power spectral densities of nodal points C and A are shown in Figures 5.10 to 5.15.

The damping ratio of the structure and all of the characteristics of earthquake ground motion are assumed to be the same as given in section 5.3, for the reservoir in empty condition.

Each of these six figures corresponds to a figure given in section 5.3, in order to investigate the effect of reservoir water on the power spectral densities of displacements. The comparison of corresponding figures show that the general characteristics of the response power spectral densities for the reservoir in full condition are the same as in empty condition and all of the general conclusions derived in section 5.3 can be applied for reservoir in full condition.

However, the following effects are noticed :

(1) As the natural frequencies are reduced in full condition (section 3.12.4) the peaks in the spectral density curves are located at these new lower frequencies.

(2) As the mode shapes are modified by the effect of reservoir water (section 3.12.4), the spectral density curves are also modified accordingly.

(3) Both the added mass effect of the reservoir water and the modification of the mode shapes cause some alterations in the contributions of individual modes.

Other than these modifications noticed on the shape of the spectral density curves, more important differences obtained in the spectral intensities of responses due to :

(1) As the depth of water in the reservoir increases, the natural frequencies of the structure decrease, because of the added mass effect of the reservoir water. This reduction brings the natural frequencies closer to the predominant frequencies of the earthquake as shown in Figure 5.1. On the other hand, the unit modal receptance defined in section 4.8 increases with the natural frequency decreases (Figure 4.7). Both of these effects serve to increase the individual modal responses.

(2) The additional mass introduced by the hydrodynamic effect of the reservoir water and the modifications occurring in the mode shapes also serve to increase the dynamical forces acting on the structure (equation 4.96a) so that the modal responses are increased.

All of these effects cause the response of the arch dam for the reservoir in full condition to become larger than the response for the reservoir in empty condition.

In order to give a better visualization for the effect of reservoir water on the response of an arch dam, the calculated responses of the crown cantilever, for earthquake duration 30 seconds, in both reservoir empty and full conditions, are shown in Figure 5.16A comparatively. The differences between

the two cases, which correspond to the response due to only the hydrodynamic effect, are given in Figure 5.16B. This deflection pattern is very much like the deflection pattern due to hydrostatic loading shown in Figure 2.17. Figure 5.16C gives the ratio of dynamic responses in reservoir full/empty conditions. As it is expected, this ratio increases in the lower sections and reaches up to 1.65 at the bottom. These figures show the importance of the hydrodynamic effect of the reservoir water on the response of an arch dam subjected to a strong ground motion.

The maximum total responses of Arch Dam Type-5, including hydrostatic deflections, are shown in Figure 5.17 comparatively. The following important ratios are obtained from this figure for the maximum responses at the top of the dam :

$$\frac{\text{EARTHQUAKE, RESERVOIR EMPTY}}{\text{HYDROSTATIC LOADING}} = 0.61$$

$$\frac{\text{EARTHQUAKE, RESERVOIR FULL}}{\text{HYDROSTATIC LOADING}} = 0.78$$

$$\frac{\text{HYDROSTATIC + EARTHQUAKE, RESERVOIR FULL}}{\text{HYDROSTATIC LOADING}} = 1.78$$

These ratios show that, even for the reservoir in empty case, the dynamic response of an arch dam subjected to a strong ground motion may reach up to 61% of the deflection due to hydrostatic loading and this ratio may reach up to 78% for the reservoir in full condition, so that the total deflection may become 1.78 times the deflection due to hydrostatic loading.

## 5.6 EFFECT OF DAMPING RATIO ON THE RESPONSE OF AN ARCH DAM

Arch dams usually have a small amount of reinforcement and few construction joints, so that the structural damping is likely to be small. In fact, the prototype experiments performed by OKAMOTO & TAKAHASHI (ref.28) have shown that arch dams have damping about 3.5-4.5% of critical. However, these values have not yet been confirmed by any other experimental results and research should be carried out in this direction. It is anticipated that an investigation on the effect of damping ratio on the response of an arch dam may provide some valuable information about the importance of the damping ratio.

The responses of Arch Dam Type-5 are calculated for damping ratios varying from 2% up to 10%, and the responses obtained for the crown cantilever are given in Figure 5.18 comparatively. However, this figure shows the effect of damping ratio on the responses; for a better visualization, the damping ratio 4% is taken as the base damping ratio and the average ratios of the responses are calculated for the other damping ratios and the results obtained are given in Figure 5.19. As it can be noticed from this figure that as the damping ratio is assumed to decrease from 4% to 2%, the responses are increased slightly more than 40%, while the damping ratio is increased from 4% up to 10%, the responses are decreased about 35%.

These results show clearly the importance of damping ratio and the necessity of reliable information about the actual damping ratio present in the arch dams. This is particularly important as the responses are much more sensible for very light damping, and an over-estimation of the damping ratio may cause large amount of underestimation of responses and this leads to unconservative design and endangers the structure in the case of a strong earthquake.

In ref.28, OKAMOTO & TAKAHASHI have pointed out that the damping present in the arch dams gives higher ratios for the higher modes and they have measured damping ratios of about 6-7% in their experimental research. This assumption is also taken into consideration in this study and damping ratios 4.0, 4.5, 5.0, 5.5 and 6.0% are assumed for the first five modes, respectively; and the responses of Arch Dam Type-5 are re-calculated. As it can be expected, the contributions of higher modes are getting smaller, and in the response components where the higher modes contribute considerably, a reduction of about 15% is obtained.

Another interesting point to demonstrate the importance of the damping ratio, is to compare the effect of damping ratio with the effect of the accuracy of the computed natural frequencies of the structure. For this purpose,  $\pm 10\%$  error is assumed in the calculation of natural frequencies and the responses of Arch Dam Type-5 are calculated with a constant damping ratio 4% for these under and overestimated frequencies. For the case where  $-10\%$  error is involved, the responses are increased about 25% and for the case where  $+10\%$  error is involved, the responses are reduced about 17%. These values correspond to about  $-1.5\%$  and  $+2\%$  differences in the damping ratio respectively, as shown in figure 5.19.

## 5.7 EFFECTS OF EARTHQUAKE CHARACTERISTICS ON THE RESPONSE OF AN ARCH DAM

5.7.1 In the previous sections, the effects of some factors related with the vibrating system have been discussed. In this section, the factors related with the earthquake ground motion and their effects on the response of an arch dam are to be discussed. Apart from the direction of action, these factors are the shape of the power spectral density and the spectral

intensity of earthquake ground acceleration; duration of earth tremor and the velocity of earthquake waves.

### 5.7.2 Power Spectral Density and the Spectral Intensity of Earthquake Ground Acceleration

Since the response of an arch dam is a linear function of the excitation, which is defined by the power spectral density of ground acceleration, then the response increases with the spectral intensity of ground acceleration. The spectral intensity of ground acceleration can be defined in terms of the mean square value of the power spectral density of ground acceleration as :

$$SI_a = \langle \ddot{u}_g^2(t) \rangle = \int_0^{\infty} S_{\ddot{u}_g}(f) df \quad \dots (5.1)$$

As there is no doubt about the relationship of the response and the spectral intensity of excitation, no further investigation is necessary to demonstrate this relationship. However, the shape of the spectral density curve affects the responses considerably, as the individual modal responses are directly related with the shape of this curve.

The predominant frequency of strong earthquake ground motions is generally about 2.5 Hz. Most of the energy involved is in the frequency range up to 5 Hz. and for higher frequencies the power contents decrease very fast so that the frequencies higher than 10 Hz. have practically no importance (see Figure 5.1). Such a spectral character results in the higher modes providing less and less contributions to the response.

It would be interesting to demonstrate the effect of the shape of the power spectral density on the response of an arch dam by means of comparing the results obtained for a spectral density given in Figure 5.1 with those

obtained for a white-noise excitation which has the same spectral intensity in the frequency range 0-10 Hz. As the spectral intensity of the spectral density curve given in Figure 5.1 is equal to  $3820 \text{ cm}^2 \text{ sec}^{-4}$ , the constant spectral density of the white-noise excitation is taken equal to  $382 \text{ cm}^2 \text{ sec}^{-4} \text{ Hz}^{-1}$ . The responses of Arch Dam Type-5 are calculated for this white-noise excitation and, as an example, the displacement power spectral densities obtained for nodal point A are shown with broken lines in Figure 5.20 in comparison with the response obtained for EL-CENTRO 1940 earthquake. In this figure, the spectral densities of EL-CENTRO earthquake and the white-noise excitation are also shown comparatively.

This figure clearly shows that the contributions of lower modes is getting smaller, while the contributions of higher modes are becoming more noticeable. As a matter of fact, in case of white noise excitation, the responses on which the fundamental mode predominates, reduce to about 0.75 of the actual earthquake and the responses on which the fifth mode predominates increase up to about 1.50 times the response obtained for the actual earthquake.

These results confirm that the responses are very much dependent upon the shapes of the spectral density curve, even the spectral intensities of these curves are assumed to be constant.

### 5.7.3. Duration of Earthquake

The relation between the power spectral density and the root mean square value of response is given by equation (4.88). This characteristic value is related with the duration of earthquake as described in section 4.5.7 and the mean maximum values for a given earthquake duration can be calculated from equation (4.90). The most important quantity in that equation is the

"magnification factor" which indicates the most probable level of the response and it is a function of both the power spectral density of response and earthquake duration.

The variation of the magnification factor with respect to the predominant frequency appeared on the response spectral density curve, is investigated with the earthquake duration taken as a parameter. The results obtained are given in Figure 5.21. As it can be noticed that the magnification factor increases with the predominant frequency and the values obtained for 15 seconds to 40 seconds duration do not vary largely. It seems that the magnification factor can be taken equal to 3.0 as this value may give a good approximation for most of the practical cases.

#### 5.7.4 Velocity of Earthquake Waves

The effect of the velocity of earthquake waves on the modal responses has already been discussed in section 4.9. In this section the effect of the velocity of earthquake waves on the responses of arch dams are to be investigated.

In this investigation, the responses of nodal points C and A are calculated with respect to various wave velocities by means of equation (4.86). In these calculations the earthquake direction is assumed once parallel to the axis of symmetry and once perpendicular; damping ratio of the structure is taken 4% and duration of the earthquake is assumed 30 seconds.

The results obtained are shown in Figure 5.22A and B. It can easily be seen that, in case of the earthquake direction being parallel to the axis of symmetry, the wave velocities larger than 1000 m/sec have no significant effect on the responses. But in the case of the earthquake direction being perpendicular to the axis of symmetry, the wave velocities less than 4000 m/sec have considerable effect on the responses. Taking the dimensions and frequencies of the

Arch Dam Type-5 into account, it seems that the wave lengths longer than 3.5-4 times the maximum dimension of the structure in the direction of excitation, have practically no effect on the responses.

As a matter of fact, the arch dams are generally constructed on quite sound rock foundations, through which the earthquake shear (secondary or "S") waves, travel with velocities not less than 3000 m/sec. (ref.88) so that, with the exception of extremely large dams, the effect of earthquake wave velocity on the response of arch dams may be neglected.

On the other hand, the effect of the wave velocities on the responses seems to be on the conservative side. This can easily be explained by inspection of Figure 4.12 and 4.13 presented in section 4.9. The modal responses shown in these figures reduce with the velocity of waves decreasing with the exception of the third mode. This is due to the fact that, for simple mode shapes where all the deflections have the same sign, the inclusion of the time lags corresponding to the wave velocity causes the change of the sign of the dynamic forces acting at some of the nodal points, so that some force cancellations take place, that is the modal responses are always reduced. For more complex mode shapes, such as the third mode, the condition is reversed and the modal responses may increase. However, as the contribution of these higher modes which have complex mode shapes is generally very small, the increases due to these higher modes are cancelled by the dominated reductions occurring due to lower modes. As the result, the consideration of the velocity of earthquake waves serves to reduce the responses of arch dams. According to these results, for a conservative design, it is recommended not to include the velocity of earthquake waves in response calculations.

## 5.8 THE DIRECTION OF ACTION OF THE GROUND ACCELERATION

5.8.1 During an earthquake, the ground moves both horizontally and vertically, with acceleration which has a complex pattern comprising oscillatory horizontal and vertical pulses random in magnitude and direction. Therefore, accelerograms consist of records in two perpendicular horizontal directions and the vertical direction can provide a complete record. For the conventional building structures, as they have considerable inherent strength in the vertical direction, the effect of vertical component of ground motion is relatively unimportant and negligible, so that it is sufficient to consider the more intense component acting in the plane of least stiffness of the structure. However, a three-dimensional structure like an arch dam is subjected to both horizontal components acting simultaneously and the effect of vertical component may be of some significance. Therefore, the response calculations of arch dams to earthquakes must include the consideration of both of the horizontal and also the vertical components of earthquake ground accelerations.

5.8.2 The method developed in this study allows the application of any component of ground motion, whichever is needed; then the responses obtained for each individual forcing direction may easily be combined. As an example, the responses of the top arch of Arch Dam Type-5, subjected to horizontal earthquake acceleration acting at various angles with respect to the axis of symmetry, are shown in Figure 5.23A and B for the reservoir in empty and full conditions respectively. By the aid of these figures, the angles of earthquake direction which produce maximum responses for various points at the top arch are determined for Arch Dam Type-5 and given in Figure 5.24.

As it can be noted from these figures that, for the responses of crown cantilever, earthquake acting along the axis of symmetry of the dam ( $0^\circ$  angle) produces the maximum response, while, for the responses of other sections the lateral horizontal component plays an important part and the angle of earthquake direction which produces maximum response is increased towards abutment.

As a matter of fact, the results given in Figure 5.24 may not be general, because the relative amplitudes due to two horizontal components of earthquake ground motion depends upon the modal responses of symmetric and anti-symmetric modes of vibration, i.e. the power spectral density of ground acceleration, the natural frequencies and mode shapes and also the geometrical characteristics of the particular arch dam. This fact is reflected by the differences obtained for the same structure but for different loading conditions, namely reservoir in empty and full conditions. The hydrodynamic effect of reservoir water is more intense for the accelerations acting in the direction of symmetry axis, so that the responses of symmetrical modes are increased considerably, but the same effect is relatively small for the anti-symmetrical modes. Therefore, for the reservoir in full condition, the relative amplitudes due to symmetrical modes are more intense than those in empty condition, so maximum responses occur for smaller angles of incidence.

5.8.3 The responses of Arch Dam Type-5 have also been calculated for a vertical earthquake ground motion having the same power spectral density of acceleration as given in Figure 5.1., EL-CENTRO 1940 earthquake. The results obtained are shown in Figure 5.25 in comparison with those corresponding to horizontal excitation. It can be seen that, in case of a vertical earthquake with the same intensity as horizontal ground motion, the horizontal components

of responses are up to 0.40 of those corresponding to horizontal excitation. However, for some nodal points, the vertical component of responses is bigger than 3.0 times the corresponding vertical responses due to horizontal excitation.

Until recent years, no attempt has been made to take the vertical component of the ground excitation into consideration in the seismic design of structures, and to analyze the characteristics of this component. The first investigation on the importance of the vertical component of earthquake motions has been carried out by CHOPRA (ref.89) and velocity response spectra of the vertical components of three strong ground motions have been derived. These spectra have somewhat higher frequency components and reduce in the lower frequency range. CHOPRA has calculated the spectrum intensities for 20% critical damping and three ratios, 0.20, 0.25 and 0.31 were obtained for the vertical to horizontal component intensities for the three earthquakes considered. Among those, 0.25 corresponds to EL-CENTRO 1940 earthquake. These velocity spectra have been applied to the dynamic analysis of earth dams by the same author (ref.78).

5.8.4 Unfortunately, no power spectral density of acceleration for the vertical component of an earthquake has been derived, therefore no attempt could be made to calculate the responses of Arch Dam Type-5 for such a vertical excitation. However, by comparing the results obtained by CHOPRA with the results presented in section 5.8.3 for the responses of Arch Dam Type-5, subjected to a vertical excitation equivalent to EL-CENTRO 1940 earthquake N-S component (fig.5.1), the following conclusions can be reached.

If the Arch Dam Type-5 is assumed to be subjected to a vertical ground motion which has the same acceleration power spectral density distribution as the horizontal component of the EL-CENTRO 1940 earthquake (fig.5.1), but only 0.25 of its square root spectral intensity, then the horizontal components of responses reduces to 0.10 of those corresponding to horizontal excitation, while the vertical component of responses may still be in the same order of magnitude as the vertical components due to horizontal excitation. So that, the effect of vertical ground motion may be considered negligible on the horizontal components of deflections, but it should be taken into consideration in the maximum response calculations for vertical component of deflections.

On the other hand, CHOPRA has shown that the vertical component of ground motion has more higher frequency contents than horizontal components, so that the contributions of higher modes are expected to increase considerably by the modification of power spectral density curve in favour of higher frequencies. Therefore, especially the contribution of the fifth mode, which is considered as the fundamental vertical mode of vibration, is to be increased; that is, the effect of vertical excitation becomes more important.

Although Arch Dam Type-5 is a doubly curved arch dam, the vertical curvatures are small and it can therefore be considered as a slightly domed structure. The results discussed above have shown that, even for a slightly domed arch dam, the effect of the vertical component of ground motion on the responses of an arch dam is quite important and should be considered in the design. In case of extremely domed arch dams, this effect is expected to become much more important.

## 5.9 EFFECT OF FOUNDATION FLEXIBILITY ON THE RESPONSE OF AN ARCH DAM

In section 3.12.5, the effect of the foundation flexibility on the dynamical characteristics of Arch Dam Type-5 has been investigated. This investigation shows that the natural frequencies are reduced as the flexibility of foundation is increased and also the mode shapes are modified considerably.

As it has been described in section 5.5 for the effect of reservoir water, the reduction in natural frequencies brings these frequencies closer to the predominant frequencies of the strong ground motions which resulted to increase the responses. Besides, the modifications occurred in the mode shapes may also serve to increase the dynamical forces acting on the structure, which also resulted to increase the responses.

No attempt has been made for a complete response calculation of Arch Dam Type-5 including boundary flexibilities, because the complete set of frequencies and corresponding mode shapes have not been obtained in order not to spend excessive computing time. However, the above conclusions are so obvious and do not need any numerical proof. It is also clear that, for more flexible foundations, the responses of arch dams are expected to increase largely; therefore the effect of foundation flexibility should be included in response calculations, otherwise considerable unconservative errors obtained in the design, which endanger the safety of the arch dam.

## CHAPTER 6

### STRESSES IN ARCH DAMS DUE TO EARTHQUAKES

#### 6.1 INTRODUCTION

6.1.1 In Chapter 5, the responses of arch dams to earthquakes have been discussed and the factors affecting these responses have been investigated. Throughout this analysis, the responses were calculated in terms of the deflections of arch dams. From an engineering point of view, the stresses induced in the structure during an earthquake is more important than the deflections, as the maximum magnitude of these stresses is the best measure to the safety of the arch dam. In this Chapter, the calculation of dynamic stresses due to a prescribed earthquake ground excitation is to be described and the safety of an arch dam subjected to earthquake shall be discussed.

6.1.2 In these stress calculations, for the prescribed earthquake ground excitation, again, the acceleration power spectral density of EL-CENTRO, 1940 earthquake (Fig. 5.1.), is to be taken into consideration and the dynamic stresses due to this earthquake shall be calculated.

6.1.3 In these calculations only the hoop and vertical stresses of the crown cantilever are to be included in order to compare these results with those obtained for the static analysis of Arch Dam Type-5 given in section 2.12.3. As a matter of fact, the maximum dynamic stresses in arch dams due to earthquake excitation generally occur at the crown cantilever, so that, the comparison of these stresses may give an appropriate information about the overall behaviour of the arch dam. The stresses in the other sections of the dam can also be calculated in the same way as shall be described below.

## 6.2 CALCULATION OF DYNAMIC STRESSES DUE TO EARTHQUAKES

### 6.2.1 Response of an arch dam in terms of stresses

The calculation of response of arch dams due to earthquakes has been described in Chapter 4, where the response was calculated in terms of the deflection of the arch dam. The stresses induced in the structure can also be determined by means of the same procedure with a modification made in order to define the responses in terms of stresses.

The computation procedure described in Section 4.8 is applied without any alteration until the end of the determination of response spectral densities,  $S_r(x,f)$ , of each mode for a given loading condition. After determining the modal response spectral densities, the power spectral density of each stress component at each nodal point can be calculated from Eq. (4.98) by means of a simple modification as:

$$S_{\sigma}(l,f) = \sum_r \sigma_r^2(l) S_r(x,f) \quad \dots (6.1)$$

where;  $\sigma_r(l)$  is the "modal stress" component at nodal point "l" in the  $r^{\text{th}}$  mode, and  $S_r(l,f)$  is the power spectral density of this stress component. In here, the "normalized deflection" component in the  $r^{\text{th}}$  mode,  $\psi_r(l)$ , of Eq. (4.98) is replaced by the "modal stress" component in the  $r^{\text{th}}$  mode.

As it is known, the normalized deflections in the  $r^{\text{th}}$  mode,  $\psi_r$  are defined as the shape of the  $r^{\text{th}}$  mode of vibration. Accordingly, the modal stresses in the  $r^{\text{th}}$  mode can be defined as the maximum stresses induced in the structure while the structure is vibrating in that mode; in other words, the modal stresses,  $\sigma_r$ , are the stresses which occur in the structure, when the structure is deflected to a normalized shape of the  $r^{\text{th}}$  mode of vibration.

As the evaluation of Eq. (4.98) has been demonstrated in Chapter 5, Eq. (6.1) can also be evaluated in the same way; provided that the modal stresses

are known. So, the only problem to be solved is the determination of these modal stresses. Once these modal stresses are determined the power spectral density of stress can be obtained from Eq. (6.1), then the variance and root mean square value are calculated from Eqs. (4.87 and 4.88) and the mean maxima of the stress for a given earthquake duration can be determined by using Eq. (4.90).

### 6.2.2 Calculation of modal stresses

The calculation of element stresses and nodal point stresses by using tetrahedral finite element technique has been discussed in Section 2.9.

An adequate method, for nodal point stress calculation, which uses nodal point forces given by Eq. (2.1), has also been described in the same section.

A similar method can be used to calculate the dynamic stresses occurring during the vibration of the structure in a particular mode of vibration. The only difference of the method developed for the dynamic stress calculation, from the method used for static analysis, is in the calculation of nodal point forces, where, in the static analysis, these nodal forces are calculated by using Eq. (2.1), while for the dynamic stress analysis, nodal forces can be calculated from Eq. (3.16) which includes the inertia forces as;

$$\{S_i\}_r = [k_i] \{\psi_i\}_r - \omega_r^2 [m_i] \{\psi_i\}_r \quad \dots (6.2)$$

where;  $\{S_i\}_r$  = nodal point forces for element  $i$  in the  $r^{\text{th}}$  mode,

$[k_i]$  = element stiffness matrix,

$[m_i]$  = element consistent mass matrix,

$\omega_r$  = circular frequency (eigenvalue) of  $r^{\text{th}}$  mode,

$\{\psi_i\}_r$  = normalized displacements (eigenvector) of the corners of of the  $i^{\text{th}}$  element in the  $r^{\text{th}}$  mode.

After determining the nodal point forces for each element, the procedure described in Section 2.9 can be followed for calculating the nodal point stresses. The eigenvalues and eigenvectors given in Chapter 3 will be used to calculate the modal stresses.

### 6.2.3 Stresses in various modes

In Chapter 5, it has been shown that the maximum radial responses at the crown cantilever are obtained for the excitation of the dam in the direction parallel to the axis of symmetry. It means that, only the symmetrical modes contribute to the radial responses, which produce the maximum dynamic stresses in the crown cantilever. For this reason, the modal stresses of the first three symmetrical modes are to be calculated and these modal stresses shall be used in the maximum stress calculations. Obviously, for other sections of the dam, the modal responses of antisymmetrical modes may also be necessary.

The natural frequencies and corresponding mode shapes of the Arch Dam Type-5 are given in Section 3.12.3. for the reservoir in empty condition, and in Section 3.12.4. for the reservoir in full condition. By using these frequencies and mode shapes and applying the method of calculation described in Section 6.2.2; the modal stresses of the first, third and fifth modes, which are the first three symmetrical modes; are calculated. The modal stresses obtained for the reservoir in empty condition are given in Fig. 6.1 and those for the reservoir in full condition are given in Fig. 6.2. In these figures, no sign is given to the stresses, but, the relative directions of the stresses on the water and air faces are preserved.

The comparison of Fig. 6.1 and 6.2 shows the effect of reservoir water on the modal stresses. The stresses obtained for the reservoir in full condition are generally bigger than those in empty condition, at the lower sections of the dam.

In both cases, the hoop stresses obtained indicate, that during an earthquake, considerable amount of moments are acting on the arches at the upper sections of the dam, while, the vertical moments at the mid sections are getting more significant. As it is noticed, the modal stresses in more complex mode shapes are bigger than those in simple mode shapes.

### 6.3. MAXIMUM DYNAMIC STRESSES

Modal response spectral densities,  $S_r(x, f)$ , have been calculated in Section 4.9 for the first five modes in three earthquake directions and those corresponding to the reservoir in empty condition have been shown in Figs. 4.8, 4.9 and 4.10. In those calculations, the acceleration power spectral density of EL-CENTRO, 1940 earthquake is taken as the input force, the damping of the Arch Dam Type-5 is assumed to be 4% of critical and the velocity of earthquake waves is equal to infinity.

Since, both the modal response spectral densities and modal stresses are determined, the spectral densities of each stress component at any point can be calculated by the application of Eq. (6.1). These calculations have been carried out for the hoop and vertical stresses of the crown cantilever for both the reservoir empty and full conditions. Mean maximum stresses are determined from the power spectral densities of stress components for an earthquake duration 30 seconds.

The results obtained are given in Fig. 6.3 for both reservoir in empty and full conditions, comparatively. These stresses are almost entirely due to the first mode and the contributions of higher modes are negligible. This is because; in spite of the result obtained in Section 6.2.3 about the modal stresses which are greater in higher modes than those in simple mode shapes; the relative modal responses of higher modes in the case of

excitation in the direction parallel to the axis of symmetry, are very small in comparison with the response of fundamental mode.

No definite sign is given to these dynamic stresses, as they may be tension or compression, according to the upstream or downstream deflection. The stresses corresponding to the reservoir in full condition are bigger than those in empty condition.

Fig. 6.3 shows that during a strong ground motion very high dynamic hoop stresses may develop in the top arch and high dynamic vertical stresses may develop at the bottom of crown cantilever of an arch dam.

#### 6.4 MAXIMUM STRESSES IN AN ARCH DAM DURING EARTHQUAKE

6.4.1 In the above sections, the method of calculation of the most probable maximum dynamic stresses in an arch dam during a strong earthquake ground motion has been presented. As described in section 1.2, various types of static loads, other than the dynamic loading due to earthquake, are acting on an arch dam simultaneously. So that, the most critical maximum stresses which may develop in the arch dam can be determined by means of algebraically combining the dynamic stresses due to an earthquake with the static stresses due to the other static loads.

In this study, only two major static loads, which are the hydrostatic loads and the gravity loads have been taken into consideration. In section 2.12.3 the results obtained were given in Fig. 2.17 and 2.18 respectively, for the crown cantilever of Arch Dam Type-5. Those results shall be taken into consideration in the following calculations in order to determine the probable maximum stresses in Arch Dam Type-5 for EL-CENTRO, 1940 earthquake.

6.4.2 The most probable critical maximum stresses in the arch dam may be developed mainly for two critical loading combinations;

(I) Reservoir in empty condition - in this case, the only acting static load is the gravity loading, so that, it must be combined with the earthquake dynamic loading corresponding to the reservoir in empty condition.

(II) Reservoir in full condition - in this case, the hydrostatic and gravity loads are acting together as the total static loading and these loadings must be combined with the earthquake dynamic loading corresponding to the reservoir in full condition.

For both of these loading combinations, the dynamic loads must be considered acting once in the upstream direction and once in the opposite (downstream) direction.

6.4.3 According to the above mentioned loading combinations the envelopes of maximum compressive and tensile, hoop and vertical stresses for the crown cantilever of Arch Dam Type-5 are calculated and shown in Figs. 6.4 to 6.7, in comparison with the static stresses due to hydrostatic and gravity loadings. In each of these figures, the stresses obtained for the water and air faces are given together for both reservoir in empty and full conditions. By examining these figures the following conclusions can be derived:

#### 6.4.3.1 Maximum Compressive Hoop Stresses

Fig. 6.4 shows that, the total maximum compressive hoop stress is developed at the top of the dam on the water face which is due to the earthquake loading acting together with the hydrostatic loads for the reservoir in full condition. The value of this total maximum compressive hoop stress is about 2.5 times the maximum compressive hoop stress due to static loadings. Even for the reservoir in empty case, the total maximum compressive hoop stress at the same location is about 1.5 times the

corresponding static stress. On the air face and at the lower sections the compressive hoop stresses are not so critical.

#### 6.4.3.2 Maximum Tensile Hoop Stresses

Fig. 6.5 shows that the total maximum tensile hoop stress is developed at the top of the dam on the water face, for the reservoir in empty condition and when the earthquake loading acting from downstream to upstream. The magnitude of this tensile hoop stress is about half of the maximum compressive stress obtained in section 6.4.3.1. For the reservoir in full condition the maximum tensile stress developed at the top is about 2/3 of the corresponding tensile stress in empty case, but considerable amount of tensile stresses are also developed on the water face at the bottom sections. On the air face, in empty condition for the earthquake acting from upstream to downstream, slightly critical tensile stresses are noticeable at the top of the dam.

#### 6.4.3.3 Maximum Compressive Vertical Stresses

Fig. 6.6 shows that, the total maximum compressive vertical stress is developed at the bottom of the crown cantilever on the air face which is due to the earthquake loading acting together with the hydrostatic loads for the reservoir in full condition. The value of this total maximum compressive vertical stress is about 1.35 times the maximum compressive vertical stress due to static loadings. On the water face and at the upper sections and also for the reservoir in empty condition the compressive vertical stresses are not so critical.

#### 6.4.3.4 Maximum Tensile Vertical Stresses

Fig. 6.7 shows that, the total maximum tensile vertical stress is developed at the bottom of the crown cantilever on the water

face which is due to the earthquake loading acting together with the hydrostatic loads for the reservoir in full condition. The value of this total maximum tensile vertical stress is about 1.60 times the maximum tensile vertical stress due to static loadings. On the air face, at the upper sections considerable amount of tensile stresses are developed which are also due to the same loading combination. For the reservoir in empty condition, the tensile vertical stresses are not so critical.

#### 6.5 DISCUSSION OF RESULTS

The numerical values for the maximum stresses given above, may not be general for every arch dam, but these results may represent the general behaviour of arch dams subjected to earthquake ground motions. Therefore, the following general conclusions can be drawn from the above investigations:

6.5.1 Maximum total stresses in an arch dam develop in two critical loading conditions:

(I) Reservoir in full condition, earthquake loading acting from upstream to downstream

- Very large compressive hoop stresses may develop at the upper arches on the water face,
- Very large compressive vertical stresses may develop at the bottom of the crown cantilever on the air face,
- Very large tensile vertical stresses may develop at the bottom of the crown cantilever on the water face,
- Considerable amount of vertical tensile stresses may develop at the upper sections of the crown cantilever on the air face.

(II) Reservoir in empty condition, earthquake loading acting from downstream to upstream:

- Large tensile hoop stresses may develop at the top arch on the water face.
- These tensile stresses are reduced at the bottom sections, but they are effective on the upper half of the dam.

6.5.2 From the structural point of view, the effect of these large stresses on the safety of the arch dam can be interpreted as follows:

In the upper portion of the dam where the large tensile hoop stresses are computed, if cracking occurs it will manifest itself as slight and temporary openings in the vertical contraction joints. These cracks will close as the structure deflects in the opposite direction and will be permanently closed when vibration of the structure ceases.

The maximum total compressive stress is to be considered as the important indicator of the ultimate strength of the dam. For the aseismic design of an arch dam to resist earthquakes, to accept a maximum total compressive stress of one half the ultimate compressive strength of the concrete is considered to be proper design (ref. 21).

The vertical tensile stresses developed at the bottom on the water face and at the upper section on the air face may also cause some horizontal crackings but they may not be closed as the structure goes into the opposite phase of the oscillation, as in that region in both of the phases the tensile stresses may predominate. Therefore some special precautions, such as using reinforcement, should be taken in those regions in order not to allow the occurrence of large cracks.

6.5.3 The maximum dynamic stresses in the case of vertical ground motion are also considered in this investigation. The intensity of this vertical ground motion is assumed 0.25 of horizontal component of earthquake. The calculations show that mostly the fifth mode contributes to the stresses and the first mode has only small amount of effect. As a result of these calculations, in case of a vertical ground motion, dynamic stresses about 8-9% of horizontal earthquake are obtained. It seems that, for a slightly domed arch dam, like Arch Dam Type-5, the dynamic stresses due to vertical earthquake may be neglected. But for extremely domed arch dams, these stresses must be taken into consideration.

## CHAPTER 7

### CONSIDERATIONS ON SEISMICITY OF THE DAM SITE

#### AND THE SUMMARY OF THE PRINCIPAL RESULTS

##### 7.1 INTRODUCTION

In the response calculations of arch dams, subjected to seismic disturbances, presented in the previous Chapters, the input excitation has been characterised by the acceleration power spectral density of the ground motion and the responses have been computed considering the acceleration power spectral density of a recorded past earthquake, in order to give an example of the application of the methods introduced.

As a matter of fact, the seismic activity is not exactly the same at any region in the world; therefore, for the design of structures to withstand earthquakes, the seismic characteristics of the particular region, where the structure is to be constructed, must be estimated in a probabilistic way and the dynamic loading must be calculated according to these estimated characteristics of that region.

In this Chapter, firstly the methods to estimate the seismic characteristics in a particular region are to be considered briefly; later, the methods presented in this study for the dynamic analysis of arch dams subjected to seismic disturbances and the general results obtained are to be summarized.

##### 7.2 ESTIMATION OF SEISMIC CHARACTERISTICS OF A PARTICULAR REGION

###### 7.2.1 Intensity measures of Earthquakes

Since the early studies on the seismic design of structures, because of the absence of suitable instruments for measuring the severity of the ground

motion, it is the usual practice to assess the intensity of ground motion on the basis of human reactions and observed damage. The well-known MODIFIED MERCALLY INTENSITY SCALE (ref.90) is most commonly used for this purpose. However, this scale is not suited to convey engineering information on the forces to be used in earthquake design; it may only facilitate comparison between different earthquakes and between different locations during the same earthquake when appropriate instrumental recordings are not available.

Another approximate method presented by RICHTER (ref.91) is to classify ground shocks according to the amount of energy released, which is based on the so-called MAGNITUDE of an earthquake. The name magnitude is defined, for shallow shocks, to mean the logarithm to the base 10 of the maximum trace amplitude expressed in thousandths of a millimetre with which the standard short period torsion seismometer would register that earthquake at an epicentral distance of 100 Km. Actually, the magnitude is a measure of the intensity of ground motion at a point 100 Km. from the epicenter. For engineering purposes, the magnitude is informative as an indication of the size of the earthquake, but does not provide a complete knowledge about the intensity of ground shaking at various points in the disturbed area.

A precise measure of the intensity of ground motion can be based on instrumental recordings. Such an intensity measure has firstly been suggested by HOUSNER (ref.73) who has introduced the SPECTRUM INTENSITY, in relation with the earthquake response spectra (see section 4.7), which is defined to be the area under the velocity response spectrum curve between 0.4 and 10 Hz, which is the frequency range of structures to be encountered during an earthquake (see figure 5.8).

A similar approach has been suggested by BORGESS (discussion on ref.73) in relation with the concept of the power spectral density of the ground acceleration, so that, the POWER SPECTRAL INTENSITY of the earthquake is defined in terms of the mean square value of the power spectral density of ground acceleration as :

$$SI_a = \langle \ddot{u}_g^2(t) \rangle = \int_0^{\infty} S_{\ddot{u}_g}(f) df . \quad \dots (7.1)$$

As the spectral density curve decreases very fast and the frequencies higher than 10 Hz. have practically no importance, (see fig.5.1), the upper limit of the integral can be taken as 10 Hz.

The concepts of power spectral density and power spectral intensity of the ground acceleration are directly related to the treatment of earthquake ground motions as series of random events, thus bringing the subject under the scope of the theory of random processes. As it has already been shown in Chapter 4 that, the application of random vibration processes to the response calculations of structures subjected to earthquake type excitation gives very satisfactory results. Accordingly, it is suggested that, the characteristics of an earthquake can be defined in terms of power spectral density and power spectral intensity of ground acceleration in the most appropriate way for design purposes.

### 7.2.2 Seismic Regionalization

In order to estimate the above mentioned characteristics of a representative earthquake which shall be used in the probabilistic design of a structure, large amount of dependable recorded data is necessary about the earthquakes which have occurred in the past in that region. As this

data recording is a very expensive process which consists of establishing a very fine network of seismogram stations, great care should be taken to reduce these costs to minimum. This can be done by the considerations of macro- and micro-regionalizations.

The subject of seismic zoning, which has so many important implications for earthquake engineers, has been summarized in a general way by MEDVEDEV (ref.92) who outlines the basic methods now in use and describes the way in which data on past earthquakes, geotectonic studies and investigations of local conditions by recording of small earthquakes may be combined to give the best picture consistent with a current state of knowledge. The seismic zoning map of USSR territory prepared during 1961-64 has also been presented in MEDVEDEV's paper which embodies many recent investigations including consideration of various soil conditions.

The problems of micro-regionalization, which is particularly important for arch dam design in a highly seismic region, have been illustrated by BUNE (ref.93) by the intensive study of a particular area. This study involved some 10-18 seismographic stations located 30-60 km. apart. In a five year period about 2000 epicenters were located and this large amount of data permitted a much more comprehensive study of the relation between epicenter locations and geological faults. The relationships between occurrence of earthquakes and the local and general geotectonic status of the region were explored. Methods of employing such data for the formulation of seismic zoning maps were also investigated.

### 7.2.3 Seismicity of an Area

The seismicity of an area can be expressed in several ways. The basic method is to simply mark all the epicenters on a map. To refine this

slightly, one might indicate an epicentre by a circle, the radius of which is proportional to the magnitude of the earthquake represented. Others have expressed seismicity in terms of strain-energy release in some selected unit area and time. This method seems to define the active tectonic zones within the area under study.

A mathematical approach is to calculate the magnitude-frequency of occurrence relationship which indicates the number of earthquakes of a given magnitude per unit of time. Another mathematical technique of expressing the same feature is to use the extreme value theorem of statistics to estimate the largest earthquake with a return period of a certain number of years.

From the design engineering point of view, the last method, namely, extreme value theorem of statistics, seems to be the most appropriate way to define the seismicity of an area, as it may provide the necessary earthquake characteristics in that area for seismic design of structures.

#### 7.2.4 Application of extreme value theorem of statistics to earthquakes

7.2.4.1 One of the aims of the statistical theory of extreme values is to analyse observed extremes valid for a given period and to forecast extremes that may be expected to occur within a certain time. As the theory of extreme values has been described in detail elsewhere (ref. 94), no attempt will be made to describe it in this thesis.

7.2.4.2 The mathematical techniques of extreme value statistics have first applied to the earthquake problem by NORDQUIST (ref. 95), who has analysed the world's largest earthquakes and also the earthquakes occurred in Southern California regions. Nordquist has shown that all the points plotted on a GUMBEL's probability paper for the earthquakes of the entire world can be represented fairly well by a straight line, while the same is also true for

the plotted points for each smaller region separately. These results are the first indication that in each case the observed distribution of the magnitudes of the largest earthquakes is in good agreement with the theory of largest values.

Recently, DICK (ref. 96) has used these methods to examine the seismicity of New Zealand, and to compare that area with the world and with the Southern California experience investigated by Nordquist. It is shown that this statistical approach gives results which fit the past record of experience very well, and which leads to meaningful statements about the occurrence of future large earthquakes.

Similar conclusions as to the validity of extreme value statistics are arrived at by MILNE and DAVENPORT (ref. 97), who have applied these techniques to a small region of Western Canada. They have suggested that the basic parameters used in extreme value statistics might well be adapted as a fundamental measure of seismicity, since these parameters point directly to the type of information on maximum expected earthquakes which is of prime interest to design engineers.

7.2.4.3 In all of these investigations, the intensity of earthquake has been expressed in terms of RICHTER's MAGNITUDE scale. As it is described in section 7.2.1 that, the magnitude scale does not provide a complete knowledge for design purposes and the most appropriate way to define the earthquake characteristics is to use the power spectral density and the power spectral intensity of ground acceleration.

For the probabilistic design methods presented in this thesis, these power spectral characteristics are taken into consideration, therefore, earthquake data about these characteristics are needed. Unfortunately, up to date very little study has been done on this area and there is

not enough data to demonstrate the application of extreme value theorem of statistics to estimate the probable maximum power spectral intensity of ground acceleration for a return period of a certain number of years. However, there is no doubt that, the use of power spectral intensities of past earthquakes will also provide the necessary information about the estimation of future earthquakes.

7.2.4.4 In the application of extreme value theorem to the power spectral densities of ground accelerations recorded in the past in order to estimate the power spectral characteristics of future earthquakes the following suggestions should be considered:

(I) The power spectral densities of each of three components of ground acceleration which are recorded in a particular region is to be determined using either analogue or digital computing techniques (ref. 98).

(II) The power spectral intensities of each component are calculated from Eq. (7.1).

(III) The power spectral density curves are normalized by means of dividing the ordinates of these curves by the corresponding power spectral intensities.

(IV) If these normalized spectral density curves show considerably different shapes for horizontal and vertical components or for micro tremors and strong ground motions, these curves are to be classified according to direction of earthquake or to the power spectral intensities.

(V) For each class of spectral curves, an average normalized power spectral curve is determined, among those, the one corresponding to most intense earthquakes may be taken into consideration in the design.

(VI) When enough data is collected, the extreme value theorem of statistics is to be applied to the calculated power spectral intensities and the results are plotted on a GUMBEL's probability paper. By fitting an appropriate straight line, the necessary probability parameters for estimating the power spectral intensities of future earthquakes are determined.

7.2.4.5. At this stage, a very important question arises. This question is; what is the return period to be taken into consideration in the design of a particular type of civil engineering structure? The return period is the direct indication of the magnitude of the future earthquake, therefore, should be chosen carefully. An over-estimated period will lead to an uneconomical solution, an underestimated period may endanger the safety of the structure.

The answer to this question is still being discussed, however, an appropriate answer can be given by considering the expected service life and the type of the particular structure. Arch dams are constructed for a long service life and the safety of them are of primary importance as the failure of an arch dam is a great disaster that may destroy many cities located downstream. Accordingly, for arch dams a long return period should be used. It is suggested that an optimum return period might be 500 years and for extremely critical arch dams this period might be increased up to 1,000 years.

7.2.4.6 The effect of duration of earthquake on the response calculations has been discussed and a magnification factor has been defined as a function of this duration in Section 5.7.3. The maximum probable duration of earthquake for a certain return period can also be determined by means of extreme value theorem of statistics.

However, HOUSNER has applied a very simple method (ref. 73) consisting of plotting the measured durations of strong earthquakes versus the magnitude of these earthquakes and has predicted that, upper bound for the duration of strong ground motion is approximately 45 seconds.

### 7.3 SUMMARY OF THE METHODS OF ANALYSIS

7.3.1. Three dimensional finite element technique is applied to the static and dynamic analysis of arch dams. Simple tetrahedral elements with four nodal points, each of them allowed three degrees-of-freedom are used for the idealization of an arch dam (Section 2.3). It is demonstrated that this idealization allows the application of any arbitrary geometrical shape without introducing any simplification of the valley or the structure itself and it is particularly suitable for the idealization of arch dams.

7.3.2 The stiffness properties of the simple tetrahedral elements are derived (Section 2.4) by assuming linear three dimensional displacement functions (Eq. 2.16). The element stiffness matrix is obtained almost explicitly and very little matrix calculations are left to be executed in the computer (Appendix A.1). It is shown that all of the element stiffness matrices can be calculated according to a global coordinate system, so that, the stiffness of the complete structure can easily be combined according to this global coordinate system without necessitating any transformation of the element stiffness matrices from local to global coordinate systems (Section 2.6).

7.3.3 In the static analysis of arch dams using finite element techniques, a very large number of simultaneous equilibrium equations are involved which necessitated a large amount of computer storage. In order to satisfy the storage requirements of the existing computers and to minimize the rounding-off errors, a three dimensional iterative method is developed (Section 2.7). A special procedure is derived

for the application of constraints to the boundary nodal points (Section 2.8). This iterative method of solution of simultaneous equations has proved to be very suitable for finite element analysis.

Calculation of nodal point stresses, in the case of simple tetrahedral finite elements, needs special care. It is shown that the usual averaging method of element stresses does not give satisfactory results for sharply varying stress conditions and an appropriate way to calculate the nodal point stresses is derived by using the nodal point forces acting in sections of the structure (Section 2.9).

There are various ways of idealizing an arch dam by means of tetrahedral elements. A comparison between the results obtained from different idealizations showed that, a double combination of five tetrahedral elements to build a brick-like block was the most convenient one to use (Section 2.10).

7.3.4. For the dynamic analysis of arch dams by finite element methods, the inertia properties of tetrahedral element is derived (Section 3.3) and the consistent mass matrix of tetrahedral element is obtained entirely explicitly (Appendix A.4).

Since the dynamic equilibrium of the complete structure involves a very large number of equations, a special computer procedure which uses so called planar storage is applied for calculating the natural frequencies and mode shapes of the arch dams (Section 3.5).

The hydrodynamic effect of the reservoir water is also considered in the calculations. The hydrodynamic pressure coefficients, which are derived from an electrolytic potential analogue are used to calculate the hydrodynamic forces (Section 3.8) and these forces are incorporated in the general vibration problem by assuming the added mass effect of

the reservoir water (Section 3.9).

The analysis is also extended to include the effect of the boundary flexibility. This is easily achieved by considering some more elements inside the valley which have given in-situ modulus of elasticity (Section 3.10).

7.3.5 General theory of stationary random vibrations is applied to a three-dimensional solid system subjected to multiple discrete stationary random exciting forces (Section 4.5.4.). The general formula (Eq. 4.49) which gives the power spectral density of response is extended for the cases of fully correlated excitation (Eq. 4.55) and convected excitation (Eq. 4.64).

The relations between the power spectral density and probability density of a random variable are considered (Section 4.5.5) and by using the general results obtained for the Gaussian peak distribution (Section 4.5.6) the "mean maxima" of the random variable for a prescribed time duration is determined (Section 4.5.7).

7.3.6 Considering the response of linear single degree-of-freedom system to earthquake ground motion, the possibilities of applying the results obtained for the response calculations to stationary random excitation, are investigated (Section 4.6). The formula for calculating the responses of structures which uses the power spectral density of earthquake ground acceleration as input is derived (Eq. 4.84). This formula is extended to include the velocity of earthquake waves (Eq. 4.86). Using the probability relationships, the mean maxima of the responses for a prescribed earthquake duration is determined (Eq. 4.90). These formulations satisfy the requirements of the probabilistic design which is necessitated by the unpredictable, random nature of the earthquake ground motion.

7.3.7 Dynamic stresses in arch dams due to earthquakes are calculated (Section 6.2) by defining the responses of the structure in terms of stresses

and modifying the general displacement response formula accordingly (Eq. 6.1). In this formula, the normalized displacements are replaced by modal stresses which are defined as the maximum stresses developed in the structure while the structure is vibrated in that particular mode. These stresses are calculated by applying the stress calculation methods given for static analysis, the only difference is, for the dynamic stresses, the formula which is used to calculate the nodal point forces includes the inertia forces (Eq. 6.2).

The most critical maximum stresses which may develop in the arch dam is determined by means of algebraically combining the maximum dynamic stresses due to an earthquake with the static stresses due to the static loads acting on the arch dam (Section 6.4).

7.3.8. In all of the response calculations, the power spectral density of a representative earthquake ground acceleration is taken as input excitation. For probabilistic seismic design of an arch dam, the shape of the power spectral density curve and the power spectral intensity must be estimated from the recorded accelerograms of the past earthquakes occurred in the region where the structure is to be built. In the estimation of these important characteristics of the representative earthquake it is suggested that, the extreme value theorem of statistics will be a very useful tool (Section 7.2.4).

#### 7.4 SUMMARY OF THE PRINCIPAL RESULTS

7.4.1 In this thesis, the application of three dimensional finite element techniques to static and dynamic analysis of arch dams is demonstrated. By developing special computer procedures, the storage requirements of the existing computers are satisfied and the rounding-off errors are minimized. The results obtained prove the efficiency of the finite element techniques for the analysis of three dimensional structures, under static and dynamic loading, which have complex geometrical shapes and also arbitrary boundary condition.

7.4.2 The simplest three-dimensional element, a tetrahedron, is chosen as the finite element. Derivations of the stiffness and consistent mass matrices of tetrahedral elements are shown to be straightforward. The consistent mass matrix is obtained entirely explicitly, and the stiffness matrix almost explicitly, where very little computation is left to be executed in the computer. In these derivations there is no need for any local coordinate system. Although, in case of the tetrahedral element, a very large number of elements are necessary for a satisfactory result, as the derivation of element properties and assembling the corresponding overall properties of the structure are very simple, the computing time spent is not excessive.

The main difficulty met in the analysis by using tetrahedral elements is the calculation of nodal point stresses. However, an appropriate method to give suitable answers is developed; the method necessitates some hand calculations to be executed by the engineer.

The results presented in section 2.12.3 for the static analysis of Arch Dam Type-5 under hydrostatic and gravity loads show that the simple tetrahedral element gives results with reasonable accuracy, even only one element layer through thickness is used in the idealization.

7.4.3 In the dynamic analysis of arch dams, the use of three-dimensional finite elements makes it possible to determine the vertical and tangential modes of vibrations which may contribute to the response of the structure considerably during excitation in vertical or cross valley direction (section 3.12.3).

The natural frequencies and mode shapes calculated for Arch Dam Type-5 resemble those obtained experimentally for a similar prototype arch dam (section 3.12.7).

The hydrodynamic effect of the reservoir water on the dynamical characteristics of arch dams are investigated by using the results of electrolytic potential analogue and incorporating the calculated hydrodynamic forces in the general vibration problem by assuming the added mass effect. The results obtained show that this effect reduces the natural frequencies of arch dams to 0.89-0.92 of the frequencies corresponding to the reservoir in empty condition (table 3.1) and the mode shapes are also modified considerably (figure 3.15). The agreement between these results and those obtained experimentally from model and prototype investigations on arch dams (table 3.5) confirms the validity of the assumption that the hydrodynamic effect can be represented as an added mass and the use of electrolytic potential analogue technique to predict the excessive pressure coefficients.

The flexibility of the foundation should be taken into consideration for the dynamic analysis of arch dams, especially when the in situ modulus of elasticity of the foundation is less than 1/2 of the modulus of elasticity of concrete, as in such cases large amounts of reductions in the natural frequencies are to be expected (figure 3.17).

7.4.4 The application of random vibration theory to the response calculations of arch dams subjected to seismic disturbances is demonstrated (section 4.6) and the results obtained are compared with those obtained by response spectra methods (section 5.4). It is suggested that the methods developed satisfy the requirements of probabilistic design and will provide a very useful tool for the aseismic design of arch dams.

As most of the energy involved in the ground motion is in the frequency range up to 5 Hz and the frequencies higher than 10 Hz have practically no

importance, the spectral density of the ground acceleration can be taken in the frequency range from 0 to 10 Hz (figure 5.1) . For the horizontal components of strong ground motions, generally, the predominant frequency is about 2.5 Hz and for higher frequencies the power content is decreasing very fast. This character of excitation and the complex shapes of the higher modes resulted that the contribution of higher modes are generally much smaller than lower modes (section 4.9). The only exception is noticed in vertical vibration, where a higher mode (in the case of Arch Dam Type-5 the fifth mode) may have bigger contribution than the lower modes; this effect may increase as the power content of vertical ground motion is considerably larger for higher frequencies.

In the case of the earthquake acting parallel to the axis of symmetry and in vertical direction, the antisymmetrical modes have no contribution and only the symmetrical modes contribute. For the excitation perpendicular to the axis of symmetry (cross valley direction) the symmetrical modes have no contribution and only the antisymmetrical modes contribute.

7.4.5 The effects of various factors on the response of arch dams subjected to earthquakes are investigated and the following conclusions are derived :

(1) The responses of the arch dam for the reservoir in full condition are larger than the responses for the reservoir in empty condition. This increase is due to the hydrodynamic effect of the reservoir water, which reduces the natural frequencies of the structure so that this reduction brings the natural frequencies closer to the predominant frequencies of the ground motion and also the additional mass introduced by the hydrodynamic effect serves to increase the dynamical forces acting on the structure (section 5.5).

The maximum dynamic radial displacement at the top of the dam under a strong ground excitation may reach to 0.61 of hydrostatic loading for the reservoir in empty condition and up to 0.78 for the reservoir in full condition (figure 5.16).

(2) The response of lightly damped structures is very sensible to the damping ratio presented in the structure. However, the arch dams are assumed to be lightly damped, there is not enough reliable information about the damping ratio presented. It is shown in this investigation that if the damping ratio is assumed to decrease from 4% to 2%, the responses are increased slightly more than 40%, while the damping ratio is increased from 4% up to 10% the responses are decreased about 35% (figure 5.19). These results show clearly the importance of damping ratio and the necessity of more reliable information about the actual damping present in the arch dams.

(3) The responses of arch dams are increased as the flexibility of the foundation increases. This is mainly due to the larger reductions in the natural frequencies of the structure in the cases of very flexible foundations and for a conservative design the flexibility of the foundation must be taken into consideration in response calculations (section 5.9).

(4) As the response is directly related to the power spectral intensity of earthquake ground acceleration, the response increases as the intensity of earthquake increases. On the other hand, the relative responses of individual modes are dependent on the shape of the power spectral density of ground acceleration (section 5.7.2) so that both the power spectral density curve and the power spectral intensity of the ground acceleration must be chosen very carefully. In order to satisfy the requirements of probabilistic design, in the choice of these characteristics, the extreme value theorem of statistics is suggested to be a valuable tool.

(5) Duration of the earthquake is another important value which must be considered in the aseismic design. However, the magnification factor, which is defined as a function of the earthquake duration, is shown to increase with the predominant frequency, the values obtained for 15 seconds to 40 seconds duration do not vary largely (figure 5.21) and it seems that a value equal to 3.0 for the magnification factor can be used as a good approximation for most of the practical cases.

(6) The effect of the velocity of earthquake waves on the responses of arch dams is also considered. It is shown that the wavelengths longer than 3.5-4 times the maximum dimension of the structure in the direction of excitation, have no significant effect on the responses of an arch dam. On the other hand, it is proved that the consideration of the velocity of earthquake waves seves to reduce the responses (figure 5.22). According to these results, for a conservative design, it is recommended not to include the velocity of earthquake waves in response calculations.

(7) During an earthquake, the ground moves both horizontally and vertically. Therefore the response calculation of arch dams to earthquakes must include the consideration of both of the horizontal and also the vertical components of earthquake ground accelerations. The methods developed in this study allow the application of any component of ground motion, then the responses obtained for each individual forcing direction may easily be combined.

The results obtained for Arch Dam Type-5 show that, for the responses of the crown cantilever, the earthquake acting along the axis of symmetry of the dam produces the maximum response (figure 5.23), while, for the responses of other sections, the lateral horizontal component plays

an important part and the angle of earthquake direction, which produces maximum response, is increased towards abutment (figure 5.24).

The responses calculated for the vertical component of ground motion (figure 5.25) show that, even for a slightly domed arch dam, the effect of the vertical component of ground motion is quite important and in case of extremely domed arch dams, this effect is expected to become much more important, and should be considered in the design.

7.4.6 From an engineering point of view, the stresses induced in the structure during an earthquake are more important than the deflections, as the maximum magnitude of these stresses is the best measure to the safety of the arch dam.

The direct calculation of the maximum dynamic stresses using the random vibration analysis techniques is demonstrated (section 6.2). In these calculations both reservoir in empty and full conditions are considered. The most critical maximum stresses which may develop in the arch dam are determined by means of algebraically combining the dynamic stresses due to an earthquake with the static stresses due to the other static loads acting according to the condition of the reservoir.

The most probable critical maximum stresses in an arch dam may be developed for two critical loading combinations; the first one is, reservoir in empty condition, earthquake loading acting from downstream to upstream, and the second combination is, reservoir in full condition, earthquake loading acting from upstream to downstream (section 6.4).

In the first case, large tensile hoop stresses may develop at the top arch on the water face and the tensile stresses are effective on the upper half of the dam.

In the second case, very large compressive stresses may develop at the upper arches on the water face; very large compressive vertical stresses at the bottom of the crown cantilever on the air face; very large tensile vertical stresses at the bottom of the crown cantilever on the water face, and considerable amount of vertical tensile stresses at the upper sections of the crown cantilever on the air face.

The numerical results obtained for Arch Dam Type-5 subjected to EL-CENTRO 1940 earthquake show that, if an arch dam is subjected to a very strong earthquake ground motion within an epicentral distance of 50 Km, the total maximum compressive hoop stress may reach up to 2.5 times the maximum compressive hoop stress due to static loadings, which may endanger the stability of the arch dam.

The maximum dynamic stresses due to vertical ground motion are also considered and dynamic stresses about 8-9% of horizontal earthquake are obtained. For extremely domed arch dams, these stresses are expected to become more effective and should not be neglected in the aseismic design of arch dams.

7.4.7 Finally, the attention is once more focussed on the importance of the statistical information about the past earthquakes occurring in the particular region where the structure is to be built. A careful consideration on seismic regionalization will certainly reduce the cost of the collection of required data for probabilistic aseismic design (section 7.2). The power spectral density function and the power spectral intensity of earthquake ground acceleration seem to be the most useful measures of the earthquakes from the point of view of design engineering. The extreme value theorem

of statistics is an appropriate tool to estimate the most probable power spectral intensity of the earthquake to be expected in that particular region. The minimum return period to be considered in the probabilistic design of arch dams is suggested to be 500 years and for extremely critical arch dams this period may be increased up to 1,000 years.

APPENDIX A.1

DERIVATION OF THE STIFFNESS MATRIX FOR THE TETRAHEDRAL ELEMENT

By means of the application of the formulae obtained in section 2.4 the stiffness matrix for the tetrahedral element is obtained as follows .

The displacement functions are given by equation (2.16) as

$$\left. \begin{aligned} u &= A_1 + A_2x + A_3y + A_4z \\ v &= A_5 + A_6x + A_7y + A_8z \\ w &= A_9 + A_{10}x + A_{11}y + A_{12}z \end{aligned} \right\} \dots (A.1.1)$$

The displacement pattern becomes

$$[N(x,y,z)] = \begin{bmatrix} 1 & x & y & z & \circ \\ \circ & \circ & \circ & \circ & 1 & x & y & z & \circ & \circ & \circ & \circ \\ \circ & 1 & x & y & z \end{bmatrix} \dots (A.1.2)$$

The generalized displacements in equation (2.2) can be written as :

$$\begin{Bmatrix} u \\ v \\ w \end{Bmatrix} = \begin{bmatrix} 1 & x & y & z & \circ \\ \circ & \circ & \circ & \circ & 1 & x & y & z & \circ & \circ & \circ & \circ \\ \circ & 1 & x & y & z \end{bmatrix} \begin{Bmatrix} A_1 \\ A_2 \\ \circ \\ \circ \\ \circ \\ \circ \end{Bmatrix} \dots (A.1.3)$$

With respect to the global Cartesian coordinate system the nodal point coordinate matrix [C] can be formed by the following transformations (see figure A.1) :

$$\left. \begin{aligned} a_j &= x_j - x_i & , & & a_k &= x_k - x_i & , & & a_\ell &= x_\ell - x_i \\ b_j &= y_j - y_i & , & & b_k &= y_k - y_i & , & & b_\ell &= y_\ell - y_i \\ c_j &= z_j - z_i & , & & c_k &= z_k - z_i & , & & c_\ell &= z_\ell - z_i \end{aligned} \right\} \dots (A.1.4)$$

the equation (2.3) can be written as :

$$\begin{Bmatrix} u_i \\ v_i \\ w_i \\ u_j \\ v_j \\ w_j \\ u_k \\ v_k \\ w_k \\ u_\ell \\ v_\ell \\ w_\ell \end{Bmatrix} = \begin{bmatrix} 1 & \cdot \\ \cdot & \cdot & \cdot & \cdot & 1 & \cdot \\ \cdot & 1 & \cdot & \cdot & \cdot \\ 1 & a_j & b_j & c_j & \cdot \\ \cdot & \cdot & \cdot & \cdot & 1 & a_j & b_j & c_j & \cdot & \cdot & \cdot & \cdot \\ \cdot & 1 & a_j & b_j & c_j \\ 1 & a_k & b_k & c_k & \cdot \\ \cdot & \cdot & \cdot & \cdot & 1 & a_k & b_k & c_k & \cdot & \cdot & \cdot & \cdot \\ \cdot & 1 & a_k & b_k & c_k \\ 1 & a_\ell & b_\ell & c_\ell & \cdot \\ \cdot & \cdot & \cdot & \cdot & 1 & a_\ell & b_\ell & c_\ell & \cdot & \cdot & \cdot & \cdot \\ \cdot & 1 & a_\ell & b_\ell & c_\ell \end{bmatrix} \begin{Bmatrix} A_1 \\ A_2 \\ A_3 \\ A_4 \\ A_5 \\ A_6 \\ A_7 \\ A_8 \\ A_9 \\ A_{10} \\ A_{11} \\ A_{12} \end{Bmatrix} \dots (A.1.5)$$

The strains and differential matrix of displacement patterns are given

by :

$$\{\epsilon\} = [B(x,y,z)] \{A\} =$$

$$\begin{Bmatrix} \epsilon_x \\ \epsilon_y \\ \epsilon_z \\ \gamma_{xy} \\ \gamma_{yz} \\ \gamma_{zx} \end{Bmatrix} = \begin{Bmatrix} \frac{\partial u}{\partial x} \\ \frac{\partial v}{\partial y} \\ \frac{\partial w}{\partial z} \\ \frac{\partial v}{\partial x} + \frac{\partial u}{\partial y} \\ \frac{\partial w}{\partial z} + \frac{\partial v}{\partial y} \\ \frac{\partial w}{\partial x} + \frac{\partial u}{\partial z} \end{Bmatrix} = \begin{bmatrix} \cdot & 1 & \cdot \\ \cdot & \cdot & \cdot & \cdot & \cdot & \cdot & 1 & \cdot & \cdot & \cdot & \cdot & \cdot \\ \cdot & 1 \\ \cdot & \cdot & 1 & \cdot & \cdot & 1 & \cdot & \cdot & \cdot & \cdot & \cdot & \cdot \\ \cdot & 1 & \cdot & \cdot & 1 & \cdot \\ \cdot & \cdot & \cdot & 1 & \cdot & \cdot & \cdot & \cdot & \cdot & 1 & \cdot & \cdot \end{bmatrix} \begin{Bmatrix} A_1 \\ A_2 \\ \cdot \\ \cdot \\ \cdot \\ \cdot \\ A_{12} \end{Bmatrix} \dots (A.1.6)$$

The matrix of material constants  $[D]$  is given for three-dimensional elasticity, as

$$[D] = \begin{bmatrix} D_1 & D_2 & D_2 & \cdot & \cdot & \cdot \\ D_2 & D_1 & D_2 & \cdot & \cdot & \cdot \\ D_2 & D_2 & D_1 & \cdot & \cdot & \cdot \\ \cdot & \cdot & \cdot & D_3 & \cdot & \cdot \\ \cdot & \cdot & \cdot & \cdot & D_3 & \cdot \\ \cdot & \cdot & \cdot & \cdot & \cdot & D_3 \end{bmatrix} \quad \dots (A.1.7)$$

where :

$$D_1 = \frac{E(1 - \nu)}{(1 + \nu)(1 - 2\nu)}$$

$$D_2 = \frac{E \cdot \nu}{(1 + \nu)(1 - 2\nu)}$$

$$D_3 = \frac{E}{2(1 + \nu)}$$

where,  $E$  is the modulus of elasticity of the element material and  $\nu$  is the Poisson's ratio.

The matrix product  $[B(x,y,z)]^T [D] [B(x,y,z)]$  can be obtained explicitly:

$$[B(x,y,z)]^T [D] [B(x,y,z)] = \begin{bmatrix} \cdot & \cdot \\ \cdot & D_1 & \cdot & \cdot & \cdot & \cdot & D_2 & \cdot & \cdot & \cdot & \cdot & D_2 \\ \cdot & \cdot & D_3 & \cdot & \cdot & \cdot & D_3 & \cdot & \cdot & \cdot & \cdot & \cdot \\ \cdot & \cdot & \cdot & D_3 & \cdot & \cdot & \cdot & \cdot & \cdot & D_3 & \cdot & \cdot \\ \cdot & \cdot \\ \cdot & \cdot & D_3 & \cdot & \cdot & \cdot & D_3 & \cdot & \cdot & \cdot & \cdot & \cdot \\ \cdot & D_2 & \cdot & \cdot & \cdot & \cdot & D_1 & \cdot & \cdot & \cdot & \cdot & D_2 \\ \cdot & D_3 & \cdot & \cdot & D_3 & \cdot \\ \cdot & \cdot \\ \cdot & \cdot & \cdot & D_3 & \cdot & \cdot & \cdot & \cdot & \cdot & D_3 & \cdot & \cdot \\ \cdot & D_3 & \cdot & \cdot & D_3 & \cdot \\ \cdot & D_2 & \cdot & \cdot & \cdot & \cdot & D_2 & \cdot & \cdot & \cdot & \cdot & D_1 \end{bmatrix} \dots (A.1.8)$$

As all the coefficients of the matrix product in equation (A.1.8) are independent of the coordinates, then the integral of the matrix product over the volume is simply obtained by multiplying the matrix by the volume of the tetrahedron. This result gives the generalized stiffness matrix  $[\tilde{k}]$  as

$$[\tilde{k}] = \int_V [B(x,y,z)]^T [D] [B(x,y,z)] dV = V \cdot [B(x,y,z)]^T [D] [B(x,y,z)] \dots (A.1.9)$$

where the volume of the tetrahedron  $V$  is given explicitly by :

$$V = \frac{1}{6} \det \begin{bmatrix} 1 & \cdot & \cdot & \cdot \\ 1 & a_j & b_j & c_j \\ 1 & a_k & b_k & c_k \\ 1 & a_l & b_l & c_l \end{bmatrix} \dots (A.1.10)$$

For tetrahedral elements, it is possible to determine the inverse matrix of the coordinate matrix  $[C]$  explicitly as :

$$[c^{-1}] = \begin{bmatrix} 1 & \cdot \\ c_{21} & \cdot & \cdot & c_{22} & \cdot & \cdot & c_{23} & \cdot & \cdot & c_{24} & \cdot & \cdot \\ c_{31} & \cdot & \cdot & c_{32} & \cdot & \cdot & c_{33} & \cdot & \cdot & c_{34} & \cdot & \cdot \\ c_{41} & \cdot & \cdot & c_{42} & \cdot & \cdot & c_{43} & \cdot & \cdot & c_{44} & \cdot & \cdot \\ \cdot & 1 & \cdot \\ \cdot & c_{21} & \cdot & \cdot & c_{22} & \cdot & \cdot & c_{23} & \cdot & \cdot & c_{24} & \cdot \\ \cdot & c_{31} & \cdot & \cdot & c_{32} & \cdot & \cdot & c_{33} & \cdot & \cdot & c_{34} & \cdot \\ \cdot & c_{41} & \cdot & \cdot & c_{42} & \cdot & \cdot & c_{43} & \cdot & \cdot & c_{44} & \cdot \\ \cdot & \cdot & 1 & \cdot \\ \cdot & \cdot & c_{21} & \cdot & \cdot & c_{22} & \cdot & \cdot & c_{23} & \cdot & \cdot & c_{24} \\ \cdot & \cdot & c_{31} & \cdot & \cdot & c_{32} & \cdot & \cdot & c_{33} & \cdot & \cdot & c_{34} \\ \cdot & \cdot & c_{41} & \cdot & \cdot & c_{42} & \cdot & \cdot & c_{43} & \cdot & \cdot & c_{44} \end{bmatrix} \quad \dots (A.1.11)$$

where,

$$\begin{aligned} c_{21} &= \frac{1}{6V} (b_j c_{\ell} - b_j c_k + b_k c_j - b_k c_{\ell} + b_{\ell} c_k - b_{\ell} c_j) \\ c_{22} &= \frac{1}{6V} (b_k c_{\ell} - b_{\ell} c_k) \\ c_{23} &= \frac{1}{6V} (-b_j c_{\ell} + b_{\ell} c_j) \\ c_{24} &= \frac{1}{6V} (b_j c_k - b_k c_j) \\ c_{31} &= \frac{1}{6V} (a_j c_k - a_j c_{\ell} + a_k c_{\ell} - a_k c_j + a_{\ell} c_j - a_{\ell} c_k) \\ c_{32} &= \frac{1}{6V} (-a_k c_{\ell} + a_{\ell} c_k) \\ c_{33} &= \frac{1}{6V} (a_j c_{\ell} - a_{\ell} c_j) \\ c_{34} &= \frac{1}{6V} (-a_j c_k + a_k c_j) \\ c_{41} &= \frac{1}{6V} (a_j b_{\ell} - a_j b_k + a_k b_j - a_k b_{\ell} + a_{\ell} b_k - a_{\ell} b_j) \\ c_{42} &= \frac{1}{6V} (a_k b_{\ell} - a_{\ell} b_k) \\ c_{43} &= \frac{1}{6V} (-a_j b_{\ell} + a_{\ell} b_j) \\ c_{44} &= \frac{1}{6V} (a_j b_k - a_k b_j) \end{aligned} \quad \dots (A.1.12)$$

The stiffness matrix, then, can be obtained by means of simple matrix operations :

$$[k] = [C^{-1}]^T [\tilde{k}] [C^{-1}] \quad \dots (A.1.13)$$

The explicit formulation of this product is quite lengthy and in the computations, these matrix multiplications are performed by the computer for each element.

One important point to note is that there is no need for any local coordinate system for the derivation of stiffness matrix for tetrahedral elements. This makes it possible to avoid the transformation process from local to global coordinates which is necessary for some other types of elements, during the formation of overall stiffness matrix.

APPENDIX A.2

APPLICATION OF ITERATION METHOD TO  
THREE DIMENSIONAL FINITE ELEMENT TECHNIQUE

The general equilibrium equation (section 2.6, equation (2.25)) can be written for the equilibrium of a nodal point as follows :

$$\{S_n\} = [K_{nn}] \{U_n\} \quad \dots (A.2.1)$$

where

$$\{S_n\} = \left\{ \begin{array}{c} S_x \\ S_y \\ S_z \end{array} \right\}_n \quad \dots (A.2.2a)$$

$$\{U_n\} = \left\{ \begin{array}{c} u \\ v \\ w \end{array} \right\}_n \quad \dots (A.2.2b)$$

$$[K_{nn}] = \begin{bmatrix} K_{xx} & K_{xy} & K_{xz} \\ K_{yx} & K_{yy} & K_{yz} \\ K_{zx} & K_{zy} & K_{zz} \end{bmatrix}_{nn} \quad \dots (A.2.2c)$$

$S_n$  is the vector of external forces applied to the nodal point  $n$ ;  
 $U_n$  is the vector containing the components of the displacement of the nodal point  $n$ ; and  $K_{nn}$  is the stiffness matrix of the nodal point  $n$ .

Equation (A.2.1) can be rewritten for the nodal point displacements as:

$$\{U_n\} = [K_{nn}^{-1}] \{S_n\} \quad \dots (A.2.3)$$

There is important physical significance in the terms of equation (A.2.3). The term  $[K_{nn}^{-1}]$  is the flexibility of nodal point  $n$ . This represents the nodal point displacements resulting from unit nodal point forces, and can be written in the form of a submatrix,

$$[K_{nn}^{-1}] = \begin{bmatrix} f_{xx} & f_{xy} & f_{xz} \\ f_{yx} & f_{yy} & f_{yz} \\ f_{zx} & f_{zy} & f_{zz} \end{bmatrix}_{nn} \quad \dots (A.2.4)$$

The Gauss-Seidel iteration procedure can be written for an unknown displacement component as follows :

$$U_n^{(r+1)} = K_{nn}^{-1} \left[ S_n - \sum_{i=1, n-1} K_{ni} U_i^{(r+1)} - \sum_{i=n+1, N} K_{ni} U_i^{(r)} \right] \quad \dots (A.2.5)$$

where  $n$  is the number of the nodal point of the unknown displacement and  $r$  is the cycle of iteration. As this procedure can be applied simultaneously to three components of displacement at each nodal point, therefore  $U_n$  and  $S_n$  become vectors with  $x$ ,  $y$  and  $z$  components (equation (A.2.2a) and (A.2.2b)), the stiffness coefficients are expressed in the  $3 \times 3$  submatrix form of equation (A.2.2c) and flexibility of the nodal point is expressed as in equation (A.2.4).

The summation terms in equation (A.2.5) represent the elastic forces acting at nodal point  $n$  due to the deformations of the tetrahedral elements :

$$\begin{Bmatrix} Q_x \\ Q_y \\ Q_z \end{Bmatrix}_n^{(r+1)} = \sum_{i=1, n-1} \begin{bmatrix} K_{xx} & K_{xy} & K_{xz} \\ K_{yx} & K_{yy} & K_{yz} \\ K_{zx} & K_{zy} & K_{zz} \end{bmatrix}_{ni} \begin{Bmatrix} u \\ v \\ w \end{Bmatrix}_i^{(r+1)} + \sum_{i=n+1, N} \begin{bmatrix} K_{xx} & K_{xy} & K_{xz} \\ K_{yx} & K_{yy} & K_{yz} \\ K_{zx} & K_{zy} & K_{zz} \end{bmatrix}_{ni} \begin{Bmatrix} u \\ v \\ w \end{Bmatrix}_i^{(r)} \quad \dots (A.2.6)$$

The difference between these elastic forces and the applied loads is the total unbalanced forces which may be written in submatrix form :

$$\begin{Bmatrix} X \\ Y \\ Z \end{Bmatrix}_n^{(r+1)} = \begin{Bmatrix} S_x \\ S_y \\ S_z \end{Bmatrix}_n - \begin{Bmatrix} Q_x \\ Q_y \\ Q_z \end{Bmatrix}_n^{(r+1)} \quad \dots (A.2.7)$$

The change in the displacement of nodal point n between two successive cycles of iteration is obtained from :

$$\begin{Bmatrix} \Delta u \\ \Delta v \\ \Delta w \end{Bmatrix}_n^{(r)} = \begin{bmatrix} f_{xx} & f_{xy} & f_{xz} \\ f_{yx} & f_{yy} & f_{yz} \\ f_{zx} & f_{zy} & f_{zz} \end{bmatrix}_{nn} \begin{Bmatrix} X \\ Y \\ Z \end{Bmatrix}_n^{(r+1)} - \begin{Bmatrix} u \\ v \\ w \end{Bmatrix}_n^{(r)} \quad \dots (A.2.8)$$

then, the new displacement of nodal point n is determined from the following equation :

$$\begin{Bmatrix} u \\ v \\ w \end{Bmatrix}_n^{(r+1)} = \begin{Bmatrix} u \\ v \\ w \end{Bmatrix}_n^{(r)} + \beta \begin{Bmatrix} \Delta u \\ \Delta v \\ \Delta w \end{Bmatrix}_n^{(r)} \quad \dots (A.2.9)$$

where  $\beta$  is the over-relaxation factor.

With  $\beta = 1$ , the application of this equation is physically equivalent to releasing nodal point  $n$  and permitting it to move freely to a new equilibrium position. With  $\beta > 1$ , the nodal point is moved beyond its equilibrium position before proceeding to the next point.

It is particularly important to note that any desired initial nodal point displacement  $U_n^{(0)}$  may be assumed for the first cycle of iteration. A good guess of these displacements will greatly speed the convergence of the solution. In fact, if all displacements were assumed correctly, the unbalanced forces given by equation (A.2.7) would be zero and no iteration would be necessary. However, in a practical case there always will be unbalanced forces in the system at first, and the iteration process continually reduces them toward zero.

This process consists of only the inversion of nodal point stiffness matrix  $[K_{nn}]$  into the nodal point flexibility submatrix  $[K_{nn}^{-1}]$ . The inversion of a 3 x 3 matrix can easily be evaluated explicitly, and coefficients of the inverted matrix may be formulated, so that the inversion of a 3 x 3 matrix becomes a process involving only some simple arithmetic operations.

APPENDIX A.3

INSERTING THE BOUNDARY CONDITIONS

If the boundary nodal point is assumed, as an example, to be fixed in x direction where  $\Delta u = 0$  and allowed to move in yz plane, then equation (A.2.8) can be written in the form of equation (2.32) of section 2.8.

$$\begin{Bmatrix} 0 \\ \Delta v \\ \Delta w \end{Bmatrix}_n = \begin{bmatrix} f_{xx} & f_{xy} & f_{xz} \\ f_{yx} & f_{yy} & f_{yz} \\ f_{zx} & f_{zy} & f_{zz} \end{bmatrix}_{nn} \begin{Bmatrix} X - R_x \\ Y \\ Z \end{Bmatrix}_n \quad \dots (A.3.1)$$

The first equation of equation (A.3.1) may be written

$$0 = X \cdot f_{xx} - R_x \cdot f_{xx} + Y \cdot f_{xy} + Z \cdot f_{xz} \quad \dots (A.3.2)$$

and can be solved for the reaction  $R_x$  :

$$R_x = X + \frac{f_{xy}}{f_{xx}} \cdot Y + \frac{f_{xz}}{f_{xx}} \cdot Z \quad \dots (A.3.3)$$

substituting equation (A.3.3) into equation (A.3.1) and evaluating the second and third equations,  $R_x$  and X are eliminated as follows :

$$\left. \begin{aligned} \Delta v &= Y \left( f_{yy} - \frac{f_{xy} f_{yx}}{f_{xx}} \right) + Z \left( f_{yz} - \frac{f_{xz} f_{yx}}{f_{xx}} \right) \\ \Delta w &= Y \left( f_{zy} - \frac{f_{zx} f_{xy}}{f_{xx}} \right) + Z \left( f_{zz} - \frac{f_{zx} f_{xz}}{f_{xx}} \right) \end{aligned} \right\} \quad \dots (A.3.4)$$

If the terms in the parentheses are defined as the effective flexibility coefficients,  $f_{yy}^*$ ,  $f_{yz}^*$ ,  $f_{zy}^*$ , and  $f_{zz}^*$ , where :

$$\left. \begin{aligned} f_{yy}^* &= f_{yy} - \frac{f_{xy} f_{yx}}{f_{xx}} & f_{yz}^* &= f_{yz} - \frac{f_{xz} f_{yx}}{f_{xx}} \\ f_{zy}^* &= f_{zy} - \frac{f_{zx} f_{xy}}{f_{xx}} & f_{zz}^* &= f_{zz} - \frac{f_{zx} f_{xz}}{f_{xx}} \end{aligned} \right\} \dots (A.3.5)$$

then, the effective flexibility matrix for  $\Delta u = 0$  is obtained by rearranging equation (A.3.4) in matrix form :

$$[K_{nn}^{*-1}] = \begin{bmatrix} 0 & 0 & 0 \\ 0 & f_{yy}^* & f_{yz}^* \\ 0 & f_{zy}^* & f_{zz}^* \end{bmatrix} \dots (A.3.6)$$

The same procedure can easily be applied in order to obtain the effective flexibility matrices, in case of the other boundary conditions.





are the coordinates of the centroid of the tetrahedron, and

$$\left. \begin{aligned}
 r_{xx}^2 &= \frac{\int_V x^2 dV}{V} \\
 r_{yy}^2 &= \frac{\int_V y^2 dV}{V} \\
 r_{zz}^2 &= \frac{\int_V z^2 dV}{V}
 \end{aligned} \right\} \dots (A.4.7)$$

$$\left. \begin{aligned}
 r_{xy}^2 &= \frac{\int_V xy dV}{V} \\
 r_{zx}^2 &= \frac{\int_V zx dV}{V} \\
 r_{yz}^2 &= \frac{\int_V yz dV}{V}
 \end{aligned} \right\} \dots (A.4.8)$$

are the radius of gyrations with respect to the given axes.

With reference to figure A.1 and figure A.2 these integrals can be obtained for a tetrahedral element as follows :

$$\int_V dV = V = \frac{1}{6} \det \begin{bmatrix} 1 & . & . & . \\ 1 & a_j & b_j & c_j \\ 1 & a_k & b_k & c_k \\ 1 & a_l & b_l & c_l \end{bmatrix} \dots (A.4.9)$$

$$\left. \begin{aligned} \int_V x \, dV &= V \cdot \bar{x} = \frac{V}{4} (a_j + a_k + a_\ell) \\ \int_V y \, dV &= V \cdot \bar{y} = \frac{V}{4} (b_j + b_k + b_\ell) \\ \int_V z \, dV &= V \cdot \bar{z} = \frac{V}{4} (c_j + c_k + c_\ell) \end{aligned} \right\} \dots (A.4.6a)$$

$$\left. \begin{aligned} \int_V x^2 \, dV &= I_{xx} = V \cdot r_{xx}^2 = \frac{V}{10} [a_j(a_j+a_k+a_\ell) + a_k(a_k+a_\ell) + a_\ell^2] \\ \int_V y^2 \, dV &= I_{yy} = V \cdot r_{yy}^2 = \frac{V}{10} [b_j(b_j+b_k+b_\ell) + b_k(b_k+b_\ell) + b_\ell^2] \\ \int_V z^2 \, dV &= I_{zz} = V \cdot r_{zz}^2 = \frac{V}{10} [c_j(c_j+c_k+c_\ell) + c_k(c_k+c_\ell) + c_\ell^2] \end{aligned} \right\} \dots (A.4.7a)$$

$$\left. \begin{aligned} \int_V xy \, dV &= I_{xy} = V \cdot r_{xy}^2 = \frac{V}{20} [a_j(2b_j+b_k+b_\ell) + a_k(b_j+2b_k+b_\ell) + a_\ell(b_j+b_k+2b_\ell)] \\ \int_V yz \, dV &= I_{yz} = V \cdot r_{yz}^2 = \frac{V}{20} [b_j(2c_j+c_k+c_\ell) + b_k(c_j+2c_k+c_\ell) + b_\ell(c_j+c_k+2c_\ell)] \\ \int_V zx \, dV &= I_{zx} = V \cdot r_{zx}^2 = \frac{V}{20} [c_j(2a_j+a_k+a_\ell) + c_k(a_j+2a_k+a_\ell) + c_\ell(a_j+a_k+2a_\ell)] \end{aligned} \right\} \dots (A.4.8a)$$

The element mass matrix can be carried out explicitly by substituting the above formulae in equation (A.4.5) and premultiplying by  $[C^{-1}]^T$ , and postmultiplying by  $[C^{-1}]$  which are given in Appendix (A.1), as follows :

$$[m] = [C^{-1}]^T [\hat{m}] [C^{-1}] \dots (A.4.10)$$

then :

$$[m] = \frac{\rho V}{4} \begin{bmatrix} 2/5 & . & . & 1/5 & . & . & 1/5 & . & . & 1/5 & . & . \\ . & 2/5 & . & . & 1/5 & . & . & 1/5 & . & . & 1/5 & . \\ . & . & 2/5 & . & . & 1/5 & . & . & 1/5 & . & . & 1/5 \\ 1/5 & . & . & 2/5 & . & . & 1/5 & . & . & 1/5 & . & . \\ . & 1/5 & . & . & 2/5 & . & . & 1/5 & . & . & 1/5 & . \\ . & . & 1/5 & . & . & 2/5 & . & . & 1/5 & . & . & 1/5 \\ 1/5 & . & . & 1/5 & . & . & 2/5 & . & . & 1/5 & . & . \\ . & 1/5 & . & . & 1/5 & . & . & 2/5 & . & . & 1/5 & . \\ . & . & 1/5 & . & . & 1/5 & . & . & 2/5 & . & . & 1/5 \\ 1/5 & . & . & 1/5 & . & . & 1/5 & . & . & 2/5 & . & . \\ . & 1/5 & . & . & 1/5 & . & . & 1/5 & . & . & 2/5 & . \\ . & . & 1/5 & . & . & 1/5 & . & . & 1/5 & . & . & 2/5 \end{bmatrix} \dots (A.4.11)$$

The above consistent mass matrix for tetrahedral element is surprisingly very simple in form.

The simple process of "obvious" lumping would have resulted in a unit diagonal matrix multiplied by  $\rho V/4$

APPENDIX A.5

SUMMARY OF PRINCIPAL RESULTS RELATED WITH  
RANDOM VIBRATION THEORY

The DISTRIBUTION FUNCTION  $P(x)$  of a quantity  $x(t)$  or a process  $\langle x(t) \rangle$  is defined as the probability that, at any instant,  $x(t)$  shall not be greater than  $x$ , or in symbols

$$P(x) = \text{Pr} [ x(t) \leq x ] \quad \dots (A.5.1)$$

This probability distribution for any instant of time also describes the way in which the values of  $x(t)$  are distributed with respect to time over any sufficiently long record.

The PROBABILITY DENSITY  $p(x)$  is defined by

$$p(x) = \frac{dP(x)}{dx} \quad \dots (A.5.2)$$

or

$$P(x) = \int_{-\infty}^x p(x) dx \quad \dots (A.5.3)$$

A signal  $x(t)$  with zero mean value is said to have GAUSSIAN DISTRIBUTION if

$$p(x) = \frac{1}{\sigma \sqrt{2\pi}} e^{-x^2/2\sigma^2} \quad \dots (A.5.4)$$

where the quantity  $\sigma^2$  is called the VARIANCE and is simply the MEAN-SQUARE VALUE of the signal, i.e.,

$$\sigma^2 = \langle x^2(t) \rangle \quad \dots (A.5.5)$$

A function  $x(t)$  and its FOURIER TRANSFORM  $A(if)$  are related by

$$\left. \begin{aligned} x(t) &= \int_{-\infty}^{\infty} A(if) e^{i2\pi ft} df \\ A(if) &= \int_{-\infty}^{\infty} x(t) e^{-i2\pi ft} dt \end{aligned} \right\} \dots (A.5.6)$$

The SPECTRAL DENSITY  $S(f)$  of a quantity  $x(t)$  is defined, by way of these relations, such that

$$\langle x^2(t) \rangle = \int_0^{\infty} S(f) df \dots (A.5.7)$$

Here  $S(f)$  is in fact given by

$$S(f) = \lim_{T \rightarrow \infty} \left[ \frac{2}{T} |A_T(if)|^2 \right], \dots (A.5.8)$$

where  $A_T(if)$  is the Fourier transform of a function  $x_T(t)$  defined to coincide with  $x(t)$  over the interval  $-T/2 < t < T/2$  and to be zero elsewhere. A spectrum is said to be WHITE if  $S(f)$  is constant at all frequencies.

The AUTOCORRELATION FUNCTION  $R(\tau)$  of a quantity  $x(t)$  is defined by

$$R(\tau) = \langle x(t) x(t + \tau) \rangle \dots (A.5.9)$$

There exists between spectral density and autocorrelation function a Fourier transform relationship such that

$$\left. \begin{aligned} S(f) &= \int_{-\infty}^{\infty} 2R(\tau) e^{-i2\pi f\tau} d\tau \\ R(\tau) &= \int_{-\infty}^{\infty} \frac{1}{2} S(f) e^{i2\pi f\tau} df \end{aligned} \right\} \dots (A.5.10)$$

It follows from equation (A.5.10) and equation (A.5.7) that for a process with a Gaussian distribution a knowledge of either spectral density or autocorrelation function is sufficient to define  $\sigma^2$  and so, by equation (A.5.4) the whole probability distribution.

Two signals  $x(t)$  and  $y(t)$  have also a CROSS-SPECTRAL DENSITY  $S_{xy}(f)$  and a CROSS-CORRELATION FUNCTION  $R_{xy}(\tau)$  defined such that

$$R_{xy}(\tau) = \langle x(t) y(t + \tau) \rangle \quad \dots (A.5.11)$$

$$S_{xy}(f) = \int_{-\infty}^{\infty} R_{xy}(\tau) e^{-i2\pi f\tau} d\tau \quad \dots (A.5.12)$$

APPENDIX A.6

RESPONSE TO RANDOM LOADING

(I) DERIVATION OF RECEPTANCE:

The equation of motion in the  $r^{\text{th}}$  normal mode is

$$\mathcal{M}_r \ddot{\xi}_r + \mathcal{C}_r \dot{\xi}_r + \mathcal{K}_r \xi_r = E_r \quad \dots (A.6.1)$$

The generalized force  $E_r$  corresponding to  $\xi_r$  is obtained by considering the work done,  $\delta W$ , in a virtual displacement  $\delta q(\alpha)$  at the nodal point  $\alpha$ , where the load  $P(\alpha, t)$  is acting. Since  $P(\alpha, t) = P_0(\alpha) e^{i\omega t}$  is assumed:

$$\delta W = P_0(\alpha) e^{i\omega t} \delta q(\alpha) = P_0(\alpha) e^{i\omega t} \sum_r \psi_r(\alpha) \delta \xi_r \quad \dots (A.6.2)$$

As  $E_r$  must be such that  $\delta W = \sum_r E_r \delta \xi_r$  as equation (4.9),

$$E_r = \psi_r(\alpha) P_0(\alpha) e^{i\omega t} \quad \dots (A.6.3)$$

is obtained. By substituting equation (A.6.3) into equation (A.6.1),

$$\mathcal{M}_r \ddot{\xi}_r + \mathcal{C}_r \dot{\xi}_r + \mathcal{K}_r \xi_r = \psi_r(\alpha) P_0(\alpha) e^{i\omega t} \quad \dots (A.6.4)$$

and solving equation (A.6.4) in the usual way

$$\xi_r = \frac{\psi_r(\alpha) P_0(\alpha) e^{i\omega t}}{\mathcal{M}_r (\omega_r^2 - \omega^2 + i2\zeta_r \omega_r \omega)} \quad \dots (A.6.5)$$

is obtained. Using the relationship between the displacement at nodal point "1" and the normal coordinates which is given by

$$w(1, t) = \sum_r \psi_r(1) \xi_r(t) \quad \dots (A.6.6)$$

the following equation is obtained :

$$w(1,t) = P_0(\alpha) e^{i\omega t} \sum_r \frac{\psi_r(1) \psi_r(\alpha)}{\mathcal{M}_r(\omega_r^2 - \omega^2 + i2\zeta_r \omega_r \omega)} \quad \dots (A.6.7)$$

since  $w(1,t)$  is proportional to  $e^{i\omega t}$  ; assuming  $w(1,t) = w_0(1) e^{i\omega t}$  ,  
by the definition, the receptance is obtained as :

$$\frac{1}{Z_{1\alpha}(i\omega)} = \frac{w_0(1)}{P_0(\alpha)} = \sum_r \frac{\psi_r(1) \psi_r(\alpha)}{\mathcal{M}_r(\omega_r^2 - \omega^2 + i2\zeta_r \omega_r \omega)} \quad \dots (A.6.8)$$

The receptance is usually required to be expressed in terms of frequency and by using the relationship between the frequency and the circular frequency,

$$\frac{1}{Z_{1\alpha}(if)} = \sum_r \frac{\psi_r(1) \psi_r(\alpha)}{4\pi^2 \mathcal{M}_r(f_r^2 - f^2 + i2\zeta_r f_r f)} \quad \dots (A.6.9)$$

is obtained.

## (II) RESPONSE TO A SINGLE RANDOM LOADING:

The relationship between the loading and response of a linear system may be expressed in terms of Duhamel's integral :

$$x(t) = \int_0^{\infty} h(\tau) P(t - \tau) d\tau \quad \dots (A.6.10)$$

The impulsive response function  $h(t)$  and the receptance of the system are

related by

$$\frac{1}{Z(if)} = \int_0^{\infty} e^{-i2\pi f\tau} h(\tau) d\tau \quad \dots (A.6.11)$$

The autocorrelation function of the response is given by definition:

$$R_x(\tau) = \langle x(t) x(t + \tau) \rangle \quad \dots (A.6.12)$$

From equation (A.6.10),

$$\left. \begin{aligned} x(t) &= \int_0^{\infty} h(\tau_1) P(t - \tau_1) d\tau_1 \\ x(t + \tau) &= \int_0^{\infty} h(\tau_2) P(t + \tau - \tau_2) d\tau_2 \end{aligned} \right\} \quad \dots (A.6.13)$$

by substituting equation (A.6.13) into equation (A.6.12) and evaluating :

$$R_x(\tau) = \int_0^{\infty} h(\tau_1) \int_0^{\infty} h(\tau_2) R_p(\tau_1 - \tau_2 + \tau) d\tau_2 d\tau_1 \quad \dots (A.6.14)$$

is obtained, where  $R_p(\tau)$  is the autocorrelation function of the loading.

Considering the relationship between the spectral density and autocorrelation function given by equation (A.5.10) in Appendix (A.5), the relationship between the spectral densities of response and loading can be obtained easily by evaluating equation (A.6.14) :

$$\begin{aligned}
S_x(f) &= 2 \int_{-\infty}^{\infty} R_x(\tau) e^{-i2\pi f\tau} d\tau \\
&= 2 \int_{-\infty}^{\infty} \left[ \int_0^{\infty} h(\tau_1) \int_0^{\infty} h(\tau_2) R_p(\tau_1 - \tau_2 + \tau) d\tau_2 d\tau_1 \right] e^{-i2\pi f\tau} d\tau \\
&= 2 \int_0^{\infty} h(\tau_1) e^{i2\pi f\tau_1} d\tau_1 \int_0^{\infty} h(\tau_2) e^{-i2\pi f\tau_2} d\tau_2 \\
&\quad \times \int_{-\infty}^{\infty} R_p(\tau_1 - \tau_2 + \tau) e^{-i2\pi f(\tau_1 - \tau_2 + \tau)} d(\tau_1 - \tau_2 + \tau) \quad \dots (A.6.15)
\end{aligned}$$

The separate factors of this expression are recognised from equation (A.6.11) and equation (A.5.10) as  $1/Z^*(if)$ ,  $1/Z(if)$  and  $S_p(f)/2$ , so that

$$S_x(f) = 2 \cdot \frac{1}{Z^*(if)} \cdot \frac{1}{Z(if)} \cdot \frac{1}{2} \cdot S_p(f) \quad \dots (A.6.16)$$

or, finally,

$$S_x(f) = \left| \frac{1}{Z(if)} \right|^2 S_p(f) \quad \dots (A.6.17)$$

is obtained.

### (III) RESPONSE TO MULTIPLE RANDOM LOADINGS:

When more than one random force act together, the above analysis can be extended without difficulty, although of course the equations become lengthier. On the other hand, the spectral density of the response cannot be determined from a knowledge only of the spectral densities of the applied forces; a knowledge of the cross spectral densities is also necessary.

Considering the response,  $x_1(t)$ , of a system, at point "1" in a given direction, the random loadings  $P(\alpha,t)$ ,  $P(\beta,t)$ , ....., acting simultaneously, it can again be possible to obtain an expression giving the autocorrelation function,  $R_x(1,\tau)$ , by expanding  $\langle x_1(t) x_1(t + \tau) \rangle$  in terms of the autocorrelation functions  $R_p(\alpha,\tau)$ ,  $R_p(\beta,\tau)$ , ....., and the cross-correlation functions  $R_p(\alpha,\beta,\tau)$ , ....., and this result can be used to express the spectral density  $S_x(1,f)$ , of  $x_1(t)$  in terms of the spectral densities  $S_p(\alpha,f)$ ,  $S_p(\beta,f)$  ....., and cross spectral densities  $S_p(\alpha,\beta,f)$ , ....., of the loadings. Proceeding in this way (ref.70):

$$\begin{aligned}
 S_x(1,f) = & \frac{S_p(\alpha,f)}{Z_{1\alpha}^*(if) Z_{1\alpha}(if)} + \frac{S_p(\beta,f)}{Z_{1\beta}^*(if) Z_{1\beta}(if)} + \dots\dots\dots \\
 & + \frac{S_p(\alpha,\beta,f)}{Z_{1\alpha}^*(if) Z_{1\beta}(if)} + \dots\dots\dots \dots (A.6.18)
 \end{aligned}$$

or in a general form :

$$S_x(1,f) = \sum_{\alpha=1}^{\infty} \sum_{\beta=1}^{\infty} \frac{1}{Z_{1\alpha}^*(if) Z_{1\beta}(if)} \dots S_p(\alpha,\beta,f) \dots (A.6.19)$$

is obtained

## REFERENCES

- (1) ROCHA, Manual - "Statement of the Physical Problem of the Arch Dam" - "Theory of Arch Dams", ed. by J.R. RYDZEWSKI, Proc. of a Symposium held at the University of Southampton, pp. 3-22, Pergamon Press, April, 1964.
- (2) RYDZEWSKI, J.R. - "Recent Advances in the Theory of Arch Dams" - Applied Mechanics Reviews, vol 18, No. 10, pp. 783-787-, October 1965.
- (3) "DRAFT BIBLIOGRAPHY on The Theory of Arch Dams" - Department of Civil Engineering, University of Southampton, 1964.
- (4) NOETZLI, F.A. - "Arch Action in Curved Dams" - Engineering and Contracting, vol 55, p. 372, April 1921.
- (5) WESTERGAARD, H.M. - "Arch Dam Analysis by Trial Loads Simplified" - Engineering News Rec. 106, p. 141, 1931.
- (6) ALLEN, D.N. de G., L. CHITTY, A.J. PIPPARD and R.T. SEVERN - "The Experimental and Mathematical Analysis of Arch Dams with Special Reference to Dokan" - Proc. I.C.E., 5 pt.1, p. 198, 1956.
- (7) RYDZEWSKI, J.R. (editor) - "Theory of Arch Dams" - Proceedings of a Symposium held at the University of Southampton; Pergamon Press, April 1964.
- (8) TURNER, M.J., R.W. CLOUGH, H.C. MARTIN, L.J. TOPP - "Stiffness and Deflection Analysis of Complex Structures" - Journal of the Aeronautical Sciences, vol 23, No. 9 pp. 805, September 1956.
- (9) CLOUGH, R.W. - "The Finite Element Method in Plane Stress Analysis" - Proceedings Second Conference on Electronic Computation, ASCE, September 1960.
- (10) CLOUGH, R.W. and J.T. TOCHER - "Analysis of Thin Arch Dams by the Finite Element Method" - Ref. 7, pp. 107-122.
- (11) ZIENKIEWICZ, O.C. and Y.K. CHEUNG - "Finite Element Method of Analysis for Arch Dam Shell and Comparison with Finite Difference Procedures" - Ref. 7, pp. 123-140.
- (12) ERGATOUDIS, J., B.M. IRONS, O.C. ZIENKIEWICZ - "Three Dimensional Analysis of Arch Dams and their Foundations" - Symposium on Arch Dams, I.C.E., paper No. 4, London, March 1968.
- (13) ARGYRIS, J.H. and S.C. REDSHAW - "Three Dimensional Analysis of Two Arch Dams by a Finite Element Method" - Symposium on Arch Dams, I.C.E., paper No. 5, London, March 1968.
- (14) DUNGAR, R. and R.T. SEVERN - "The Analysis of Arch Dams Under Static Loading by the Finite Element Method" - Symposium on Arch Dams, I.C.E., paper No. 6., London, March 1968.
- (15) GUIDO, O. - "Italian Arch Dam Design and Model Confirmation" - Journal of Structural Division, Proceedings ASCE, vol. 83, pp. 1351-1357, March 1960.

- (16) ROCHA, M. - "Structural Model Techniques, Some Recent Developments" - L.N.E.C., Memoria No. 264, Lisbon, 1965.
- (17) ERMUTLU, H.E. - "Beton Baraj Modelleri" - DSI yayinlari, No. 484, Ankara 1965. ("Models of Concrete Dams" - State Hydraulic Works, Publication No. 484, Ankara, Turkey, 1965 - in Turkish).
- (18) MORRIS, S.B. and C.E. PEARCE - "Earthquake Forces on Dams" Bull. Seism. Soc. Amer., vol 21, 1931.
- (19) WESTERGAARD, H.M. - "Water Pressures on Dams During Earthquakes" - Trans. ASCE., vol 98. pp 814-433, 1933.
- (20) ZANGAR, C.N. - "Hydrodynamic Pressures on Dams due to Horizontal Earthquake Effects" - U.S. Bureau of Reclamation, Engineering Monograph No. 11.
- (21) CRAWFORD, C.C. and M.D. COPEN - "Proposed Earthquake Loadings for the Design of Thin Arch Dams" - Presented at the ASCE Annual Meeting and Structural Engineering Conference, San Francisco, California, October 1963.
- (22) SERAFIM, J.L. and J.O. PEDRO - "Seismic Study of Arch Dams" - Proceedings ASCE. vol 91. ST 2, 1965.
- (23) TAYLOR, P.R. - "The Response of Arch Dams to Earthquakes" - Ph.D. Thesis, University of Bristol, September 1965.
- (24) KOTSUBO, S. - "Dynamic Water Pressure on Dams During Earthquakes" - Proceedings 2nd World Conference on Earthquake Engineering, pp. 799 - 814, Tokyo, Japan, 1960.
- (25) ZIENKIEWICZ, O.C. and B. NATH - "Earthquake Hydrodynamic Pressures on Arch Dams - an Electric Analogue Solution" - Proc. Inst. Civ. Eng.s - vol 25, pp. 165, 1963.
- (26) BORGES, J.F., J. PEREIRA, A. RAVARA, J. PEDRO - "Seismic Studies on Concrete Dam Models" - Symposium on Concrete Dam Models, L.N.E.C., Lisbon, 1963.
- (27) GAUKROGER, D.R., G.A. TAYLOR and SKINGLE, C.W. - "Resonance Tests on a Model Dam" - R.A.E. Technical Report 67083, March 1967.
- (28) OKAMOTO, S. and T. TAKAHASHI - "On Behaviour of an Arch Dam During Earthquakes" - Proc. of the Second World Conference on Earthquake Engineering. vol 2, pp. 1401-1412, Tokyo, Japan, 1960.
- (29) HOUSNER, G.W. - "Characteristics of Strong-Motion Earthquakes" - Bull. of the Seism. Soc of America, vol 37, 1947.
- (30) CLOUGH, R.W. and E.L. WILSON - "Dynamic Response by Step-by-Step Matrix Analysis" - Symposium on Use of Computers in Civil Engineering, L.N.E.C., Lisbon, Portugal, October 1962.
- (31) BIOT, M.A. - "Analytical and Experimental Methods in Engineering Seismology" - Trans. ASCE, paper No. 2183, p. 365, 1943.

- (32) RAVARA, A. - "Spectral Analysis of Seismic Actions" - L.N.E.C. Memoria No. 268, Lisbon 1965.
- (33) C.E.R.A. - "First Interim Report on Research on the Design of Arch Dams" - I.C.E., London, 1963.
- (34) ARGYRIS, J.H. - "Energy Theorems and Structural Analysis" - Butterworths, London, 1960.
- (35) ZIENKIEWICZ, O.C. and Y.K. CHEUNG - "The Finite Element Method" - McGraw-Hill, 1967.
- (36) DUNGAR, R. and R.T. SEVERN - "Dynamic Analysis of Arch Dams" - Symposium on Arch Dams, I.C.E., Paper No. 7, London, March, 1968.
- (37) GALLAGHER, R.H. - "Stress Analysis of Heated Complex Shapes" - A.R.S. Journal, pp. 700, 1962.
- (38) MELOSH, R.J. - "Structural Analysis of Solids" - Proc. A.S.C.E. vol 89, ST.4, pp. 205, Aug. 1963.
- (39) ARGYRIS, J.H. - "Matrix Analysis of Three Dimensional Elastic Media - Small and Large Displacements" - Journal A.I.A.A., vol 3, pp. 45, Jan. 1965.
- (40) ARGYRIS, J.H. - "Continua and Discontinua" - Proc. Conf. Matrix Methods in Structural Mechanics, Wright Patterson Air Force Base, Ohio, Oct. 1965.
- (41) ERGATOUDIS, J., B.M. IRONS and O.C. ZIENKIEWICZ - "Three Dimensional Stress Analysis of Arch Dams by the Finite Element Method" - University of Wales, Swansea, Civil Engineering Division, Report No. c/R/58/66.
- (42) MELOSH, R.J. - "Basis for Derivation of Matrices for the Direct Stiffness Method" - Journal A.I.A.A. vol. 1, pp. 1631-1637, 1963.
- (43) SOUTHWELL, R.V. - "Relaxation Methods in Engineering Science" - Oxford University Press, 1940.
- (44) WILSON, L.W. - "Finite Element Analysis of Two-Dimensional Structures" - Structures and Materials Research Department of Civil Engineering, Report No. 63-2. University of California, Berkeley, California, June 1963.
- (45) LEHMAN, F.G. - "Simultaneous Equations Solved by Over-Relaxation" - Proc. ASCE, 2nd Conf. on Electronic Computation, Pittsburgh, Pa., September, 1960.
- (46) TURNER, M.J., H.C. MARTIN, R.C. WEIKEL - "Further Developments and Application of the Stiffness Method" - AGARD, Structures and Materials Panel, Paris, July 1962
- (47) ARCHER, J.S. - "Consistent Mass Matrix for Distributed Mass Systems" - Proc. ASCE, vol 89, ST.4, pp. 161, 1963.

- (48) WILKINSON, J.H. - "Householder's Method for the Solution of the Algebraic Eigen-Problem" - Computer Journal, vol 3, No. 1, April 1960, pp 23-37.
- (49) PETYT, M. - "The Application of Finite Element Techniques to the Vibration Analysis of Cracked Plates in Tension" - Ph.D. Thesis, University of Southampton, May 1967.
- (50) FOX, L. - "An Introduction to Numerical Linear Algebra" - Oxford Clarendon Press, 1964.
- (51) BOOTH, A.D. - "Numerical Methods" - Butterworths Scientific Publications, 1955.
- (52) BRAHTZ, H.A. and C.H. HEILBORN - "Discussion to Wetergaard's paper, Trans. ASCE. vol 98, pp-453, 1933.
- (53) HOSKINS, L.M. and L.S. JACOBSEN - "Water Pressures in a Tank Caused by a Simulated Earthquake" - Bull. Seism.Soc.of Amer., vol 24, No. 1, Jan, 1934.
- (54) KOTSUBO, S. - "Dynamic Water Pressures on Dams Due to Irregular Earthquakes" 1 Memoirs Fac.of Eng., Kyushu University, Fukuoka, Japan, vol. 18, No. 4, 1959.
- (55) BUSTAMENTE, J.I., E.ROSENBLUETH, I. HERRERA, A. FLORES - "Presion Hidrodinamica en Presas y Depositos" - Bolotin Sociedad Mexicana.de Ingenieria Sismica, vol 1, No. 2, October 1963.
- (56) WERNER, P.W. and K.J. SUNDQUIST - "On Hydrodynamic Earthquake Effects" - Trans.Amer. Geophysical Union, vol 30, No. 5 October 1949. pp. 636-657.
- (57) CHZHEN-CHEN, C. - "The Effect of Dynamic Fluid Pressure on a Dam During Earthquakes" - Journal of Applied Math. and Mech. (P.M.M), vol 25, No 1, 1961.
- (58) KOTSUBO, S. - "External Forces on Arch Dams during Earthquakes" - Memoirs Fac-of Eng., Kyushu University, Fukuoka, Japan, vol 20. No. 4 1961.
- (59) CHOPRA, A.K. - "Hydrodynamic Pressures on Dams during Earthquakes"- Proc. ASCE, vol 93, EM 6, pp. 205-225, December, 1967.
- (60) BUSTAMENTE, J.I. and A. FLORES - "Water Pressures on Dams Subjected to Earthquakes" - Proc. ASCE, vol 92, EM 5. pp.115-127, October, 1966.
- (61) ZIENKIEWICZ, O.C., B. IRONS, B.MATH - "Natural Frequencies of Complex, Free or Submerged Structures by the Finite Element Method" - Vibration in Civil Engineering "Edited by B.O. SKIPP, Butterworths, pp. 83-90, London 1966.
- (62) SKINGLE, C.W., G.A. TAYLOR, D.R. GAUKROGER - "The Effect of Reservoir Water on the Dynamic Behaviour of an Idealized Model Dam" - R.A.E. Technical Report 67113, May 1967.

- (63) LAMB, H. - "Hydrodynamics" - Cambridge University Press, 1932.
- (64) BIOT, M.A. - "A Mechanical Analyser for the Prediction of Earthquake Stresses" - Bull. Seism. Soc. of Amer., vol 31, pp. 151-171, 1941.
- (65) HOUSNER, G.W. and G.D. Mc CANN - "The Analysis of Strong Motion Earthquake Records with the Electric Analog Computer" - Bull. Seism. Soc. of Amer., Vol 39, pp. 47-56, 1949.
- (66) CAUGHEY, T.K., D.E. HUDSON, R.V. POWEL - "The CIT Mark II Electric Analog Type Response Spectrum Analyser" - Earthquake Eng. Research Lab., Calif. Ins. of Tech., Pasadena, 1960.
- (67) BREMAECKER, J. CL de, P. DONOHO, J.G. MICHEL - "A Direct Digitizing Seismograph" - Bull. Seism. Soc. of Amer., vol 52, No 3 pp. 661-672, July 1962.
- (68) CLOUD, W.K. and D.E. HUDSON - "A Simplified Instrument for Recording Strong-Motion Earthquakes" - Bull. Seism. Soc. of Amer., vol 51, No. 2, pp. 159-174, April 1961.
- (69) BENDAT, J.S. - "Principles and Applications of Random Noise Theory" - John Wiley and Sons Inc. 1958.
- (70) ROBSON, J.D. - "An Introduction to Random Vibration" - Edinburgh Univ. Publications, Science and Mathematics Texts 5, Edinburgh Univ. Press, 1963
- (71) MINER, M.A. - "Cumulative Damage in Fatigue" - Jour. Appl. Mechanics, 12(3), p. A-159, 1945.
- (72) RICE, S.O. - "Mathematical Analysis of Random Noise - Bell System Tech. J., Vol 23, pp. 282, 1944 and vol 24, pp. 44, 1945.
- (73) HOUSNER, G.W. - "Density of Earthquake Ground Shaking Near Causative Fault" - Proc. of the Third World Conf. on Earthquake Engng., III-94-109, New Zealand, 1965.
- (74) BOGDANOF, J.L., J.E. GOLDBERG and M.C. BERNARD - "Response of a Single Structure to a Random Earthquake-Type Disturbance" - Bull. Seism. Soc. of Amer., vol 51, No. 2. pp. 293-310, April 1961.
- (75) TAJIMI, H. - "A Statistical Method of Determining the Maximum Response of a Building Structure During an Earthquake" - Proc. of the Second World Conf. on Earthquake Engng., vol 2, pp. 781-797, Tokyo, Japan, 1960.
- (76) BOLOTIN, V.V. - "Statistical Theory of the Aseismic Design of Structures" - Ibid. Proc. vol 2. pp. 1365-1374.
- (77) HOUSNER, G.W., R.R. MARTEL and J.L. ALFORD - "Spectrum Analysis of Strong-Motion Earthquakes" - Bull. Seism. Soc. of Amer., vol 43, pp. 97-119, April 1953.

- (78) CLOUGH, R.W. and A.K. CHOPRA - "Earthquake Stress Analysis in Earth Dams" - Jour. ASCE, vol 92, EM. 2, April 1966.
- (79) SEVERN, R.T. and P.R. RAYLOR - "Earthquake Effects on an Arch Dam by Response Spectra Methods" - "Vibration in Civil Engineering", Edited by B.O. SKIPP, pp. 221-227, Butterworths, London, 1966.
- (80) BENIOFF - "The Physical Evaluation of Seismic Destructiveness" - Bull. Seism. Soc. of Amer., vol 24, pp. 398-403, 1934.
- (81) HUDSON, D.E. - "Some Problems in the Application of Spectrum Techniques to Strong-Motion Earthquake Analysis" - Bull. Seism. Soc. of Amer., vol 52, No. 2, pp. 417-430, April, 1962.
- (82) FUNG, Y.C. - "Shock Loading and Response Spectra" - "Shock and Structural Response", Edited by M.V. BARTON, The ASME, New York 1960.
- (83) HOUSNER, G.W. - "Behaviour of Structures During Earthquakes" - Proc. ASCE, Jour. of Eng. Mech. Div., October, 1959.
- (84) CLOUGH, R.W. - "On the Importance of Higher Modes of Vibration in the Earthquake Response of a Tall Building" - Bull. Seism. Soc. of Amer., vol 45. pp. 289-301, 1955.
- (85) ROSENBLUETH, E. - "Some Applications of Probability Theory in Aseismic Design" - Proc. World Conf. on Earthquake Engng., pp. 8-1, Univ. of California, Berkeley, Calif.
- (86) JENNINGS, R.L. - "The Response of Multi-Storied Structures to Strong Ground Motion" - M.Sc. Thesis, Univ. of Illinois. Urbana.
- (87) MERCHANT, H.C. and D.E. HUDSON - "Mode Superposition in Multi-Degree of Freedom Systems Using Earthquake Response Spectrum Data" - Bull. Seism. Soc. of Amer., vol 52, No. 2. pp. 405-416, April, 1962.
- (88) BULLEN, K. - "An Introduction to the Theory of Seismology" - Cambridge Univ. Press, 1947.
- (89) CHOPRA, A.K. - "The Importance of the Vertical Component of Earthquake Motions" - Bull. Seism. Soc. of Amer., vol 56, No. 5, pp. 1163-1175, October, 1966.
- (90) WOOD, H.D., and F. NEUMANN - Bull. Seism. Soc. of Amer., Vol 21, No. 4, pp. 277, 1931.
- (91) GUTENBERG, B. and C.F. RICHTER - "Earthquake Magnitude, Intensity, Energy and Acceleration" - Bull. Seism. Soc. of Amer., Vol 32. pp. 163-191, 1942.
- (92) MEDVEDEV, S.V. - "New Seismic Regionalisation of USSR Territory" - Proc. of the Third World Conf. on Earthquake Engineering, New Zealand, 1965, III-168.

- (93) BUNE, V.I. - "Seismic Investigations in the Vaksh Area of Tadzhik Republic Relating to Large Dam Construction Projects" - Ibid Proc. III-27.
- (94) GUMBEL, E.J. - "Statistical Theory of Extreme Values and Some Practical Applications" - Applied Mathematics Series, 33, National Bureau of Standards, Feb. 1954.
- (95) NORDQUIST, J.M. - "Theory of Largest Values Applied to Earthquake Magnitudes" - Trans., Amer. Geophysical Union, Vol 26, Part I, pp. 29-31, Aug. 1945.
- (96) DICK, I.D. - "Extreme Value Theory and Earthquakes" - Proc. of the Third World Conf. on Earthquake Engineering, New Zealand, 1965, II-45.
- (97) MILNE, W.G. and A.G. DAVENPORT - "Statistical Parameters Applied to Seismic Regionalization" - Ibid. Proc. III-181.
- (98) BLACKMAN, R.B. and J.W. TUKEY - "The Measurement of Power Spectra" - New York, Dover Publications, Inc., 1958.

-007-

A cross-section through the nodal points	Element layers and nodal point forces	Stress distribution and nodal point forces	Stress calculation including moment effect and assuming linear stress distribution	Stress calculation according to simple Force/Area formula.
			$\sigma_1 = \frac{2}{bh} (2P_1 - P_2)$ $\sigma_2 = \frac{2}{bh} (-P_1 + 2P_2)$	$\sigma'_1 = \frac{2}{bh} P_1$ $\sigma'_2 = \frac{2}{bh} P_2$
			$\sigma_1 = \frac{2}{bh} (2P_1 + \frac{P_2}{2} - P_3)$ $\sigma_3 = \frac{2}{bh} (-P_1 + \frac{P_2}{2} + 2P_3)$	$\sigma'_1 = \frac{4}{bh} P_1$ $\sigma'_3 = \frac{4}{bh} P_3$
			$\sigma_1 = \frac{2}{bh} (2P_1 + P_2 - P_4)$ $\sigma_4 = \frac{2}{bh} (-P_1 + P_3 + 2P_4)$	$\sigma'_1 = \frac{6}{bh} P_1$ $\sigma'_4 = \frac{6}{bh} P_4$
			$\sigma_1 = \frac{2}{bh} (2P_1 + \frac{5}{4}P_2 + \frac{1}{2}P_3 - \frac{1}{4}P_4 - P_5)$ $\sigma_5 = \frac{2}{bh} (-P_1 - \frac{1}{4}P_2 + \frac{1}{2}P_3 + \frac{5}{4}P_4 + 2P_5)$	$\sigma'_1 = \frac{8}{bh} P_1$ $\sigma'_5 = \frac{8}{bh} P_5$

TABLE 2.1 : CALCULATION OF NODAL POINT STRESSES

Property	Unit	Concrete	Rock
Coefficient of thermal expansion	per °C	$9 \times 10^{-6}$	$9 \times 10^{-6}$
Density	kg/m <sup>3</sup>	2400	2400
Young's Modulus	kg/cm <sup>2</sup>	$0.20 \times 10^6$	$0.20 \times 10^6$ or $0.05 \times 10^6$
Poisson's Ratio		0.15	0.15

TABLE 2.2: MECHANICAL PROPERTIES OF CONCRETE AND FOUNDATION ROCK FOR ARCH DAM TYPE-5

MODE No.	MODE SHAPE	NATURAL FREQUENCIES (Hz) ON RIGID FOUNDATION		
		Reservoir Condition		$F_{(full)}/F_{(empty)}$ Ratio
		Empty	Full	
1	Symmetric	3.27	2.91	0.89
2	Antisymmetric	4.16	3.79	0.91
3	Symmetric	6.18	5.55	0.90
4	Antisymmetric	6.83	6.31	0.92
5	Symmetric	7.25	6.49	0.90

TABLE 3.1: EFFECT OF THE RESERVOIR WATER ON THE NATURAL FREQUENCIES OF ARCH DAM TYPE-5

$\frac{E(\text{boundary})}{E(\text{concrete})}$ RATIO	Fundamental Frequency (Hz.)	$\frac{F(\text{flex.})}{F(\text{rigid})}$ RATIO
$\infty$	3.27	1.000
1/1	3.10	0.947
1/2	2.96	0.905
1/4	2.75	0.840
1/8	2.46	0.752

TABLE 3.2: EFFECT OF THE FLEXIBILITY OF FOUNDATION ON THE NATURAL FREQUENCY OF FUNDAMENTAL MODE OF ARCH DAM TYPE-5

	KAMISHIIBA DAM (ref.28)	ARCH DAM TYPE-5
Height	110.0 m.	120.0 m.
Crest length	310.0 m.	320.0 m.
Radius of top arch	142.4 m.	167.3 m.
Thickness at top	7.0 m.	5.4 m.
Thickness at bottom	27.7 m.	23.4 m.
Type	Double curvature symmetrical arch dam with varying radius	

TABLE 3.3: COMPARISON OF GEOMETRICAL CHARACTERISTICS OF KAMISHIIBA DAM WITH ARCH DAM TYPE-5.

RESERVOIR CONDITION	KAMISHIIBA DAM PROTOTYPE EXPERIMENTAL (ref.28)			ARCH DAM TYPE-5 ON RIGID FOUNDATION	
	MODE		FREQUENCY (Hz.)	CORRESPONDING MODE No.	FREQUENCY (Hz.)
	No.	SHAPE			
EMPTY	1	Sym.	?	1	3.27
	2	Antisym.	4.7	2	4.16
	3	Sym.	6.3	3	6.18
	4	Antisym.	8.0	6	8.48
FULL	1	Sym.	3.8	1	2.91
	2	Antisym.	4.3	2	3.79
	3	Sym.	5.3	3	5.55

TABLE 3.4: COMPARISON OF EXPERIMENTAL RESULTS OBTAINED FOR KAMISHIIBA DAM WITH THE THEORETICAL RESULTS OBTAINED FOR ARCH DAM TYPE-5.

MODE No.	KAMISHIIBA EXPERIMENTAL (ref.28)	ARCH DAM TYPE-5 THEORETICAL	R.A.E. MODEL TESTS (ref.27)
1	?	0.89	0.85 ~ 0.92
2	0.91	0.91	
3	0.85	0.90	

TABLE 3.5: COMPARISON OF THE FREQUENCY RATIOS OBTAINED FOR THE EFFECT OF THE RESERVOIR WATER ON THE NATURAL FREQUENCIES OF ARCH DAMS

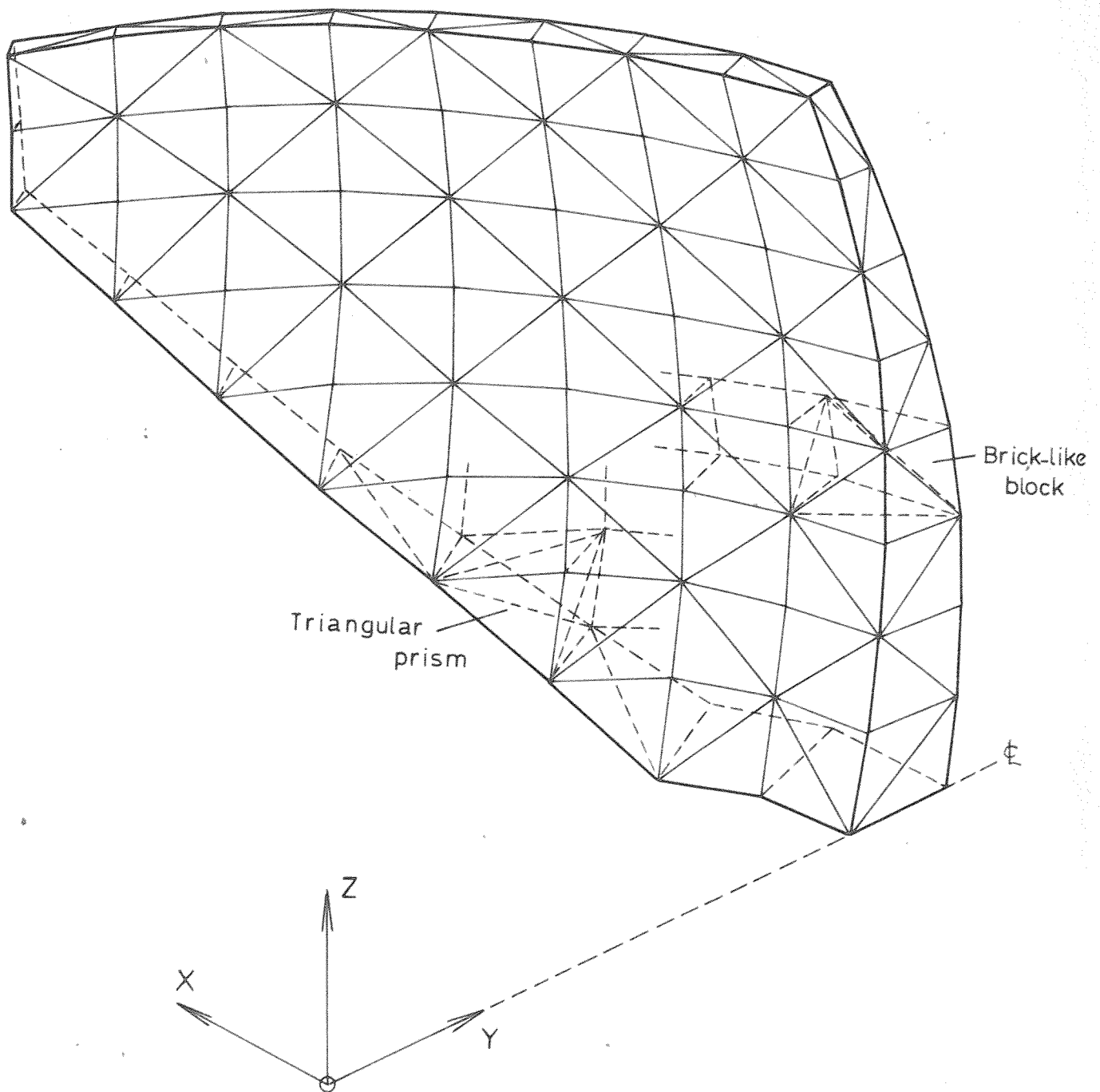


Fig.2.1. Idealization of an arch dam by means of tetrahedral elements

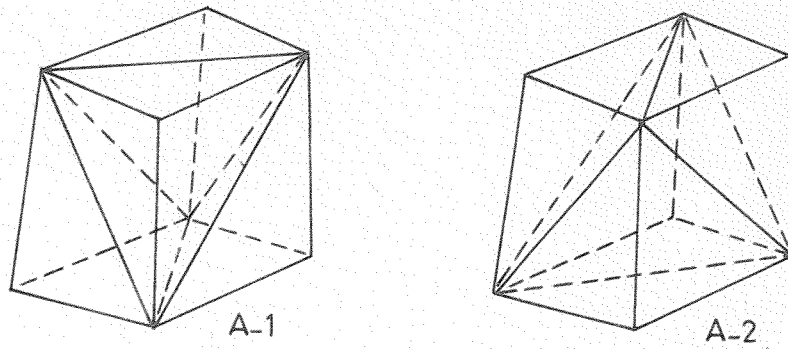


Fig.2.2. A-type idealization of a brick-like block by five tetrahedral elements

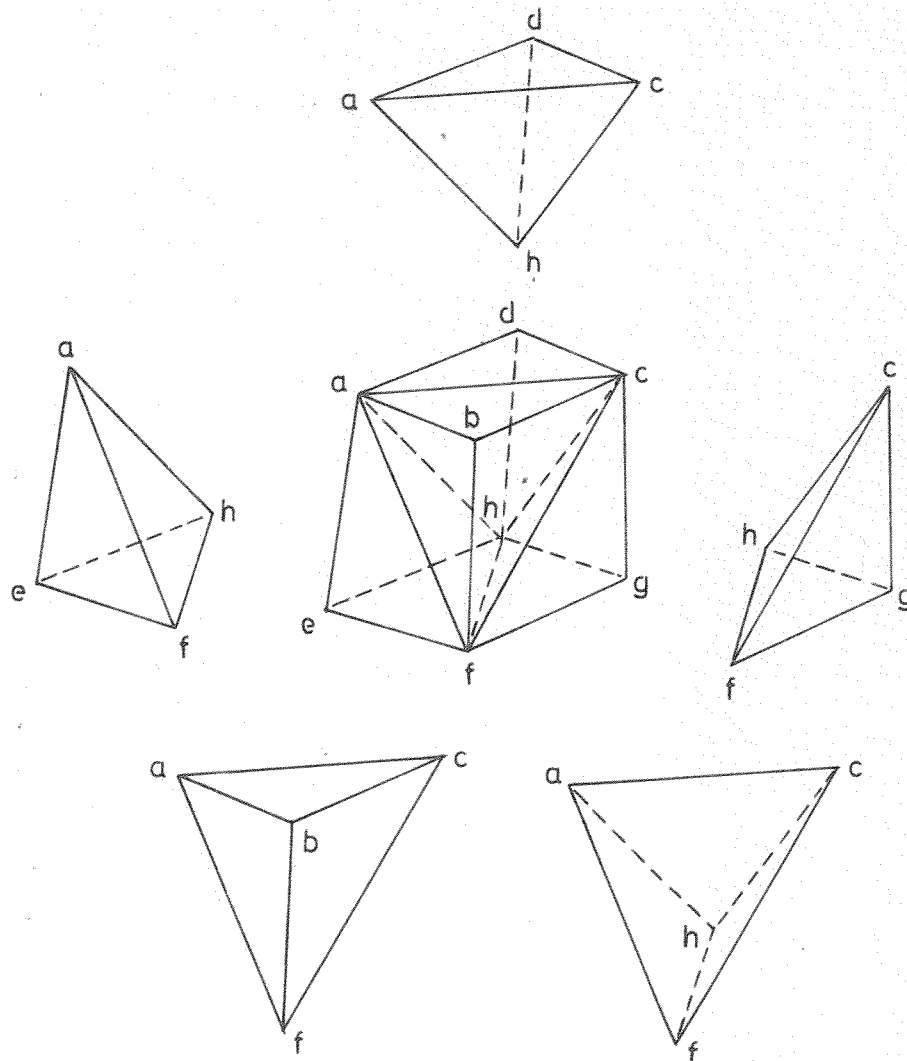


Fig.2.3. Division of a brick-like block into five tetrahedral elements (A-type idealization)

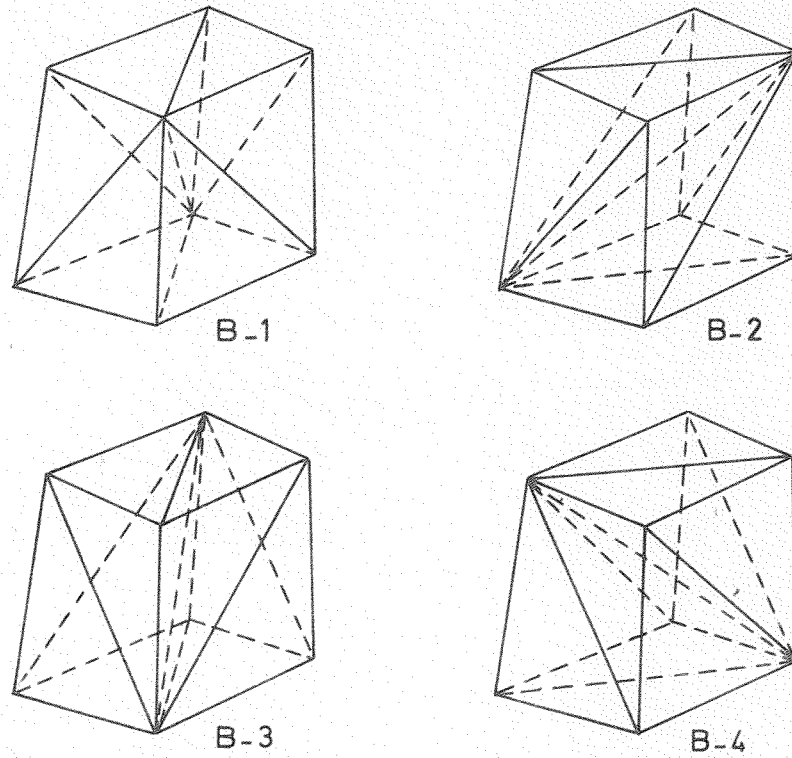


Fig.2.4. B-type idealization of a brick-like block by six tetrahedral elements

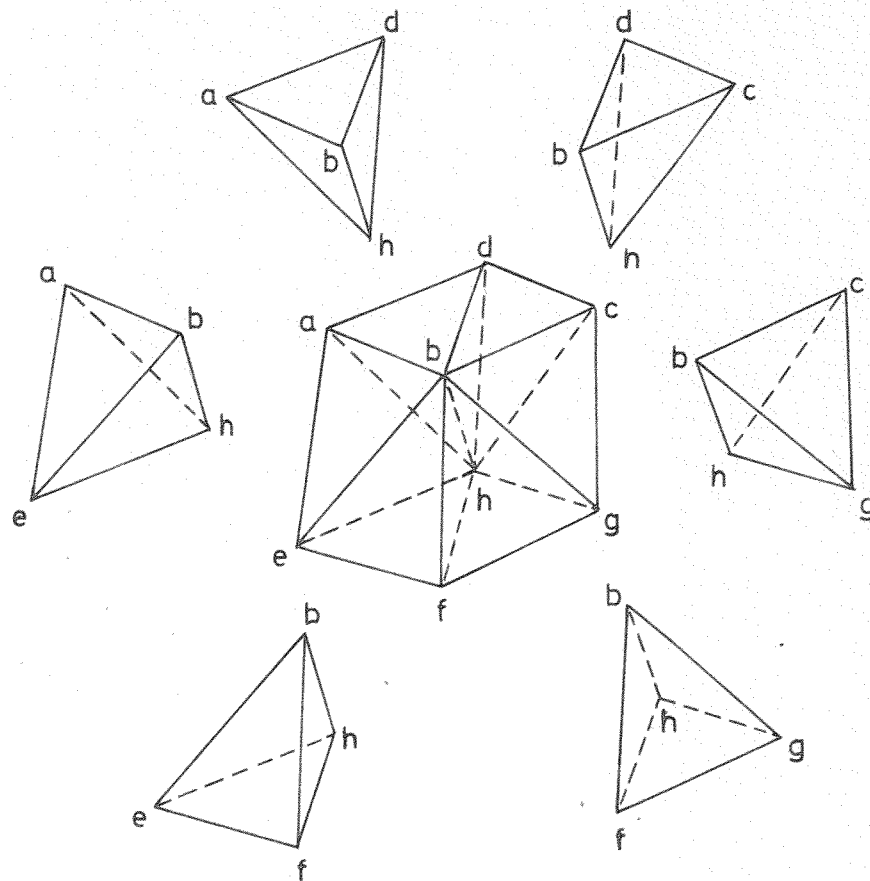


Fig.2.5. Division of a brick-like block into six tetrahedral elements (B-type idealization)

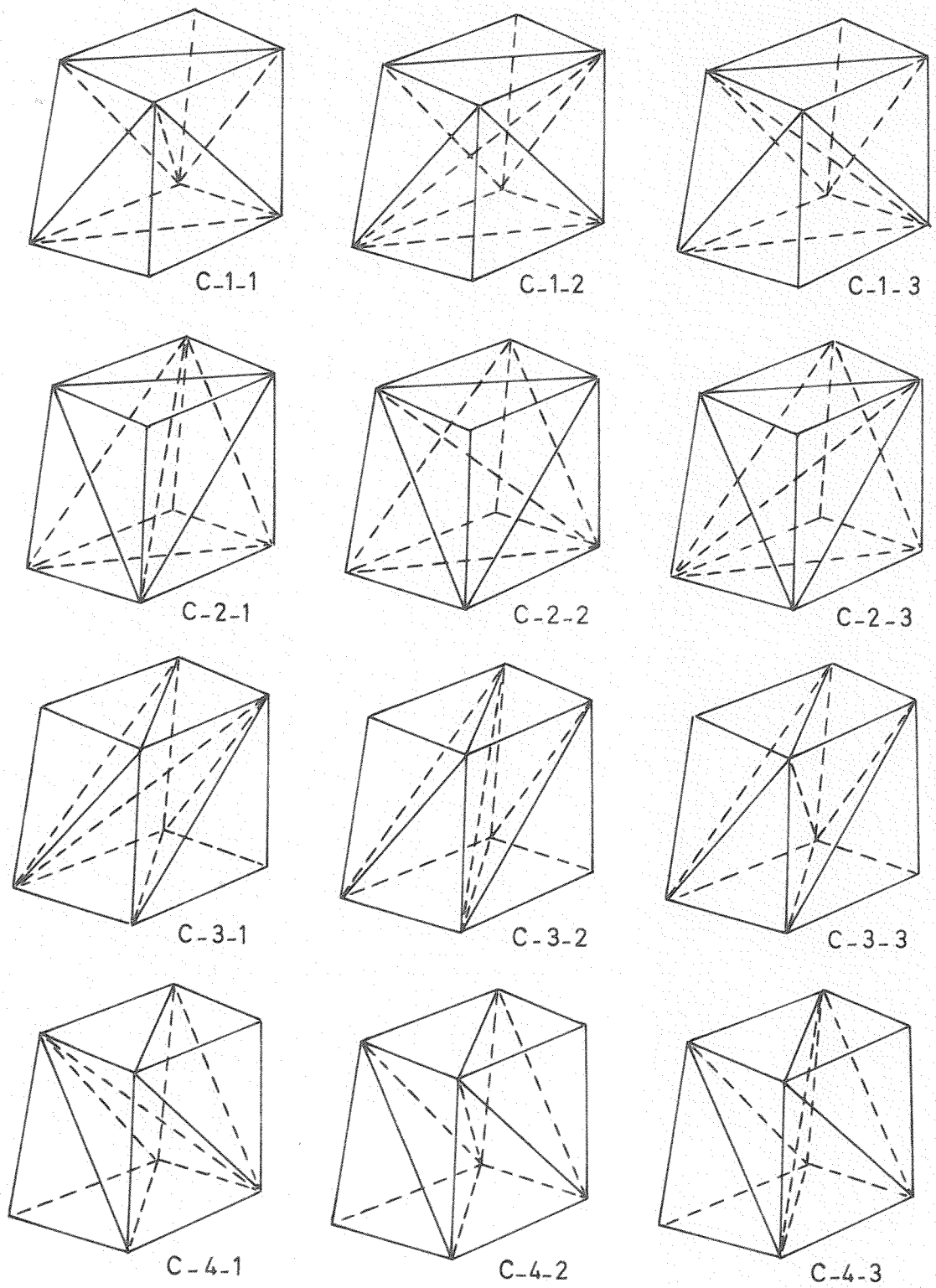


Fig.2.6. C-type idealization of a brick-like block by six tetrahedral elements

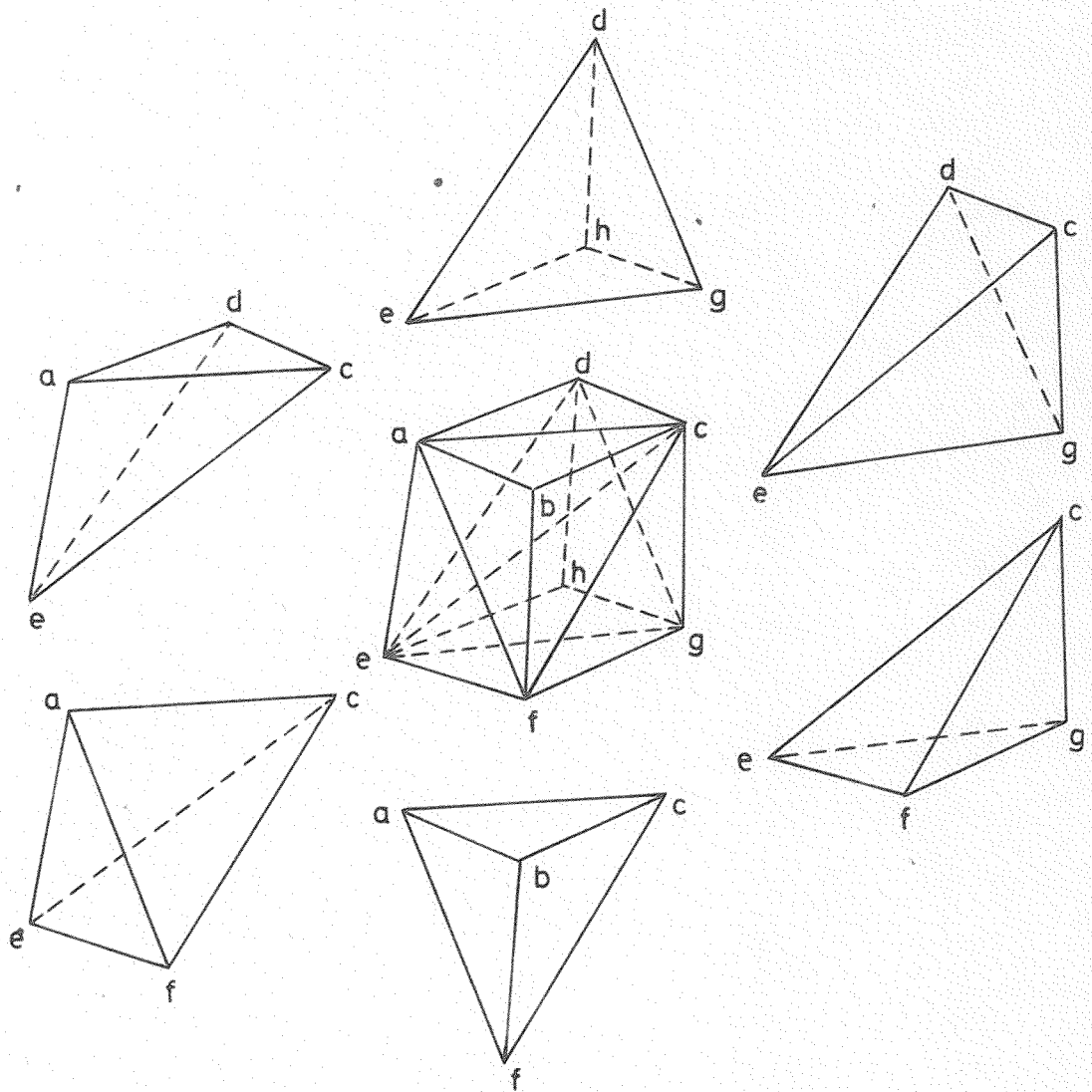


Fig.2.7. Division of a brick-like block into six tetrahedral elements (C-type idealization)

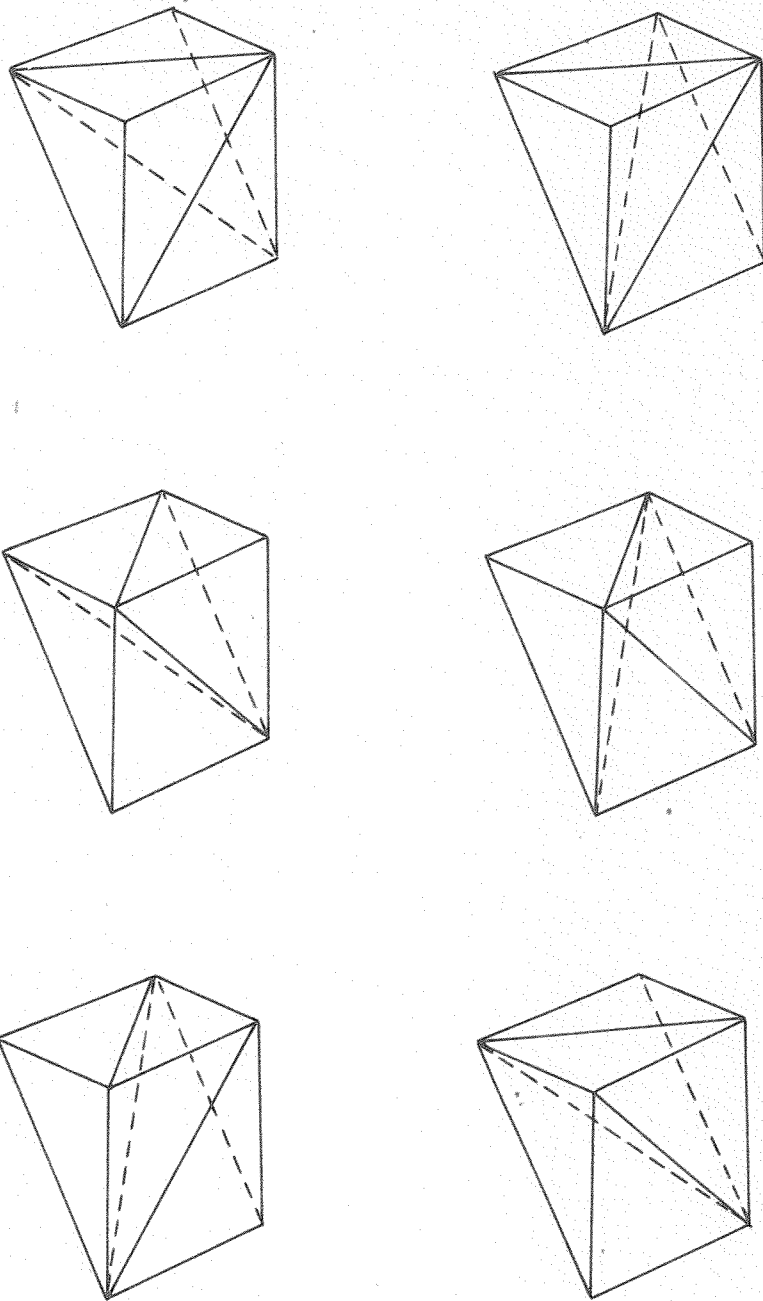


Fig.2.8. Possible combinations of three tetrahedral elements to construct a triangular prism

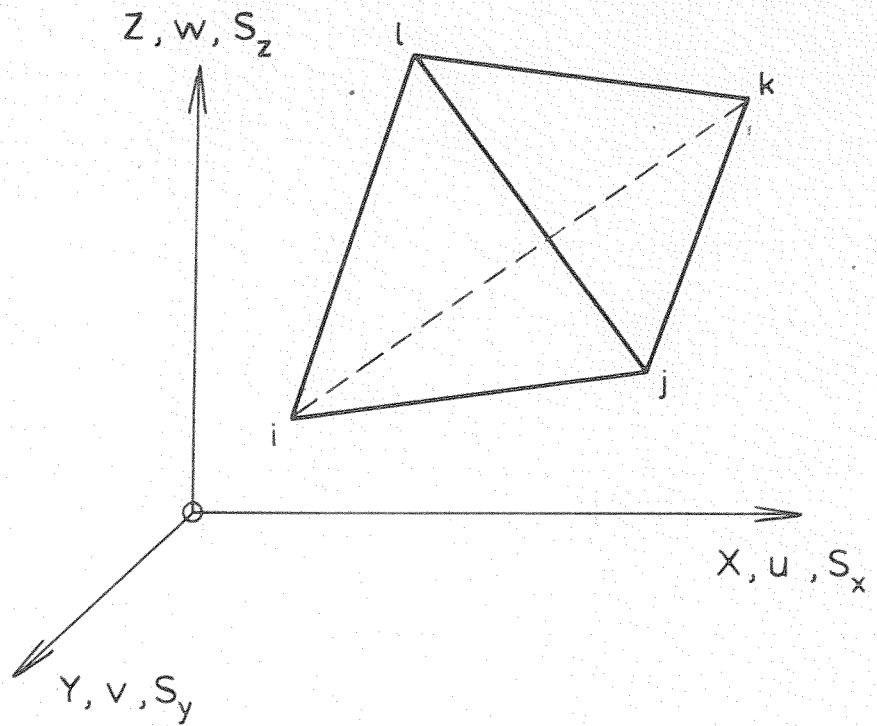


Fig.2.9. Tetrahedral element, global Cartesian co-ordinate system

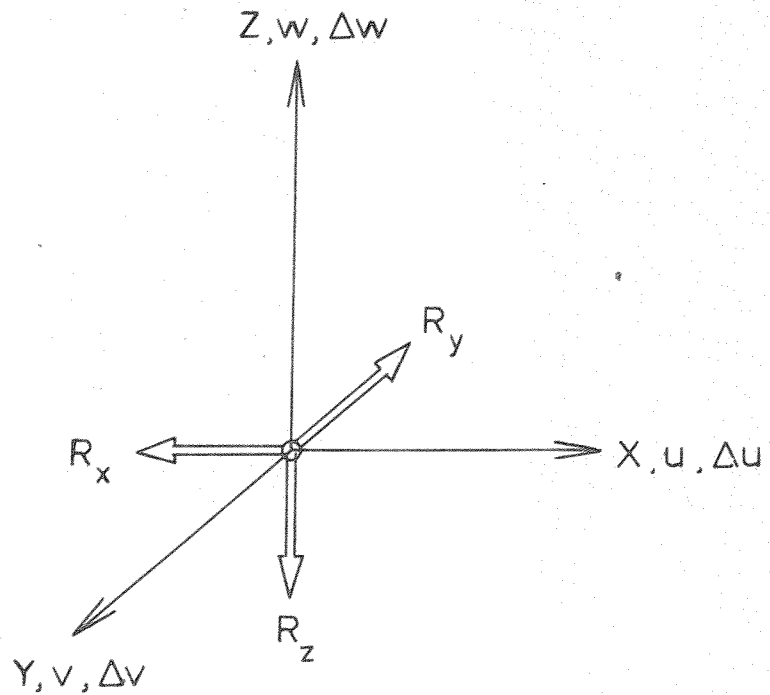


Fig.2.10. A boundary nodal point and acting forces

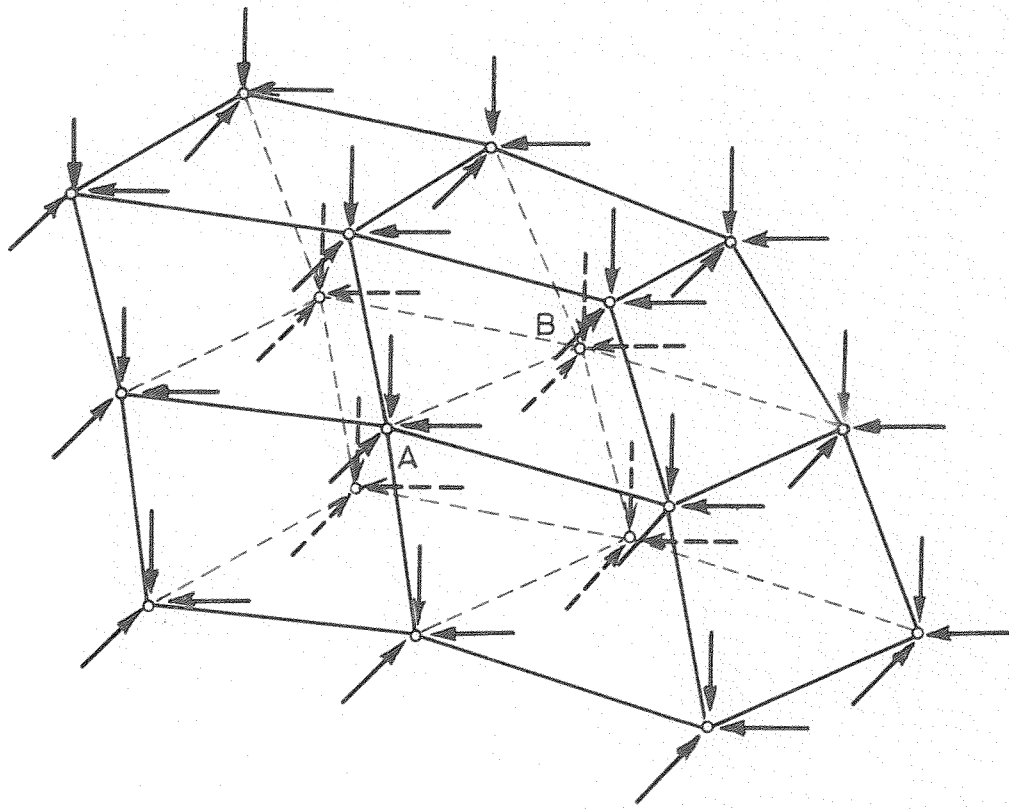


Fig.2.11.d. Nodal point forces acting on a portion of a three dimensional structure

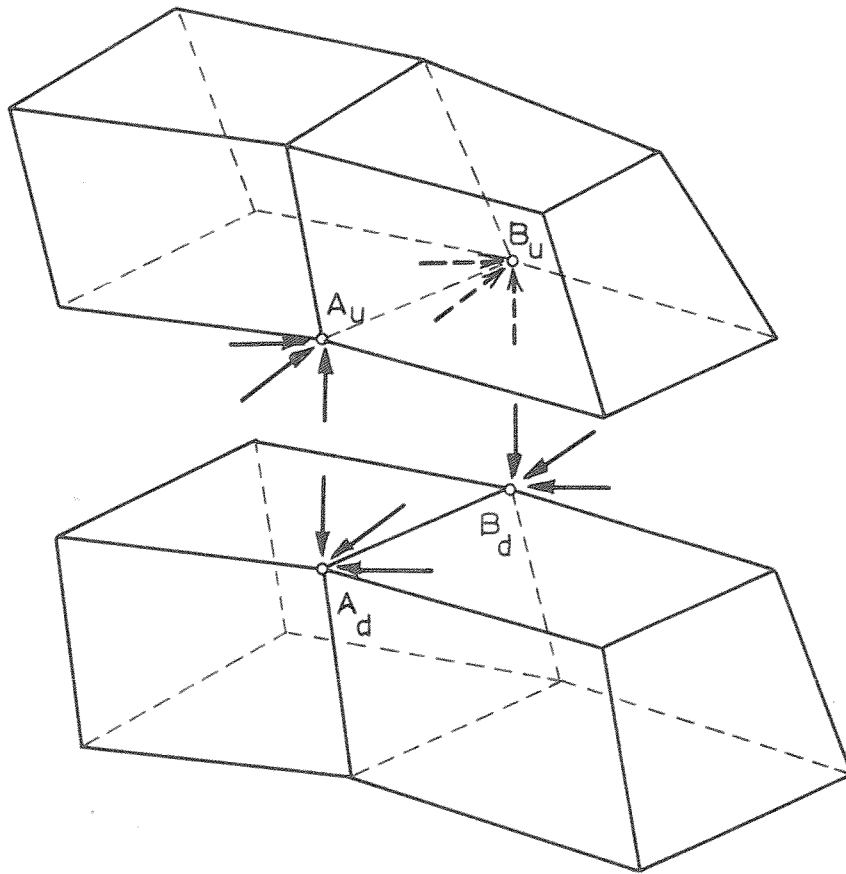


Fig.2.11.b. Horizontal cut through a section, nodal point reactions acting upwards and downwards

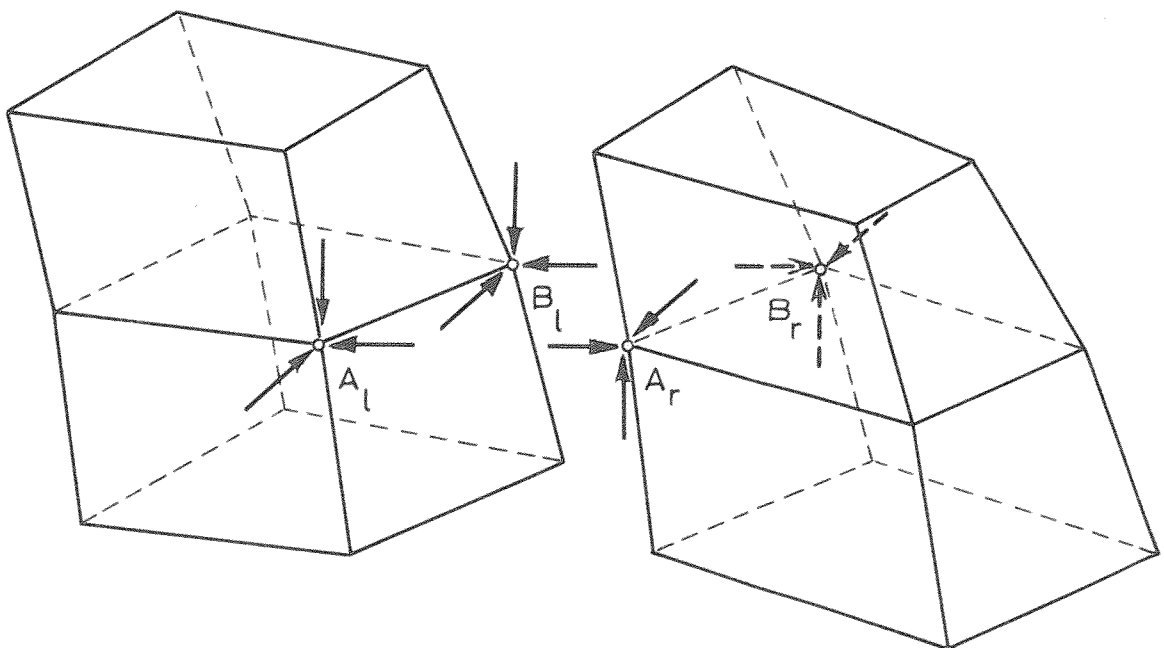
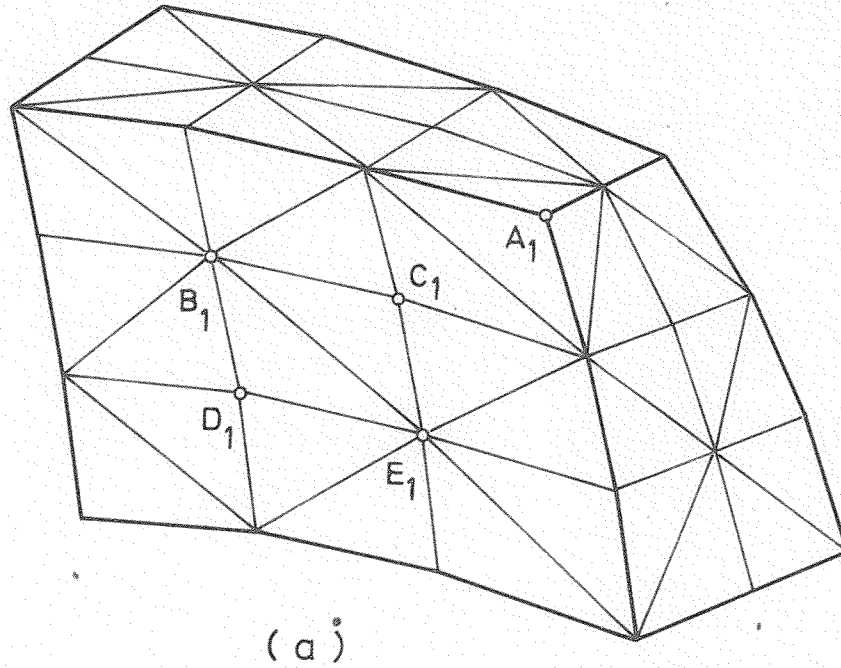
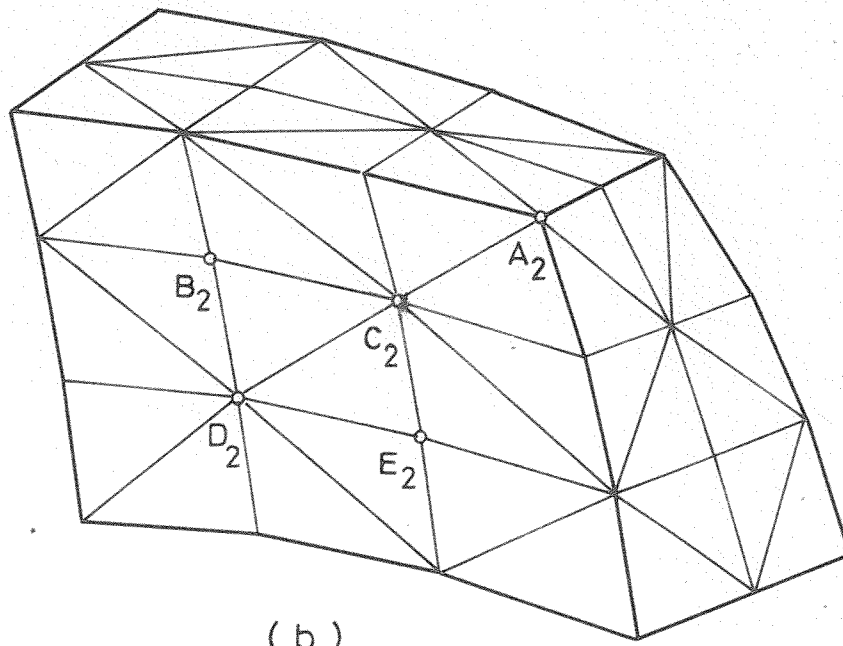


Fig.2.11.c. Vertical cut through a section, nodal point reactions acting on the left and right portions

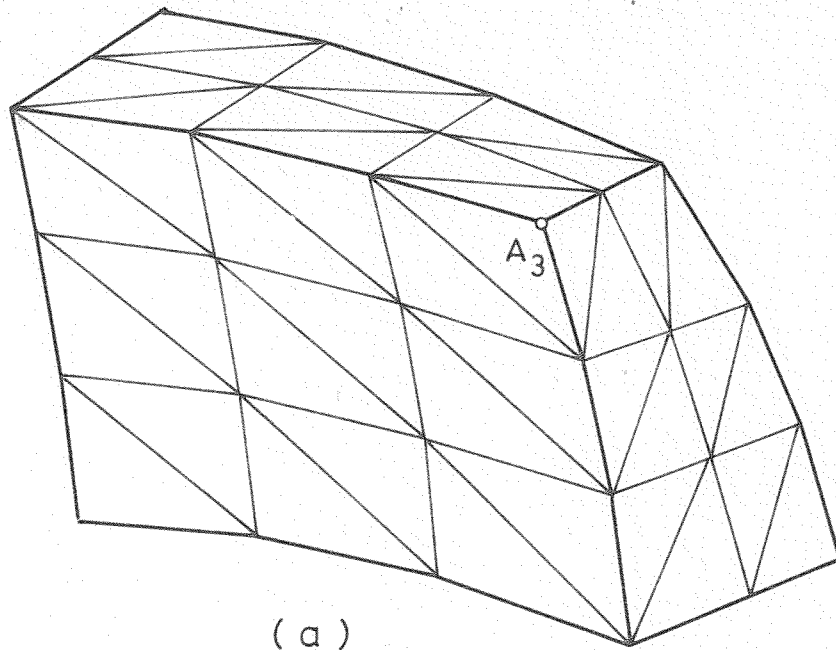


(a)

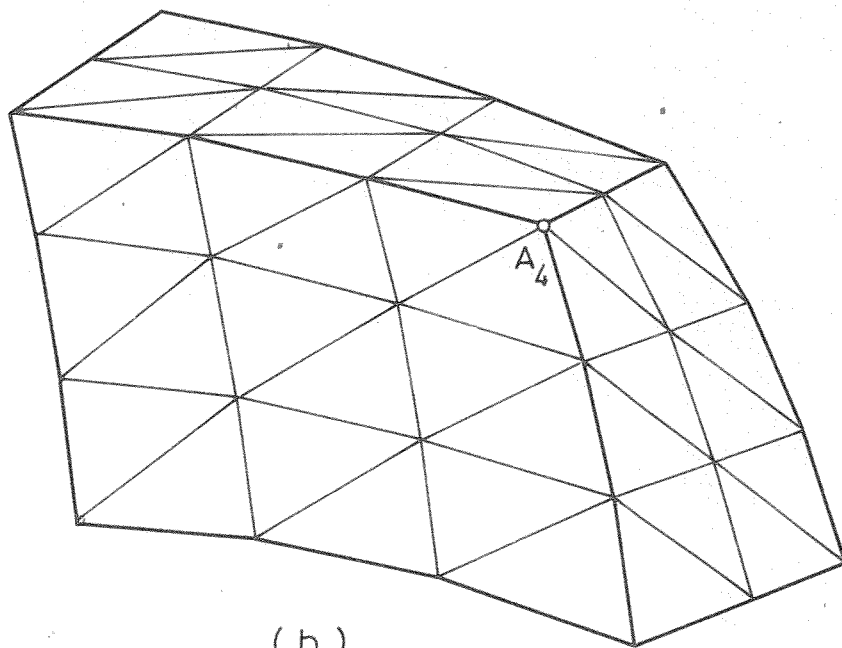


(b)

Fig.2.12. Two possible idealizations of a structure by using A-type brick-like blocks



(a)



(b)

Fig.2.13. Two of possible idealizations of a structure by using C-type brick-like blocks'

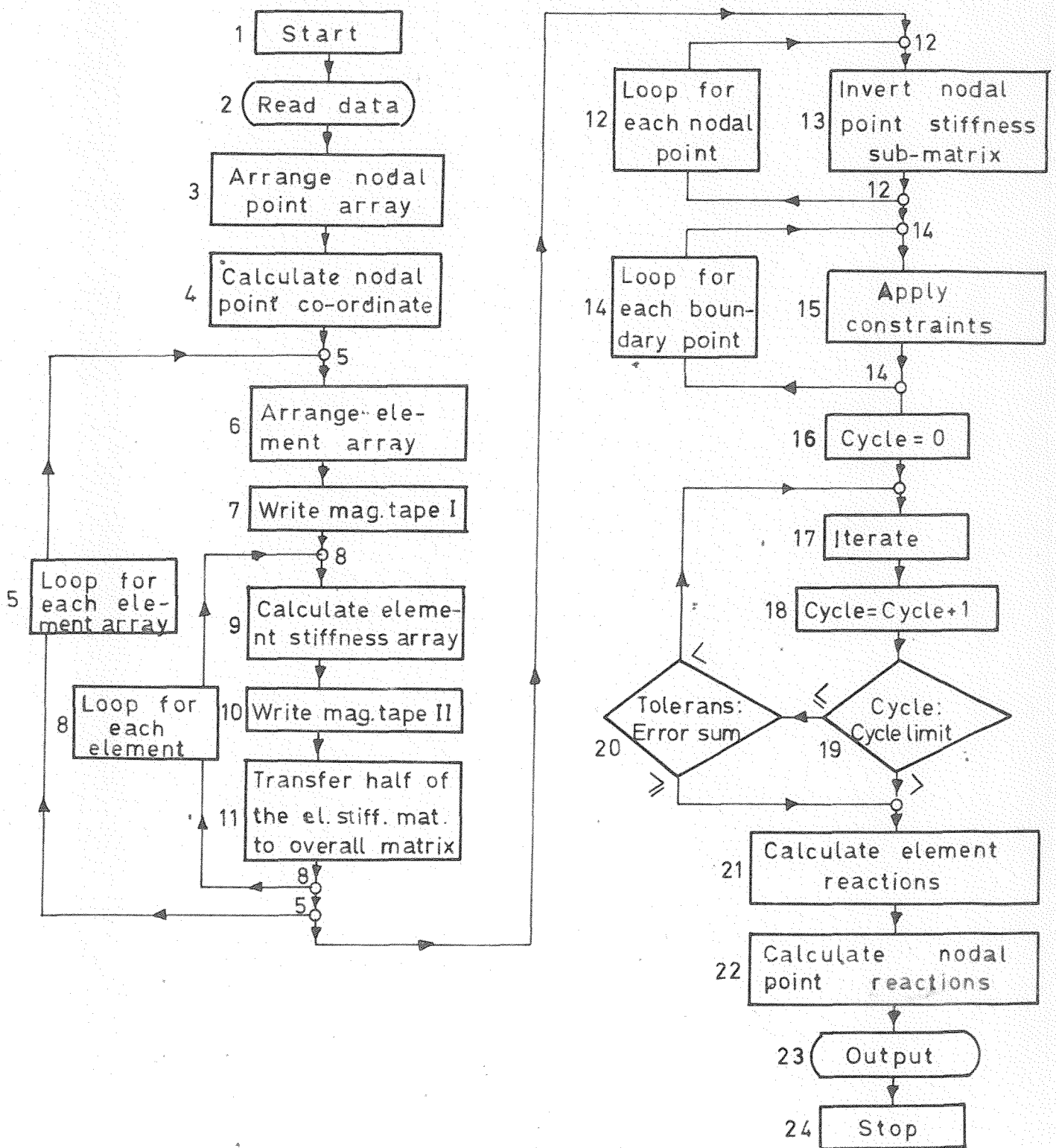
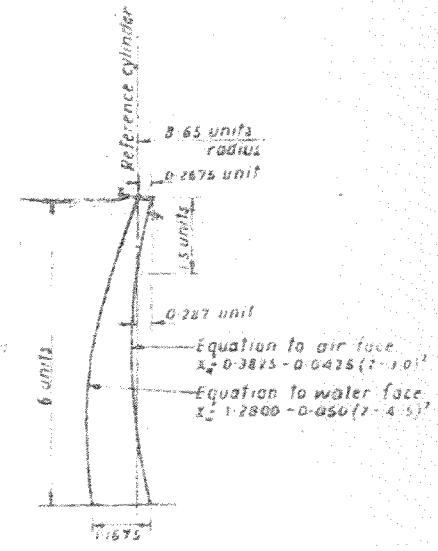
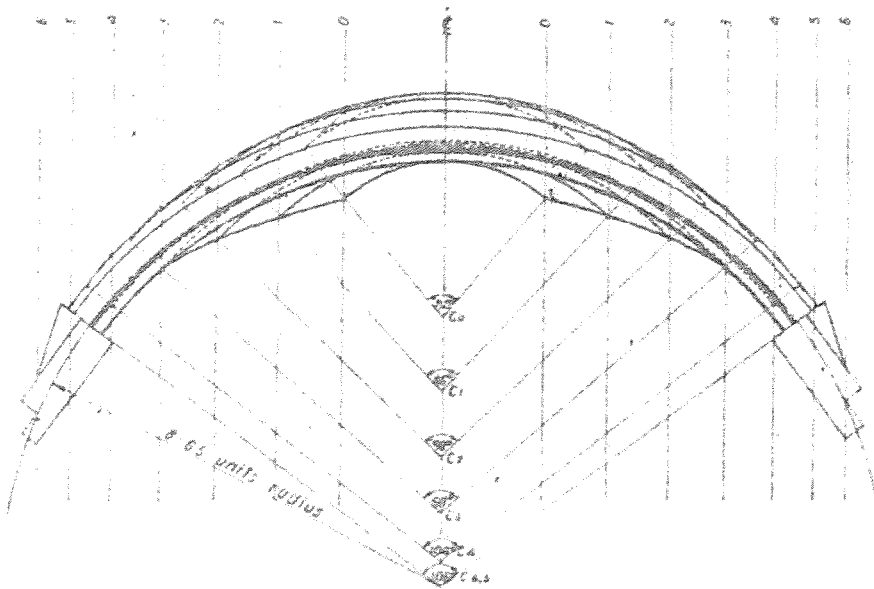
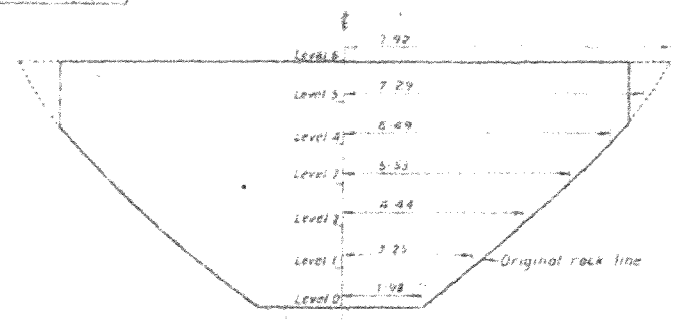


Fig.2.14. Flow diagram for static analysis of arch dams

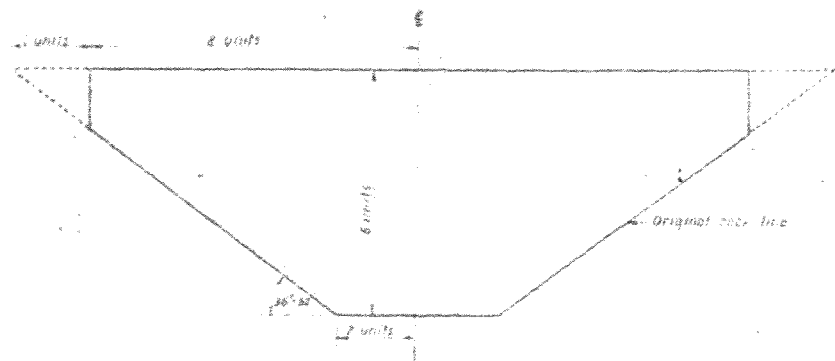


- NOTES  
 1 Centre of arch at level  $i$  indicated by  $C_i$   
 2 Radii and central angles to  $\xi$  of arches as follows

Level, units	0	1	2	3	4	5	6
Radius, units	3.67	5.29	6.64	7.72	8.54	8.85	8.50
Central angle	80°	86°	92°	98°	104°	106°	106°



Normal cross section of idealized valley



Developed surface of reference cylinder

Fig.2.15. Arch dam type-5  
 General layout

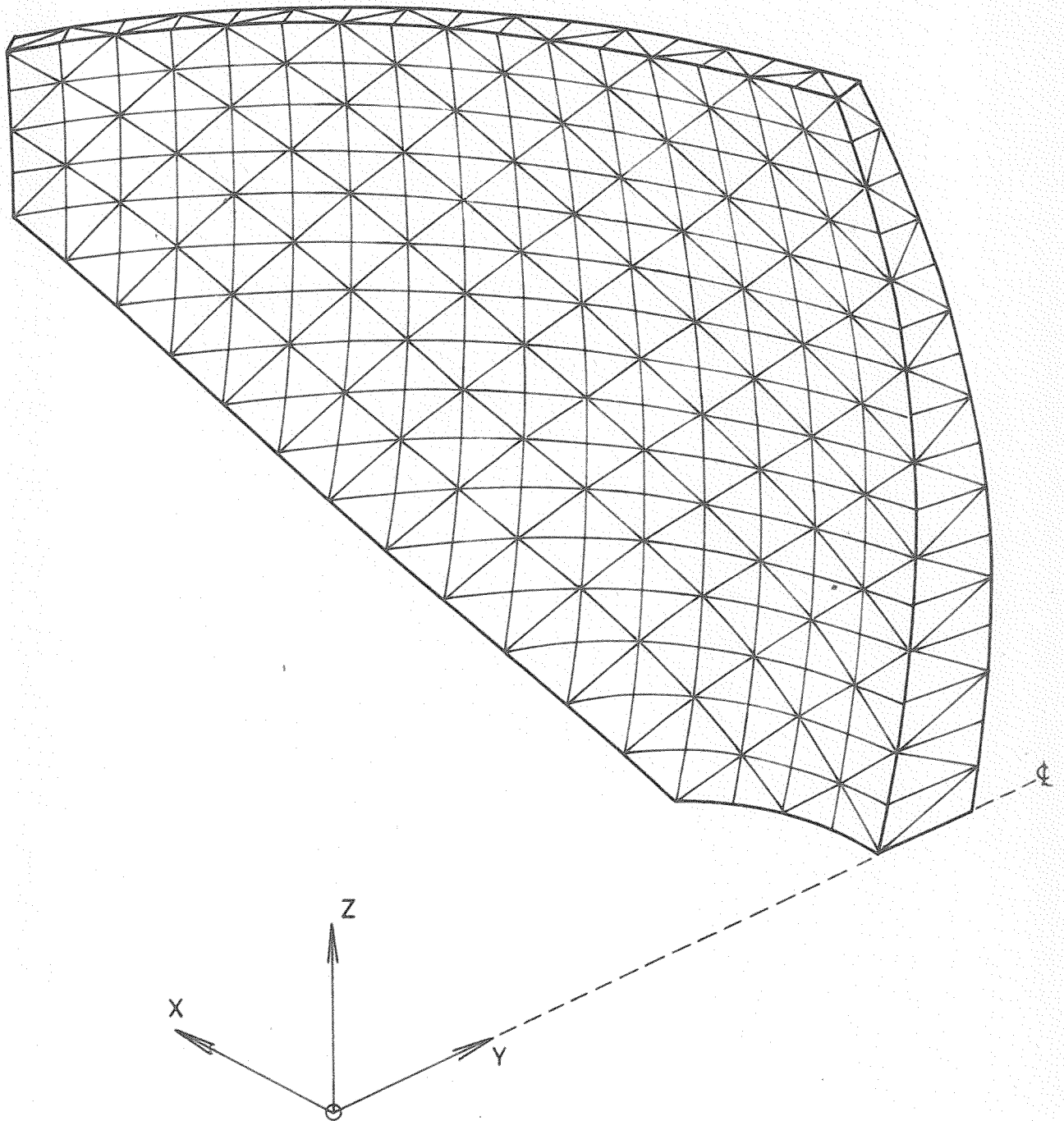


Fig.2.16. Idealization of the half of a double curvature arch dam by means of A-type brick-like blocks using five tetrahedral elements (16x1x16 mesh type)

Arch Dam Type-5, 120 m High, 100 m Span, 100 m Radius

W: Water face  
A: Air face

—○—○— Simple tetrahedron  
-x-x-x- Zienkiewicz  
--△--△-- Trial-load  
--□--□-- Kantorovich

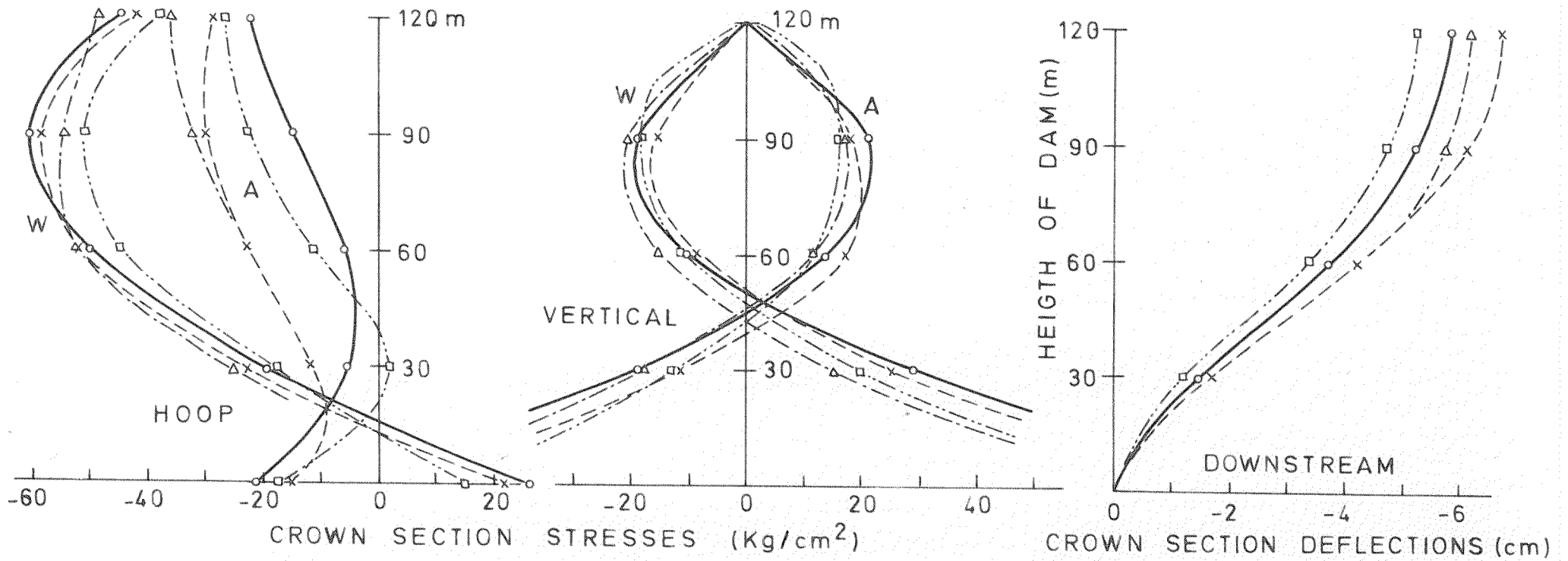


Fig.2.17. Stresses and deflections of Arch Dam Type-5 under hydrostatic loading

W: Water face  
 A: Air face

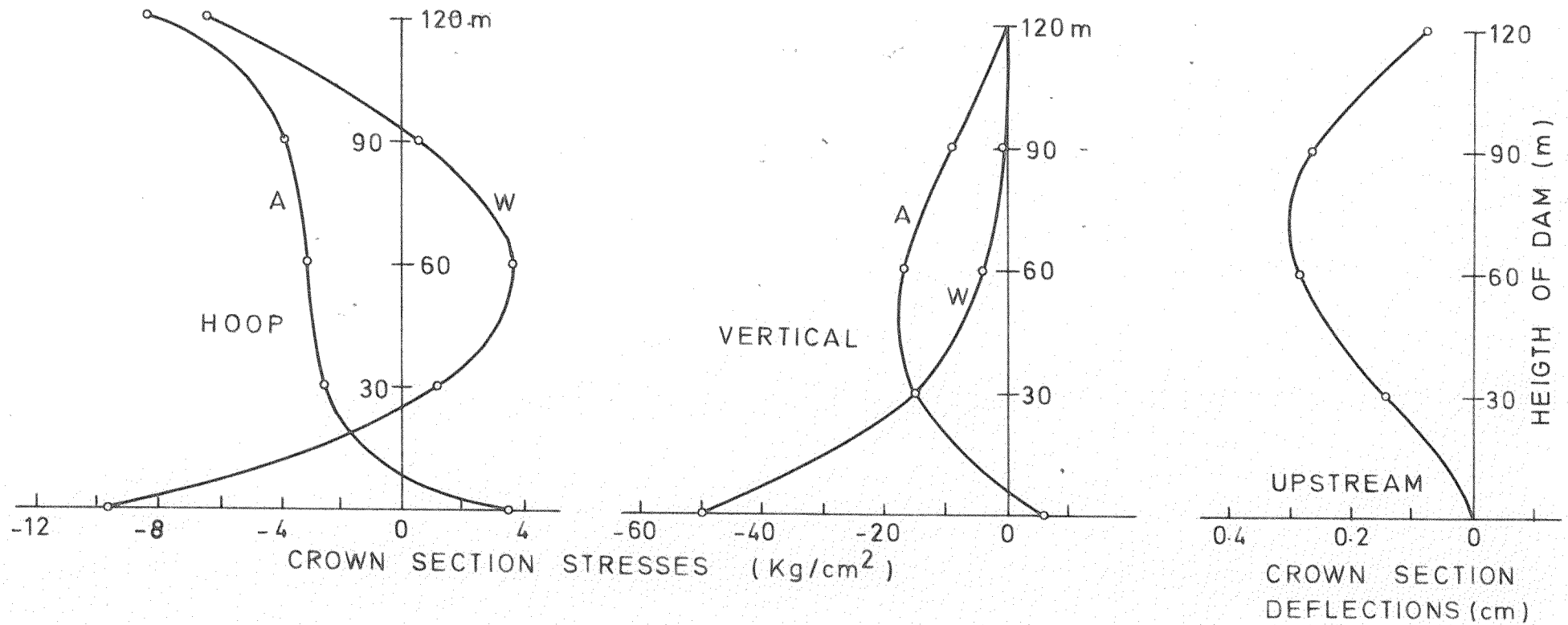


Fig.2.18. Stresses and deflections of Arch Dam Type-5 under gravity loading

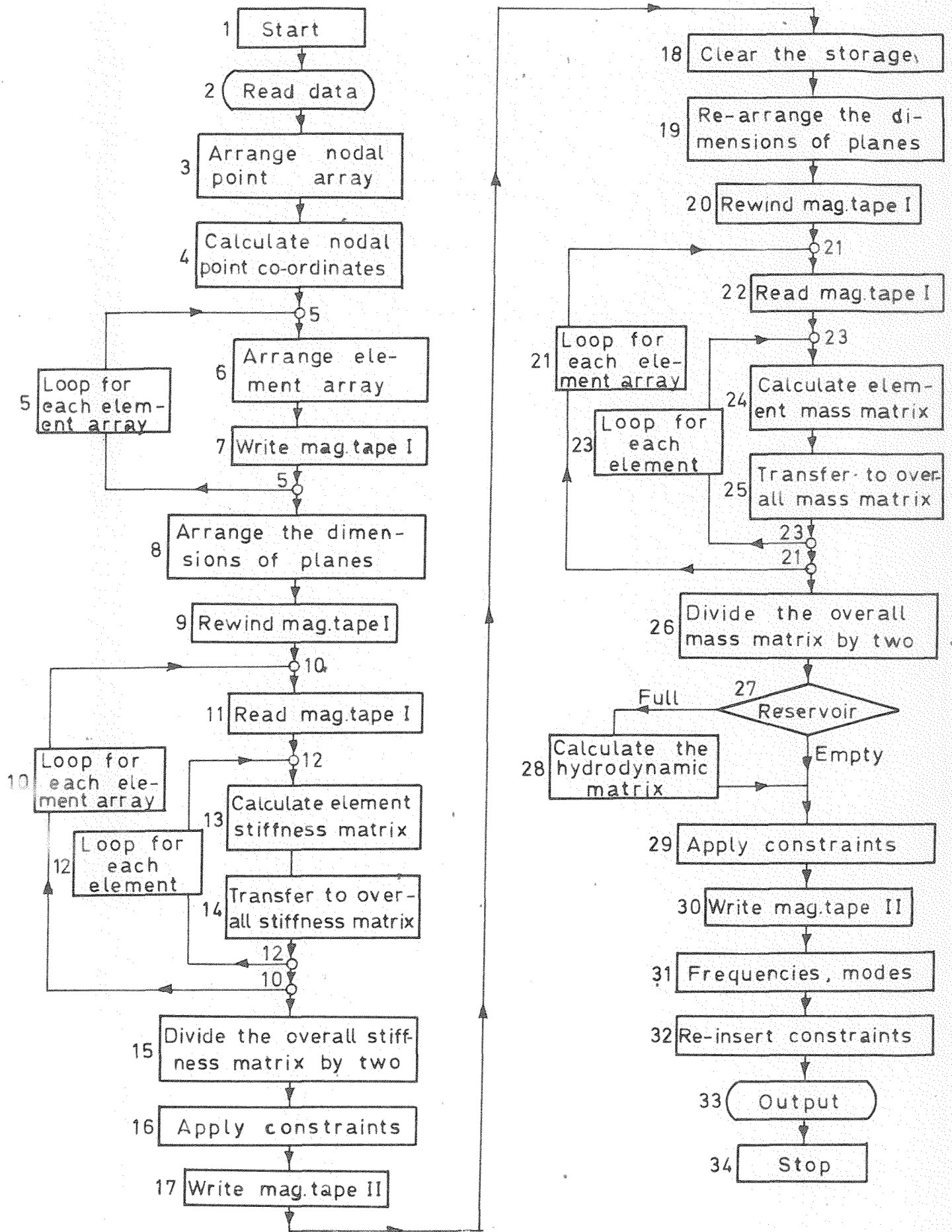


Fig.3.1. Flow diagram for calculating frequency and mode shape

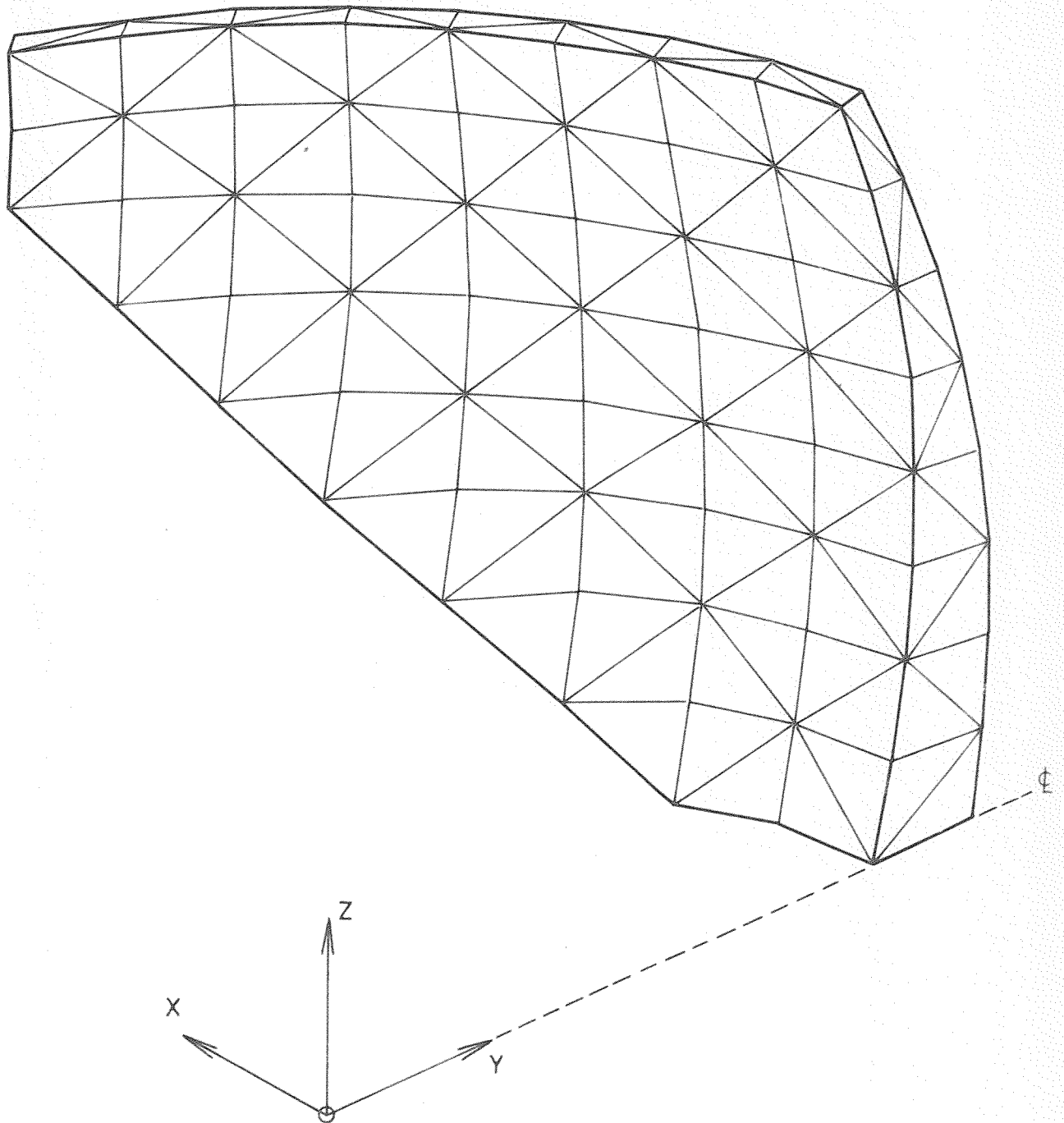
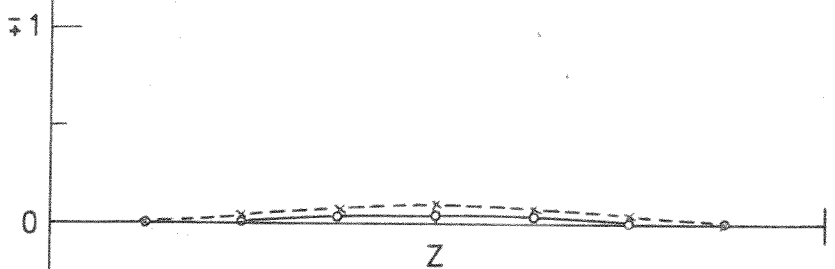
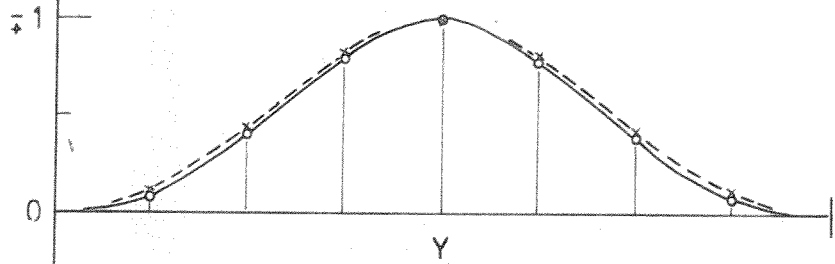
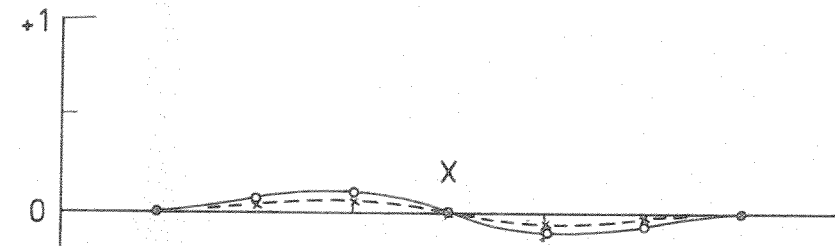
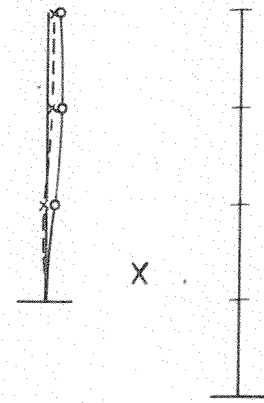
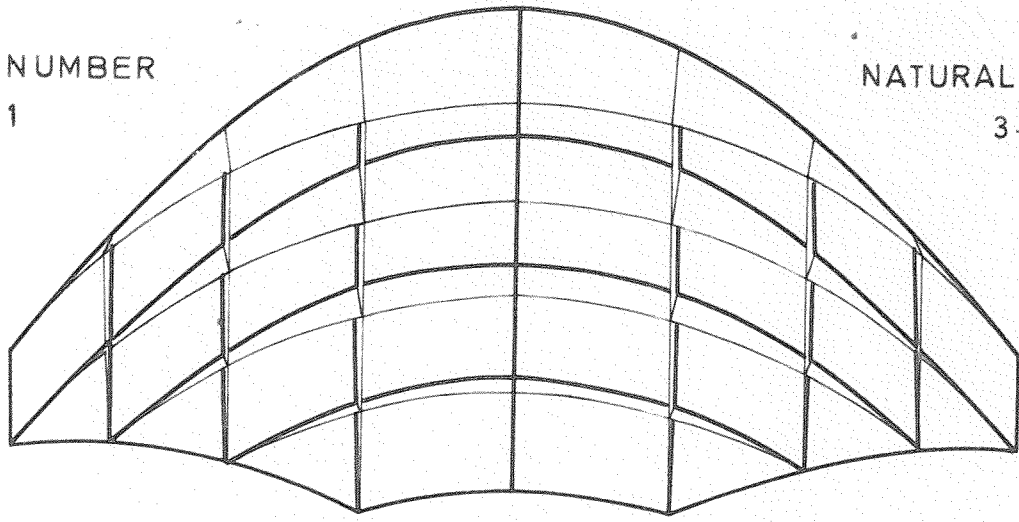


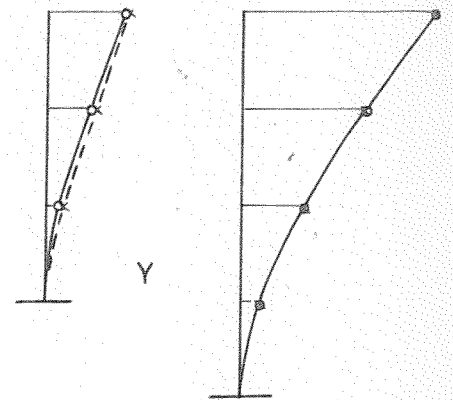
Fig.3.2. Idealization of the half of a double curvature arch dam (8x1x8 mesh type)

MODE NUMBER  
1

NATURAL FREQUENCY  
3.27 Hz



Deflections of top arch



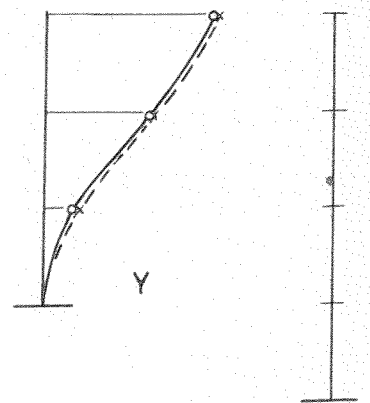
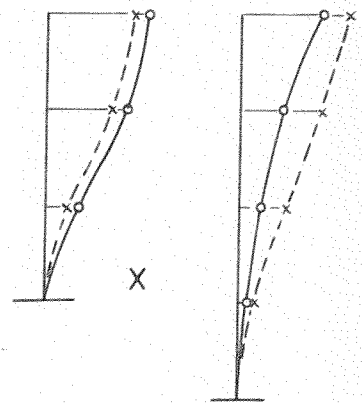
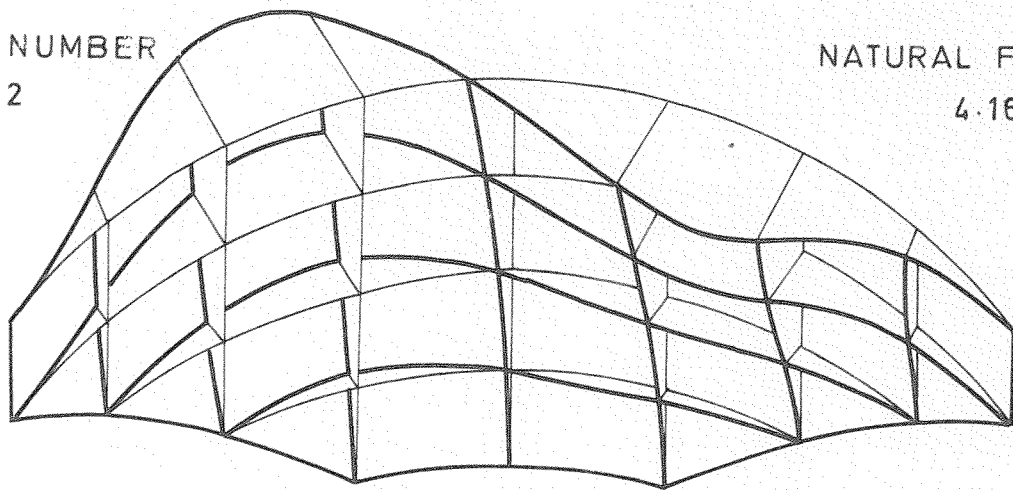
Mid Crown  
Cantilever displacements

—○—○— Water face  
-x---x- Air face

Fig.3.3. First mode of vibration of Arch Dam Type-5

MODE NUMBER  
2

NATURAL FREQUENCY  
4.16 Hz



Mid                      Crown  
Cantilever displacements

—○—○— Water face  
-x--x- Air face

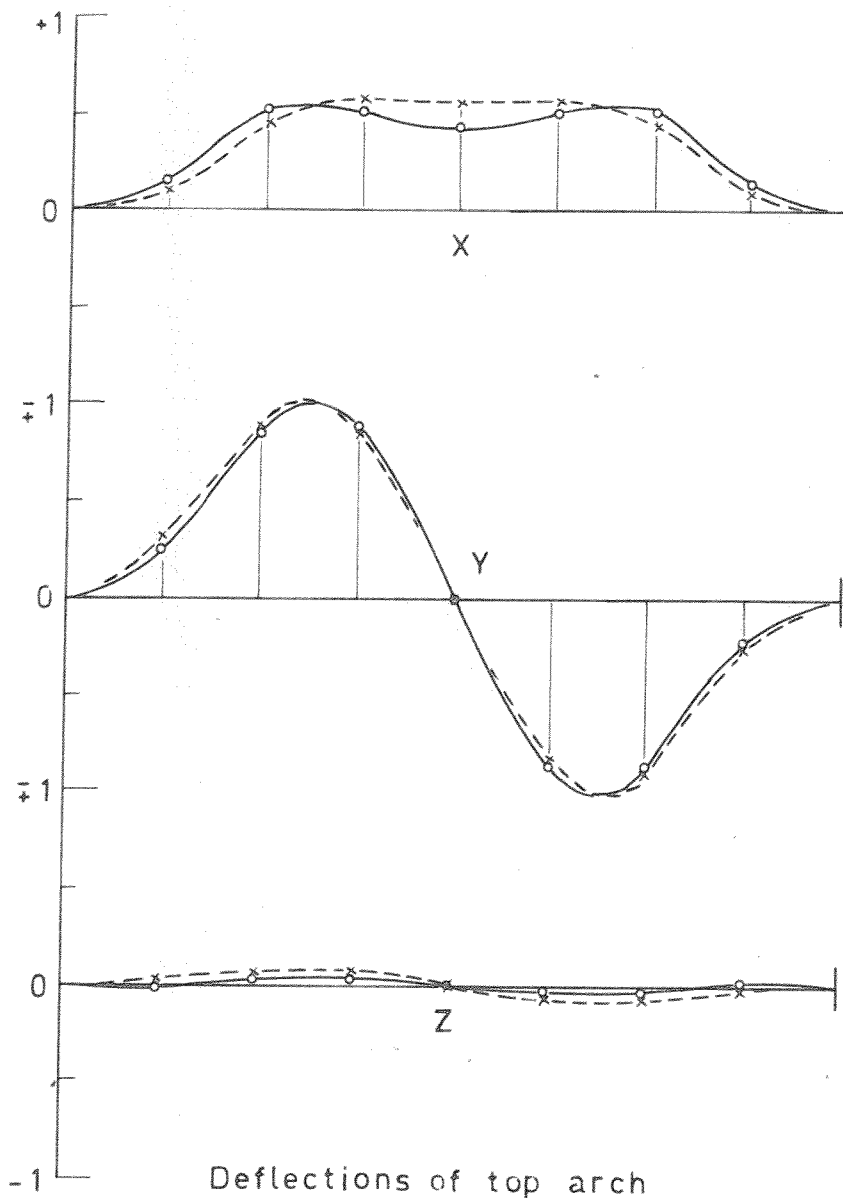
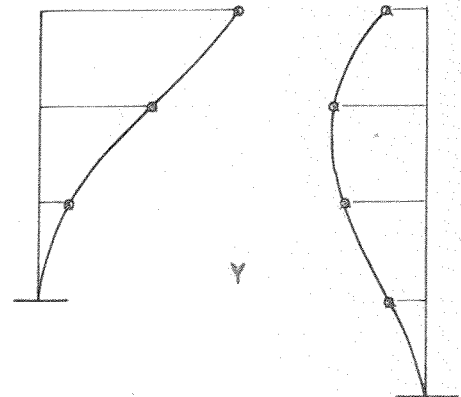
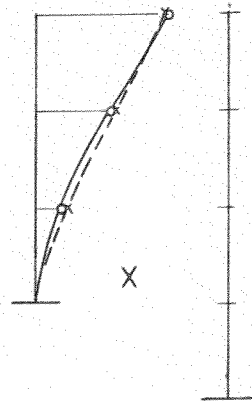
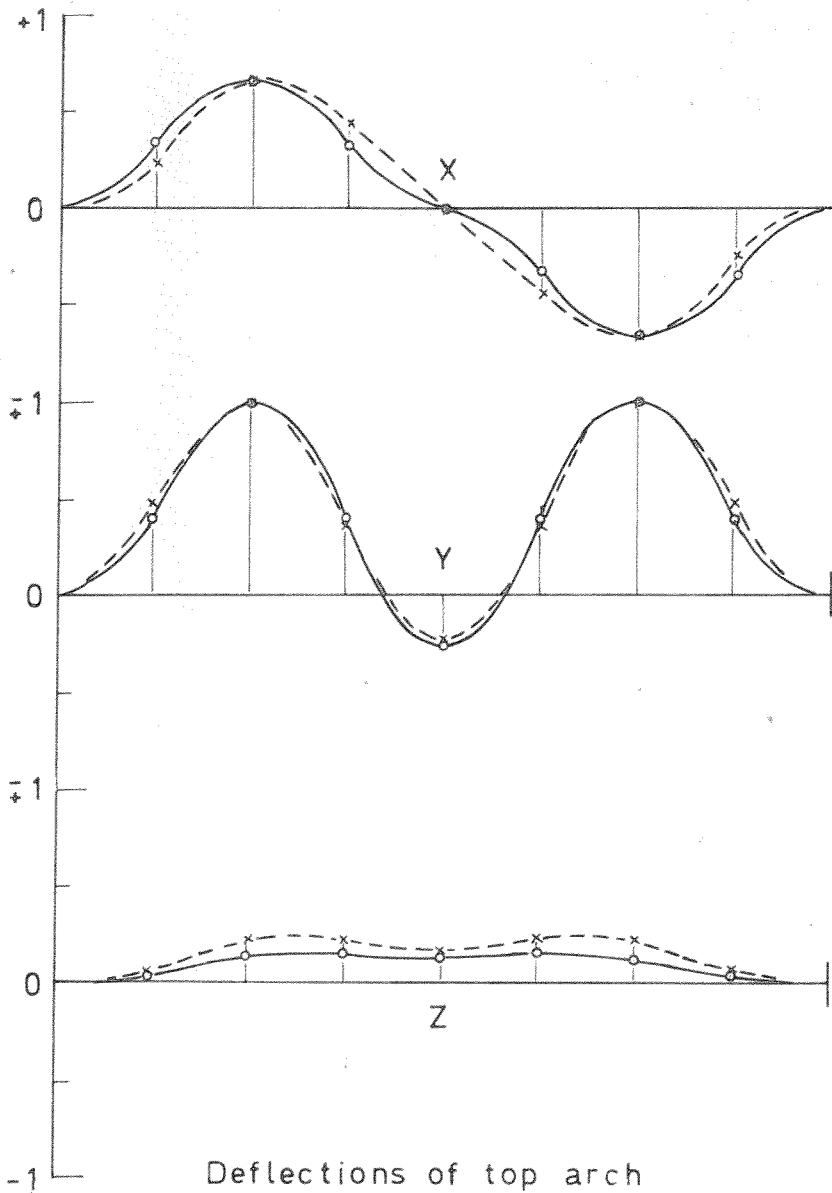
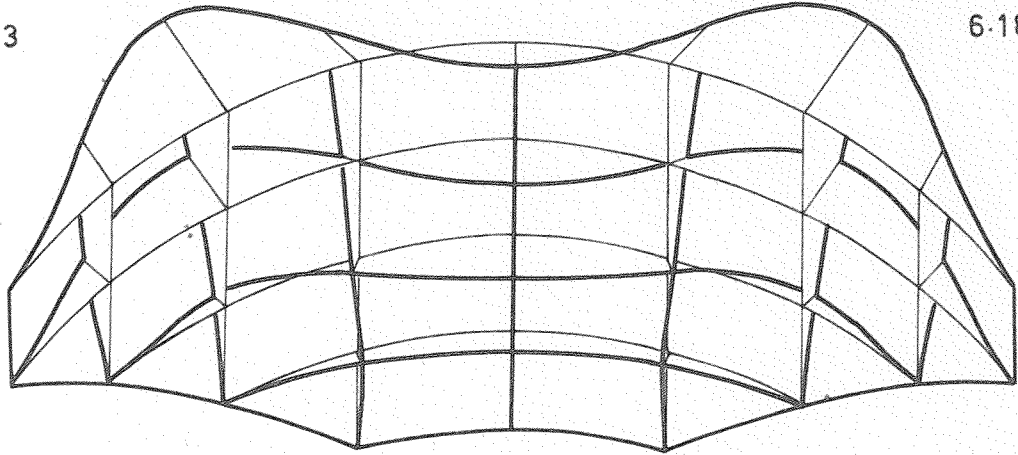


Fig.3.4. Second mode of vibration of Arch Dam Type-5

MODE NUMBER  
3

NATURAL FREQUENCY  
6.18 Hz



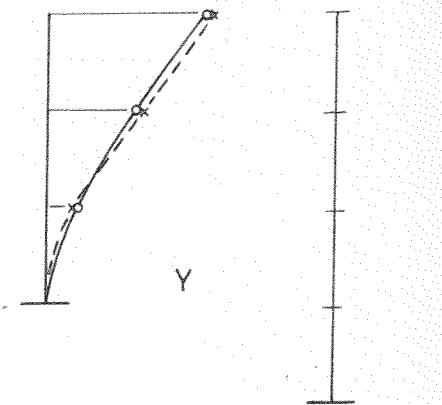
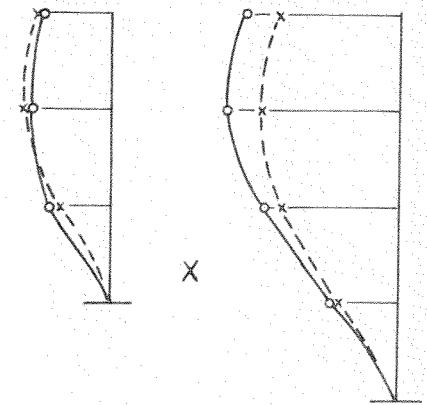
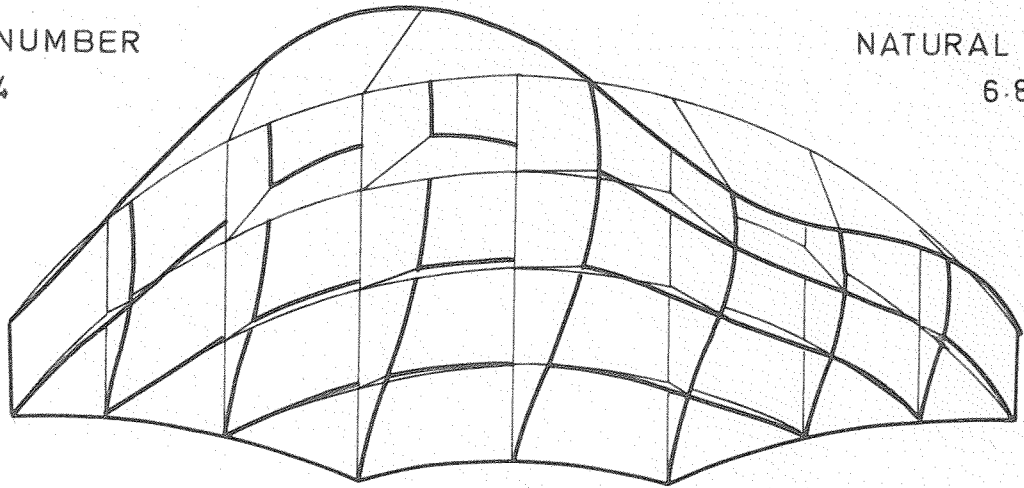
Mid Cantilever displacements

○—○ Water face  
-x--x- Air face

Fig.3.5. Third mode of vibration of Arch Dam Type-5

MODE NUMBER  
4

NATURAL FREQUENCY  
6.83 Hz



Mid Crown  
Cantilever displacements

—o—o— Water face  
-x---x- Air face

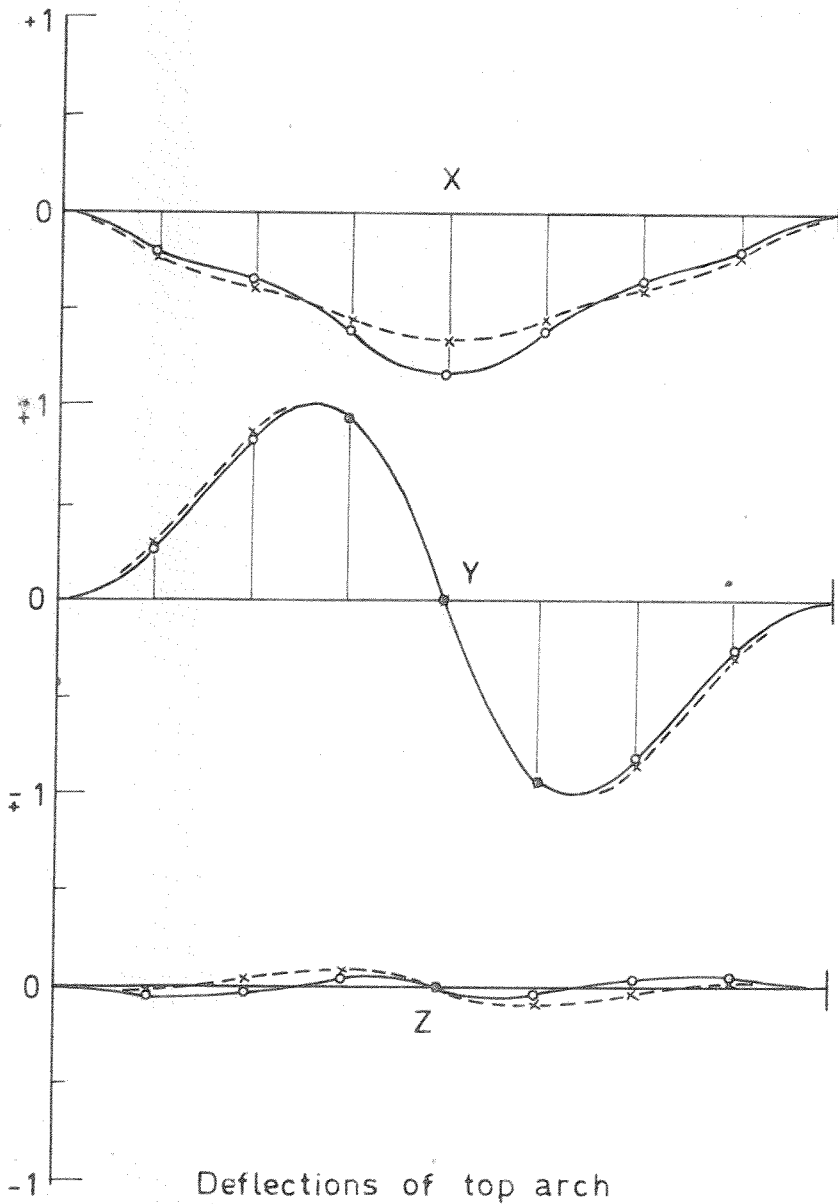
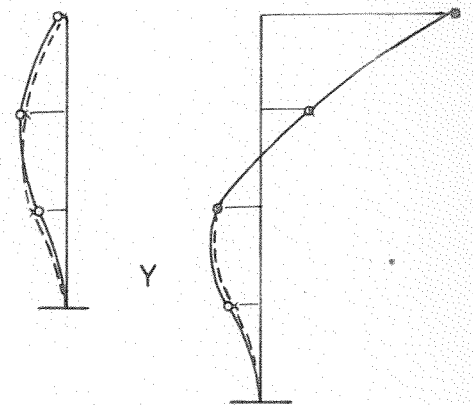
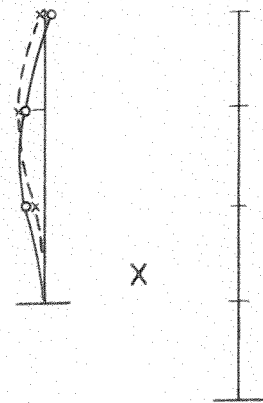
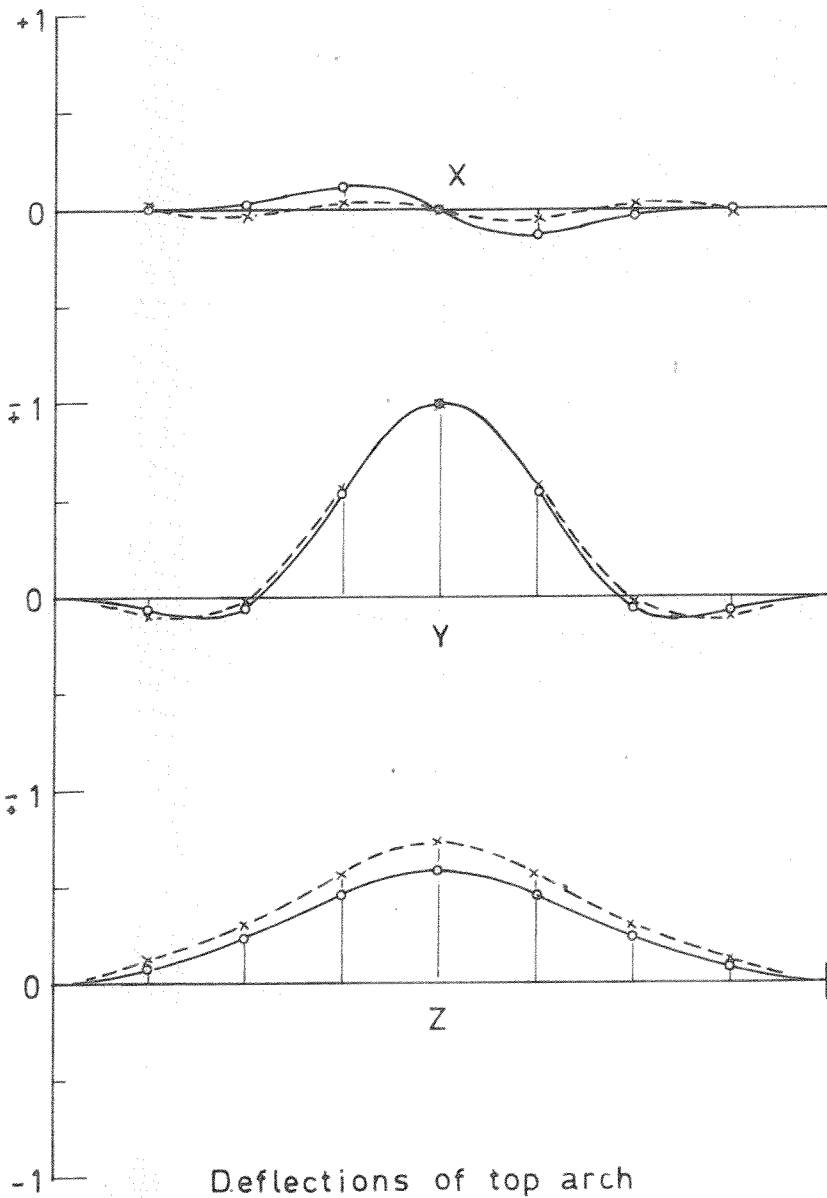
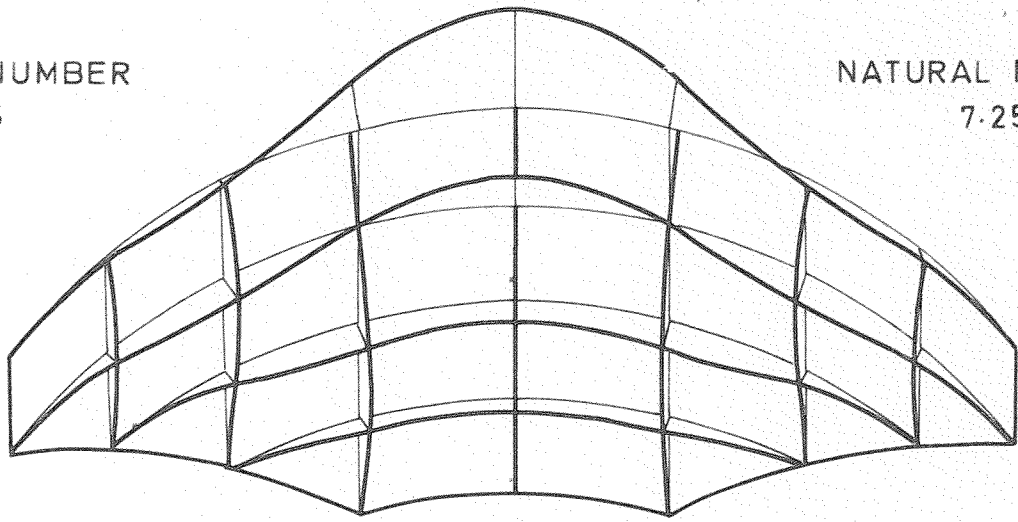


Fig.3.6. Fourth mode of vibration of Arch Dam Type-5

MODE NUMBER  
5

NATURAL FREQUENCY  
7.25 Hz



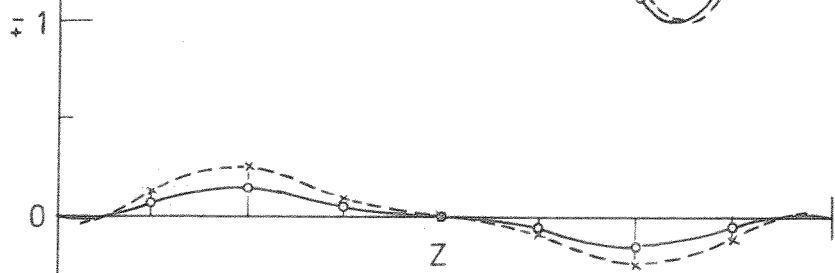
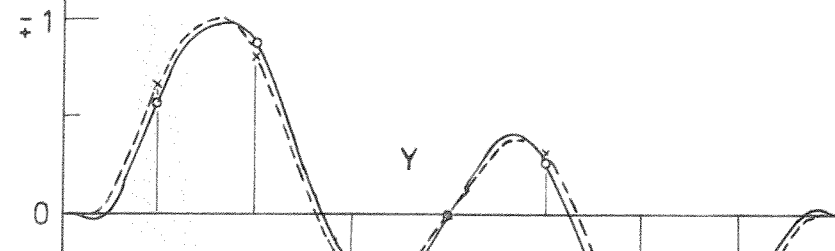
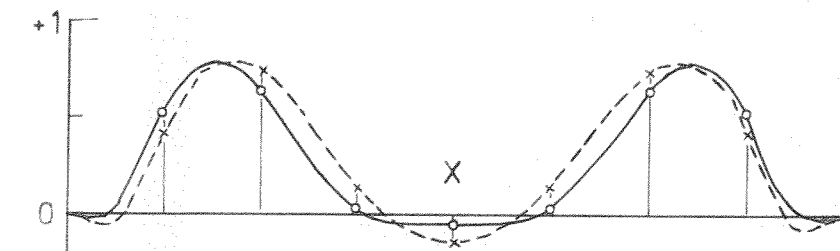
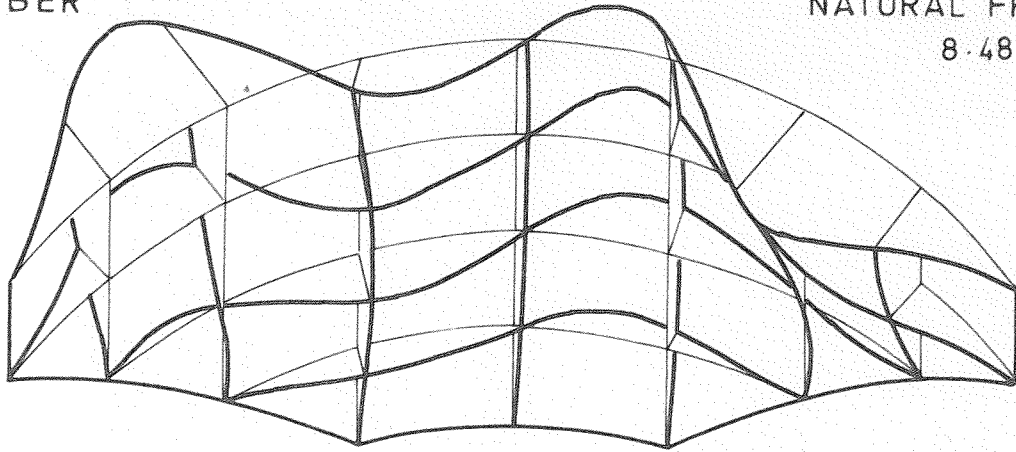
Mid      Crown  
Cantilever displacements

○—○ Water face  
-x---x- Air face

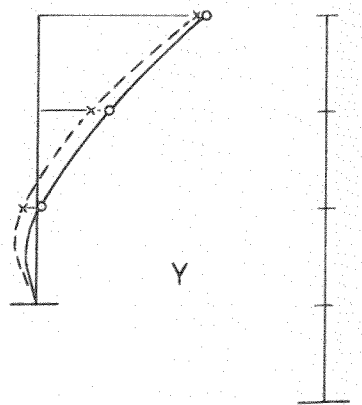
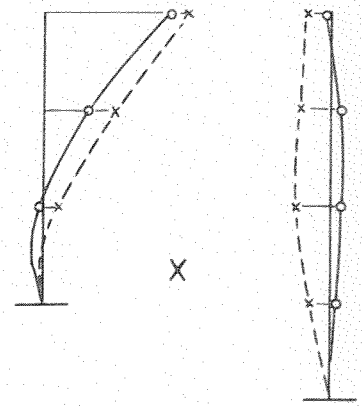
Fig.3.7. Fifth mode of vibration of Arch Dam Type-5

MODE NUMBER  
6

NATURAL FREQUENCY  
8.48 Hz



Deflections of top arch



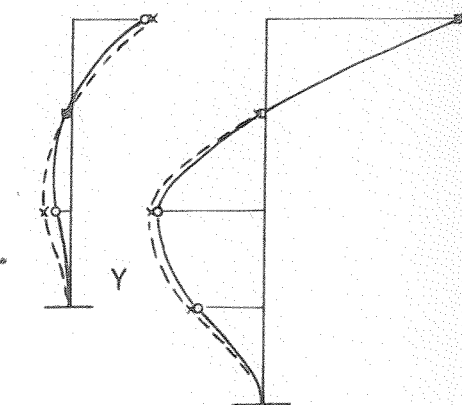
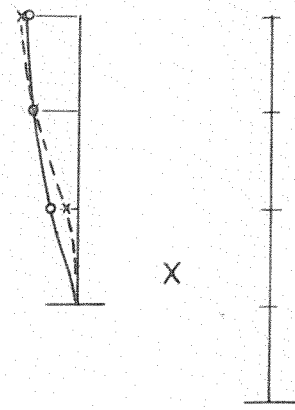
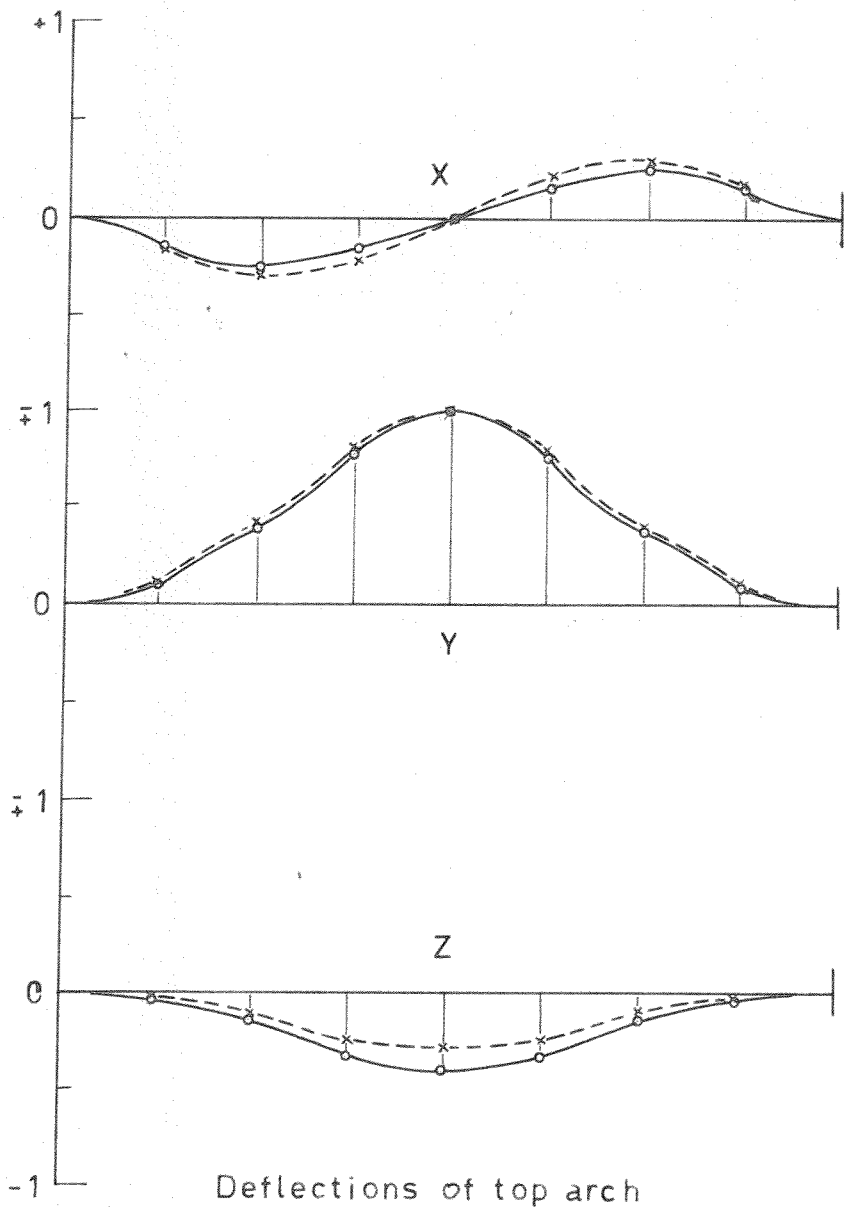
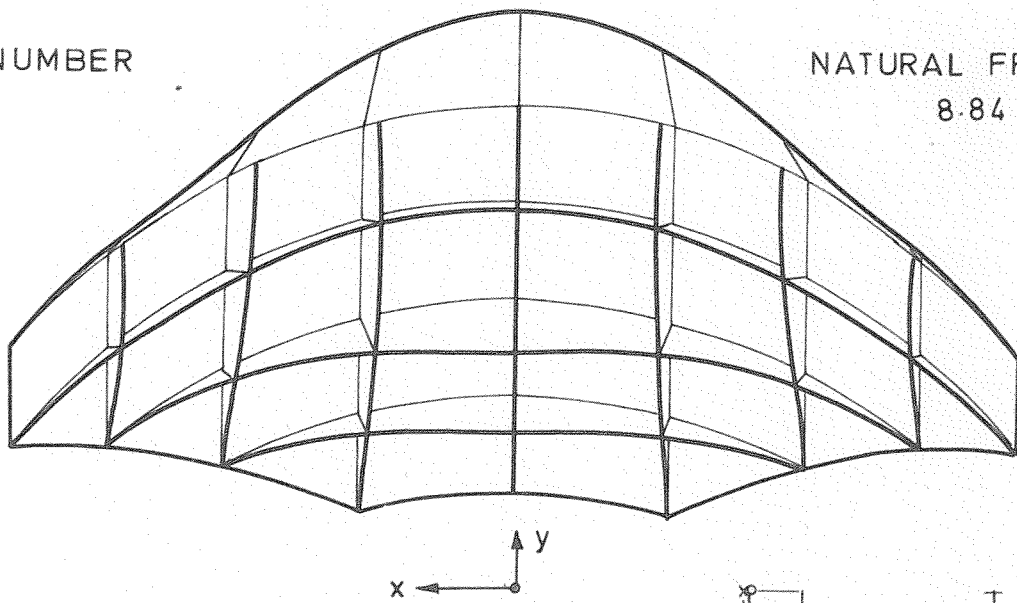
Mid                      Crown  
Cantilever displacements

—○—○— Water face  
-x---x- Air face

Fig.3.8. Sixth mode of vibration of Arch Dam Type-5

MODE NUMBER  
7

NATURAL FREQUENCY  
8.84 Hz



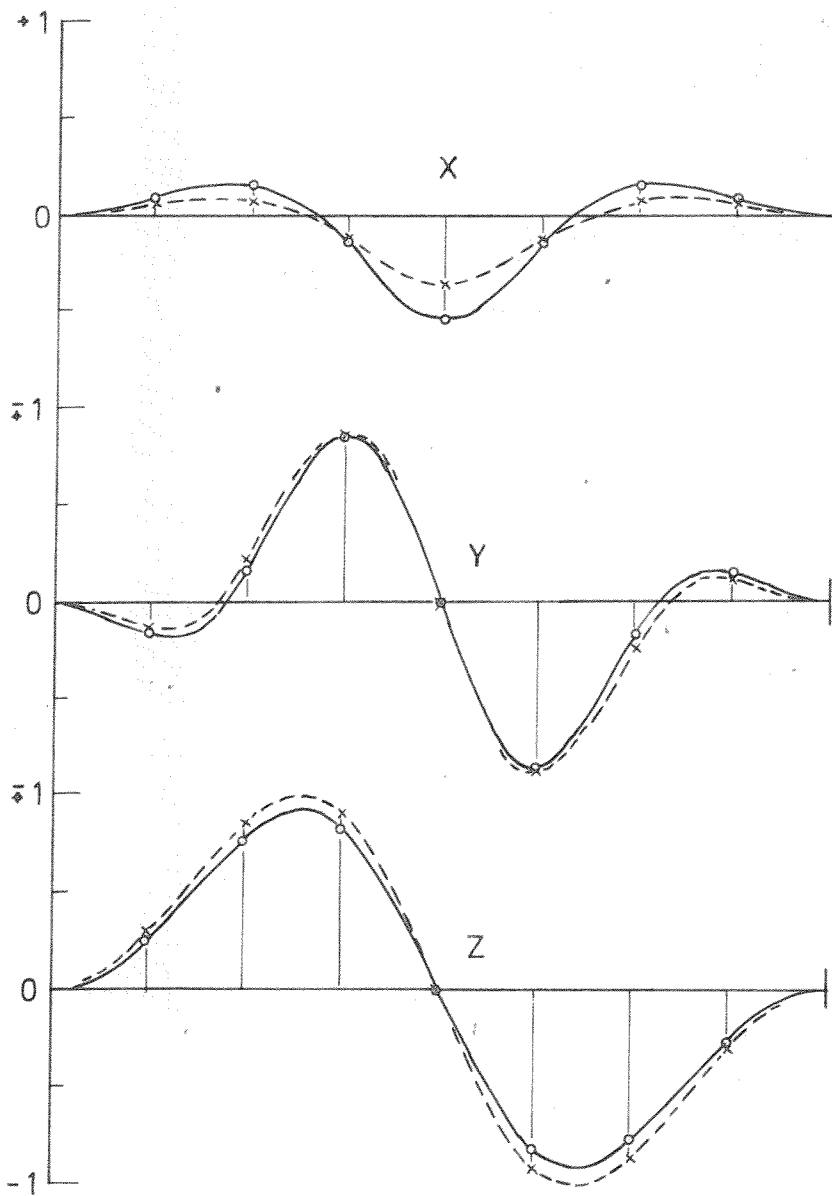
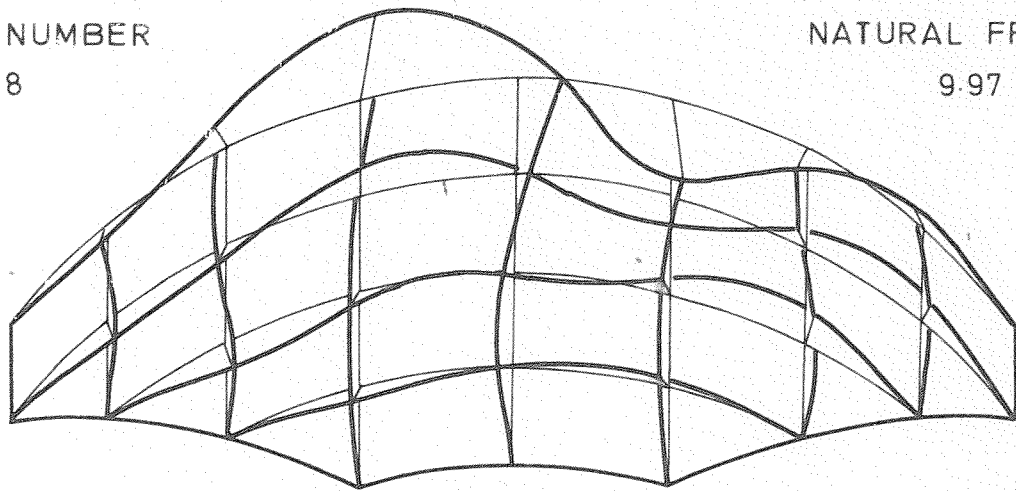
Mid Cantilever      Crown  
displacements

—○—○— Water face  
- - x - - x - Air face

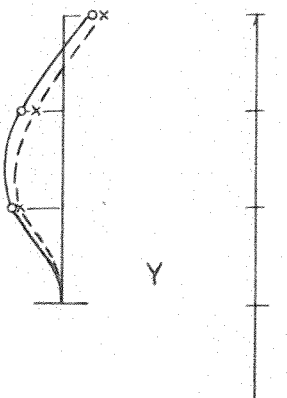
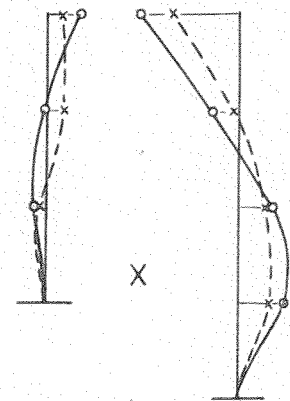
Fig.3.9. Seventh mode of vibration of Arch Dam Type-5

MODE NUMBER  
8

NATURAL FREQUENCY  
9.97 Hz



Deflections of top arch



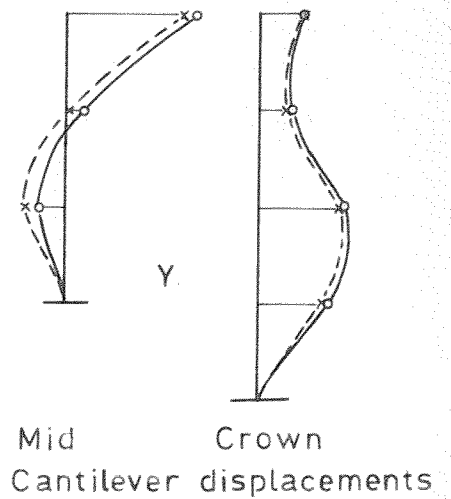
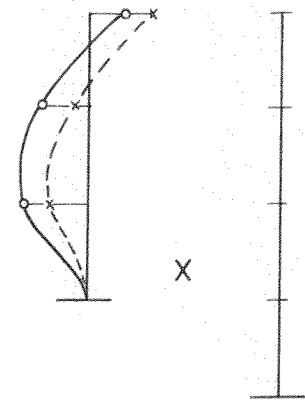
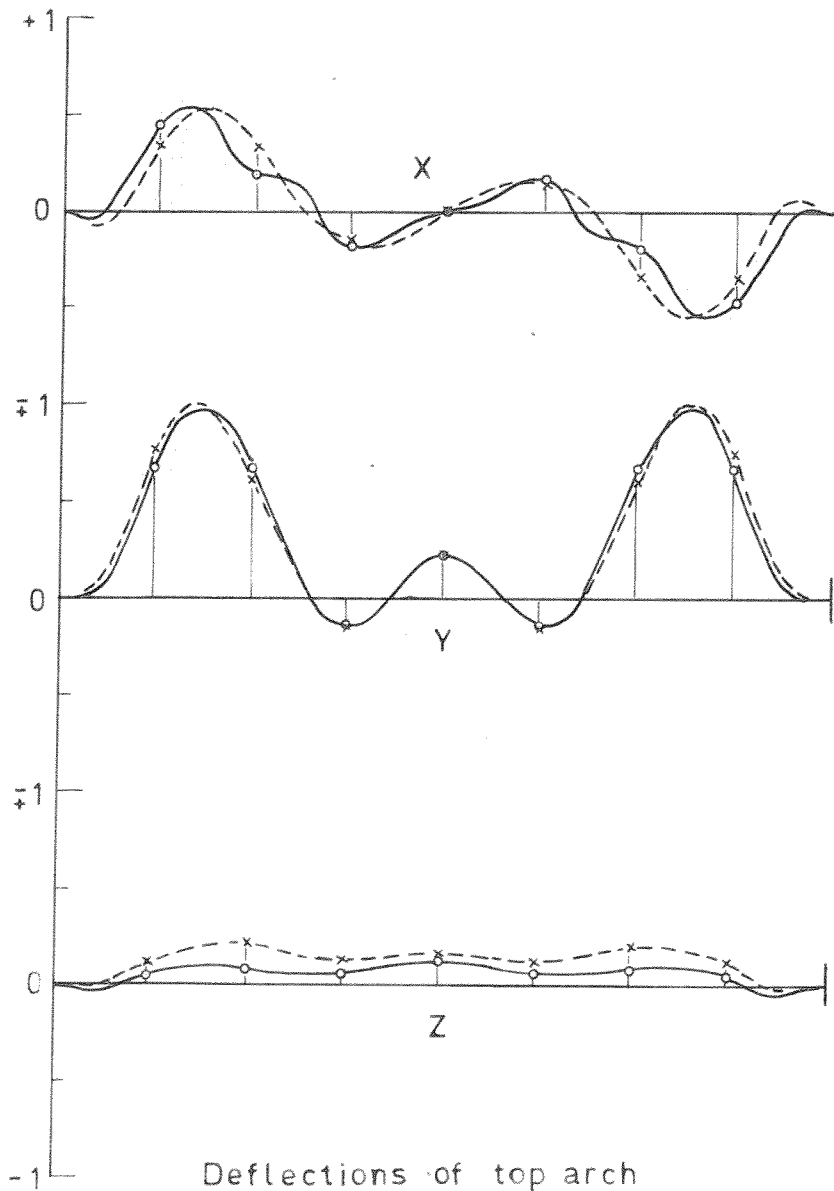
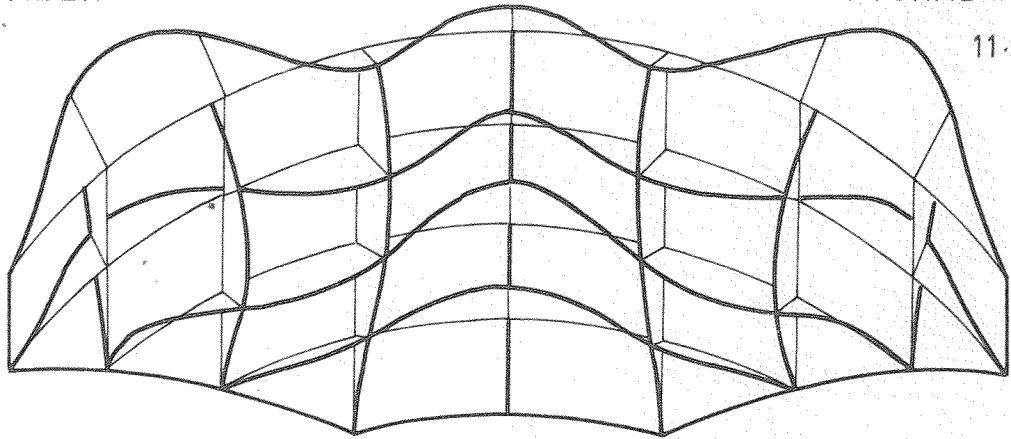
Mid                      Crown  
Cantilever displacements

—○—○— Water face  
-x---x- Air face

Fig.3.10. Eighth mode of vibration of Arch Dam Type-5

MODE NUMBER  
9

NATURAL FREQUENCY  
11.67 Hz

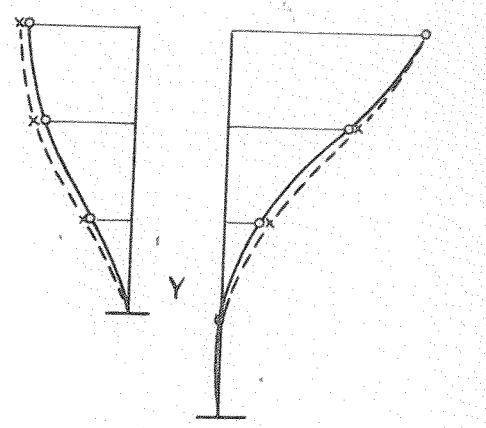
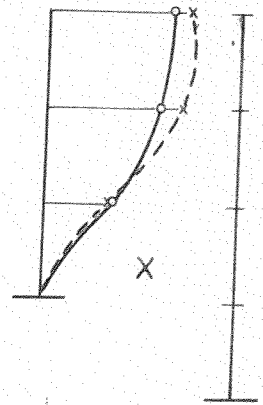
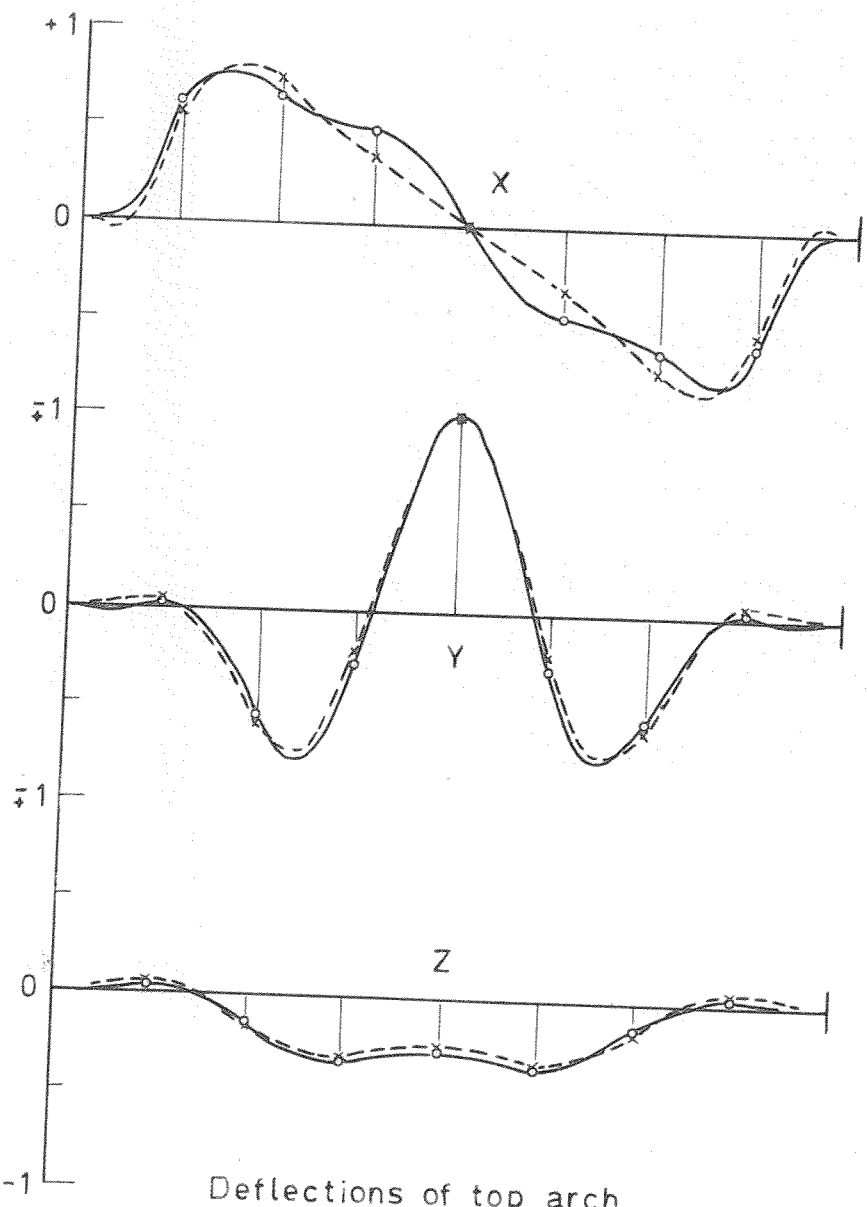
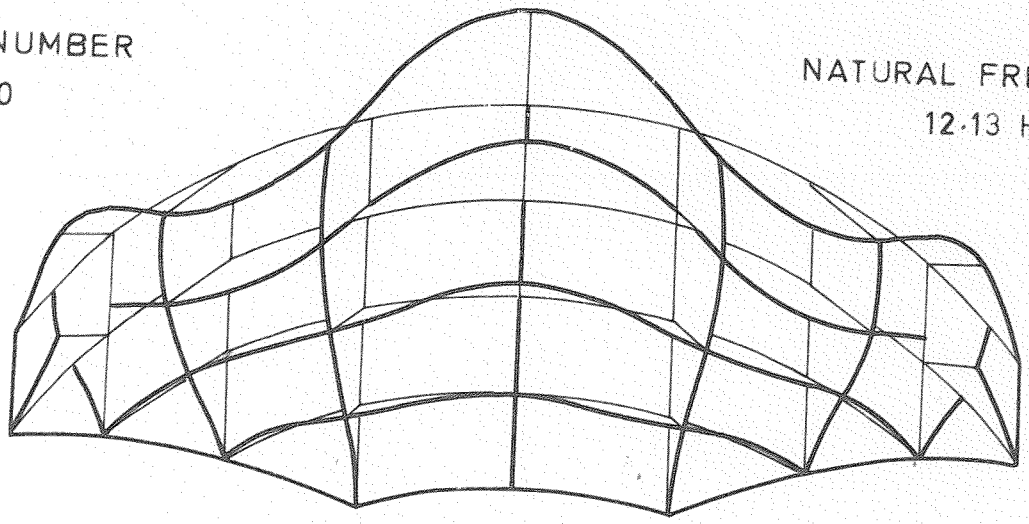


—○—○— Water face  
-x---x- Air face

Fig.3.11. Ninth mode of vibration of Arch Dam Type-5

MODE NUMBER  
10

NATURAL FREQUENCY  
12.13 Hz



Mid      Crown  
Cantilever displacements

—○—○— Water face  
-x---x- Air face

Fig.3.12. Tenth mode of vibration of Arch Dam Type-5

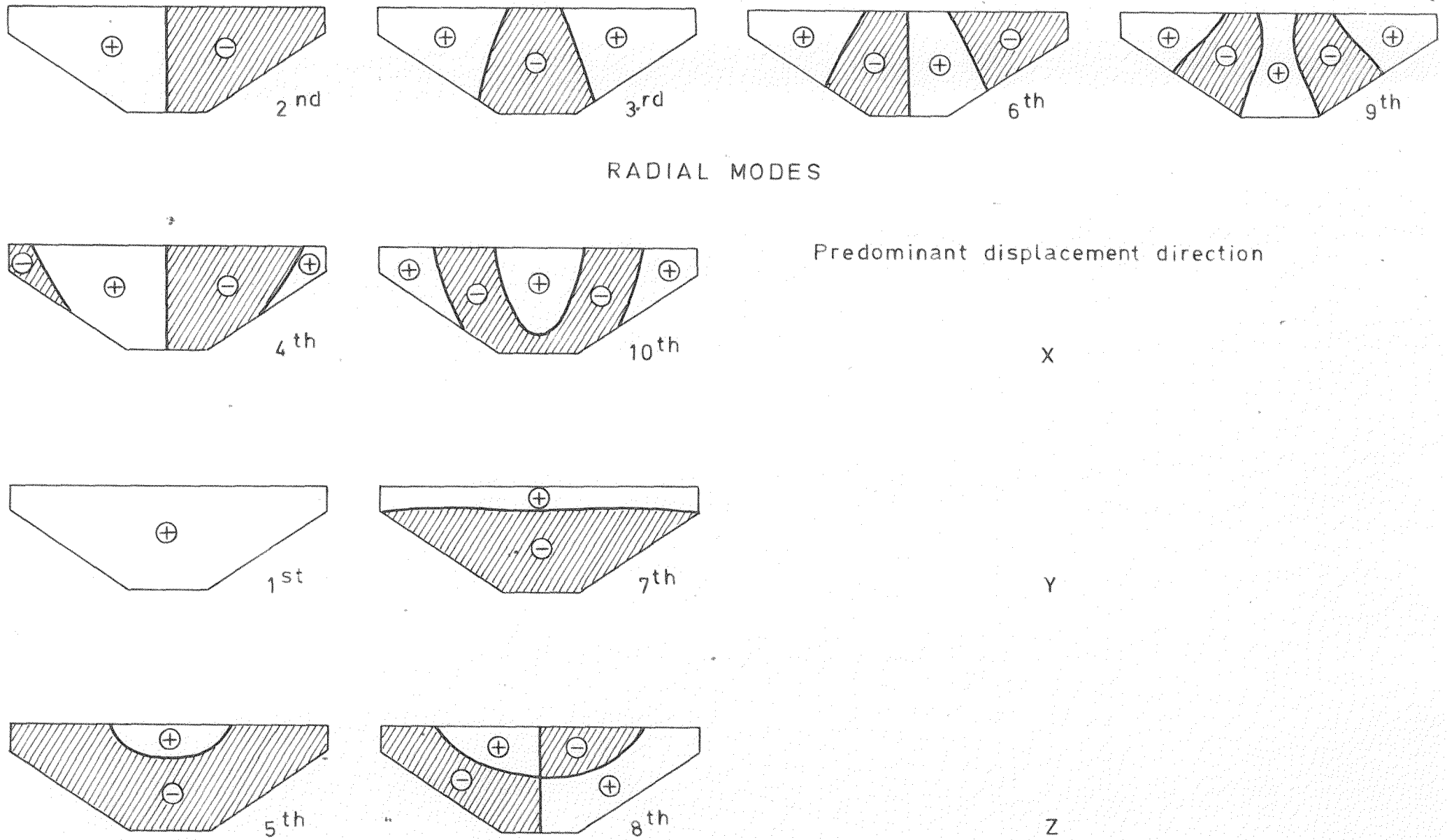


Fig.3.13. Modal lines of horizontal deflections for each mode of vibration of Arch Dam Type-5

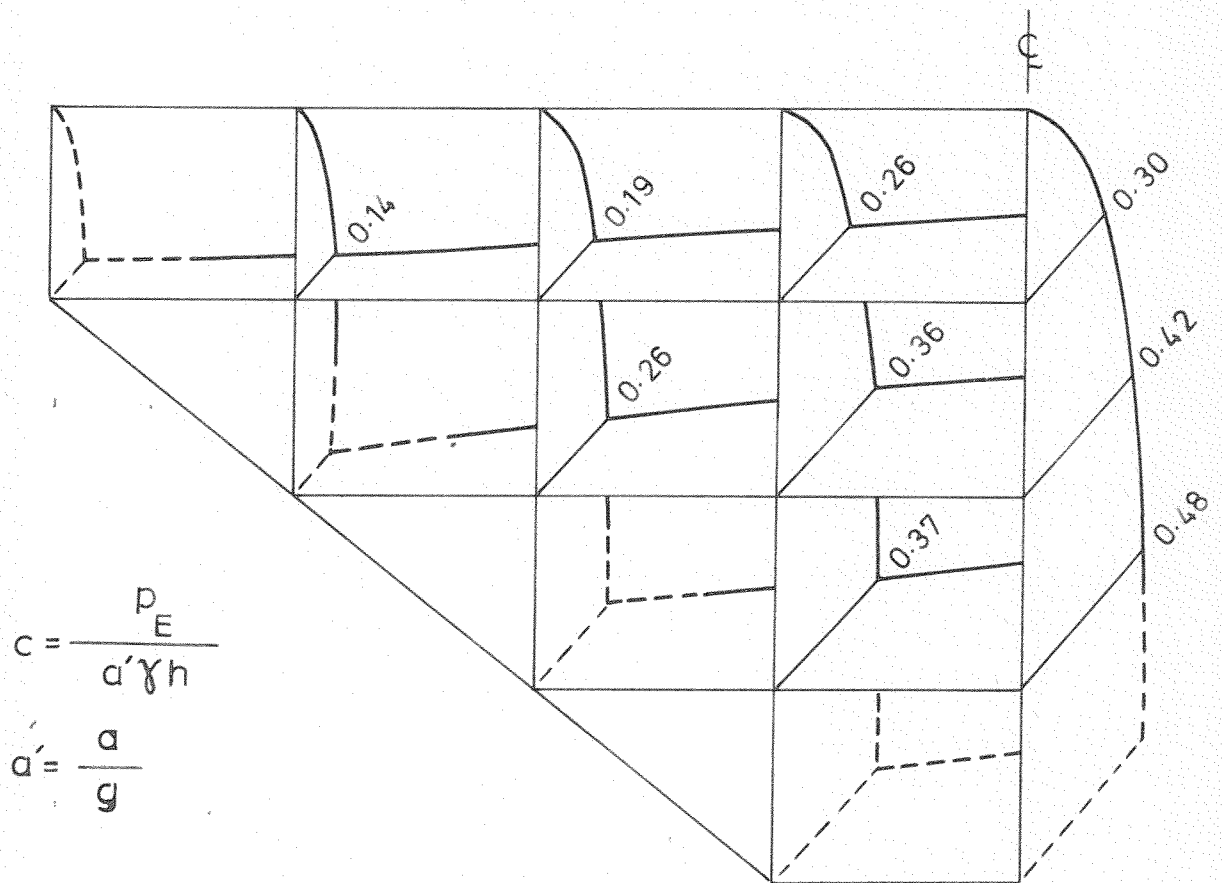


Fig.3.14. Coefficients  $c$ , of radial hydrodynamic pressures  $p_E$ , for uniform upstream acceleration  $a$  (TAYLOR, ref. 23)

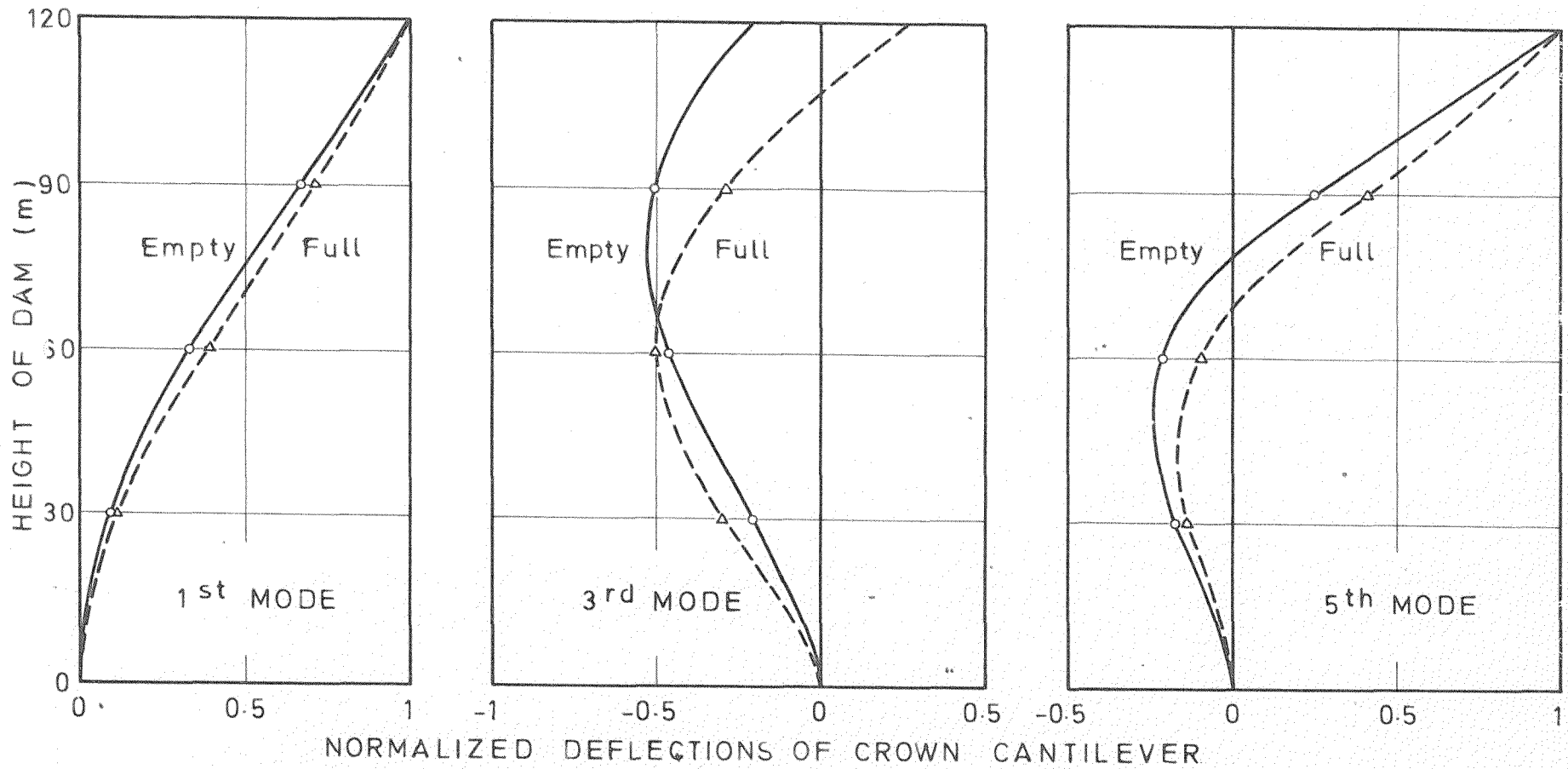


Fig.3.15. Effect of the reservoir water on the mode shapes

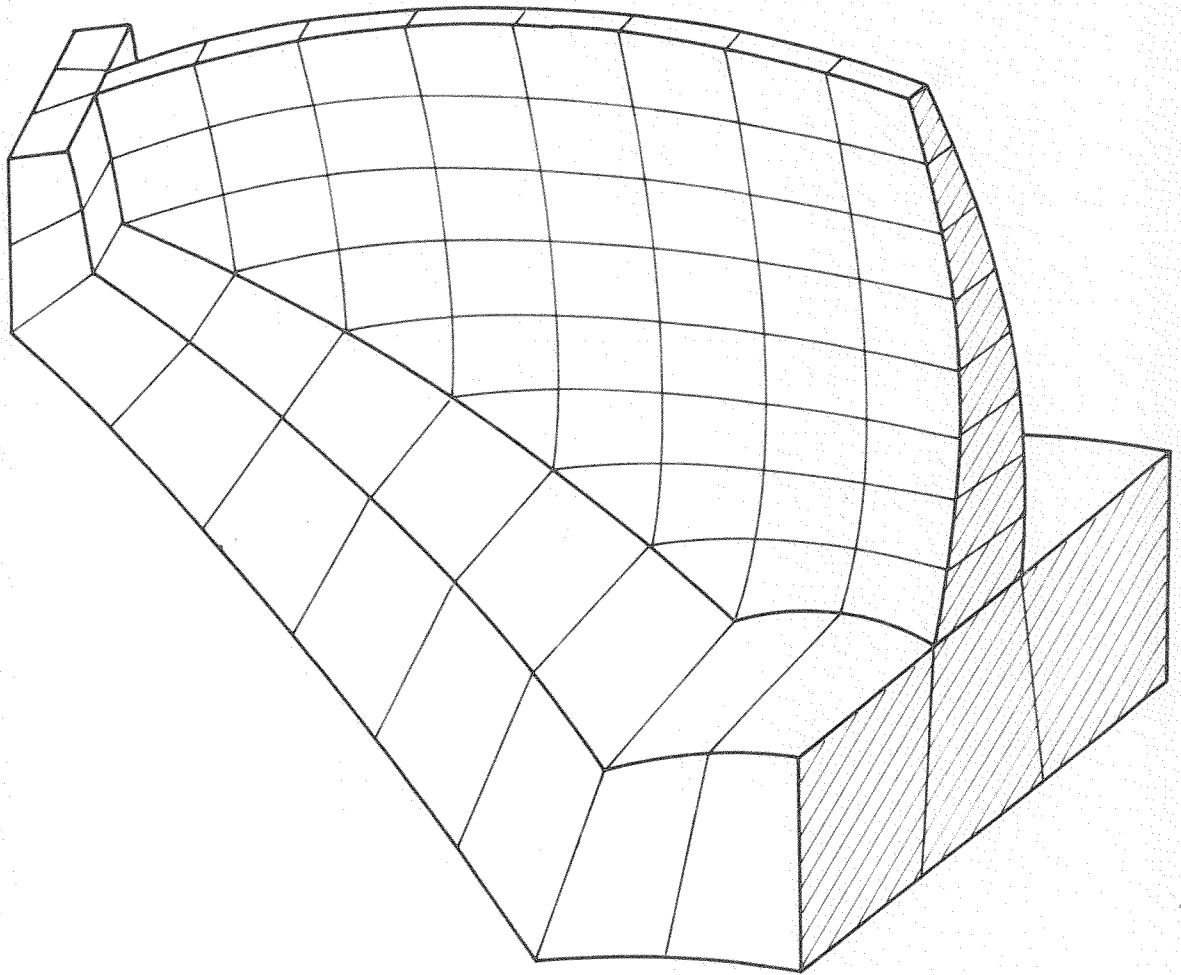


Fig.3.16. Arch dam with its foundation included

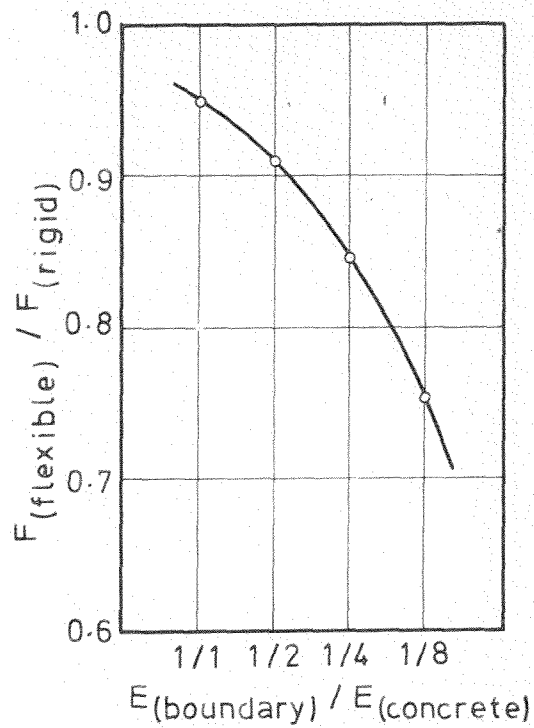


Fig.3.17. Effect of the boundary flexibility on the natural frequency of the fundamental mode (reservoir empty)

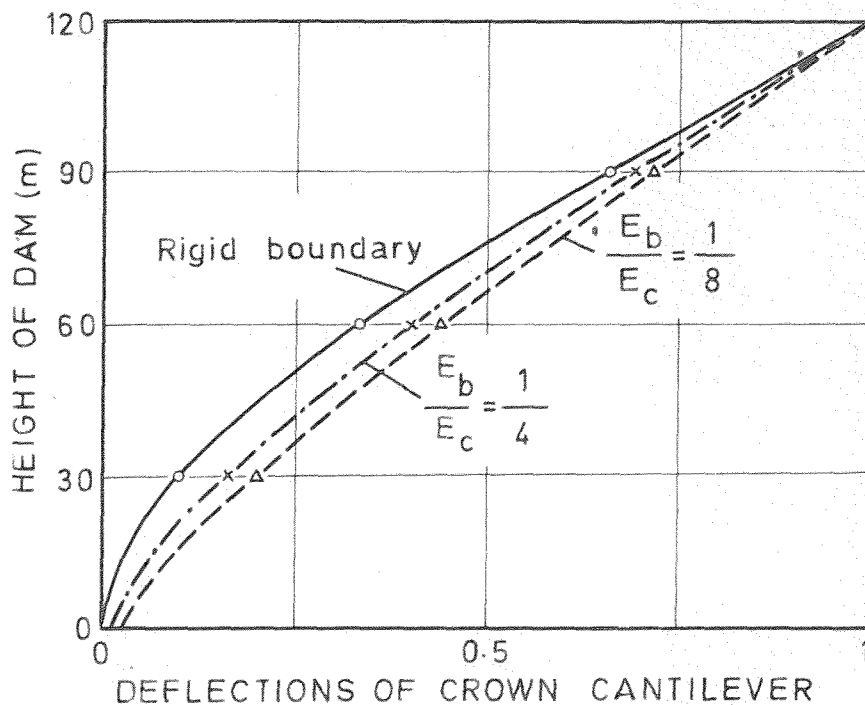


Fig.3.18. Effect of the boundary flexibility on the shape of the fundamental mode (reservoir empty)

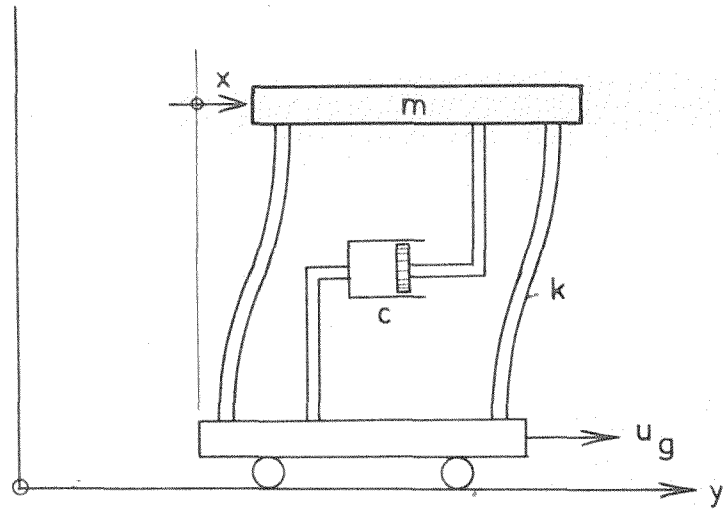


Fig.4.1. Single degree of freedom system subjected to base excitation

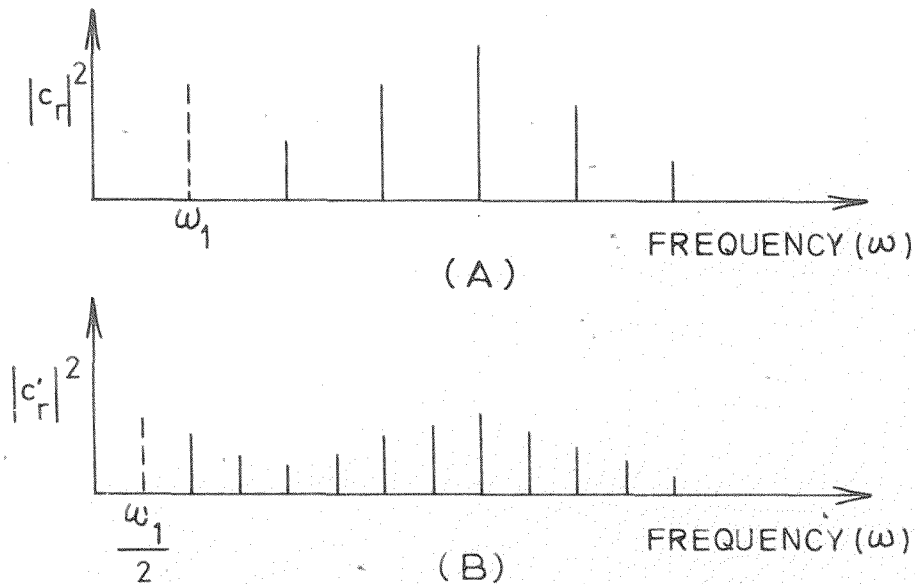


Fig.4.2. Spectrum analysis of random vibration, as determined from a magnetic tape loop. In (A) the period is  $T$ . In (B) the period is  $2T$ .

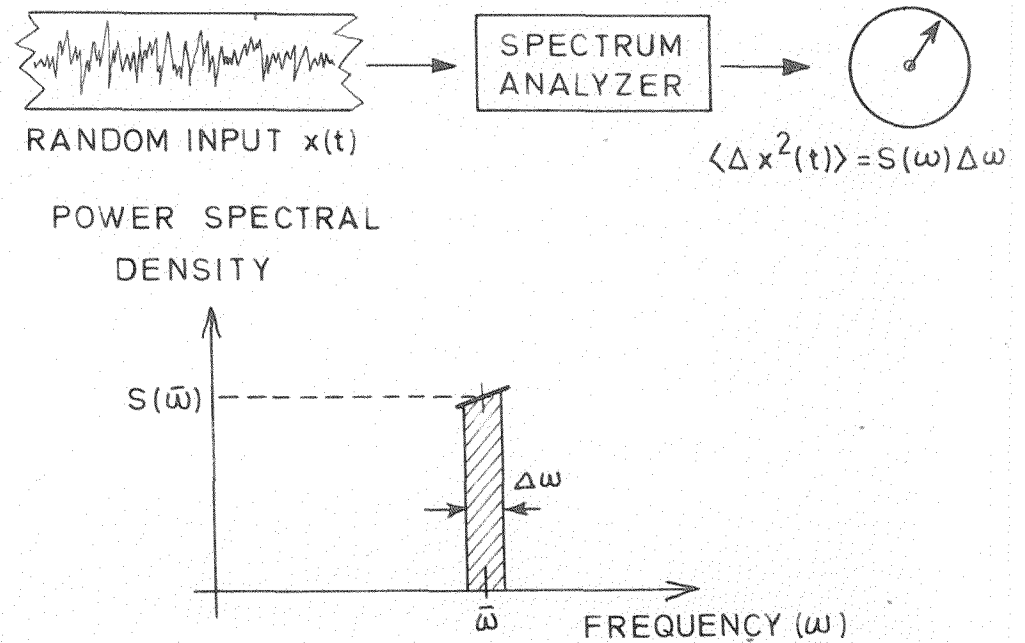


Fig.4.3. The experimental determination of the power spectral density  $S(\omega)$  of a random function  $x(t)$

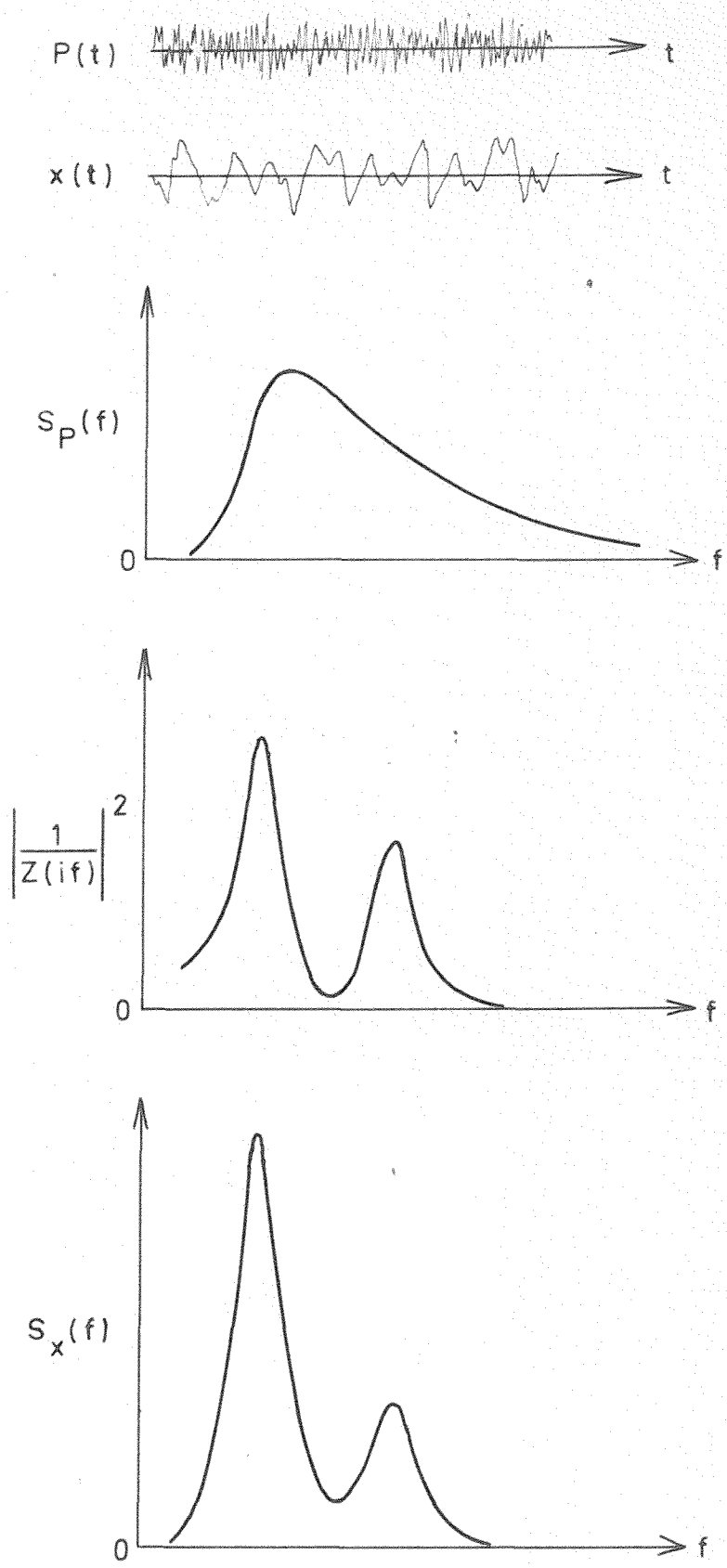


Fig.4.4. Illustration of the relationship between the input (force) and output (displacement) power spectral densities and the receptance of the system

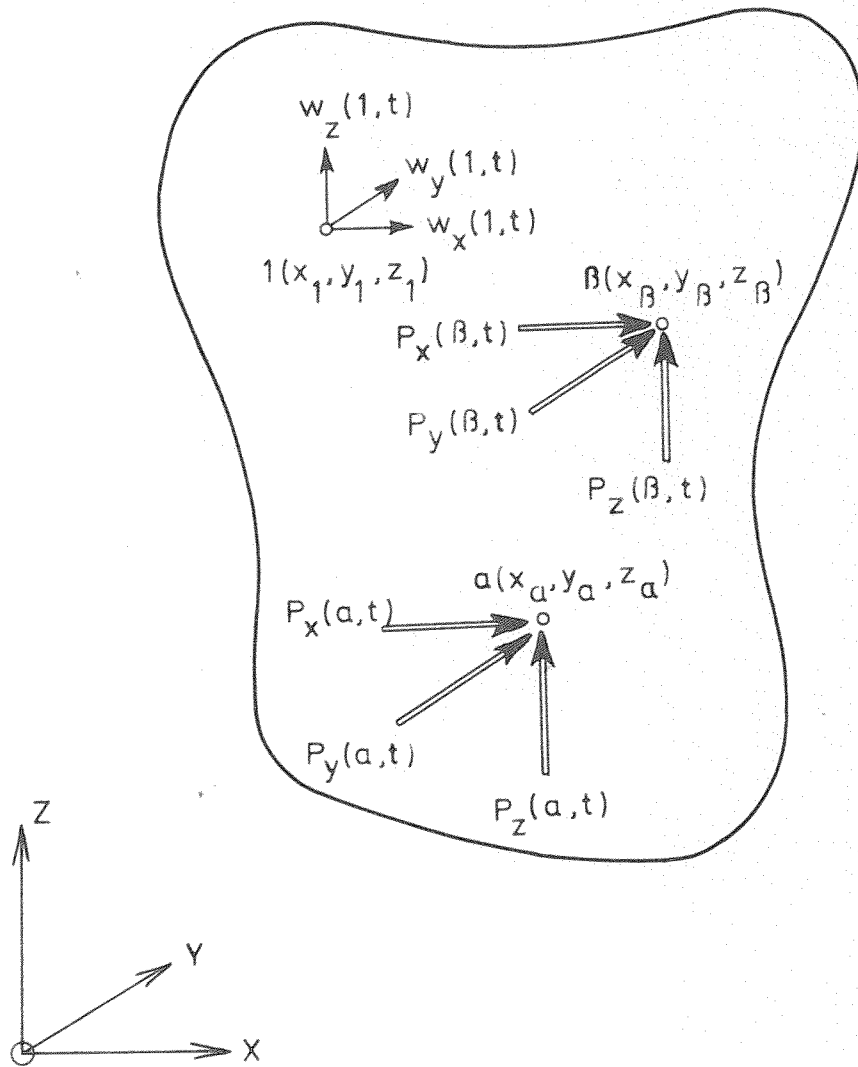


Fig.4.5. Three dimensional solid structure, acting forces and displacements

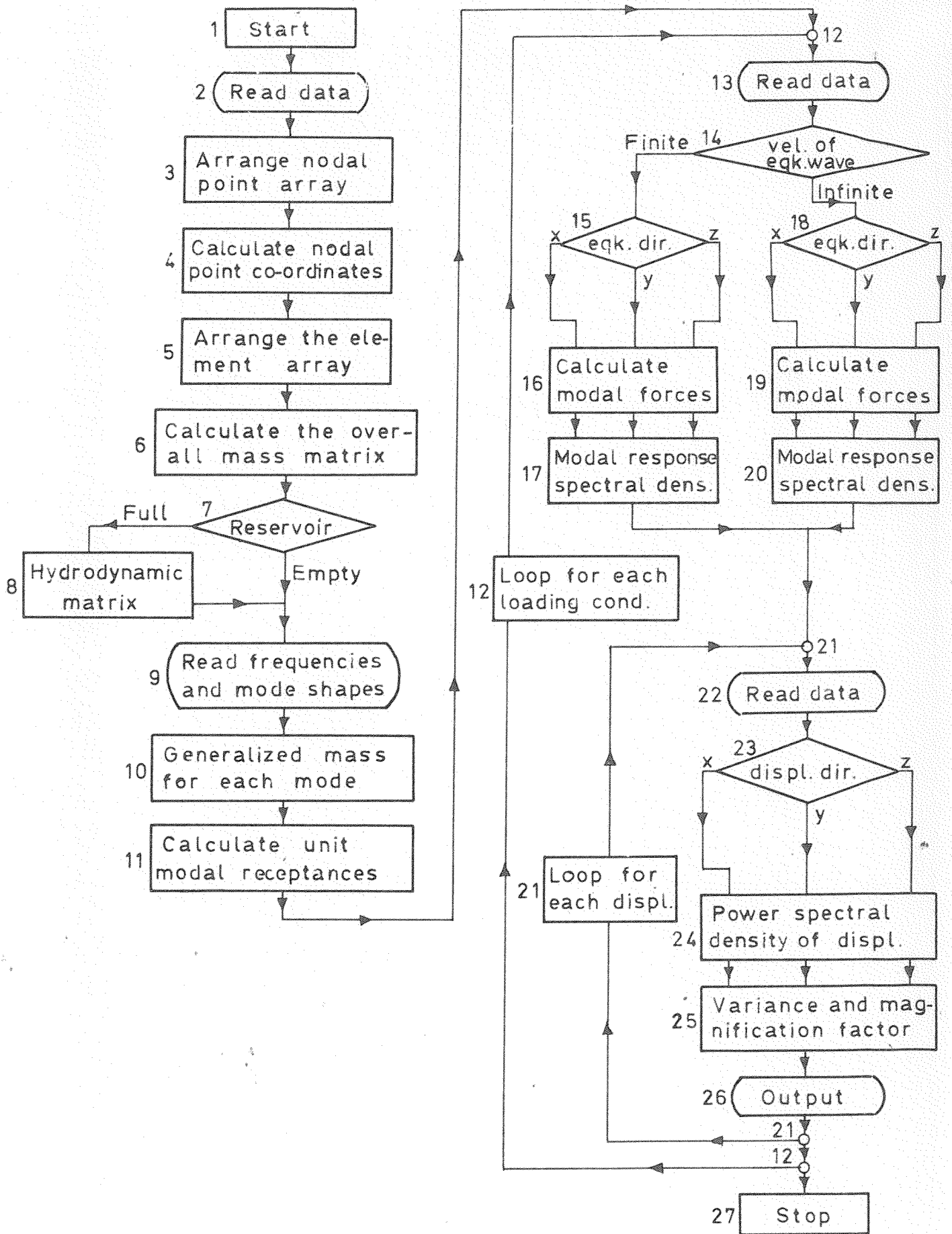


Fig.4.6. Flow diagram for calculating response by power spectral density method

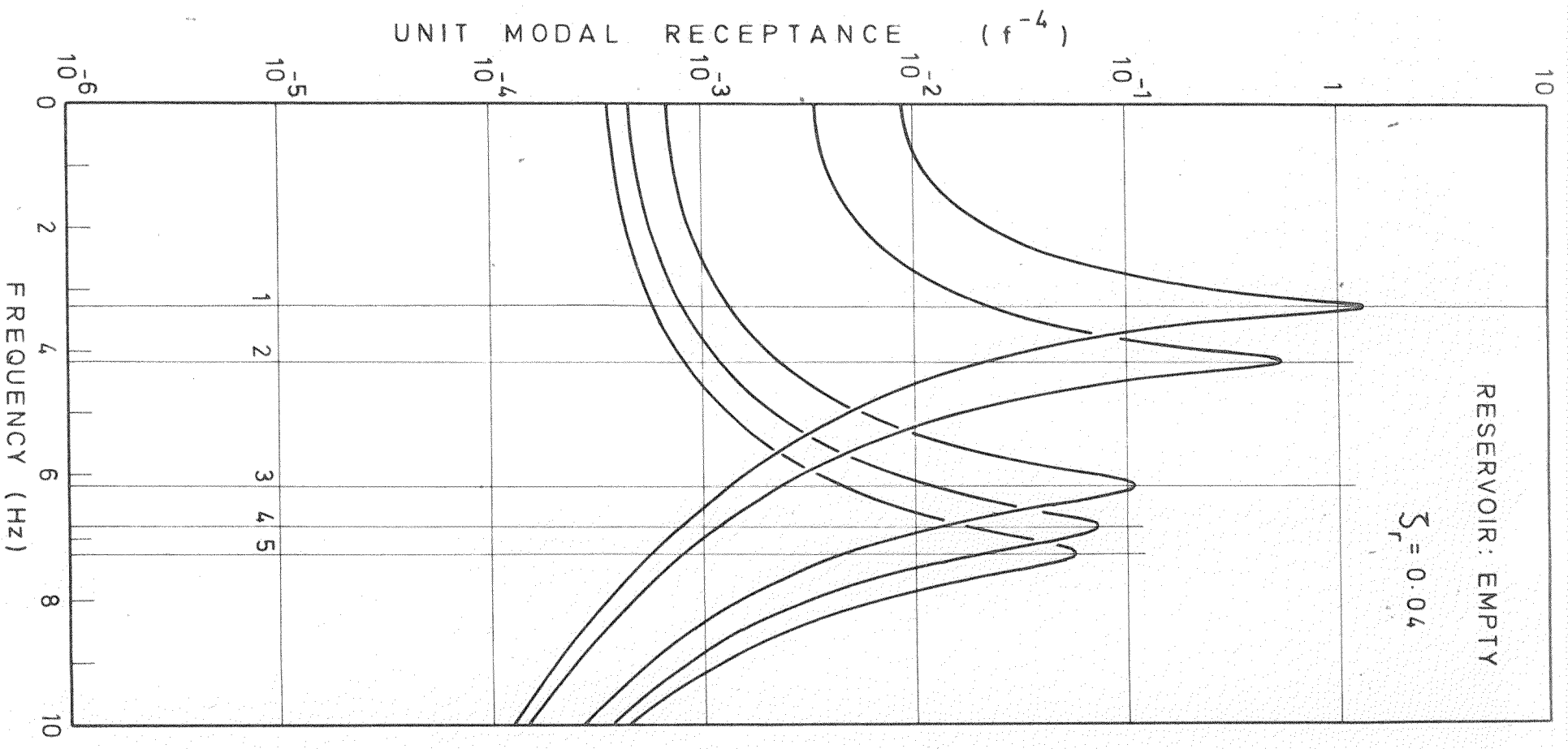


Fig.4.7. Unit modal receptances given by Eq.(4.95)

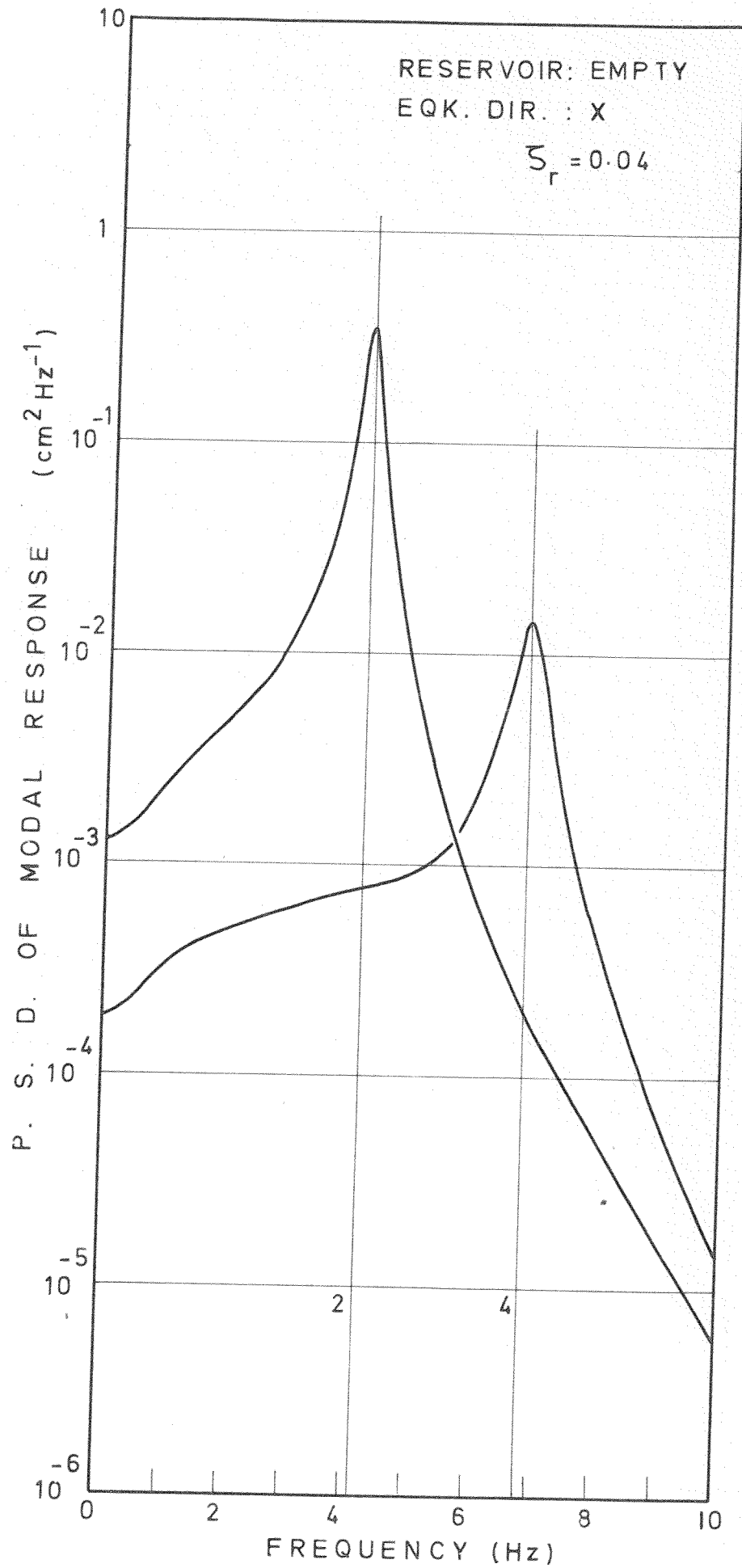


Fig.4.8. Modal response P.S.D., force direction X

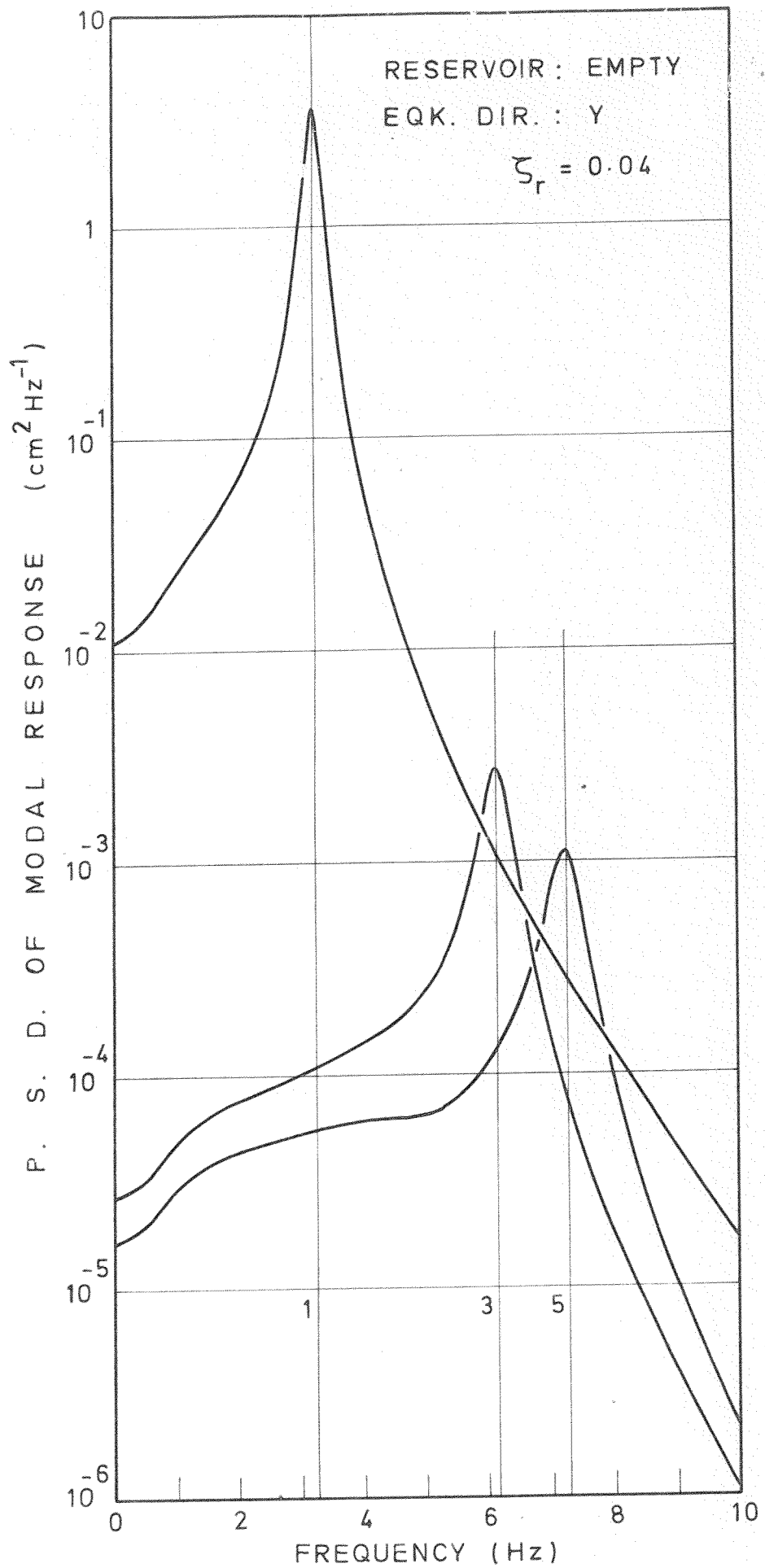


Fig.4.9. Modal response P. S. D., force direction Y

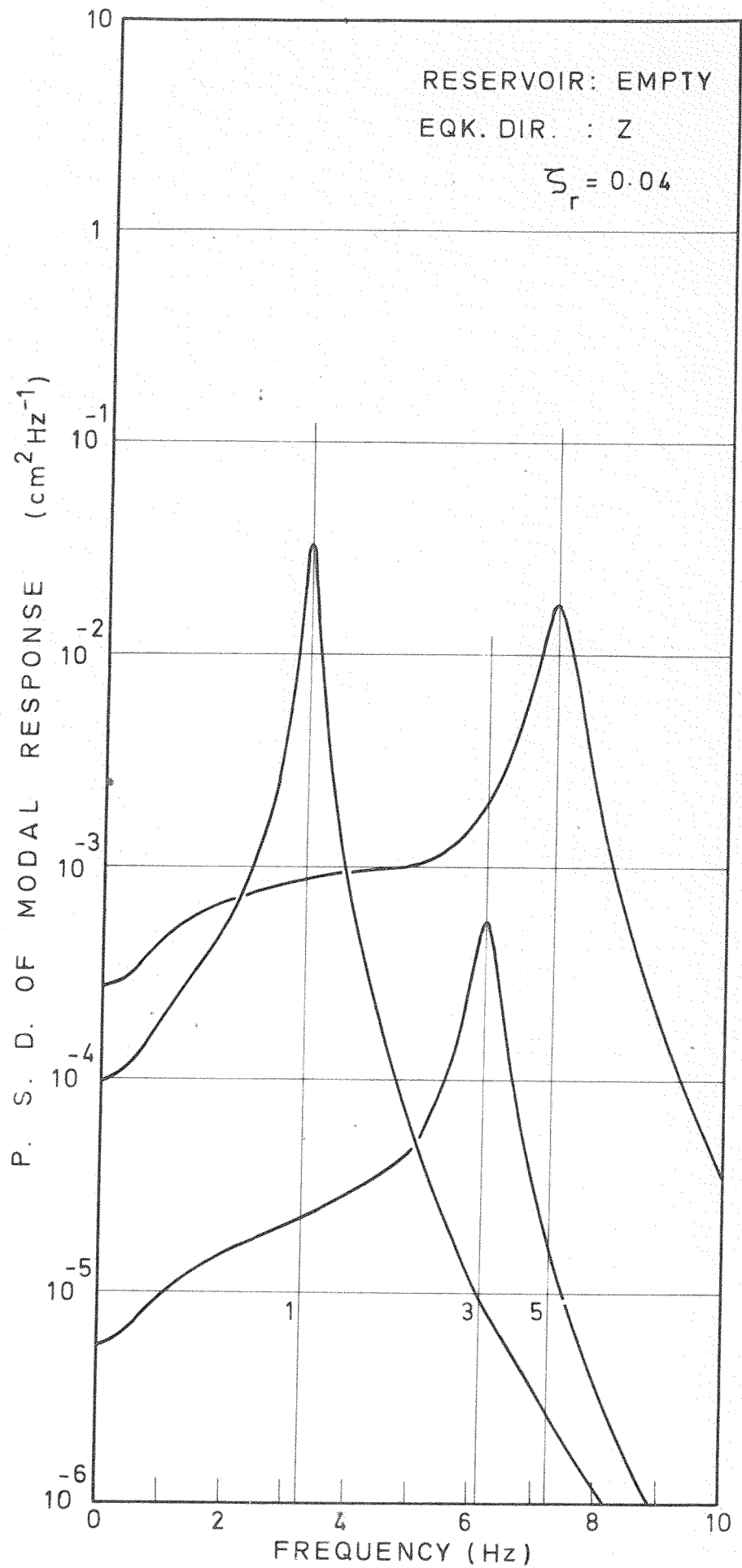


Fig.4.10. Modal response P.S.D., force direction Z

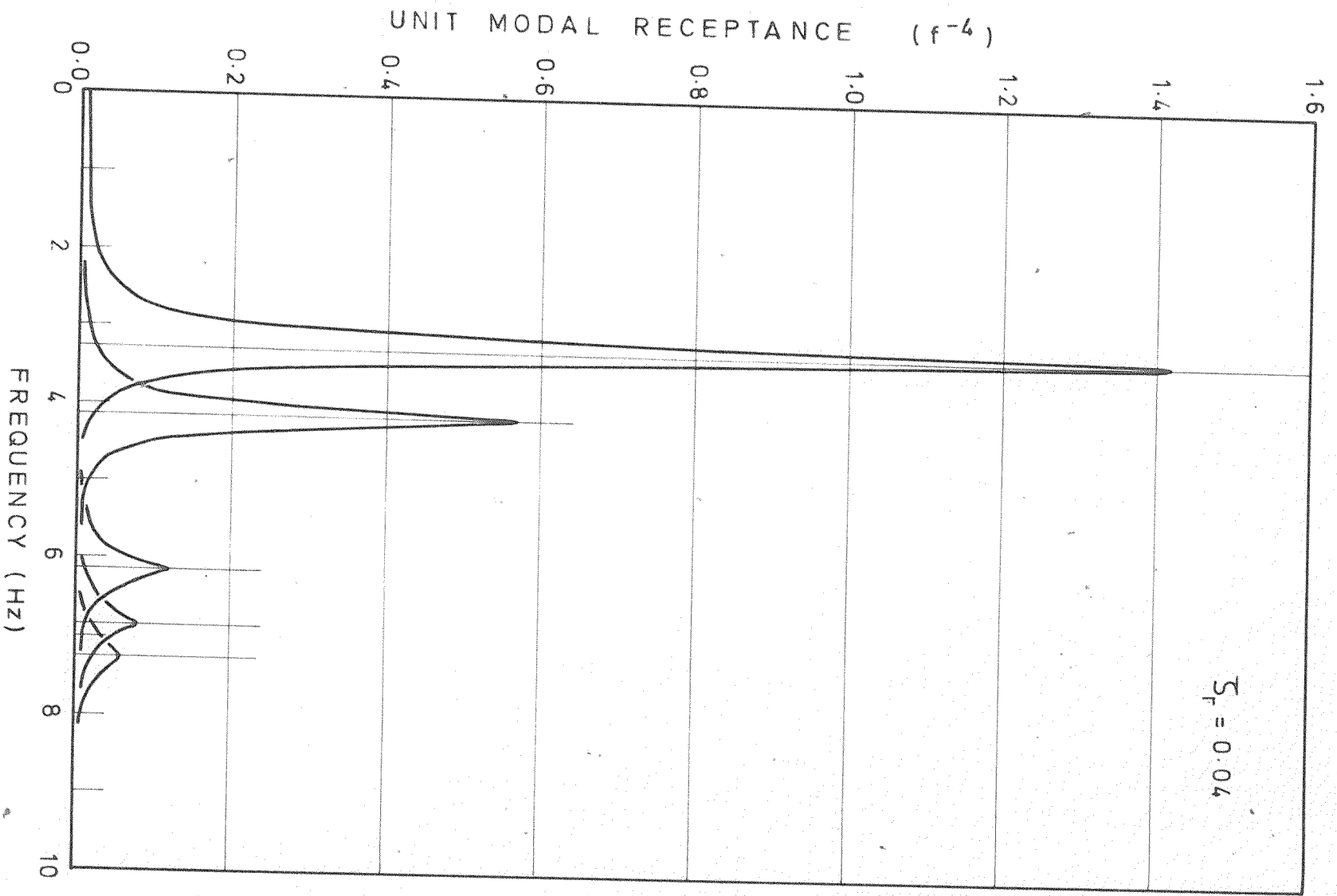


Fig.4.11. Unit modal receptances in linear scale

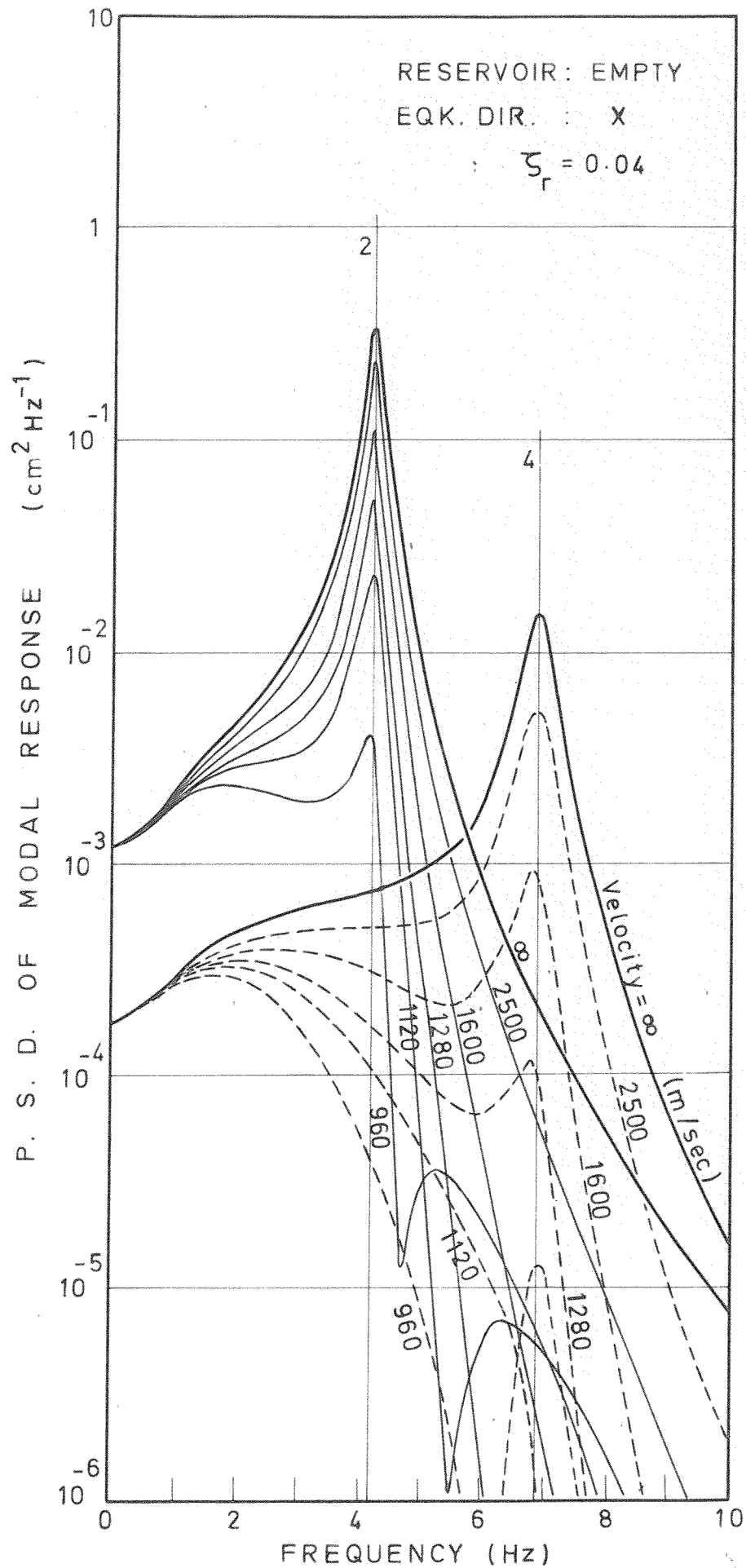


Fig.4.12. Effect of earthquake wave velocity on modal response, force direction X

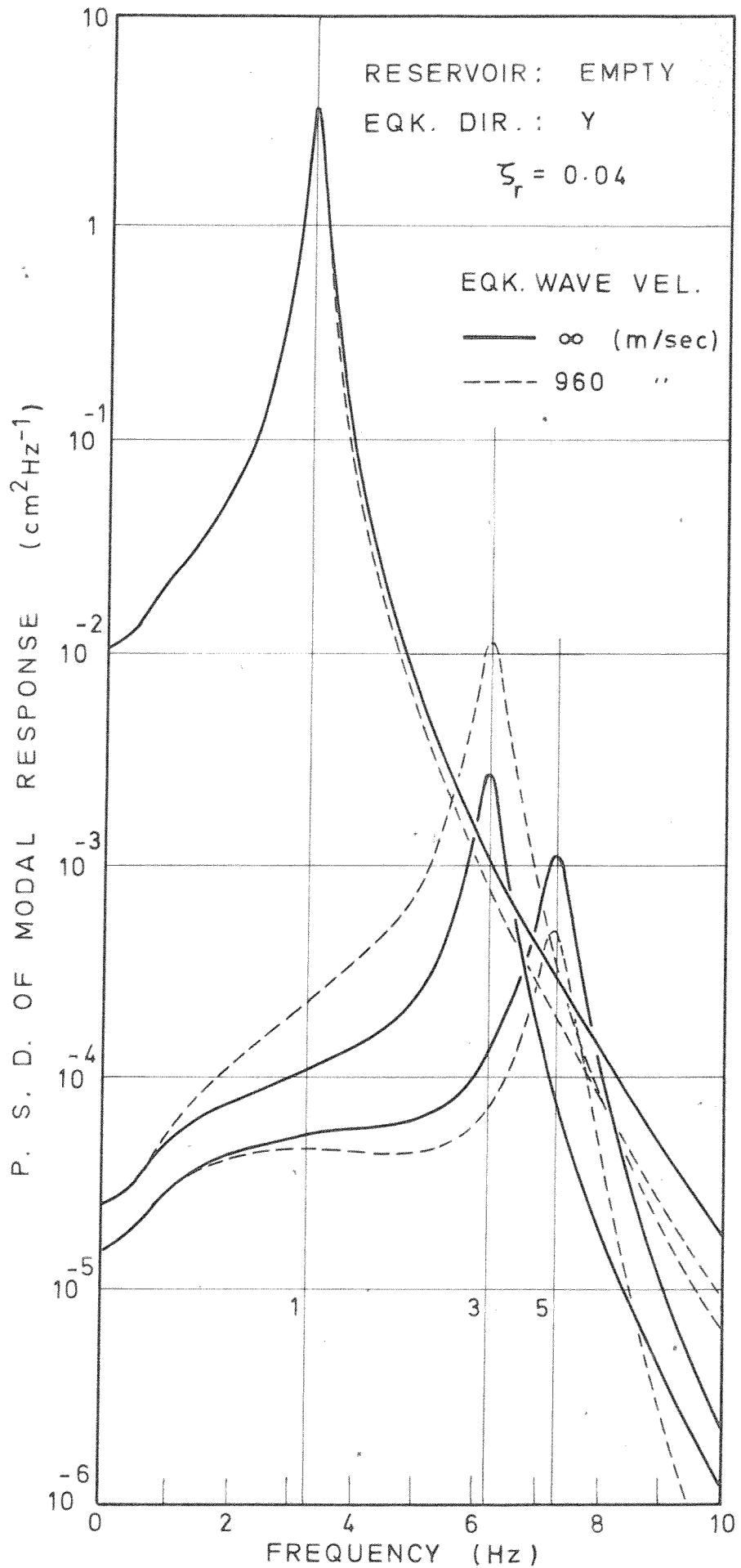


Fig. 4.13. Effect of earthquake wave velocity on modal response, force direction Y

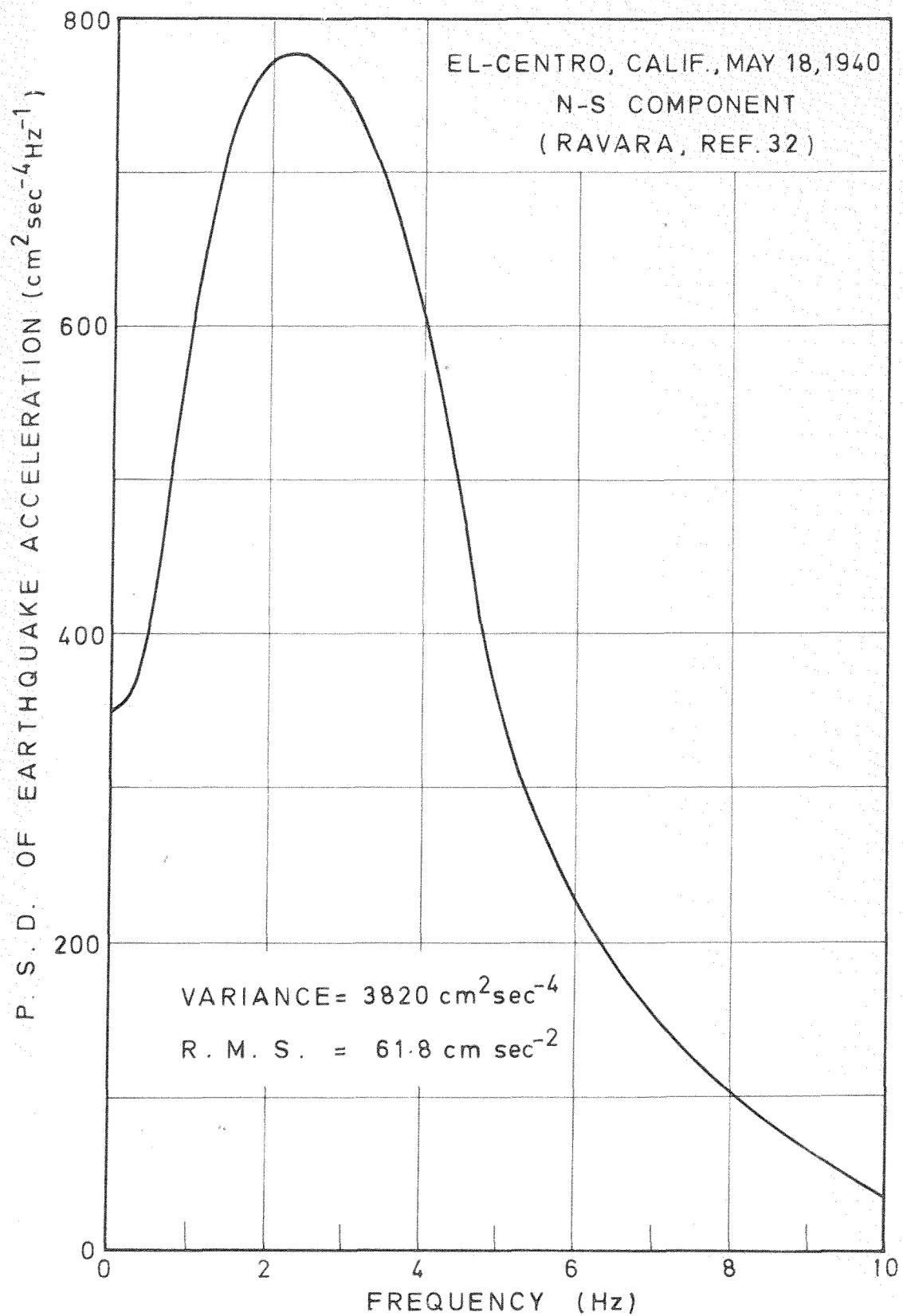


Fig. 5.1. Smoothed power spectrum of earthquake acceleration. Referred to El-Centro, 1940 intensity

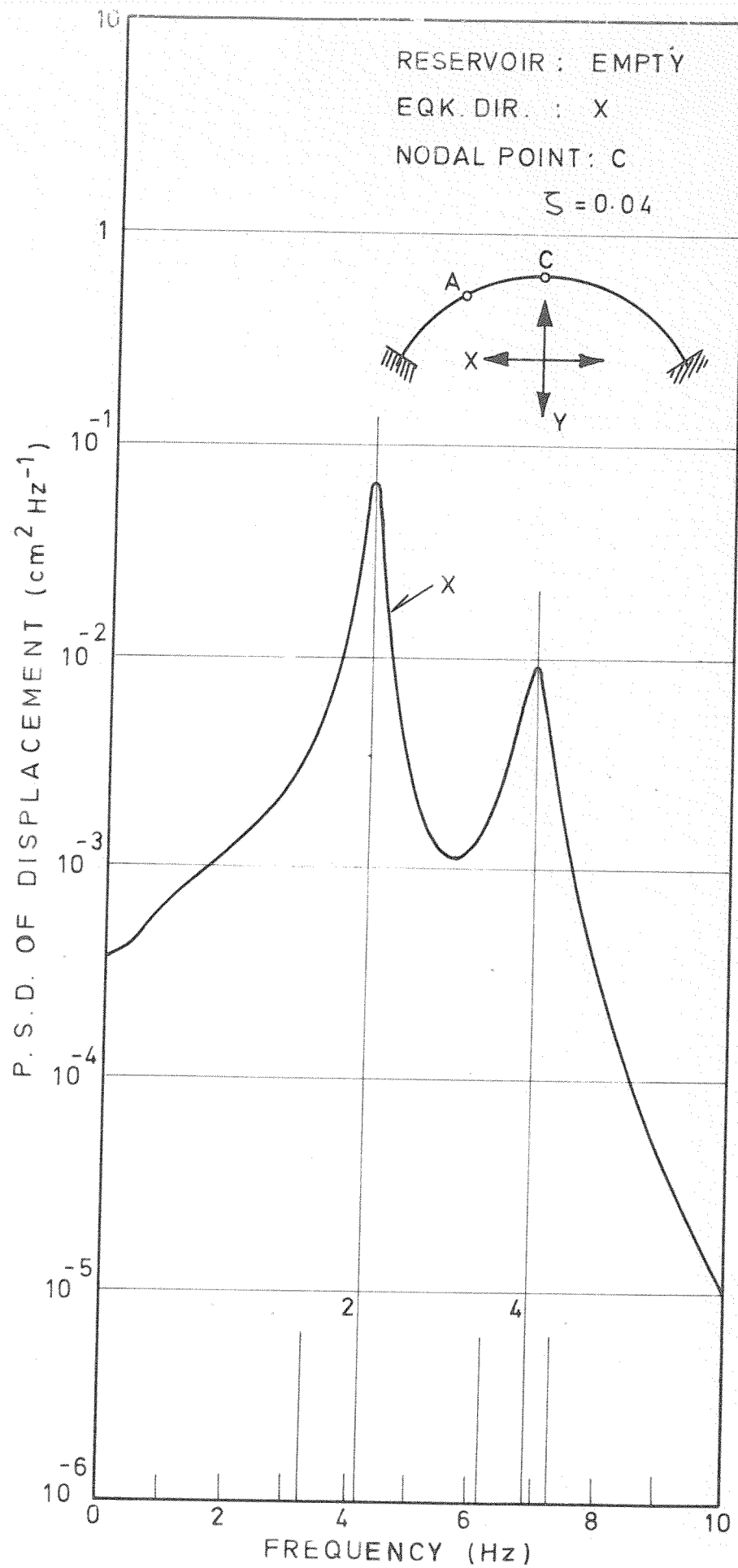


Fig. 5.2. Response power spectrum

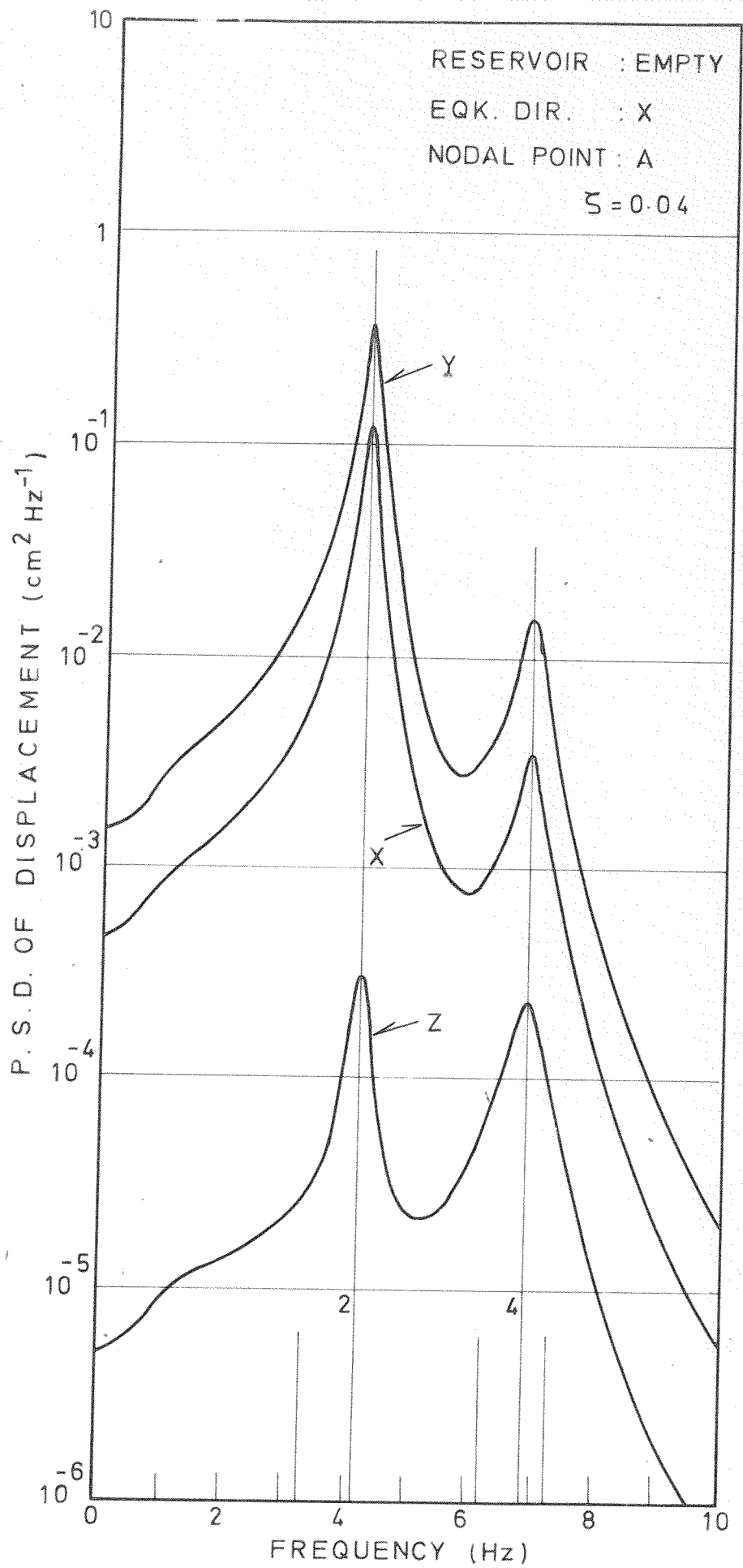


Fig.5.3. Response power spectrum

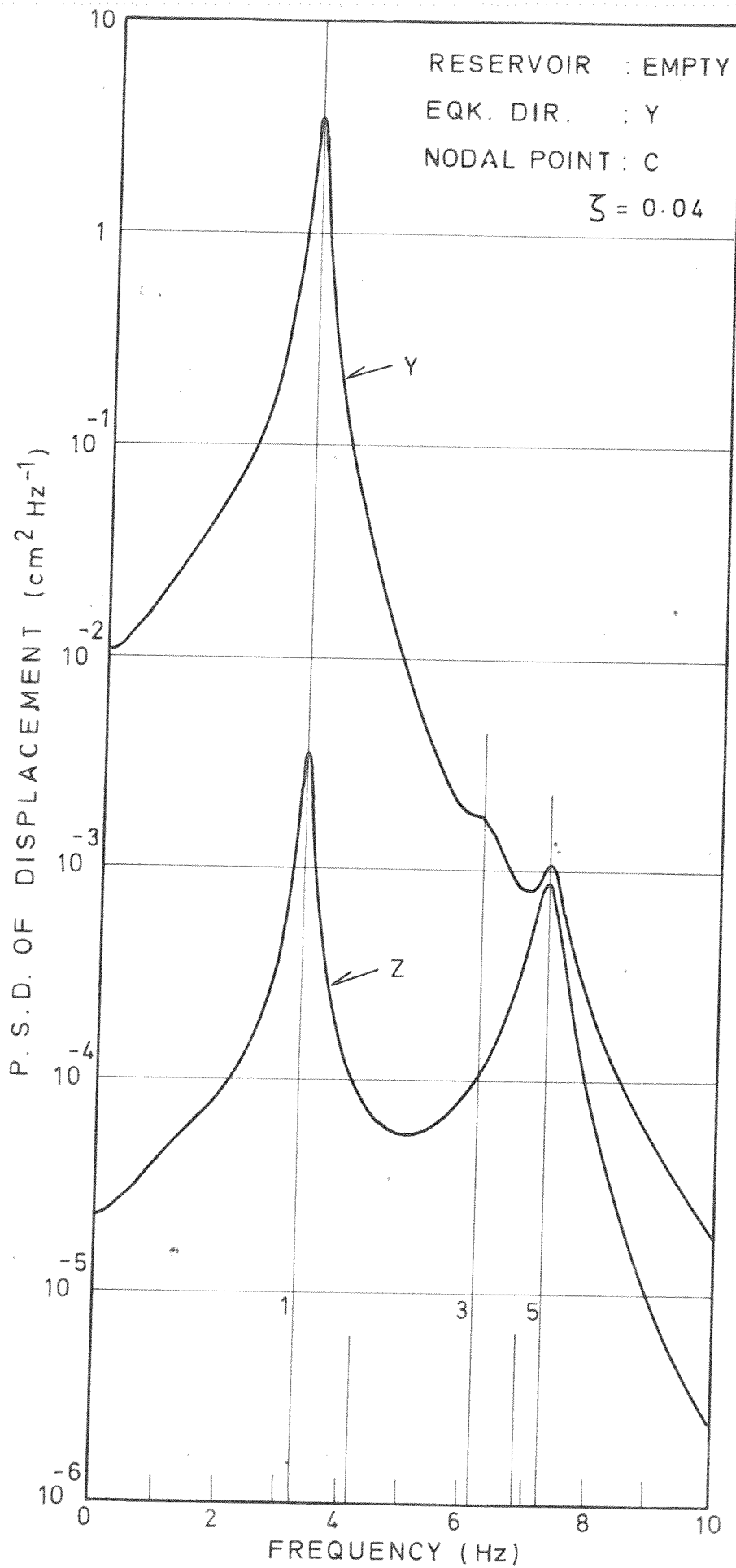


Fig.5.4. Response power spectrum

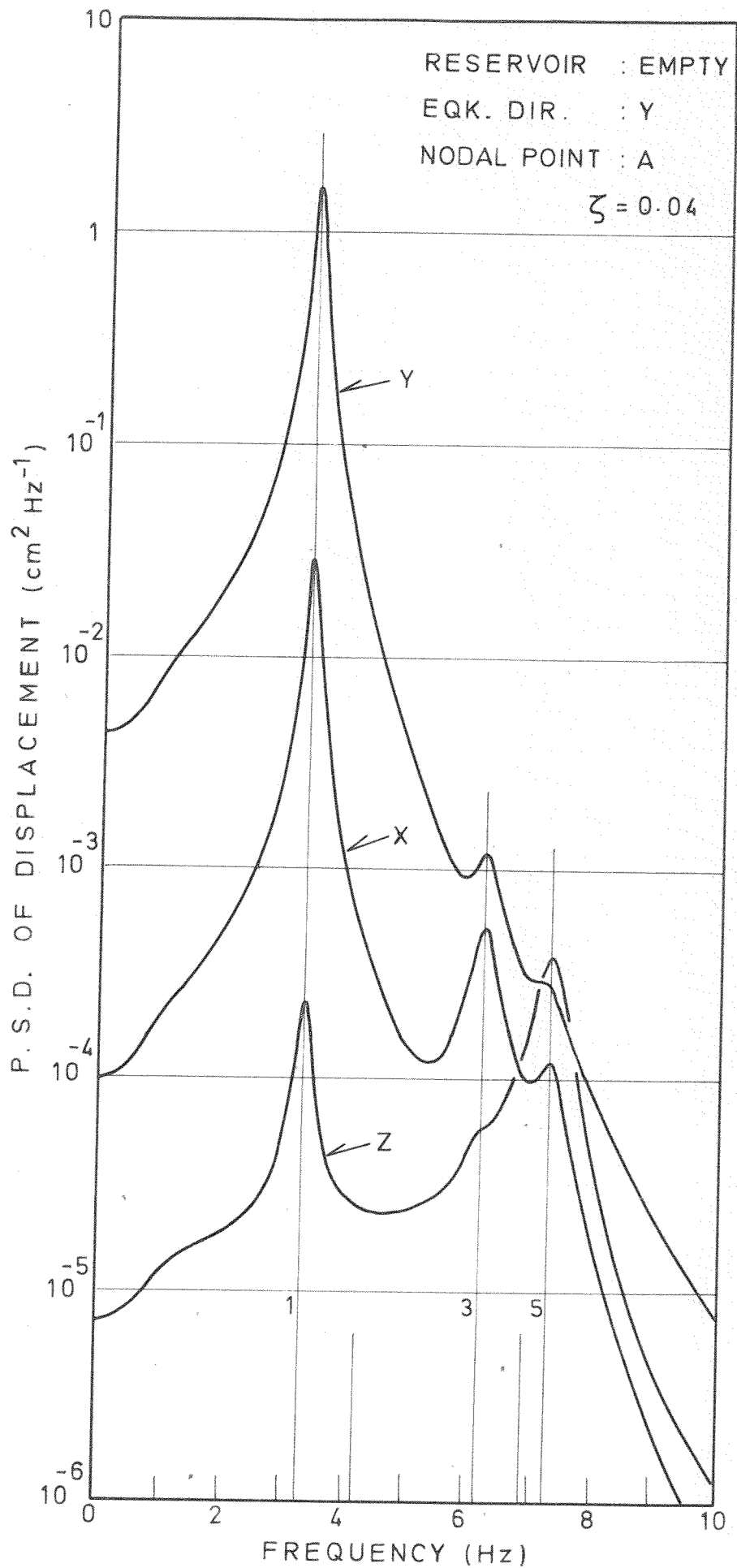


Fig. 5.5. Response power spectrum

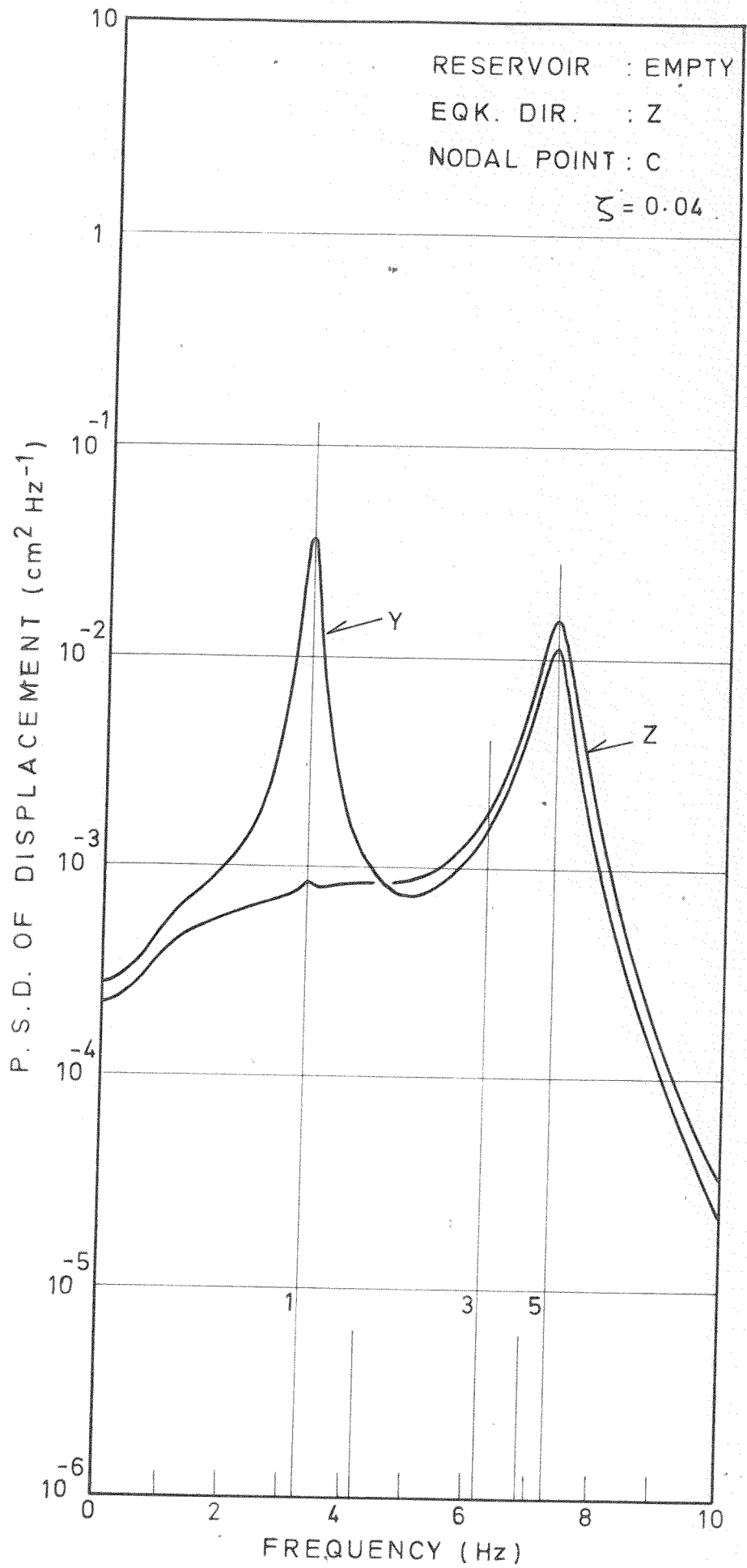


Fig.5.6. Response power spectrum

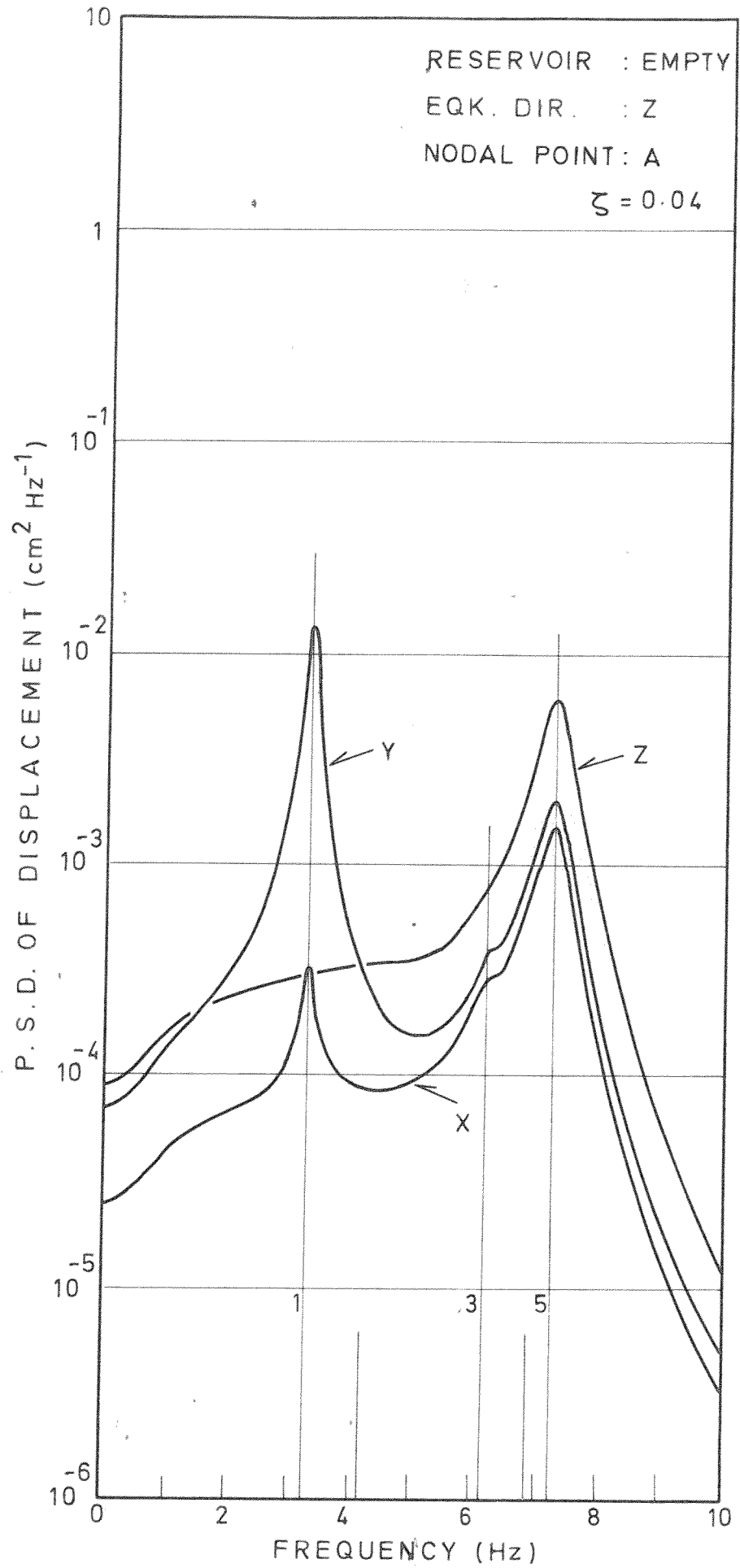


Fig. 5.7. Response power spectrum

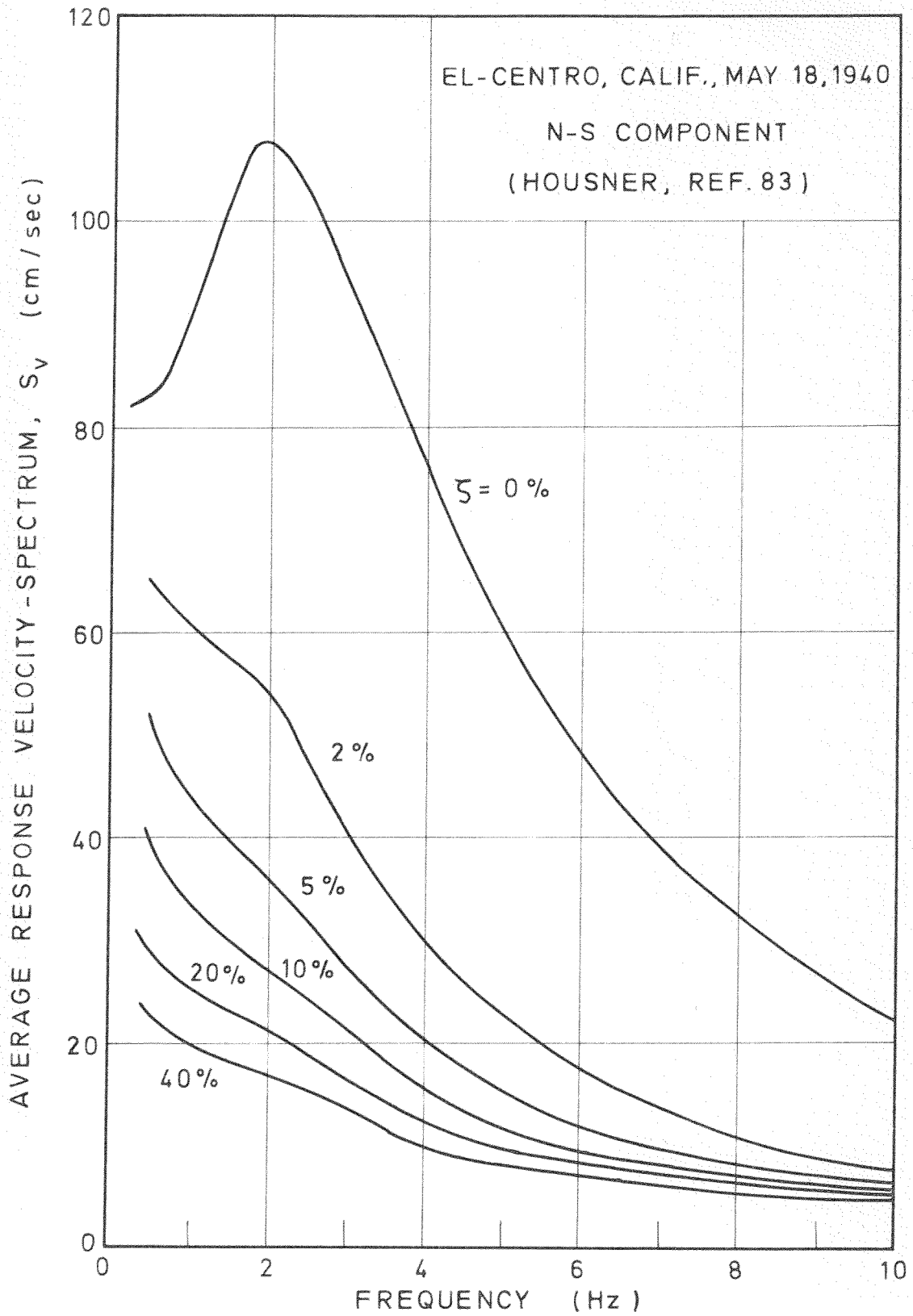


Fig.5.8. Average response velocity spectrum curves  
Intensity of ground motion recorded  
at El-Centro, Calif., 1940.

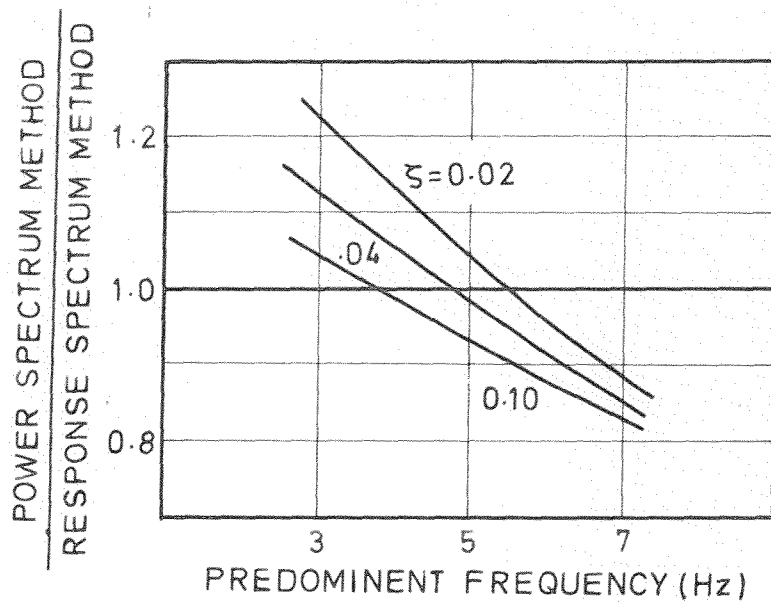


Fig. 5.9. Comparison of the responses obtained by "power" and "response" spectrum methods

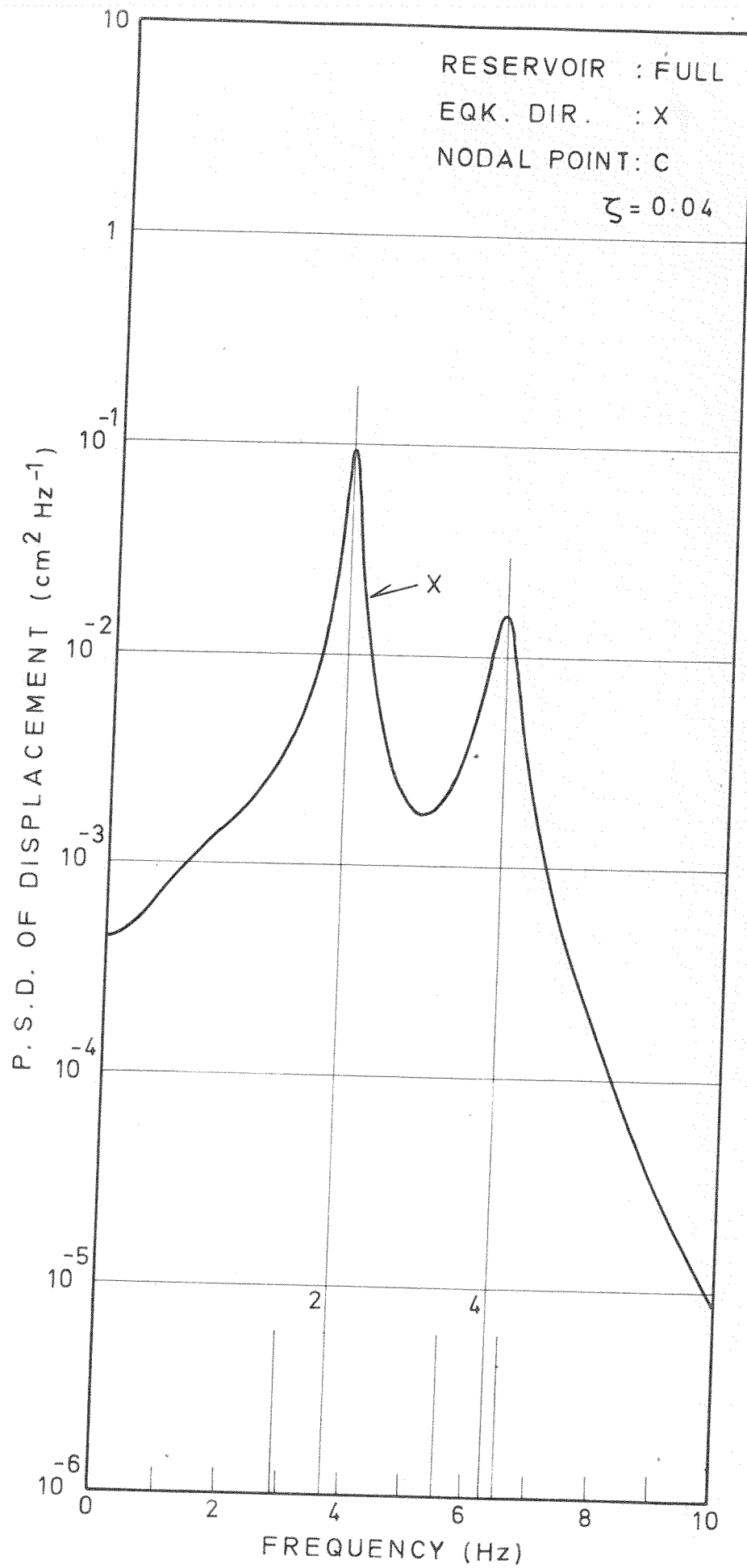


Fig. 5.10. Response power spectrum

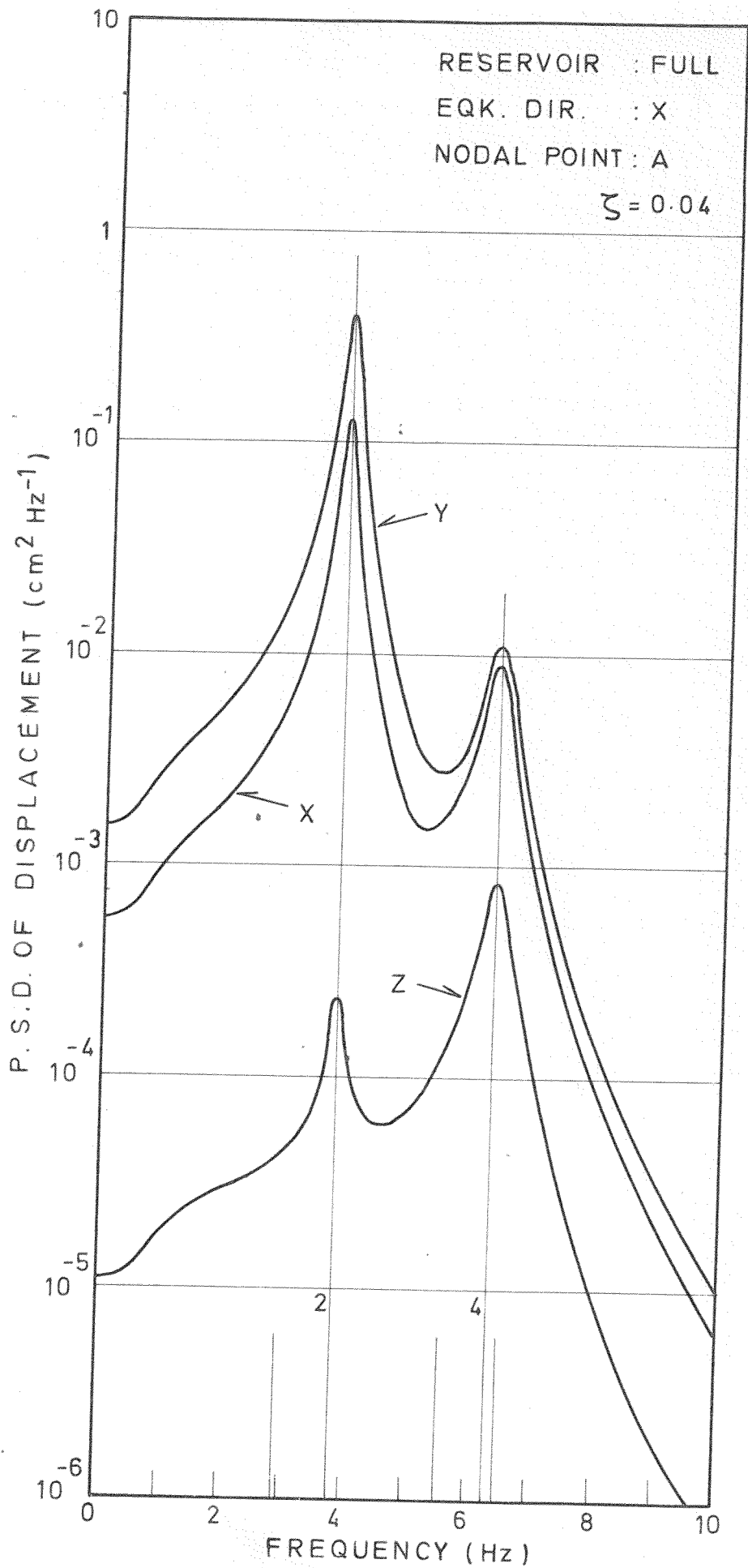


Fig. 5.11. Response power spectrum

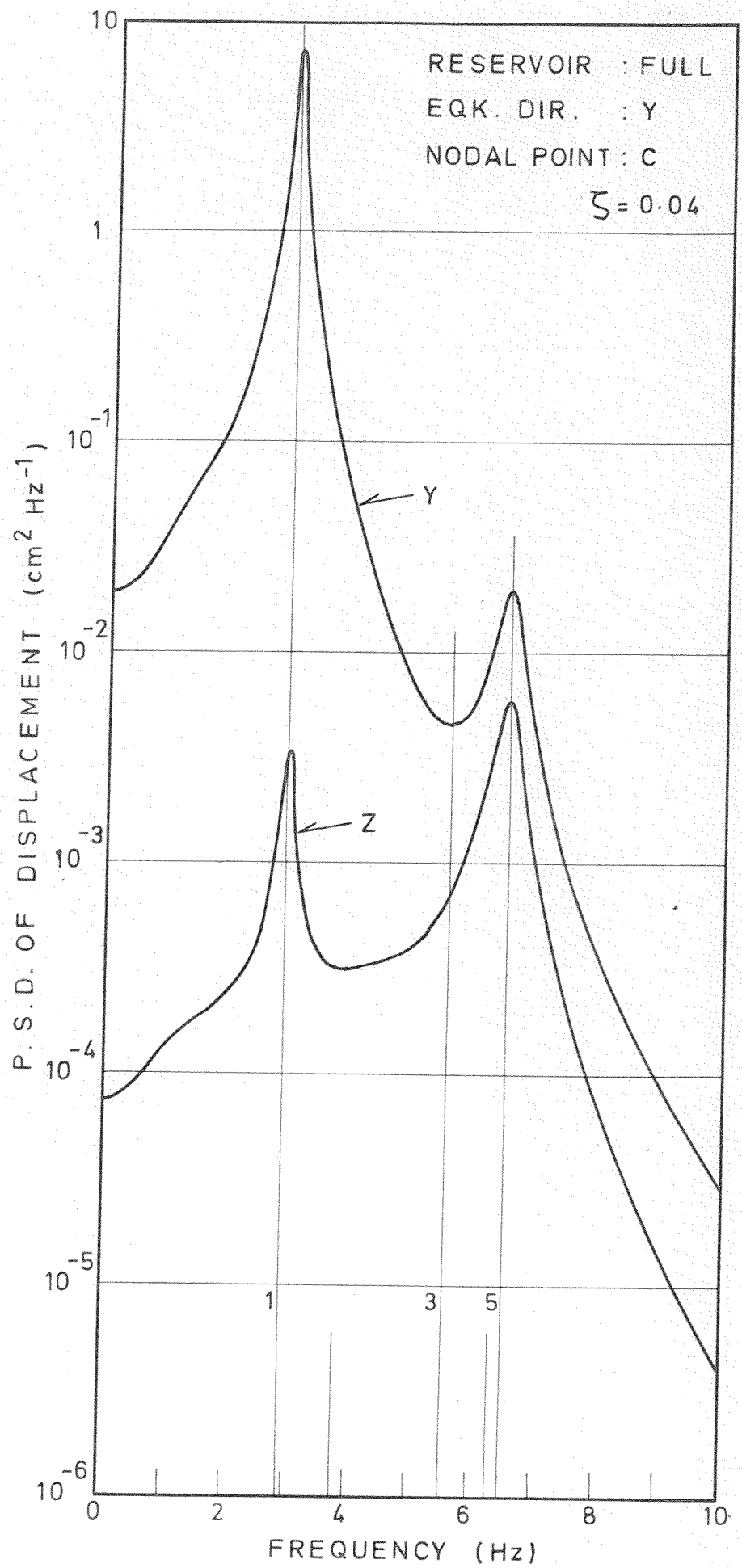


Fig.5.12. Response power spectrum

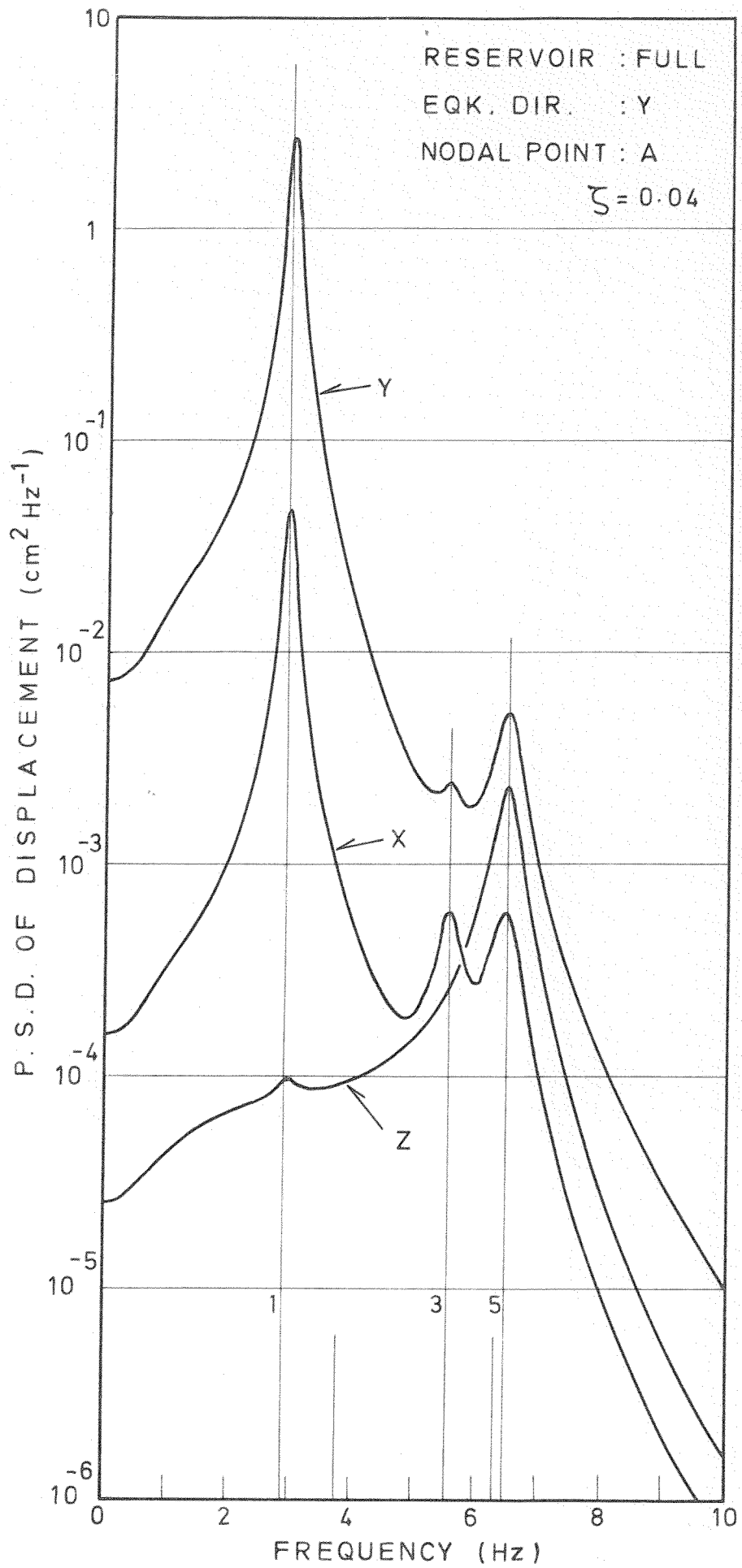


Fig. 5.13. Response power spectrum

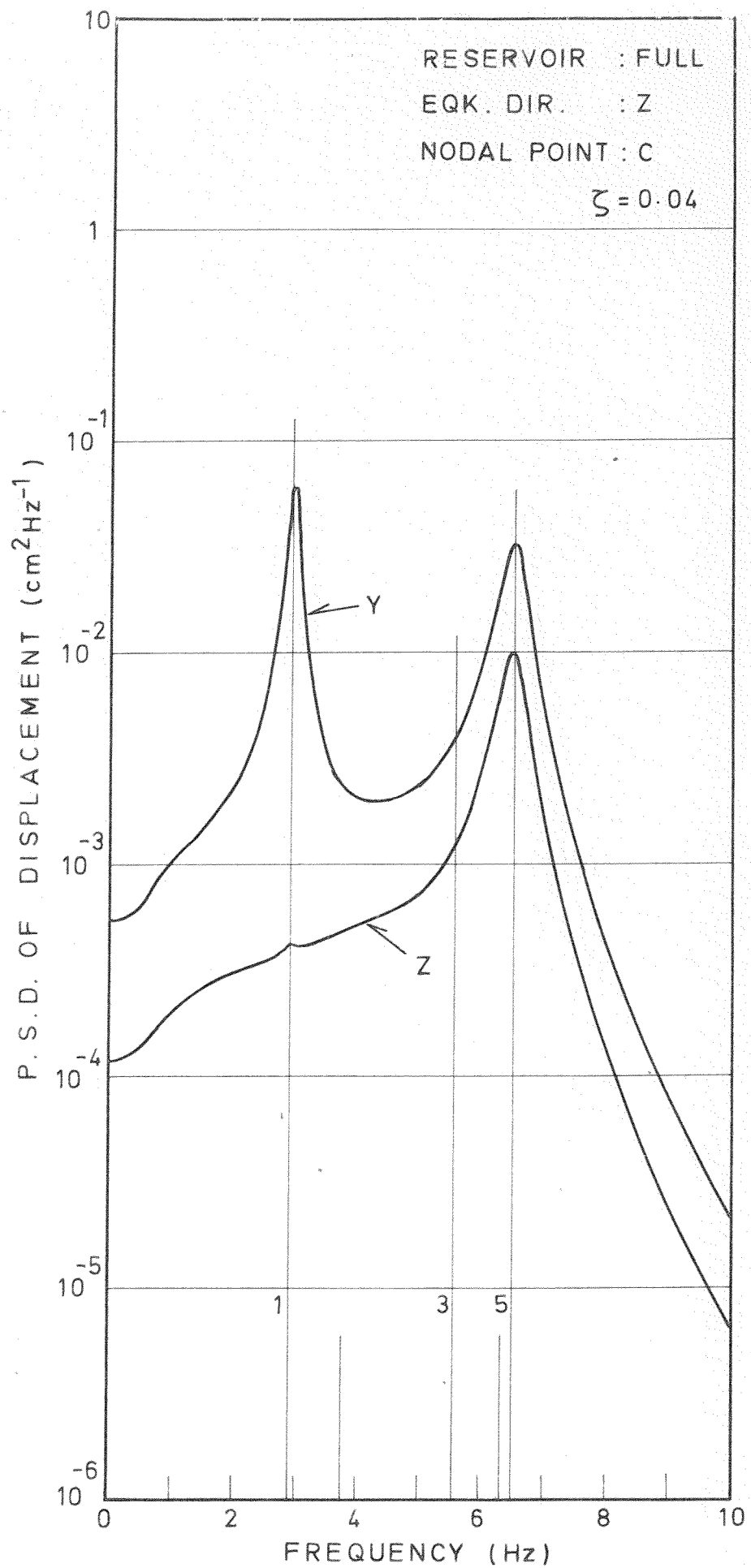


Fig.5.14. Response power spectrum

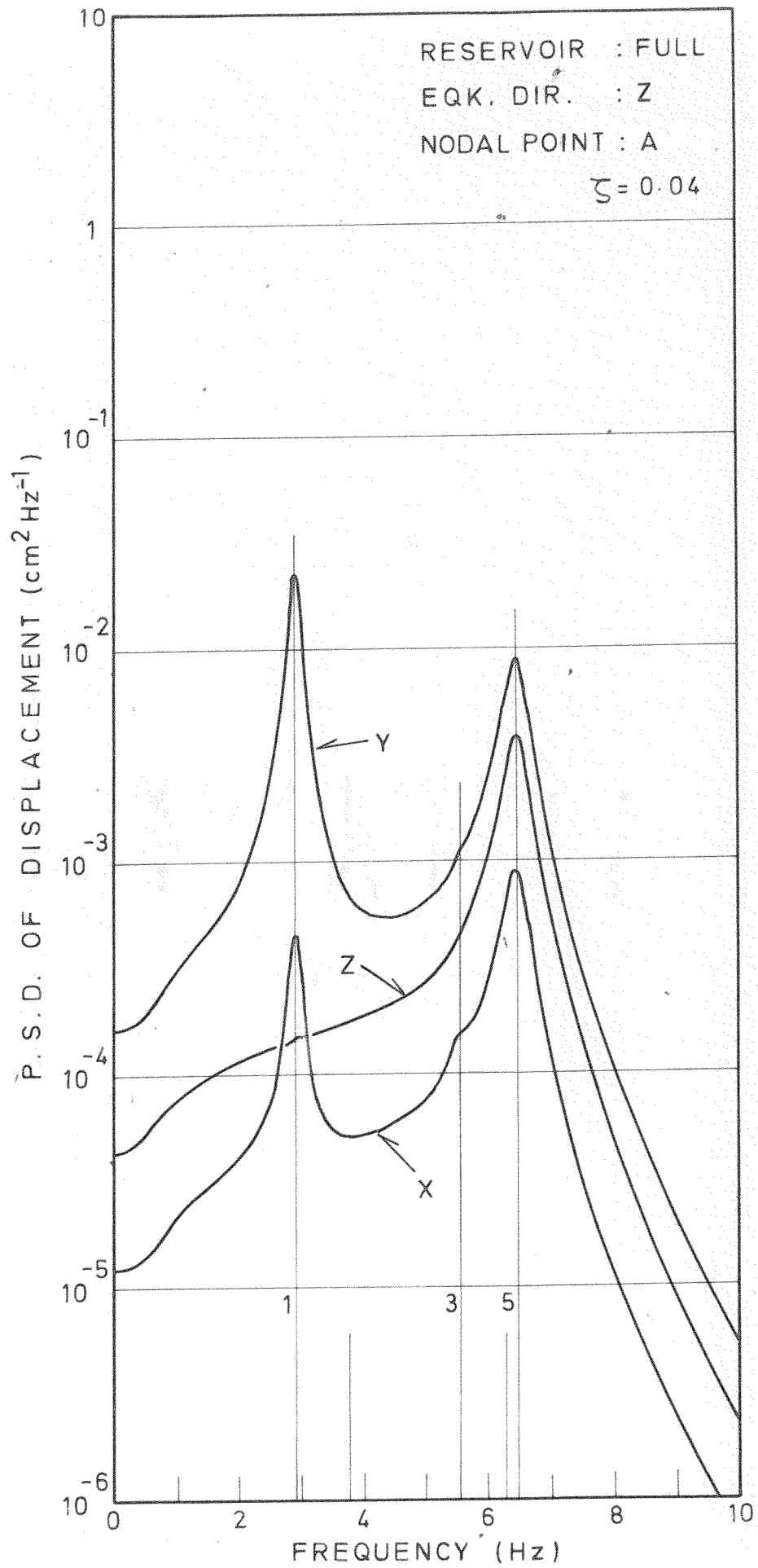


Fig.5.15. Response power spectrum

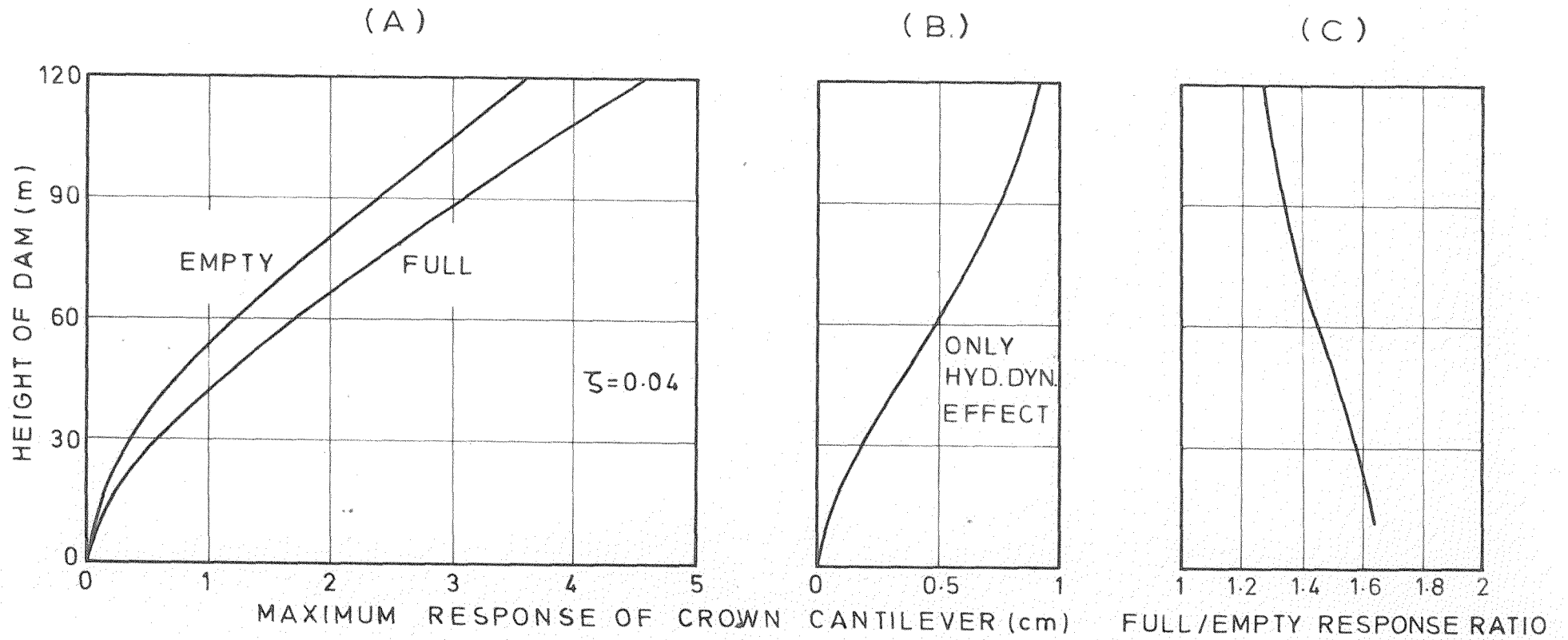


Fig.5.16. Effect of the reservoir water on the maximum response of crown cantilever

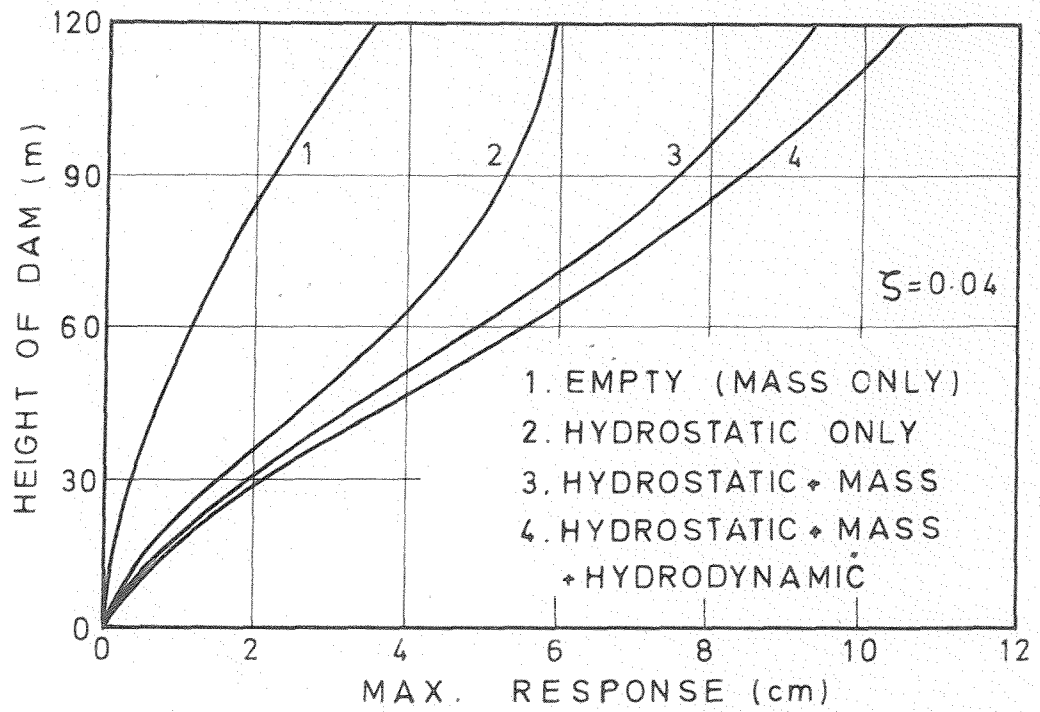


Fig.5.17. Max. response of crown cantilever in comparison with hydrostatic deflections

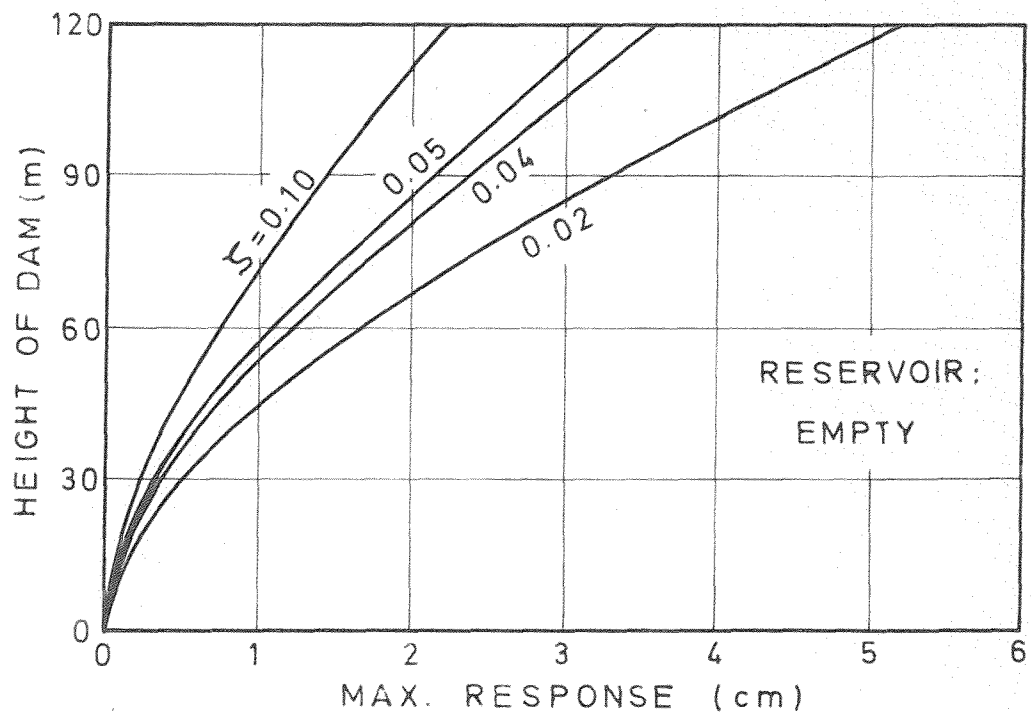


Fig.5.18. Effect of damping ratio on the response of crown cantilever

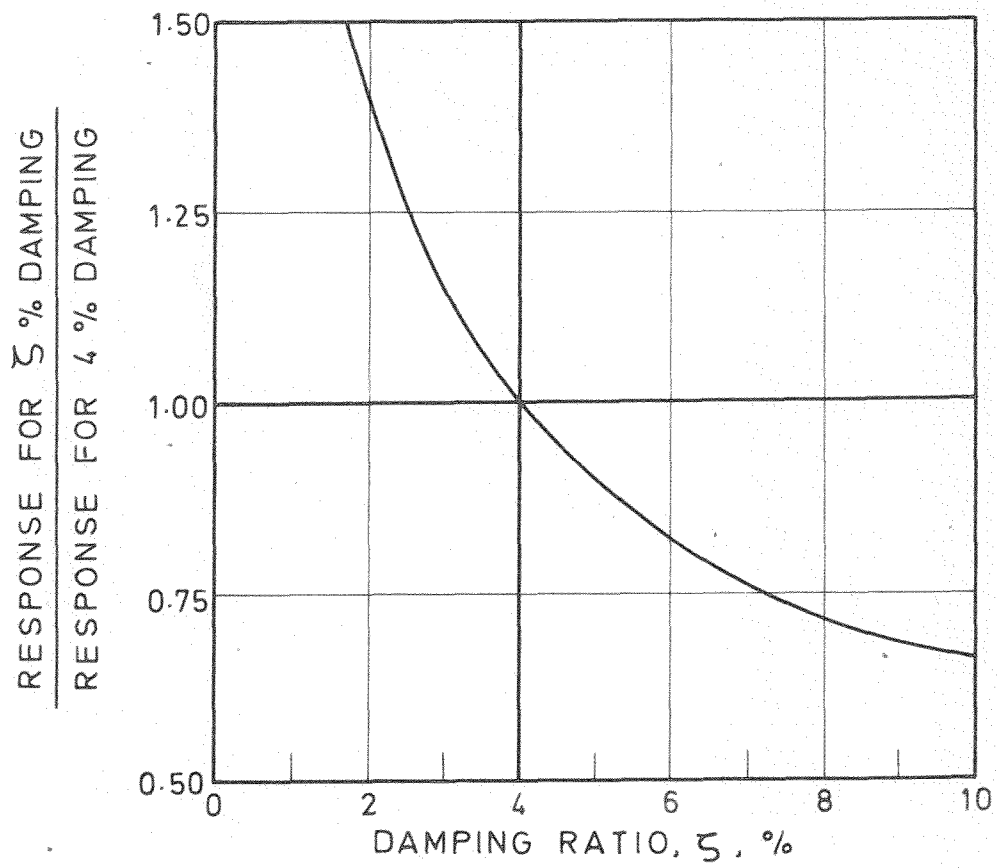


Fig. 5.19. Effect of damping ratio on the response of arch dam

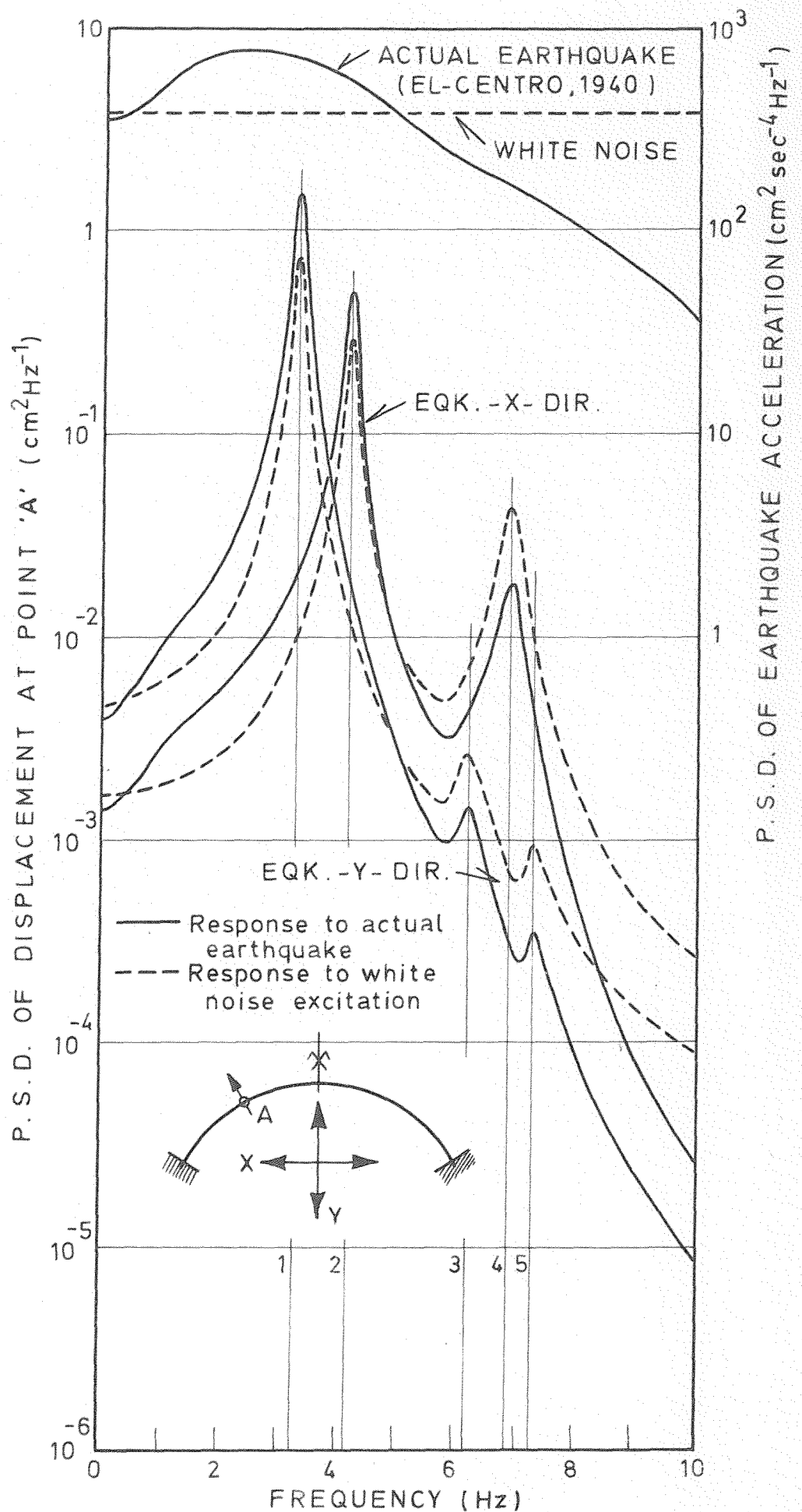


Fig.5.20. Earthquake and response power spectrums in comparison with white noise excitation

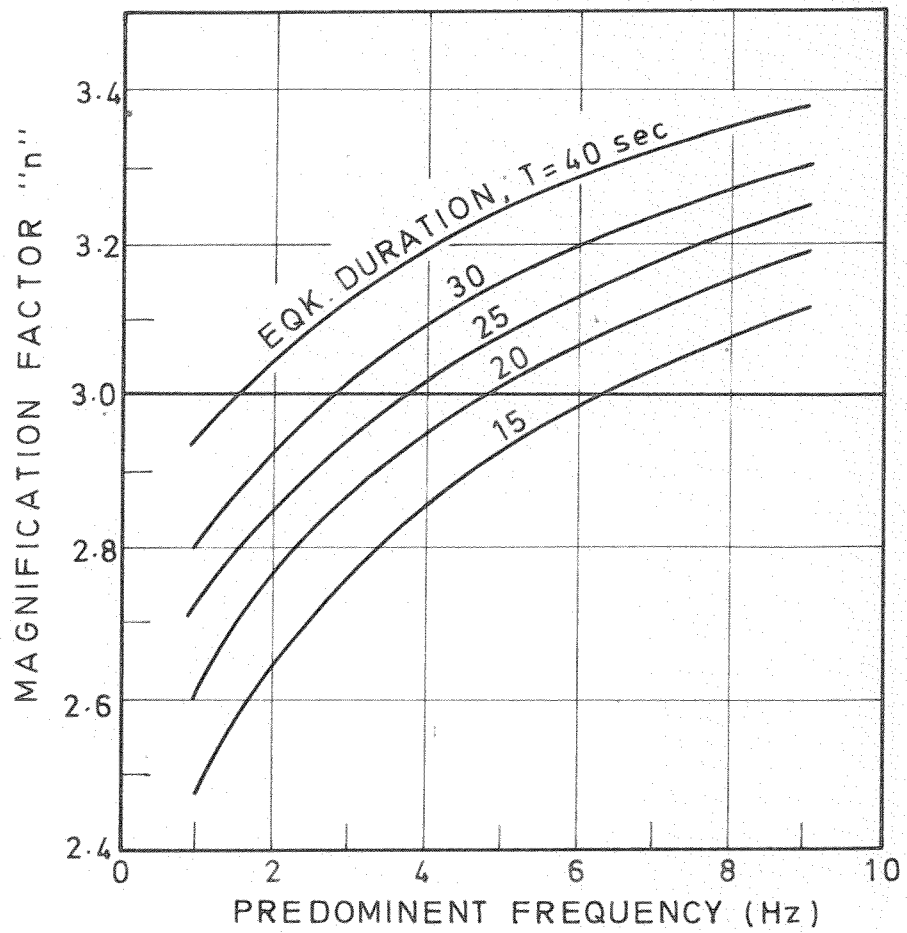


Fig.5.21. Variation of magnification factor with earthquake duration

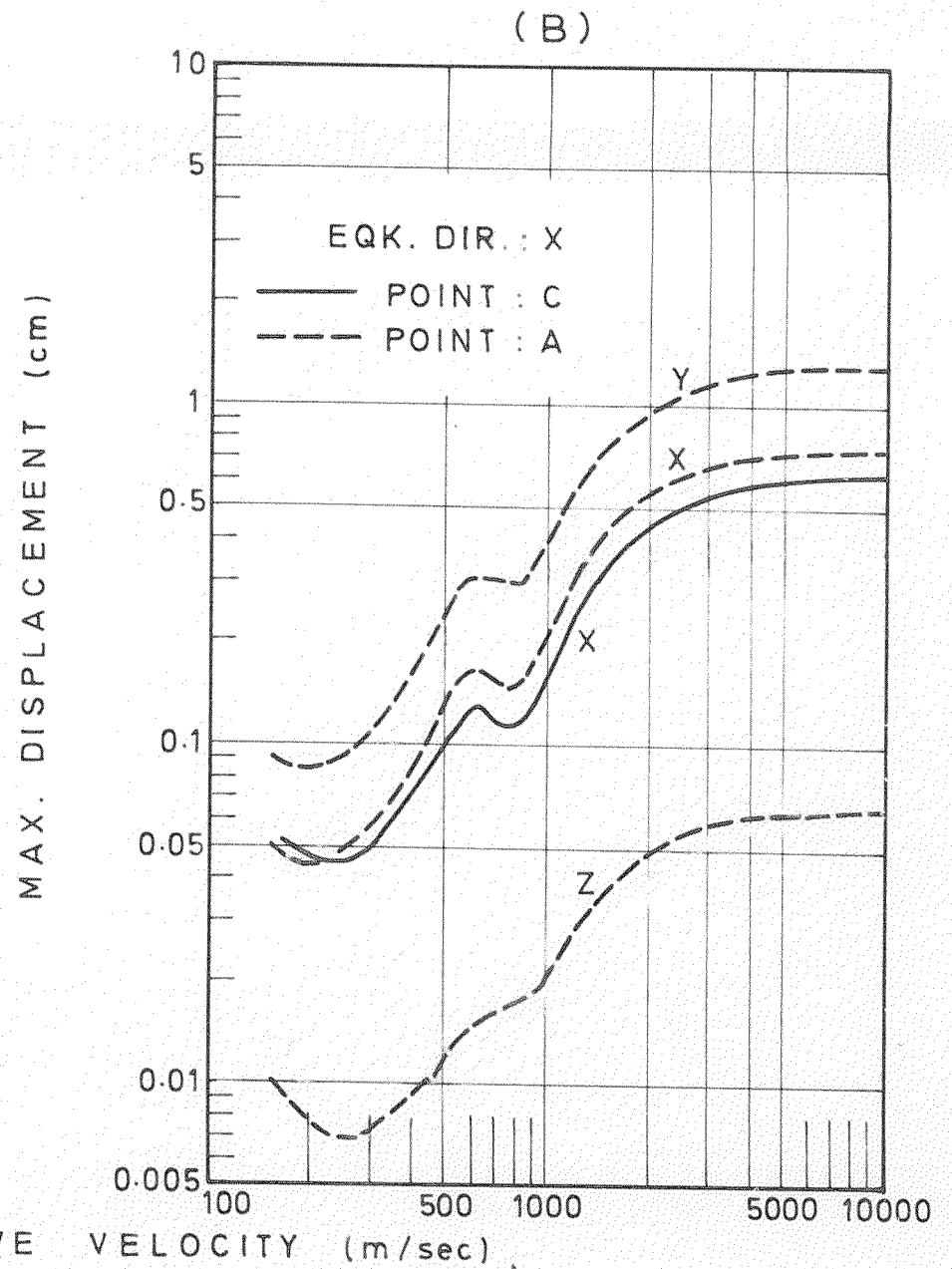
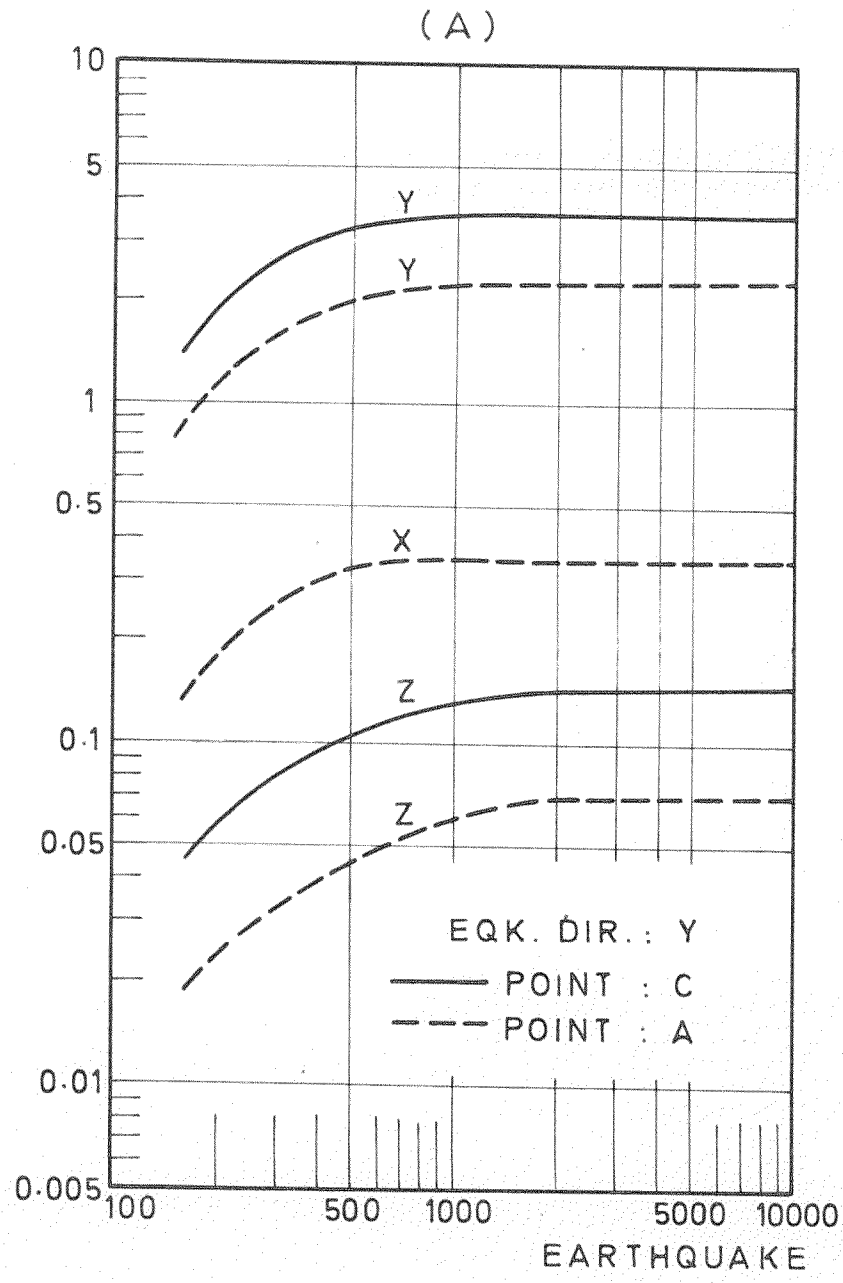


Fig.5.22. Effect of earthquake wave velocity on maximum response

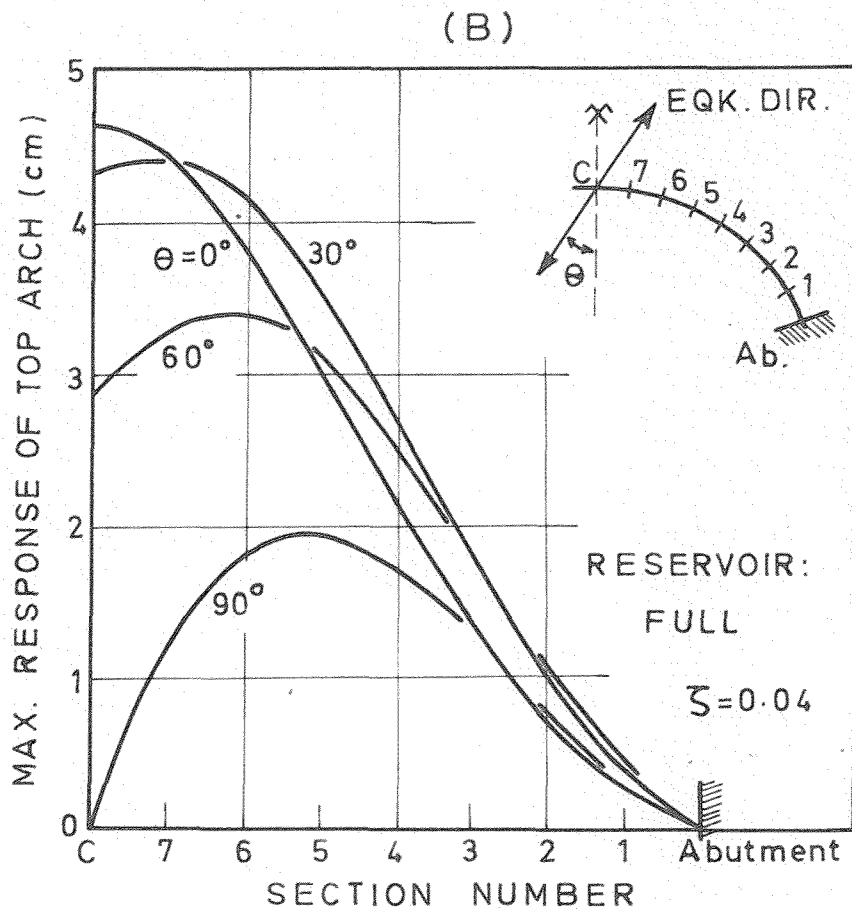
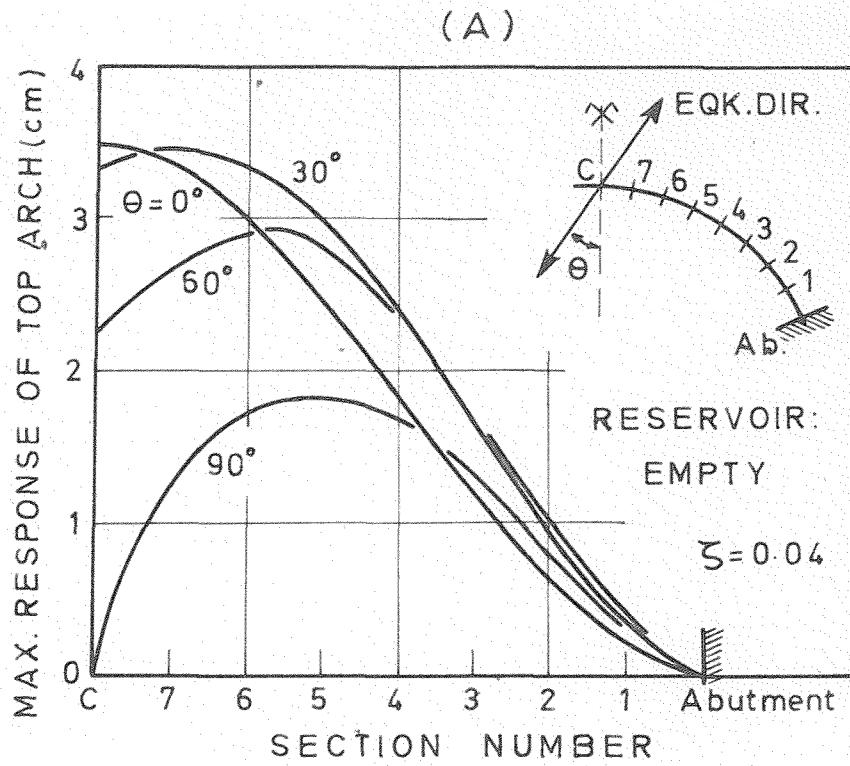


Fig.5.23. Effect of earthquake direction on the response of arch dam

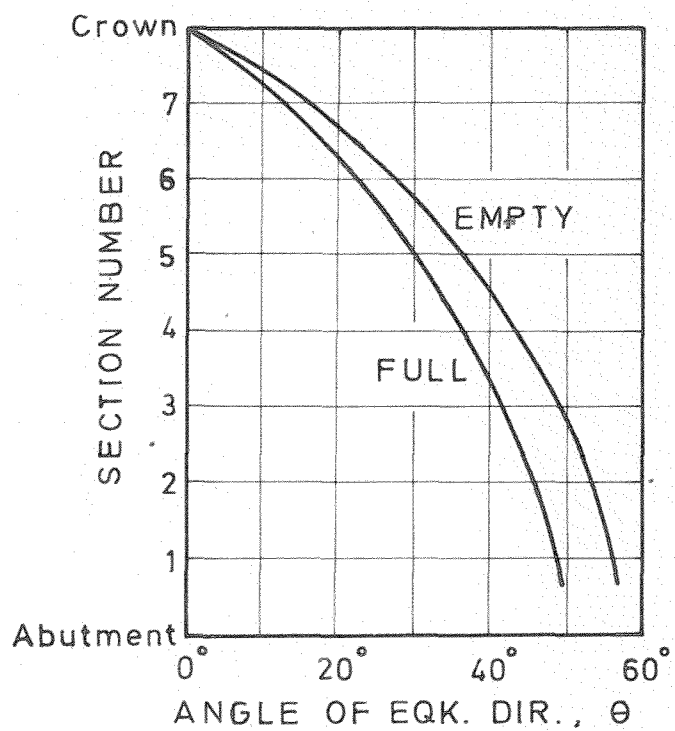
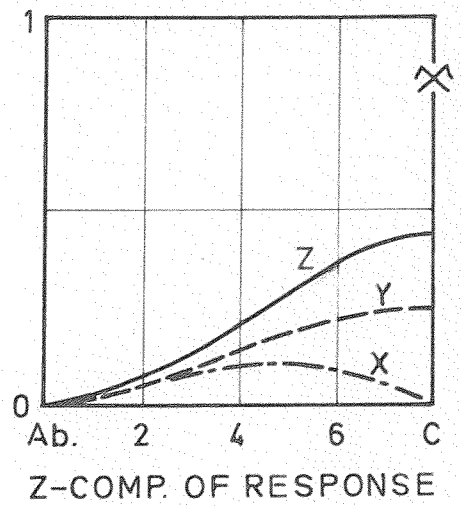
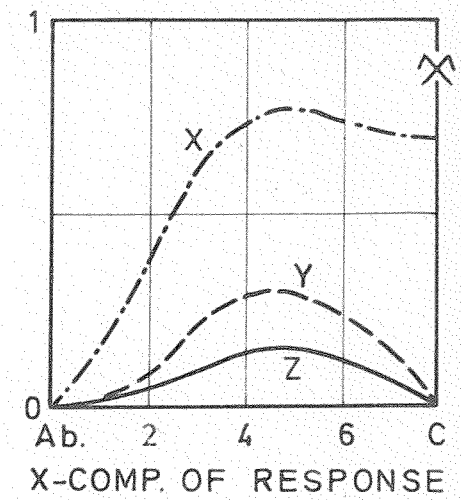
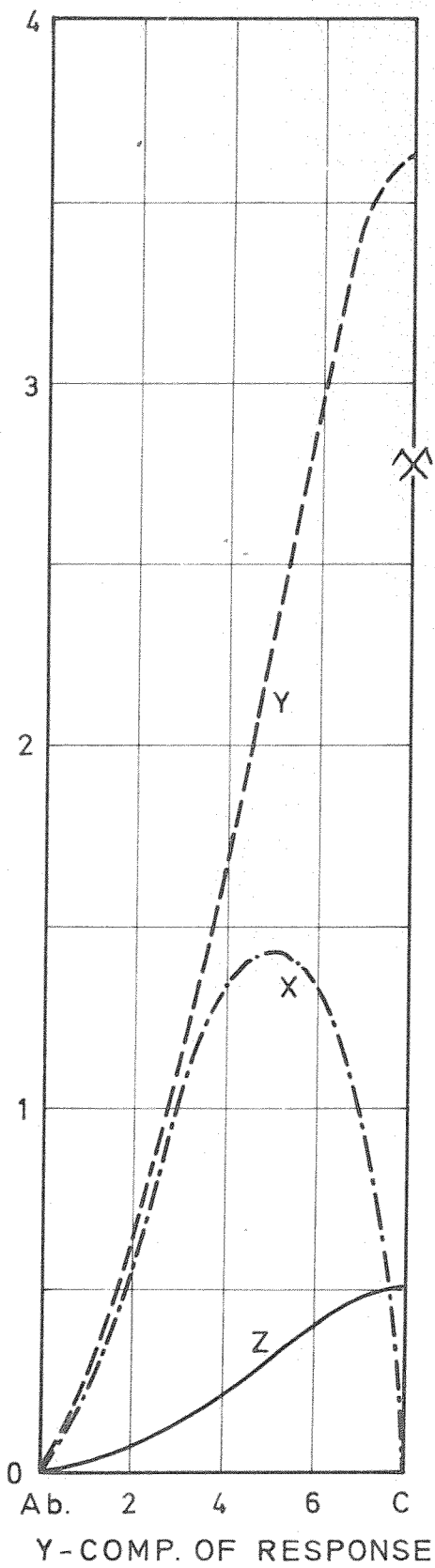


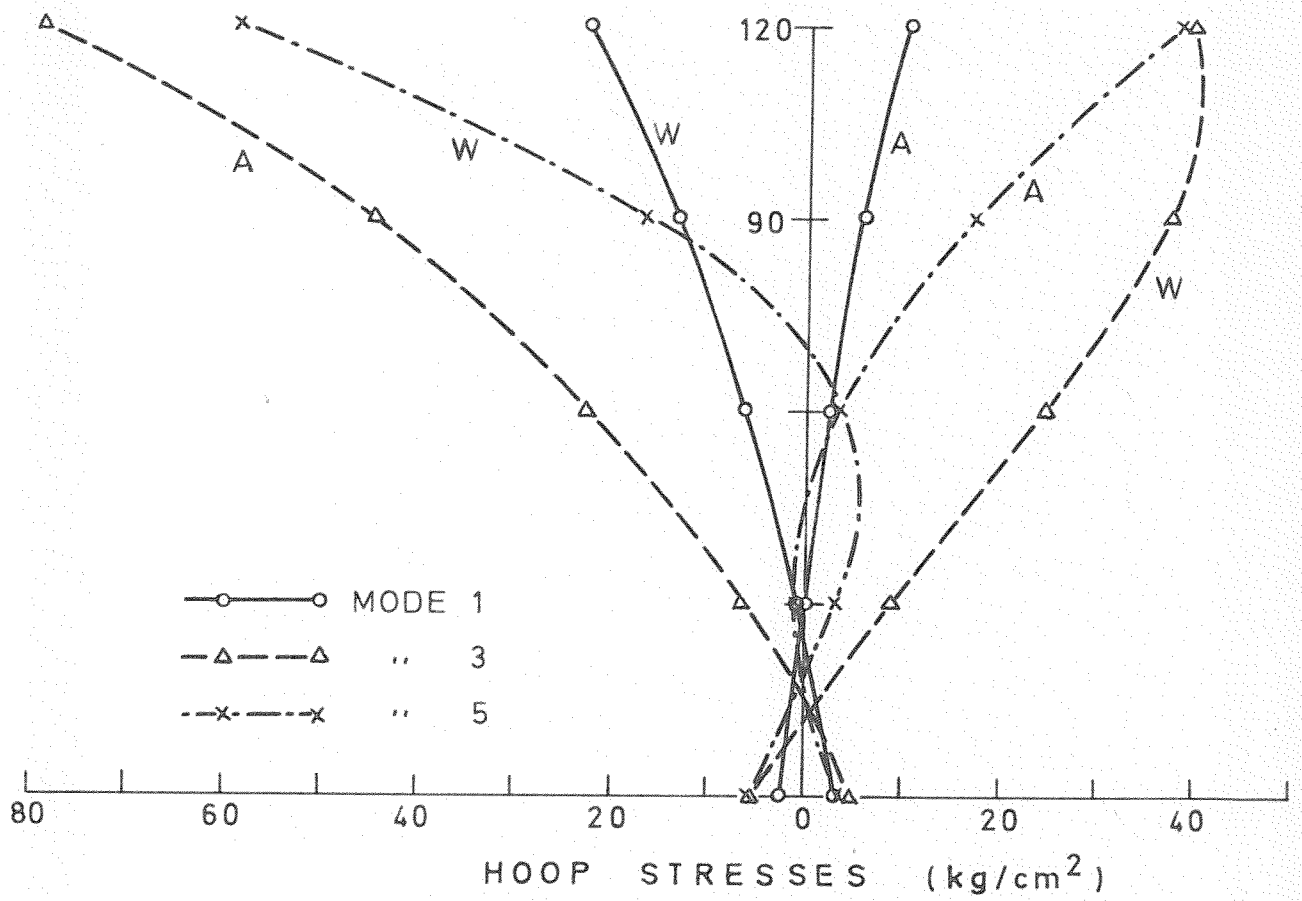
Fig.5.24. Earthquake direction which produces maximum horizontal responses at the points on the top arch



DISPLACEMENT (cm)

EQK. DIR.  
 - - - - - Y  
 - · - · - X  
 ——— Z

Fig.5.25. Comparison of response components of top arch, according to components of earthquake, having the same intensity



W: Water face  
 A: Air face

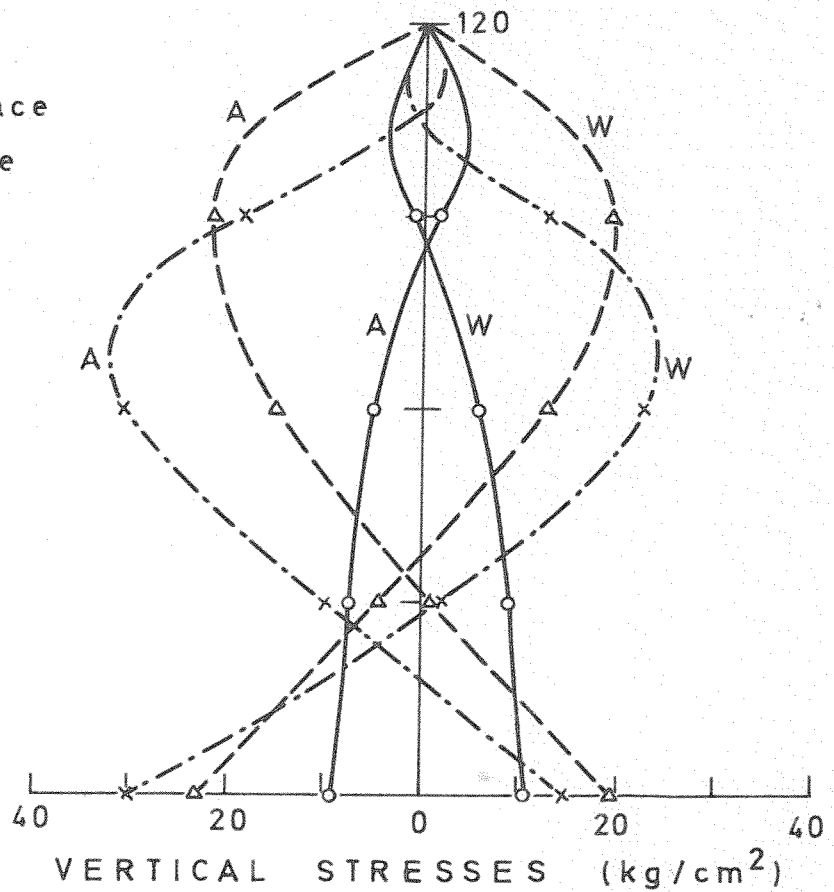
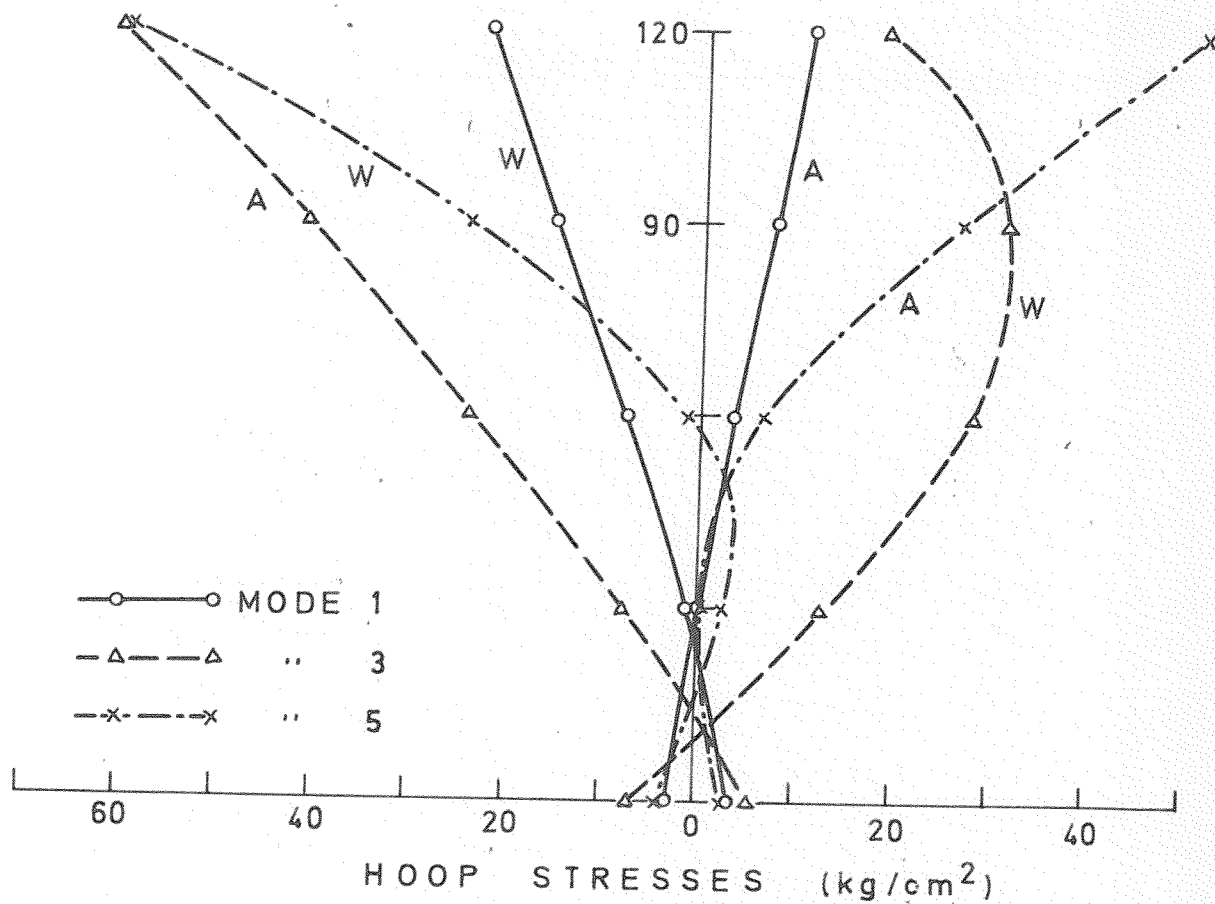


Fig.6.1. Modal stresses in crown cantilever Reservoir in empty condition



W: Water face  
A: Air face

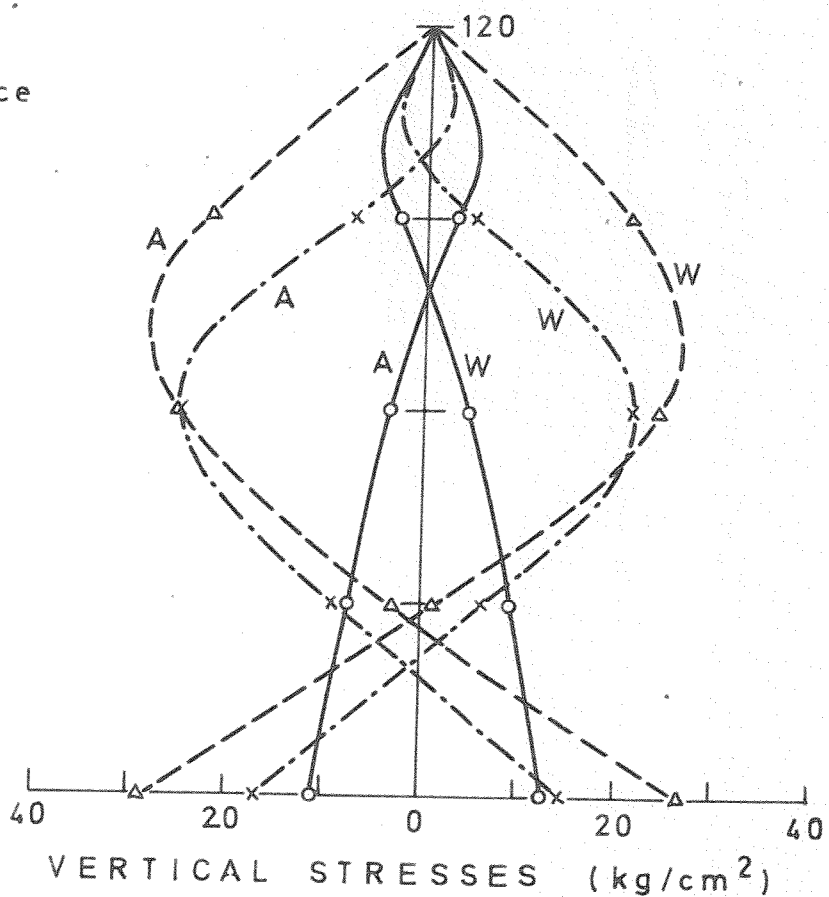


Fig.6.2. Modal stresses in crown cantilever Reservoir in full condition

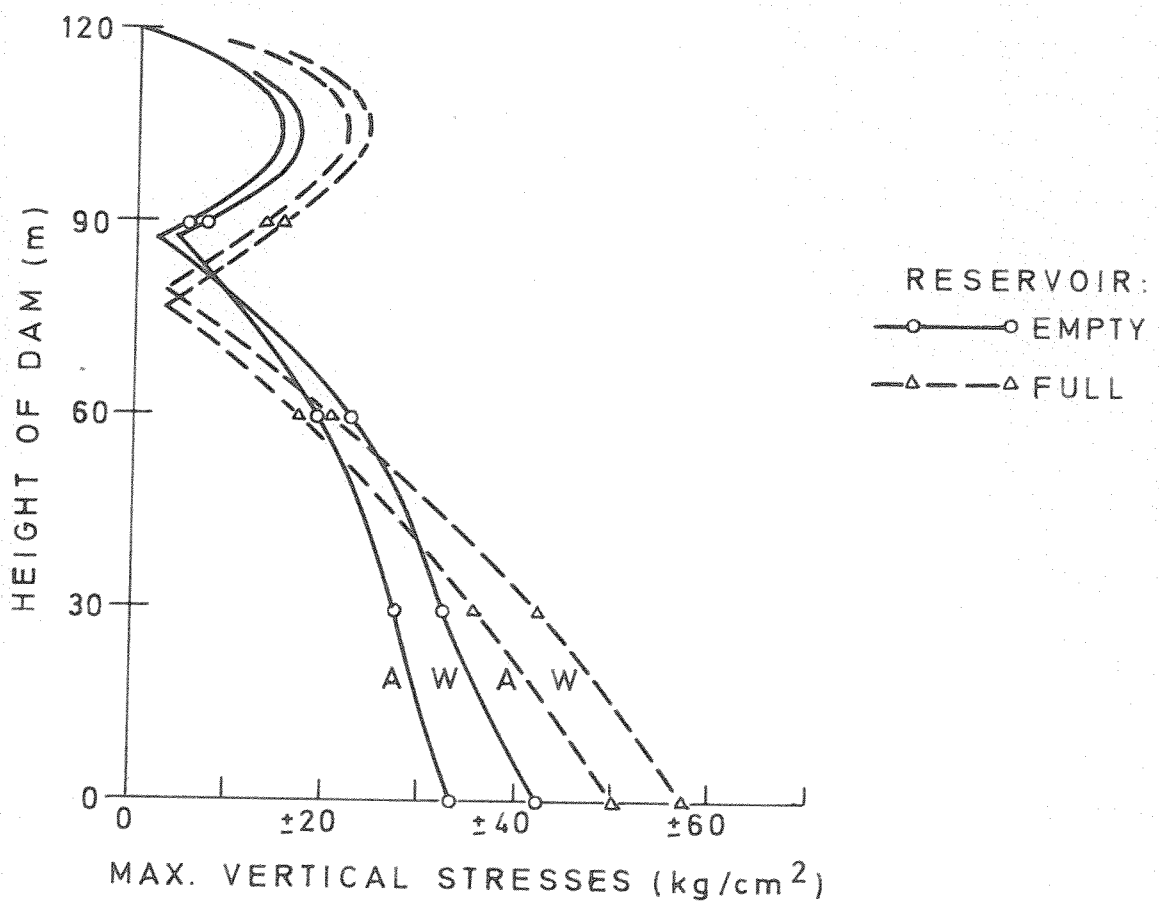
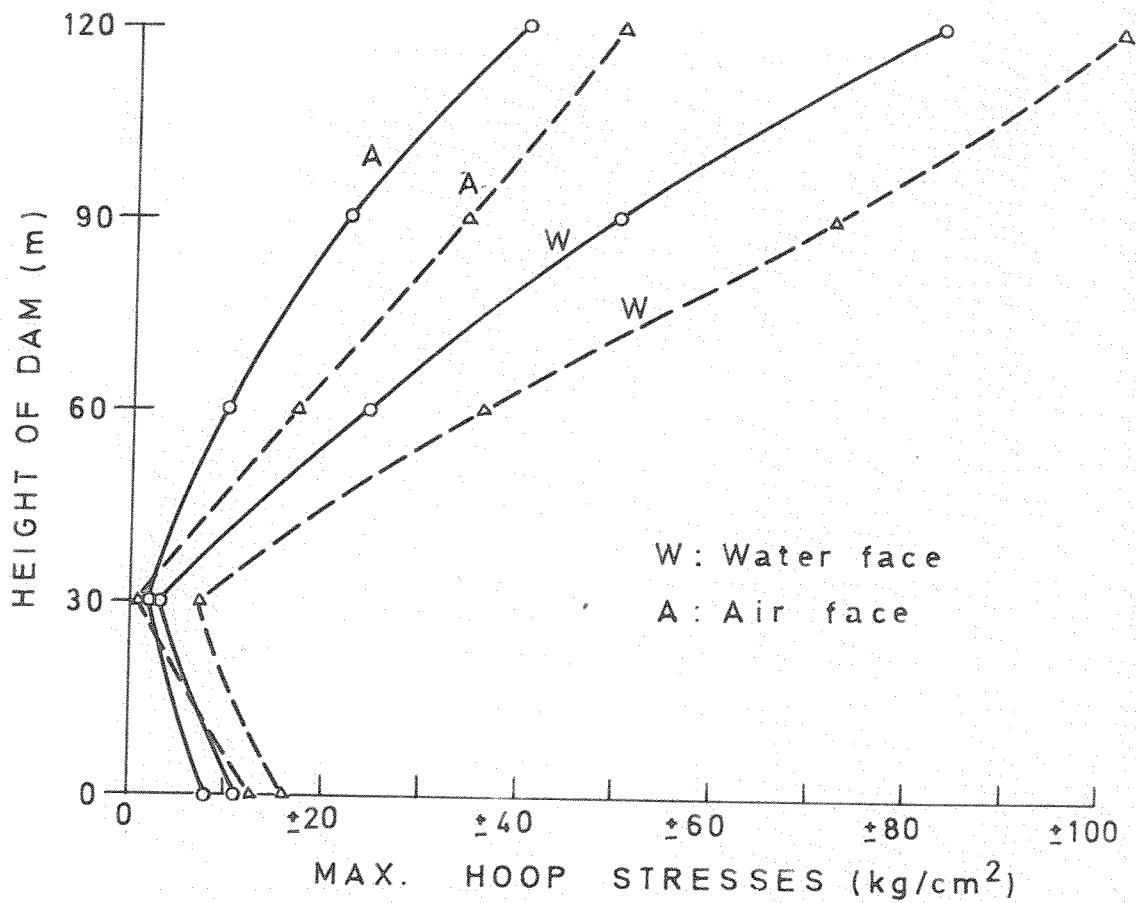


Fig. 6.3. Max. dynamic stresses in crown cantilever due to El-Centro, 1940 earthquake

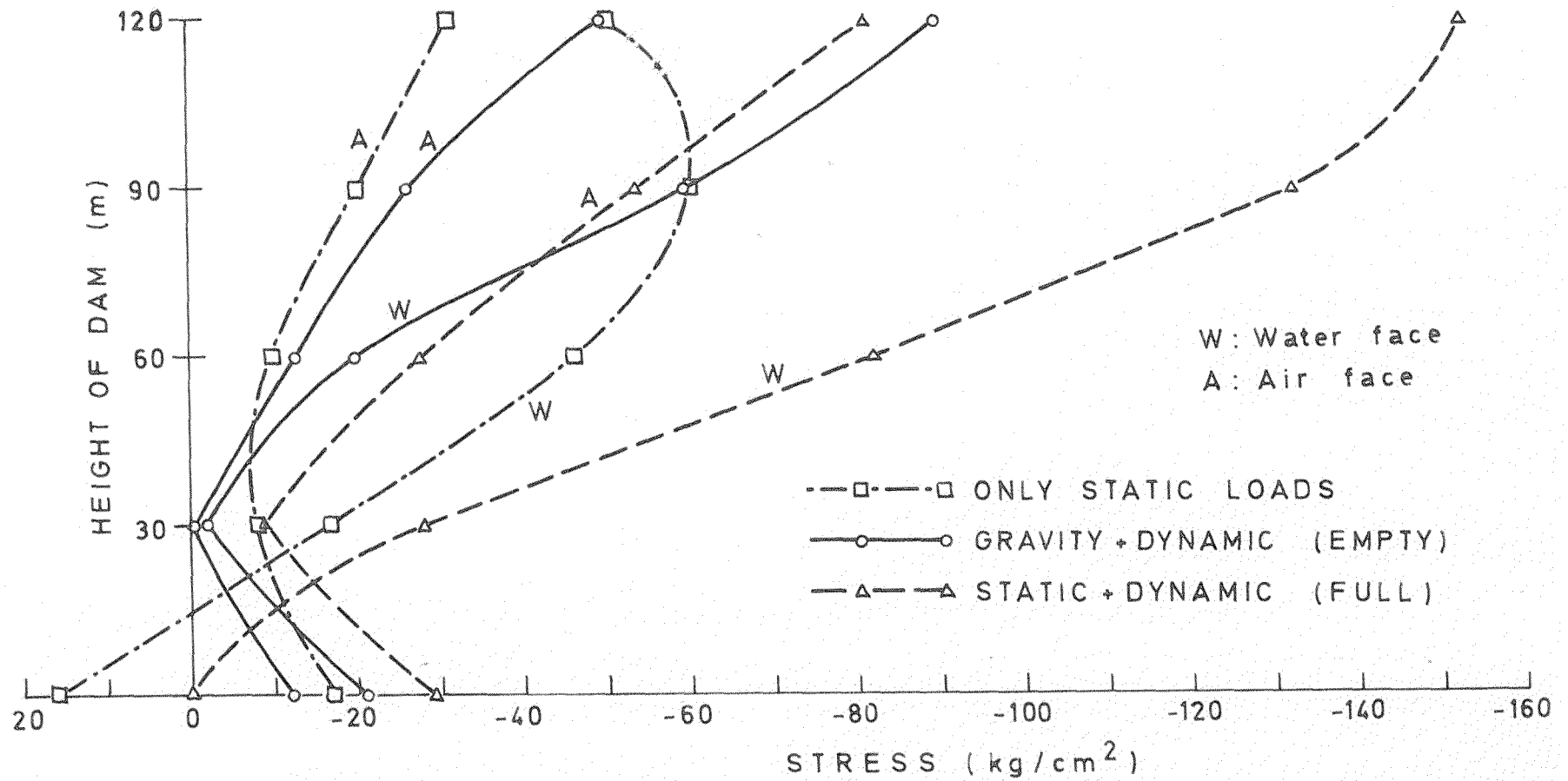


Fig.6.4. Max. total compressive hoop stresses in crown cantilever

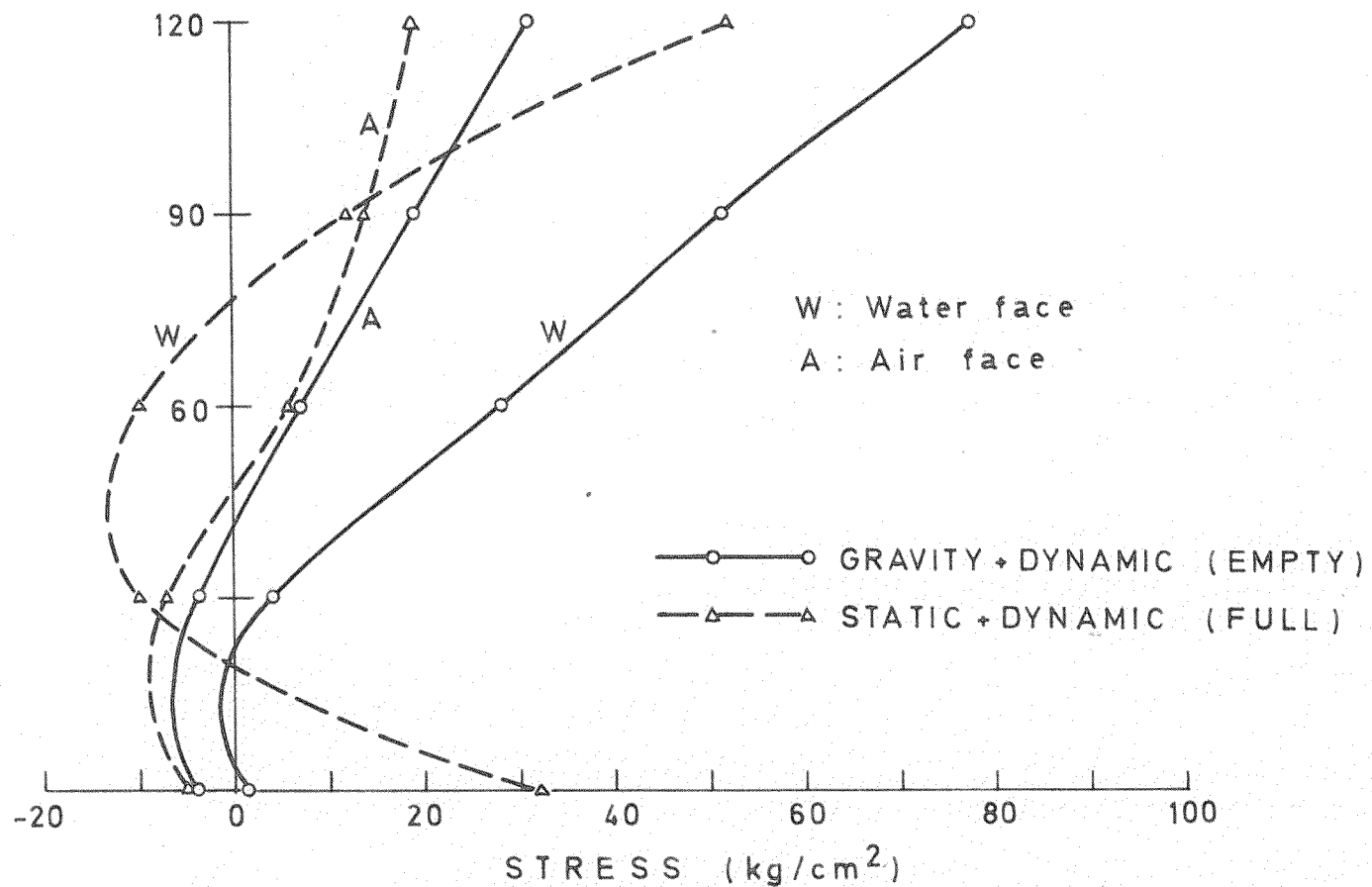


Fig.6.5. Max. total tensile hoop stresses in crown cantilever

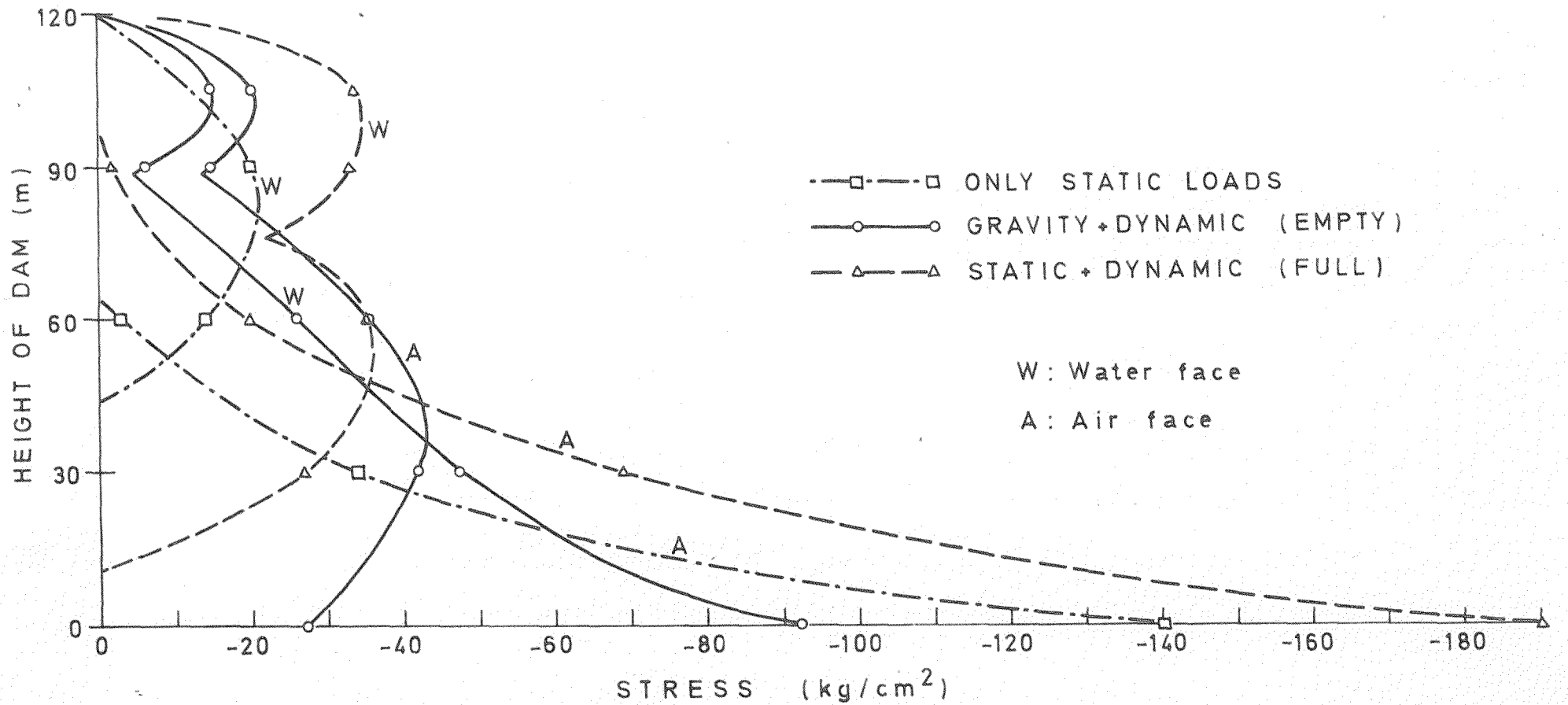


Fig.6.6. Max. total compressive vertical stresses in crown cantilever

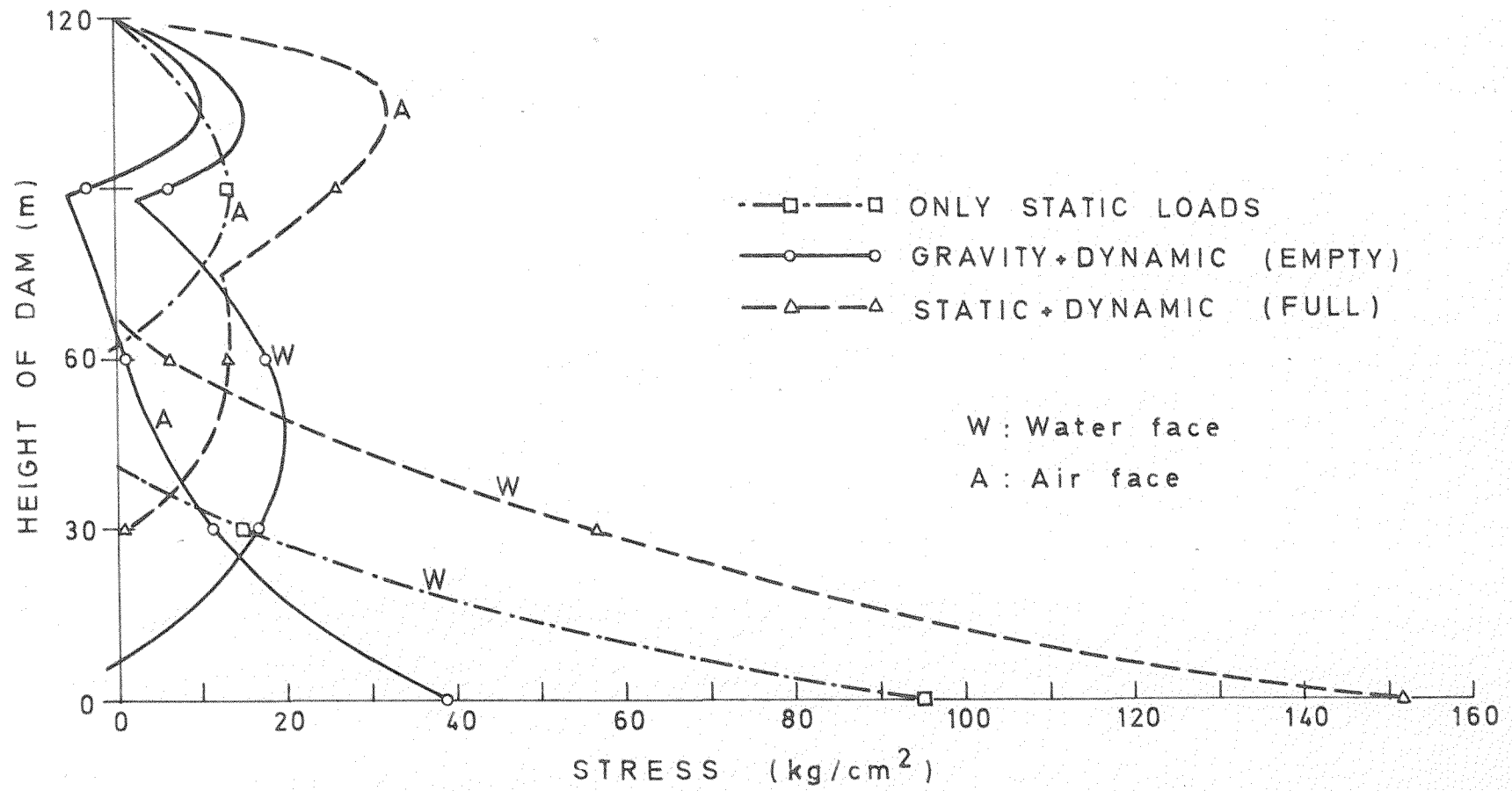


Fig.6.7. Max. total tensile vertical stresses in crown cantilever

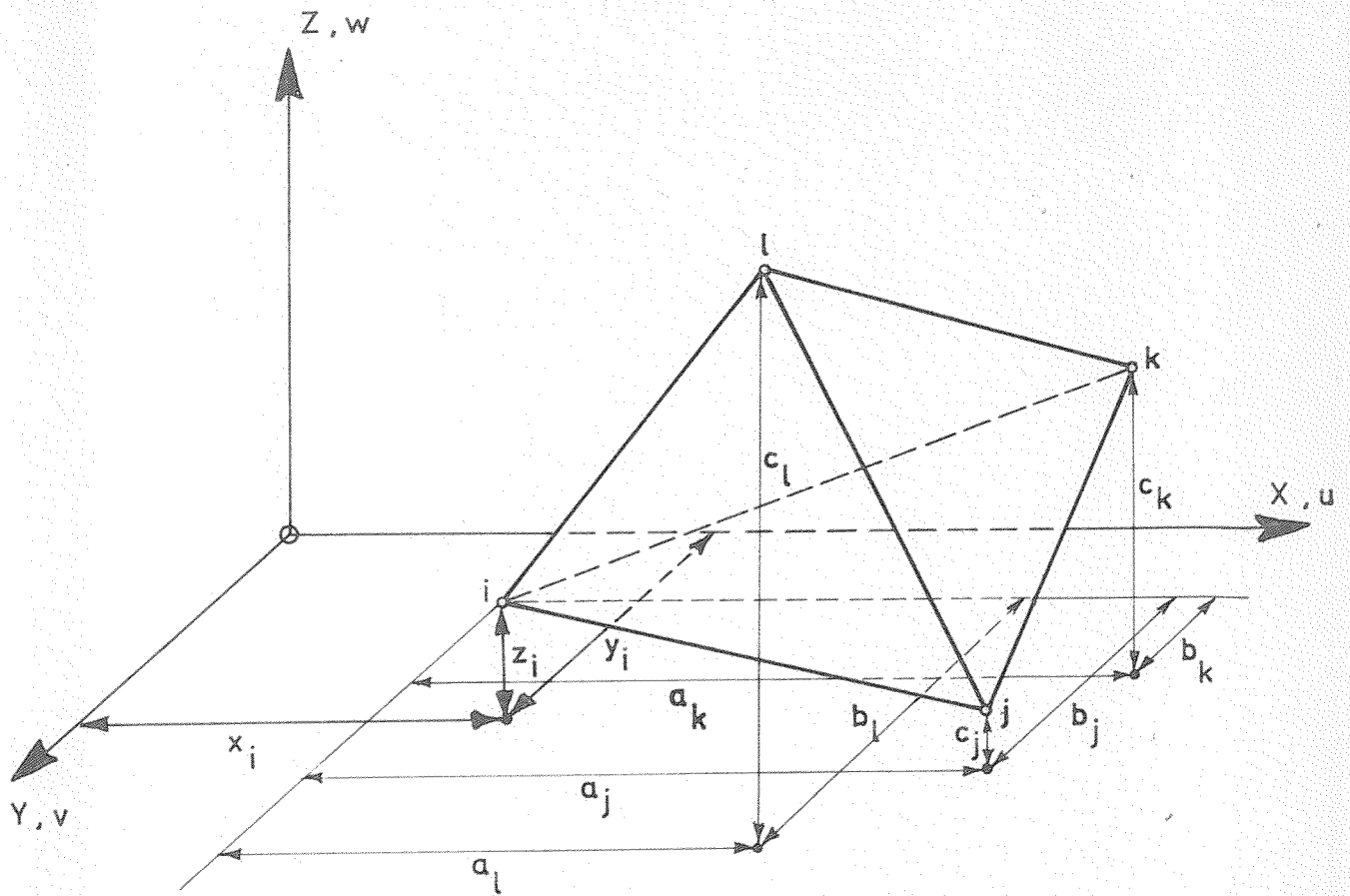


Fig.A.1. Tetrahedral finite element, co-ordinate system and dimensions

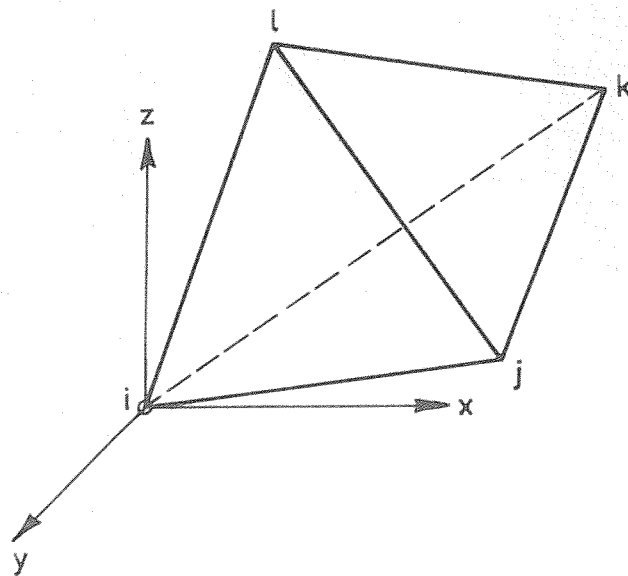


Fig.A.2. Assumed system of axis for inertia calculations